ROBUST COMPUTATIONAL METHODS FOR SINGULAR PERTURBATION PROBLEMS WITH SHIFTS AND INTEGRAL BOUNDARY CONDITIONS

Thesis Submitted
in Partial Fulfillment of the Requirements
for the Degree of

DOCTOR OF PHILOSOPHY

by

SHIVANI JAIN
(2K21/PHDAM/02)

Under the Supervision of
Prof. Aditya Kaushik
Delhi Technological University

Department of Applied Mathematics

DELHI TECHNOLOGICAL UNIVERSITY
(Formerly Delhi College of Engineering)
Shahbad Daulatpur, Main Bawana Road, Delhi-110042 India

July, 2025

DELHI TECHNOLOGICAL UNIVERSITY

(Formerly Delhi College of Engineering)

Shahbad Daulatpur, Main Bawana Road, Delhi – 110042 India

CANDIDATE'S DECLARATION

I Shivani Jain hereby certify that the work which is being presented in the thesis entitled " Robust Computational Methods for Singular Perturbation Problems with Shifts and Integral Boundary Conditions" in partial fulfillment of the requirements for the award of the Degree of Doctor of Philosophy, submitted in the Department of Applied Mathematics, Delhi Technological University is an authentic record of my own work carried out during the period from 02/08/2021 to 06/05/2025 under the supervision of Prof. Aditya Kaushik.

The matter presented in the thesis has not been submitted by me for the award of any other degree of this or any other Institute.

Shivani Jain

2K21/PHDAM/02

DELHI TECHNOLOGICAL UNIVERSITY

(Formerly Delhi College of Engineering)
Shahbad Daulatpur, Main Bawana Road, Delhi – 110042 India

CERTIFICATE

Certified that Shivani Jain (2K21/PHDAM/02) has carried out their research work presented in this thesis entitled "Robust Computational Methods for Singular Perturbation Problems with Shifts and Integral Boundary Conditions" for the award of Doctor of Philosophy from Department of Applied Mathematics, Delhi Technological University, Delhi. The thesis embodies results of original work, and studies are carried out by the student herself and the contents of the thesis do not form the basis for the award of any other degree to the candidate or to anybody else from this or any other University/Institution.

Dr. Aditya Kaushik
Professor & Supervisor
Department of Applied Mathematics
Delhi Technological University, Delhi.

Dr. Ramesh Srivastava
Professor & Head of Department
Department of Applied Mathematics
Delhi Technological University, Delhi.

Date: Tuesday 22nd July, 2025

ACKNOWLEDGEMENT

I would like to extend my sincerest gratitude to my supervisor Prof. Aditya Kaushik, Department of Applied Mathematics, Delhi Technological University, Delhi for his divine motivation, patient mentorship and substantial support throughout my research. His wisdom and humble approach were instrumental for me over the years. Indeed it's been a privilege for me to work under his supervision. The skills and insights I gained under his mentorship are the lessons that I will carry throughout my life's journey and would remain ever grateful to him for his guidance and inspiration in every step of the way.

I sincerely thank to all the DRC members, faculty members, department staff and academic branch of Delhi Technological University for extending their support and providing all the facilities necessary for my research.

I am greatly obliged to my family for their unwavering love and continuous care. Their prayer for me was what sustained me this far. Their encouragement and patience have provided me with the strength to see this journey to completion.

Last but not the least, I thank the God's almighty for giving me the opportunity and the blessings to be successful in my life's journey so far.

Date: Tuesday 22nd July, 2025 **SHIVANI JAIN**

Place: Delhi, India.

Contents

Abstract

In the present thesis, an attempt has been made to construct, apply, analyse and optimise higher-order hybrid parameter-uniform finite difference methods for solving singular perturbation problems involving a system of reaction-diffusion equations with shifts and integral boundary conditions. These problems commonly arise in the different fields of applied mathematics, for example, edge layers in solid mechanics, aerodynamics, oceanography, rafted-gas dynamics, transition points in quantum mechanics, shock and boundary layers in fluid dynamics, magnetohydrodynamics, drift-diffusion equations of semiconductor devices, plasma dynamics, skin layers in electrical applications, Stoke's line in mathematics, and rarefied-gas dynamics. These problems depend on a small perturbation parameter ε, which multiplies the highest-order derivative terms. When the value of the perturbation parameter is limited to zero, the solutions to such problems approach a discontinuous limit and exhibit a multiscale character. Often, these mathematical problems are extremely difficult (or even impossible) to solve exactly and approximate solutions are necessary in certain circumstances. Asymptotic and numerical analysis are two principal approaches to solving singular perturbation problems. Although asymptotic and numerical methods offer valuable tools for tackling singularly perturbed systems of reaction-diffusion equations, they also have limitations. Asymptotic methods struggle to provide accurate solutions in regions where multiple lengths or time scales interact. Additionally, these methods often rely on analytical approximations, which may not fully capture the system's behaviour. Numerical methods also have limitations when applied on uniform meshes. They require excessively fine meshes to capture the solution behaviour within the boundary layers, leading to computationally expensive simulations.

The analysis and solution of these systems require specialised mathematical techniques tailored to handle stiffness and boundary layer phenomena. The thesis provides higher-order hybrid numerical methods over an adaptive mesh for solving different classes of reaction-diffusion problems. The thesis consists of six chapters. A brief outline of the chapters is as follows:

Chapter 1 recalls an overview of the fundamentals of singular perturbation theory. It also presents concepts and a historical assessment of the related literature. This chapter also provides a detailed literature review of various state-of-the-art techniques developed in the recent past. In addition, the chapter illustrates the purpose and objectives of the thesis.

Chapter 2 presents a higher-order adaptive hybrid difference method to solve a singularly perturbed system of reaction-diffusion problems with Dirichlet boundary conditions. The numerical method combines a Hermite difference method with the classical central difference method on a layer-adapted

mesh. The equidistribution principle generates the mesh using a nonnegative monitor function. The mesh generation procedure automatically detects the thickness and steepness of any boundary layers present in the solution and does not require prior information about its analytical behaviour. The chapter presents a rigorous theoretical analysis and numerical results for model problems to support theoretical findings. The method is almost fourth-order accurate, converges uniformly, and is unconditionally stable. Moreover, the convergence obtained is optimal, as the estimates are free from any logarithmic term compared to the difference methods over the piecewise uniform Shishkin mesh.

Chapter 3 presents a higher-order hybrid approximation over an adaptive mesh designed to solve a coupled system of singularly perturbed reaction-diffusion equations with a shift on an equidistributed mesh. The difference method combines an exponential spline difference method for the outer layer and a cubic spline difference method for the boundary layer on the adaptive mesh generated. The mesh relies on the equidistribution principle, a nonnegative monitor function, and the second-order derivatives of the layer components of the solution. The proposed numerical method improves the accuracy of numerical solutions while maintaining computational efficiency. The proposed numerical method is consistent, stable, and converges regardless of the size of the perturbation parameter. The numerical results and illustrations support the theoretical findings.

Chapter 4 presents a semi-analytical approach to solving a system of singularly perturbed convection-diffusion equations with shifts. A careful factorisation handles complex multiscale systems by splitting them into two explicit parts: one capturing smooth solutions and the other addressing boundary layer solutions. The strategy involves factoring a coupled system of equations into explicit systems of first-order initial value problems and second-order boundary value problems. The solutions to the degenerate system correspond to the regular component. In contrast, those of the system of boundary value problems represent the singular component. The process combines the regular and singular components to obtain the complete solution. The q-stage Runge-Kutta method computes the outer solution, and an analytical approach derives the inner solution. The proposed method is unconditionally stable and converges independently of the perturbation parameters. Unlike numerical methods, the proposed technique does not require adaptive mesh generation to sustain approximation and consequently has lower computational complexity. The process is straightforward, and interdisciplinary researchers can quickly adapt the method to solve problems related to chemical kinetics, mathematical physics, and biology. The method is highly accurate, free from directional bias, and the estimates are free from logarithmic terms. The results demonstrate that the numerical method outperforms many existing methods.

Chapter 5 presents a highly efficient hybrid difference approximation for a time-dependent singularly perturbed reaction-diffusion equation with shift and integral boundary conditions. The technique utilises a modified backward difference discretisation in time on a uniform mesh and a suitable combination of the exponential and cubic spline difference methods over a layer adaptive moving mesh in space. The layer-adapted mesh in space is generated by equidistributing a nonnegative monitor function, and the modified backward difference discretisation ensures alignment with the mesh at each subsequent time level. The presented method demonstrates second-order spatial uniform convergence and first-order temporal convergence. The method improves the accuracy of numerical solutions while maintaining

computational efficiency. The method is unconditionally stable and free from directional bias. The numerical experiments validate the theoretical estimates.

Chapter 6 concludes the work done and provides insight into the author's thoughts on the future direction of the research.

List of Tables

List of Figures

Chapter 1

Introduction

1.1 Perturbation Problems

Differential equations play a crucial role in mathematical modelling by providing a structured approach to describing and analysing dynamic systems. They capture the relationship between a function and its derivatives, enabling the study of how quantities change over time or space. Ordinary differential equations (ODEs) model processes that depend on a single independent variable and are used frequently in population dynamics, mechanical systems, and electrical circuits. Partial differential equations (PDEs) extend this course to functions of multiple independent variables, making them essential for modelling heat conduction, fluid flow, and wave propagation. In contrast, systems of differential equations further enhance modelling capabilities by representing interdependent processes, such as in epidemiology, chemical reactions, and neural networks. The ability to derive, analyse, and solve these equations analytically or numerically makes them indispensable tools for predicting real-world behaviours in science, engineering, and economics. These equations offer a versatile mathematical tool set for understanding and predicting complex phenomena.

Boundary/initial value problems involving ordinary and partial differential equations describe many physical phenomena in biology, chemistry, engineering, and physics. Often, these models involve small parameters that significantly influence the behaviour of the system, making it difficult to obtain exact solutions. When solving a mathematical model, we aim to capture the essential elements by retaining significant quantities and omitting negligible ones that involve small parameters. The model that includes these small parameters is the perturbed model, while the simplified degenerate model is the unperturbed or reduced model [1]. The mathematical problems associated with these models are further classified as regular and singular perturbation problems, as will be defined later. Perturbation techniques provide systematic approaches to finding approximate solutions by expanding them in terms of small parameters. Regular perturbation problems allow solutions to be expanded in a straightforward power series of the small parameter, maintaining smooth behaviour throughout the domain [2]. In the case of singular perturbations, things get more complicated. They involve rapid variations, such as boundary layers or multiple time scales, where standard expansions fail. The solution to the unper-

turbed problem does not satisfy, in general, all the original boundary conditions and/or initial conditions, as some of the derivatives may disappear by neglecting the small parameters [3, 4]. Thus, some discrepancies may appear between the solution of the perturbed model and the corresponding reduced model [5, 6].

Let Ω be an open bounded set with smooth boundary Γ and $\bar{\Omega}$ its closure. Consider the boundary value problem [1]

$$\mathscr{P}_\varepsilon : \mathscr{L}_\varepsilon y := \mathscr{L}_0 + \varepsilon \mathscr{L}_1 = g(x,\varepsilon);\ x \in \Omega \text{ and } y(\Gamma) \text{ is given.} \tag{1.1.1}$$

Here $0 < \varepsilon \ll 1$ is a small perturbation parameter, $\mathscr{L}_\varepsilon$ denotes the differential operator, and $g(x,\varepsilon)$ is a given real-valued smooth function. We assume that the perturbation problem $\mathscr{P}_\varepsilon$ possesses a unique smooth solution $y := y_\varepsilon(x)$ for each ε. Denote by $\mathscr{P}_0$ the corresponding degenerate problem obtained by setting $\varepsilon = 0$ in (1.1.1) and by y_0 a smooth solution of $\mathscr{P}_0$. The norm we use is the standard maximum norm defined as

$$\|f\|_{\bar{\Omega}} = \sup\left\{|f(x)| : x \in \bar{\Omega}\right\}.$$

Definition 1.1.1. The perturbation problem $\mathscr{P}_\varepsilon$ is regularly perturbed with respect to some norm $\|\cdot\|$ if there exist a solution $y_0(x)$ of the reduced problem $\mathscr{P}_0$ such that $\|y_\varepsilon - y_0\| \to 0$ as $\varepsilon \to 0$. Otherwise, $\mathscr{P}_\varepsilon$ is said to be singularly perturbed with respect to the same norm.

Example 1.1.1. Consider an initial value problem $\mathscr{P}_\varepsilon$:

$$y'(x) = 2y(x) - 4\varepsilon y^2(x),\ x \in (0,1);\ y(0) = 1.$$

The exact solution of $\mathscr{P}_\varepsilon$ reads

$$y(x) := y_\varepsilon(x) = \frac{e^{2x}}{2\varepsilon(e^{2x}-1)+1},\ 0 \le x \le 1.$$

It is easy to follow that $\lim_{\varepsilon\to 0} y_\varepsilon(x) = e^{2x} := y_0$. Also, note that y_0 is the solution to the reduced problem $\mathscr{P}_0$, obtained by setting $\varepsilon = 0$. Therefore, $\mathscr{P}_\varepsilon$ is a regular perturbation problem.

Example 1.1.2. Consider the two-point boundary value problem $\mathscr{P}_\varepsilon$:

$$\varepsilon^2 \frac{d^2y(x)}{dx^2} - y(x) = 0,\ x \in (0,1);\ y(0) = A,\ y(1) = B, \tag{1.1.2}$$

where ε is the small perturbation parameter. Then, corresponding to the large real roots $\pm 1/\varepsilon$ of the characteristic polynomial, the linearly independent solutions $e^{x/\varepsilon}$ and $e^{-x/\varepsilon}$ contribute to the exact solution that reads

$$\begin{aligned} y(x) &= \frac{-Ae^{-1/\varepsilon}+B}{e^{1/\varepsilon}-e^{-1/\varepsilon}}e^{x/\varepsilon} + \frac{Ae^{1/\varepsilon}-B}{e^{1/\varepsilon}-e^{-1/\varepsilon}}e^{-x/\varepsilon} \\ &= \frac{(2-e^{-1/\varepsilon})e^{x/\varepsilon} + (e^{1/\varepsilon}-2)e^{-x/\varepsilon}}{e^{1/\varepsilon}-e^{-1/\varepsilon}} \text{ for A=1 and B=2.} \end{aligned}$$

Note that the solution $y(x) := y_1(x)$ is defined for all $\varepsilon > 0$. Moreover, for some fixed constant $\rho \in (0,1)$

$$\lim_{\varepsilon \to 0^+} y_1(x) = 0,\ x \in [\rho, 1-\rho]. \tag{1.1.3}$$

However, the solution $y_1(x)$ attains the limiting value 0 non-uniformly in the neighborhood of $x = 0$ and $x = 1$ in the sense that

$$\lim_{\varepsilon \to 0^+} \lim_{x \to 0^+} y_1(x) = 1 \neq 0 = \lim_{x \to 0^+} \lim_{\varepsilon \to 0^+} y_1(x) \text{ and}$$

$$\lim_{\varepsilon \to 0^+} \lim_{x \to 1^-} y_1(x) = 2 \neq 0 = \lim_{x \to 1^-} \lim_{\varepsilon \to 0^+} y_1(x).$$

It is important to note that the limiting value 0 is a stable solution of the corresponding degenerate equation. Let us next consider an example having the same boundary conditions and a similar reaction term but with an opposite sign.

Example 1.1.3. Consider the two-point boundary value problem $\mathscr{P}_\varepsilon$:

$$\varepsilon^2 \frac{d^2y(x)}{dx^2} + y(x) = 0,\ x \in (0,1);\ y(0) = A,\ y(1) = B, \tag{1.1.4}$$

where ε is the small perturbation parameter. Then, corresponding to the large imaginary roots $\pm \imath/\varepsilon$ of the characteristic polynomial are the linearly independent solutions $\sin x/\varepsilon$ and $\cos x/\varepsilon$, and the exact solution of the problem reads

$$y(x) \quad = \quad \frac{A \sin(1-x)/\varepsilon + B}{\sin 1/\varepsilon} = \cos x/\varepsilon + \frac{2 - \cos 1/\varepsilon}{\sin 1/\varepsilon} \sin x/\varepsilon \text{ for } A = 1 \text{ and } B = 2.$$

It is apparent that the solution $y(x) := y_2(x)$ is defined only if $\varepsilon \neq 1/n\pi$; $n = 1, 2, \ldots$. The solution is highly oscillatory for arbitrary small ε with period ε and bounded amplitude.

For Example 1.1.2, Figure 1.1 illustrates the solution for different values of perturbation parameters and verifies that the solution exhibits a multiscale character. There are regions of small widths where the solution changes rapidly and exhibits steep gradients. Note that the corresponding degenerate problem cannot satisfy all the given boundary conditions. The problem is a singular perturbation problem, and the solution reveals layer behaviour. Whereas, for Example 1.1.3, it is immediate from Figure 1.2 that the solution to the problem is highly oscillatory and it cannot satisfy a limiting relation like (1.1.3). The problem is a singular perturbation problem from a mathematical perspective.

Example 1.1.4. Consider an initial value problem $\mathscr{P}_\varepsilon$:

$$\varepsilon \frac{dy}{dx} - z = \varepsilon g_1(x),\ \varepsilon \frac{dz}{dx} + y = \varepsilon g_2(x),\ 0 < x < 1;\ y(0) = 1,\ z(0) = 0,$$

where ε is the small perturbation parameter and $g_1(x),\ g_2(x) \in C[0,1]$. It is easy to note that the given problem is a singular perturbation problem but not of the boundary layer type. This conclusion is trivial in the case $g_1(x) = g_2(x) = 0$ when the solution of the given problem reads $y(x) = \cos x/\varepsilon$ and $z(x) = -\sin x/\varepsilon$.

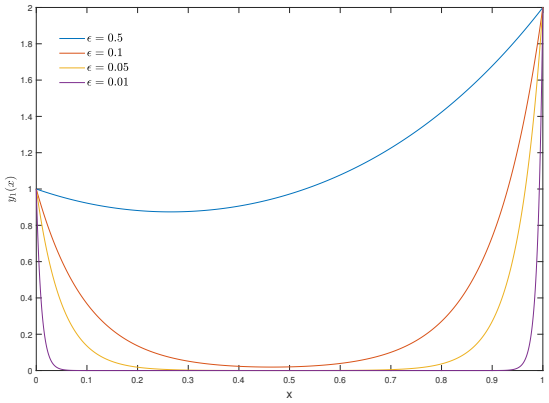

Fig. 1.1: Numerical solution of Example 1.1.2 for different values of ε.

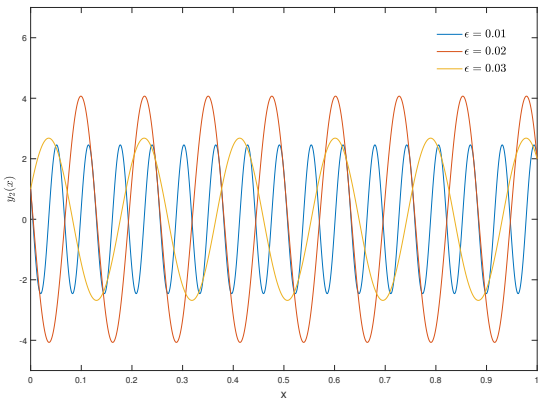

Fig. 1.2: Numerical solution of Example 1.1.3 for different values of ε.

Example 1.1.5. Consider an initial boundary value problem $\mathscr{P}_\varepsilon$:

$$\begin{cases} \varepsilon \dfrac{\partial y}{\partial t} - \dfrac{\partial^2 y}{\partial x^2} = t \sin x, \ (x,t) \in (0,\pi) \times (0,T), \\ y(x,0) = \sin x, \ x \in [0,\pi], \\ y(0,t) = 0 = y(\pi,t), \ t \in [0,T], \end{cases}$$

where ε is the small perturbation parameter and T is the given positive integer. The exact solution of the problem reads

$$y(x,t) := y_\varepsilon(x,t) = t \sin x + e^{-t/\varepsilon} \sin x + \varepsilon \left(e^{-t/\varepsilon} - 1 \right) \sin x.$$

It follows that the solution y_ε converges uniformly to the function $y_0(x,t) = t \sin x$ on every rectangle $R_\delta = \{(x,t) : 0 \le x \le \pi, \delta \le t \le T\}$, $0 < \delta < T$, but not on the entire domain. However, y_0 satisfies the reduced problem

$$-\frac{\partial^2 y}{\partial x^2} = t \sin x, \ y(0,t) = 0 = y(\pi,t), \ t \in [0,T]$$

it fails to be a uniform approximation of y_ε in the strip $S_\delta = \{(x,t) : 0 \le x \le \pi, 0 \le t \le \delta\}$. The problem is a singular perturbation problem of boundary layer type.

1.2 The D'Alembert's Paradox

In fluid dynamics, the d'Alembert paradox refers to the contradiction between theoretical predictions and real-world observations regarding drag forces in inviscid steady flows. Jean le Rond d'Alembert, an 18th-century mathematician and physicist, demonstrated that under the assumptions of ideal fluid theory - which neglects viscosity - a body moving in a steady potential flow should experience zero drag. However, everyday experience contradicts this result. When an object moves through a fluid, such as air or water, it experiences drag, a resistive force that opposes motion. The failure of ideal-fluid theory to predict this observed drag raised a fundamental question. Why does an object experience

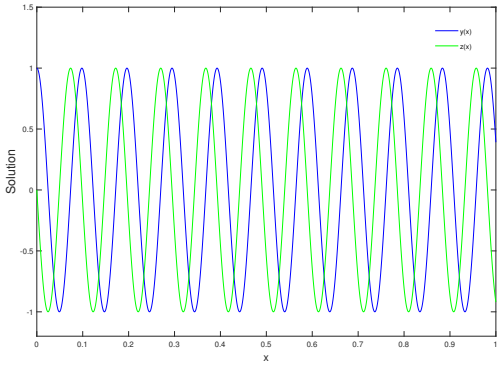

Fig. 1.3: Numerical Solution of Example 1.1.4 for $\varepsilon = 2^{-4}$.

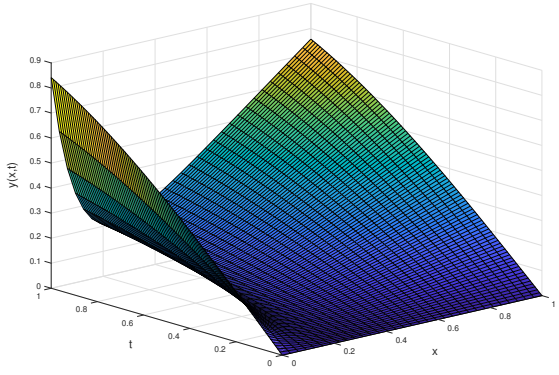

Fig. 1.4: Numerical Solution of Example 1.1.5 for $\varepsilon = 10^{-2}$.

resistance in a flow if classical hydrodynamics suggests otherwise?

This paradox was particularly puzzling because potential flow theory (which assumes an inviscid, incompressible, and irrotational fluid) produced elegant mathematical solutions that failed to capture the actual physics of fluid motion around solid bodies. The resolution of this paradox lies in recognising the role of viscosity, which the classical ideal fluid theory had ignored. The property of fluids that causes internal friction and the development of shear forces between layers of different velocities. Although viscosity is often small in common fluids such as air and water, its effects can be profound in specific flow regions [7, 8].

The impact of viscosity is best understood through the Reynolds number (Re), a dimensionless quantity given by $Re = \dfrac{\rho UL}{\mu}$ where ρ is the fluid density, U is the characteristic velocity of the flow, L is the characteristic length (such as the diameter of a sphere or chord length of an aerofoil), and μ is the dynamic viscosity of the fluid. The Reynolds number (Re) quantifies the ratio of inertial forces of a fluid to its viscous forces. At high values of Re, which is typical in air and water flows around practical objects such as aeroplanes, ships, or cars, the effects of viscosity may initially seem insignificant [9]. However, Ludwig Prandtl demonstrated that viscosity cannot be completely overlooked, as it plays a vital role in thin regions near solid surfaces known as boundary layers [8].

1.3 Prandtl's Resolution Using Boundary Layer Theory

The resolution to the d'Alembert paradox came in 1904 when Ludwig Prandtl introduced the ground-breaking boundary layer theory. Prandtl proposed that viscosity is confined to thin boundary layers near the surface in flows with high Re. Outside this layer, the flow remains largely inviscid. When a fluid flows past a solid body, the no-slip condition dictates that the velocity of the fluid at the surface must be zero relative to that of the body. However, the velocity gradually increases away from the surface until it matches the free-stream velocity. The region where this velocity transition occurs is the boundary layer. Prandtl's insight allowed for a two-region approach to fluid motion:

- The Outer Region (Potential Flow Region): Here, the viscosity is negligible, and the flow can be

approximated using ideal-fluid equations (Euler's equations).

- The Inner Region (Boundary Layer Region): Close to the solid surface, viscosity dominates, leading to significant velocity gradients and the development of shear stresses.

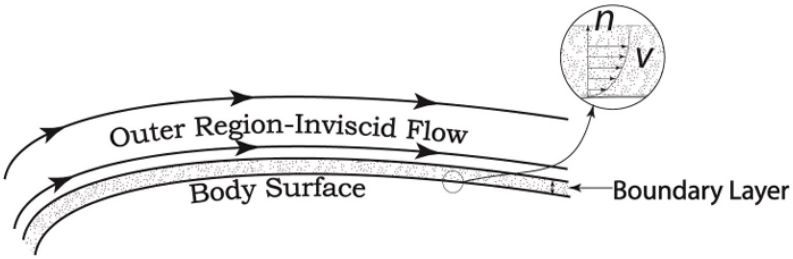

Fig. 1.5: Boundary layer concept.

Prandtl's theory provided a framework to explain how drag arises in real-world flows. In the case of streamlined bodies like aerofoils, the boundary layer remains attached, minimising drag. For bluff bodies, such as spheres and cylinders, the boundary layer tends to separate from the surface, creating a turbulent wake and resulting in pressure drag, which was not considered in the d'Alembert analysis [8]. This insight revolutionised fluid mechanics and laid the foundation for modern aerodynamics and hydrodynamics, enabling accurate predictions of drag forces and optimising designs in aviation, naval engineering, and other fluid-based applications. Beyond aerodynamics, boundary layer theory has become fundamental in various fields, including meteorology, oceanography, and biofluid mechanics.

The concept of boundary layers has also led to the singular perturbation theory, which addresses problems where small effects (such as viscosity) lead to significant consequences [7, 10, 3]. Singular perturbation problems are widespread in nature and arise in the modelling of various complicated phenomena such as in semiconductor devices [11], population dynamics [12], impulses and physiological states of nerve membrane [13], water quality problems in river networks [14], groundwater flow [15], theory of thin plates and shells [16], biochemical kinetics [17], electromagnetic field theory in moving media [18], modelling of option pricing and corporate liabilities [19], neuronal variability [20], simulation of oil extraction from underground reservoirs [21], Reissner-Mindlin plate theory [22], Fokker-Planck equation [23] and many more [7, 9, 24, 25, 26, 27, 10]. They have been extensively studied and applied, so it is pertinent to trace their historical developments.

1.4 Classification of Singular Perturbation Problems

De-Jager and Furu [28] classify singular perturbation problems as singular perturbations of the cumulative type and singular perturbations of the boundary layer type.

1. **Singular perturbation problems of cumulative type:** The class of singular perturbations of cumulative type concerns oscillating systems where the influence of the small parameter becomes observable only after a long time, for instance, after an interval of $\mathcal{O}(1/\varepsilon)$ [28]. In these

problems, the effects of the small perturbation parameter accumulate gradually over the entire domain. The solution changes slowly but significantly over the whole region rather than being localised in a specific part of the domain. A typical example occurs in multiple-scale problems, where a small perturbation affects long-term behaviour.

At the end of the 19th century, Lindstedt and Poincaré proposed the method of stretching the coordinate to obtain an asymptotic approximation of the solution to this type of problem in connection with their studies of perturbation problems in celestial mechanics [29, 30, 31]. The technique was later elaborated, refined, and applied by several others [2, 32]. Lagrange [33] first used the method of averaging and took an average of certain quantities that slowly varied over time. Gausz also employed an averaging principle in his study of the mutual influence of planets during their motion. He distributed each planet's mass over its orbit in proportion to time and replaced the planet's attracting force with that of a ring. Similarly, van der Pol [34] applied an averaging principle in his study of triode oscillations, neglecting terms with a zero average over the oscillation period. The method of averaging is widely known as the approach developed by Krylov, Bogoliubov, and Mitropolski [35], who proved the averaging principle and applied it to various problems. For a comprehensive discussion, we refer the reader to the book by Bogoliubov and Mitropolski [35], which includes numerous references to mathematicians and physicists who contributed to the asymptotic theory of nonlinear oscillations.

2. **Singular perturbation problems of boundary layer type:** The class of singular perturbations of boundary layer type involves systems where the presence of a small parameter leads to rapid changes in the solution in a localised region, usually near boundaries. Outside this region, the solution behaves more smoothly and is often approximated by a reduced problem. These problems frequently arise in fluid dynamics (e.g., boundary layers in high Re-flows). The term boundary layer, introduced by Prandtl, is in the context of fluid mechanics. They are also termed shock waves in gas motion, skin layers in electric applications, and Stokes surfaces in quantum mechanics and optics. In case the layers do not appear near the boundaries of the domain. The layers are termed interior layers or free layers. The interior layers arise in singular perturbation problems with turning points, nonsmooth coefficients, nonsmooth initial/boundary conditions, nonlinearities, and incompatibility at the domain's boundaries.

   Further, we distinguish these problems into two types: singular perturbations of the convection-diffusion type and reaction-diffusion type.

   (a) **Singularly Perturbed Convection-Diffusion Problems**: These problems involve convection (advection) and diffusion, where convection dominates certain regions. For example, a problem of the form

   $$-\varepsilon y''(x) + a(x)y'(x) + b(x)y(x) = g(x),\ x \in \Omega = (0,1);\ y(0) = y_0,\ y(1) = y_1. \qquad (1.4.1)$$

   The small parameter ε represents the diffusion coefficient, while the term $a(x)y'(x)$ represents convection. When ε is small, the convection term dominates, leading to the formation of boundary layers near the outflow boundaries.

(b) **Singularly Perturbed Reaction-Diffusion Problems**: These problems involve both reaction (source/sink terms) and diffusion, where reaction dominates in certain regions. For example, a problem of the form

$$-\varepsilon y''(x)+b(x)y(x)=g(x),\ x\in\Omega=(0,1);\ y(0)=y_0,\ y(1)=y_1.$$

The small parameter ε represents the diffusion coefficient, while the term $b(x)y(x)$ represents reaction. When ε is small, the reaction term dominates, leading to the formation of interior or boundary layers.

These problems model physical phenomena balancing three processes, namely, convection, reaction, and diffusion. Convection refers to the movement of a quantity (such as heat, mass, or momentum) owing to the bulk motion within a medium such as water or air. For example, in a river, pollutants are carried downstream by moving water. The term diffusion refers to the process by which particles spread from regions of high concentration to regions of low concentration. The reaction relates to the interaction process through which the substance is generated or consumed. Several physical and mathematical models of the convection-diffusion and reaction-diffusion problems have been mentioned in the literature, as some authors have referred to [36, 37, 38, 39, 40].

Example 1.4.1. Consider the following convection-diffusion problem $\mathscr{P}_\varepsilon$ [1]:

$$\varepsilon\frac{d^2y}{dx^2}+\frac{dy}{dx}=2x,\ 0<x<1;\ y(0)=0=y(1),$$

where ε is the small perturbation parameter. The solution of the problem $\mathscr{P}_\varepsilon$ reads

$$\begin{aligned} y(x):=y_\varepsilon(x) &= x(x-2\varepsilon)+\frac{2\varepsilon-1}{1-e^{-1/\varepsilon}}\left(1-e^{-x/\varepsilon}\right)\\ &= (x^2-1)+e^{-x/\varepsilon}+\chi_\varepsilon(x)\end{aligned}$$

where $\lim\limits_{\varepsilon\to 0}\chi_\varepsilon(x)=0$. The corresponding degenerate equation is of order one, and we can impose only one of the given boundary conditions. It is not immediately obvious which of the two possible boundary conditions we can impose. Note that y_ε converges uniformly to the function $y_0=(x^2-1)$ on every interval $[\delta,1];\ 0<\delta<1$, but not on the whole interval $[0,1]$. Clearly, y_0 satisfies the corresponding reduced problem $\mathscr{P}_0$ but $\|u_\varepsilon-u_0\|_{C[0,1]}\nrightarrow 0$ uniformly as $\varepsilon\to 0$. For small δ, y_0 is an approximation of y_ε in $[\delta,1]$, but it fails to be an approximation of y_ε in $[0,\delta]$. This small interval $[0,\delta]$ is the boundary layer region. In this region, y_ε exhibits a sharp change from its value $y_\varepsilon(0)=0$ to values close to y_0. A uniform approximation for $y_\varepsilon(x)$ is given by $y_0(x)+e^{-x/\varepsilon}$. The function $e^{-x/\varepsilon}$ is called a boundary layer function (correction). It fills the gap between y_ε and y_0 in the boundary layer region $[0,\delta]$. This behaviour of y_ε is called a boundary layer phenomenon, and the solution of the problem $\mathscr{P}_\varepsilon$ is said to have a boundary layer of the width $\mathscr{O}(\varepsilon)$ near $x=0$ as shown in Figure 1.6.

Example 1.4.2. Consider the following reaction-diffusion problem $\mathscr{P}_\varepsilon$:

$$\varepsilon\frac{d^2y(x)}{dx^2}-y(x)=0,\ x\in(0,1);\ y(0)=1,\ y(1)=2,$$

where ε is the small perturbation parameter. The solution of the problem $\mathscr{P}_\varepsilon$ reads

$$y(x) := y_\varepsilon(x) = \frac{2-e^{-1/\sqrt{\varepsilon}}}{1-e^{-2/\sqrt{\varepsilon}}}e^{-(1-x)/\sqrt{\varepsilon}} + \frac{1-2e^{-1/\sqrt{\varepsilon}}}{1-e^{-2/\sqrt{\varepsilon}}}e^{-x/\sqrt{\varepsilon}}.$$

The corresponding degenerate equation is of order zero, and we cannot impose any of the given nonzero boundary conditions. A similar analysis as in the previous example suggests that the solution of the problem $\mathscr{P}_\varepsilon$ has two boundary layers of width $\mathscr{O}(\sqrt{\varepsilon})$ near $x = 0$ and $x = 1$ as shown in Figure 1.7. Moreover, $e^{-x/\sqrt{\varepsilon}}$ and $e^{-(1-x)/\sqrt{\varepsilon}}$ are the corresponding layer correction functions, respectively.

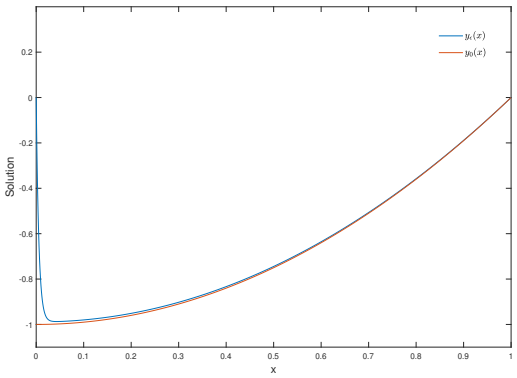

Fig. 1.6: Solution of Example 1.4.1 for $\varepsilon = 2^{-8}$.

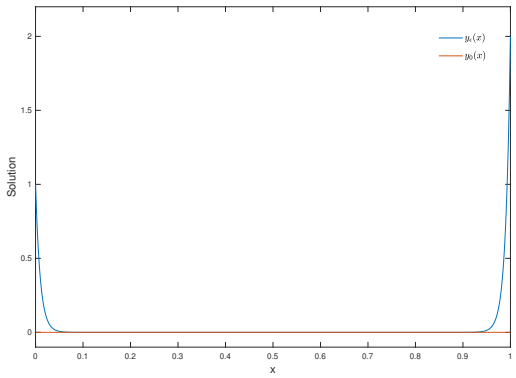

Fig. 1.7: Solution of Example 1.4.2 for $\varepsilon = 2^{-8}$.

The characteristics of the layers, such as their strength, width, and location, depend on whether the problem is of convection-diffusion or reaction-diffusion type. The coefficients and initial/boundary conditions specified in the problem also influence these characteristics. Information about the strength and location of the interior/boundary layers can be inferred from Table 1.1 and Table 1.2 for convection-diffusion and reaction-diffusion problems, respectively.

Table 1.1: **Strength and location of boundary and interior layers in convection-diffusion problems.**

Smoothness of functions			**Value of the function**	**Strength and location of**	
$b(x)$	$a(x)$	$g(x)$	$a(x)$	**Boundary Layer**	**Interior Layer**
Smooth			$<0, \forall x \in \overline{\Omega}$	Strong, at $x=0$	—
Smooth			$>0, \forall x \in \overline{\Omega}$	Strong, at $x=1$	—
Smooth		Discontinuous at $x=d \in \Omega$	$<0, \forall x \in \overline{\Omega}$	Strong, at $x=0$	Weak, on right side of $x=d$
Smooth		Discontinuous at $x=d \in \Omega$	$>0, \forall x \in \overline{\Omega}$	Strong, at $x=1$	Weak, on left side of $x=d$
Smooth	Discontinuous at $x=d \in \Omega$		$<0, \forall x \in \overline{\Omega}$	Strong, at $x=0$	Weak, on right side of $x=d$
Smooth	Discontinuous at $x=d \in \Omega$		$>0, \forall x \in \overline{\Omega}$	Strong, at $x=1$	Weak, on left side of $x=d$
Smooth	Discontinuous at $x=d \in \Omega$		$>0, x \in (0,d)$ and $<0, x \in (d,1)$	—	Strong, on both side of $x=d$
Smooth	Discontinuous at $x=d \in \Omega$		$<0, x \in (0,d)$ and $>0, x \in (d,1)$	Solution is unbounded	
—			$=0$	Problem is of reaction-diffusion type	

This thesis aims to explore and address singular perturbation problems, specifically those of the

Table 1.2: **Strength and location of boundary and interior layers in reaction-diffusion problems.**

Smoothness of functions		**Strength and location of**	
$b(x)$	$g(x)$	**Boundary Layer**	**Interior Layer**
Smooth		Strong, at both endpoints $x = 0$ and $x = 1$	—
Smooth	Discontinuous at $x = d \in \Omega$	Strong, at both endpoints $x = 0$ and $x = 1$	Strong, on both sides of $x = d$

boundary layer type.

1.5 Methods for Solving Singular Perturbation Problems

The theory of singular perturbations has been with us for more than a century. Prandtl started research on boundary layers in 1904. However, this work remained confined mainly to his institute in Göttingen for the first twenty years. It was not until his Wilbur Wright Memorial Lecture to the Royal Aeronautical Society in 1927 that the research gained wider recognition. In the 19^{th} century, A.N. Tikhonov [41, 42, 43] began to systematically study singular perturbations, although there had been some previous attempts in this direction [1, 28]. The name of H. Schlichting first appeared in 1930 with his doctoral thesis on wake flow. Shortly thereafter, Schlichting devoted significant effort to the problem of the stability of laminar boundary layer flow. Subsequent research soon confirmed the theory of stability described in the papers of Tollmien and Schlichting quantitatively and qualitatively [7]. However, the aerodynamic boundary layer was first defined by Prandtl [8]. The term singular perturbation was first used in the work of Friedrichs and Wasow [44], and the concept of the boundary layer was given greater generality in the substantial work of Wasow [45].

Many studies have focused on the mathematical justification of boundary layer theory. Studies indicate that this theory offers a first approximation within a broader framework intended for calculating the asymptotic expansions of solutions to the complete equations of motion. The problem is effectively transformed into a singular perturbation problem and solved using the method of matched asymptotic expansions. M. Van Dyke has provided a comprehensive overview of perturbation techniques in fluid mechanics [24]. In 1954, S. Kaplun studied the role of coordinate systems in boundary layer theory [46]. In 1957, in a fundamental paper [47], M.I. Vishik and L.A. Lyusternik studied linear PDEs with singular perturbations, introducing the famous method, which is today called the Vishik-Lyusternik method. It became clear that the boundary layer theory developed heuristically by Prandtl was a classic example of the solution of a singular perturbation problem. From then on, the entire literature has been devoted to this subject [48, 49, 50, 51, 52].

Despite this long history, the subject is still in a state of vigorous development. Numerous methods have been proposed to solve singular perturbation problems and are broadly classified into asymptotic and numerical methods.

1.5.1 Asymptotic Methods

Asymptotic methods for singular perturbation problems constitute a robust mathematical framework for analysing and approximating solutions to differential equations in which small parameters significantly influence the behaviour of the system. Over the years, researchers have developed various asymptotic techniques to systematically address these problems, facilitating the construction of uniformly valid approximations across different regions of the solution domain.

One of the most widely used methods is the method of matched asymptotic expansions, which partitions the domain into distinct regions, typically termed inner and outer regions. Asymptotic approximations are constructed within each region and matched to ensure a smooth transition between them. The technique begins by dividing the problem domain into an outer region, where a regular perturbation expansion (e.g. $y_{outer}(x) = y_0(x) + \varepsilon y_1(x) + \ldots$) captures the slowly varying behaviour, and an inner region, where a rescaled coordinate (e.g. $\xi = x/\varepsilon$) magnifies the rapid transition, yielding an inner expansion (e.g. $y_{inner}(\xi) = Y_0(\xi) + \varepsilon Y_1(\xi) + \ldots$). These expansions are developed independently, often solving simplified versions of the original equation tailored to each region. The critical step, matching, ensures consistency by equating the inner and outer solutions in an intermediate region where their domains overlap, using rules like van Dyke's principle to determine constants or functions. This method shines in applications like fluid dynamics, where it models boundary layers in flows with high Re or in resolving sharp gradients near boundaries. However, it has limitations such as determining the correct scaling for the inner region requires insight into the problem's physics, matching can become algebraically complex for higher-order terms, and the method assumes a clear separation of scales, which may not hold in highly nonlinear or chaotic systems. Furthermore, it provides only asymptotic (not exact) solutions, potentially missing subtle effects such as $\varepsilon \to 0$, and may fail near singularities or turning points unless supplemented by other techniques. Despite these challenges, matched asymptotic expansions remain a powerful tool for bridging multiscale phenomena with analytical clarity. During the 1950s, this method was refined and applied to numerous physical problems [53, 54, 46, 55, 56, 57, 47]. For a detailed overview, the reader can refer to the books [24, 58, 59].

The method of multiple scales is another powerful asymptotic technique to analyse problems where different time or spatial scales coexist. It is particularly useful for handling singular perturbation problems in dynamical systems, wave propagation, nonlinear oscillations, and fluid mechanics. The methodology begins by recognising that the solution operates on distinct time or spatial scales, typically a fast scale that captures rapid oscillations or transitions, and a slow scale that describes gradual evolution. To apply the method, multiple independent variables are introduced, such as t (fast time) and $\tau = \varepsilon t$ (slow time). The dependent variable is then expanded as an asymptotic series, e.g., $y(t,\varepsilon) = y_0(t,\tau) + \varepsilon y_1(t,\tau) + \varepsilon^2 y_2(t,\tau) + \cdots$, and substituted into the original equation. By treating the scales as independent, the partial derivatives transform $\left(\text{e.g.} \dfrac{d}{dt} = \dfrac{\partial}{\partial t} + \varepsilon \dfrac{\partial}{\partial \tau}\right)$, and the equation is separated into a hierarchy of problems by equating coefficients of similar powers of ε. Secular terms, unbounded growth that invalidates the perturbation expansion, are eliminated by imposing solvability conditions, yielding equations that govern slow-scale behaviour. The benefits of this approach include

its ability to capture multiscale phenomena, provide uniformly valid approximations over long intervals, and avoid the breakdown of naive perturbation methods. However, it requires careful identification of the relevant scales, can become computationally intensive for higher-order terms, and may fail if the scales are not well separated or if the problem lacks a clear asymptotic structure [60], necessitating alternative techniques such as matched asymptotic expansions. The method has been used to solve numerous singular perturbation problems in [61, 62, 63, 64, 65, 66, 67, 68].

The Wentzel-Kramers-Brillouin method is a semiclassical approximation technique widely used to solve singular perturbation problems, particularly in linear differential equations with a small parameter, such as those arising in quantum mechanics, wave propagation, and optics. The methodology assumes that the solution takes an exponential form, $y(x) = A(x)\exp\left(\frac{1}{\varepsilon}S(x)\right)$, where ε is the small parameter, $S(x)$ is the phase (or action), and $A(x)$ is the amplitude, both of which vary slowly compared to the rapid oscillations driven by $\frac{1}{\varepsilon}$. Substituting this ansatz into the differential equation, the terms are collected by powers of ε, leading to the eikonal equation for $S(x)$ (zeroth order) and a transport equation for $A(x)$ (first order). For example, in $y'' + \frac{1}{\varepsilon^2}q(x)y = 0$, the eikonal equation becomes $(S')^2 = q(x)$, so $S(x) = \int \sqrt{q(x)}\,dx$, and the amplitude is adjusted to conserve energy or probability flux. The method excels in providing approximate solutions in regions where $q(x)$ varies slowly, offering physical insight into wave behaviour and being computationally simpler than numerical methods for high-frequency problems. The method provides critical insights into the behaviour of solutions in different regions, distinguishing between oscillatory and exponentially decaying solutions depending on whether the potential function is positive or negative. However, limitations arise near turning points and Stokes lines, causing the approximation to break down due to singularities in $A(x)$, requiring connection formulas (e.g. Airy functions) to bridge regions. Furthermore, the method assumes that the solution varies rapidly compared to the problem's characteristic scale, making it less effective for problems with slow variations. Despite these challenges, the method remains a cornerstone of asymptotic analysis for singular perturbation problems. The method was first used in the 1920s to approximate solutions to the Schrödinger equation. Its historical development is documented in [69], while a comprehensive discussion of its mathematical foundations can be found in [70]. Applications of the method in quantum mechanics and solid mechanics are presented in [71] and [72], respectively. For a detailed overview, the reader may refer to [73, 74, 75].

Other significant asymptotic techniques include the homogenisation method, which addresses problems involving multiple spatial scales, such as composite materials and periodic structures [76, 77]. The Lindstedt-Poincaré method eliminates secular terms in perturbative expansions for periodic solutions in dynamical systems [78, 79, 80, 81, 82, 83]. In contrast, the renormalisation group method provides a robust framework to analyse scaling behaviours and self-similarity in singular perturbation problems [84]. The method of strained coordinates improves the perturbation approximations by modifying independent variables [85]. The Brillouin-Kramers-Wentzel method, a variant of the Wentzel-Kramers-Brillouin approach, is particularly effective in wave phenomena. The exponential asymptotic approach extends traditional asymptotic series to capture exponentially minor effects that standard asymptotic expansions often overlook. In addition, modern approaches include geometric singular

perturbation theory [86, 87, 88], which offers a geometric framework for analysing slow-fast dynamical systems, and hyperasymptotics, which refines conventional asymptotic series by incorporating higher-order corrections for exponentially small terms. Additional techniques, such as boundary function and stretched coordinate methods, further improve asymptotic approximations for problems characterised by sharp transitions [89, 90, 91]. For a comprehensive overview of the advances in the asymptotic theory of singular perturbations, see [92, 93, 60, 3].

The primary advantage of asymptotic methods is their ability to provide analytical insight into complex multiscale phenomena. They reveal the dominant physical mechanisms and their dependence on the small perturbation parameter, often yielding simpler expressions that guide further analysis or computation. However, challenges include determining the correct scaling for inner regions, ensuring proper matching, and handling higher-order terms, which can become algebraically intensive. Additionally, these methods may not capture all nonlinear effects or singularities in highly complex systems.

1.5.2 Numerical Methods

Numerical methods for differential equations are computational techniques used to approximate solutions to problems when analytical solutions are difficult or impossible to obtain. During the past few decades, many numerical methods have been developed to solve singular perturbation problems [3, 5, 4, 51]. We distinguish numerical methods into finite difference, finite element, and finite volume methods.

Finite difference methods (FDMs) are numerical techniques for solving differential equations by approximating derivatives with finite differences on a discrete grid [94, 95, 96]. By approximating derivatives using discrete differences, FDM transforms complex differential equations into algebraic systems that can be solved computationally. FDM offers several benefits, including simplicity of implementation, ease of handling various boundary conditions, and flexibility in adapting to different types of ordinary and partial differential equations. Furthermore, FDM allows for efficient computational solutions, especially when combined with modern techniques and computing power. At the same time, finite element methods (FEMs) are also versatile and widely used numerical techniques to solve differential equations [97, 98, 99]. The core idea of FEM involves dividing the problem domain into smaller, simpler subdomains called finite elements (such as triangles or quadrilaterals in 2D), over which local basis functions approximate the solution. These local approximations are then assembled into a global system of equations that models the entire problem [100, 101, 102, 103]. The method is especially powerful for handling complex geometries, irregular domains, and boundary conditions. It is significant for its flexibility, accuracy, and adaptability. It allows for mesh refinement in regions where the solution exhibits rapid changes, such as boundary layers or singularities, making it particularly useful for singularly perturbed problems. Compared to FDM, FEM offers greater flexibility in mesh design and can handle more easily irregular geometries and variable coefficients. Although FDM is often simpler to implement and computationally faster for problems on regular grids, FEM provides higher accuracy and better convergence properties for complex real-world problems. Finite volume methods (FVMs) are also widely used for solving differential equations, especially those governing conservation laws [104,

105, 106]. The FVM builds on the conservation principle as its core idea. The idea of FVM involves dividing the domain into a finite number of control volumes and integrating the governing equations over each volume. The divergence theorem converts volume integrals into surface integrals and ensures that the method accurately accounts for the fluxes entering and leaving each control volume. This local conservation property makes FVM particularly suitable for problems in computational fluid dynamics. It is significant for its ability to naturally enforce conservation laws, handle complex geometries, and provide stable and accurate solutions, even on unstructured meshes. Compared to FDM, FVM offers better conservation and can handle irregular geometries more effectively. In contrast to FEM, which is based on variational principles and is highly effective for problems involving complex geometries and material properties, FVM is more naturally suited to conservation-based problems. FEM typically provides higher-order accuracy and is preferred in structural and solid mechanics, whereas FVM is the method of choice in fluid dynamics and related fields.

Standard numerical methods on a uniform mesh fail to approximate the solution of singularly perturbed problems accurately. These methods require the mesh size and perturbation parameter to be of the same order of magnitude to maintain the approximation. However, such a fine mesh would unexpectedly increase the mesh points and the associated computational cost. The stable upwind difference scheme on a uniform mesh is only first-order uniformly convergent in the discrete maximum norm. The formally second-order convergent central difference scheme oscillates in domains where the perturbation parameter is small compared to the local step size [4]. In fact, for problems with a strongly asymmetric differential operator, the usual discretisations are either unstable, inaccurate, or direction-dependent. For example, the higher-order accurate differences based on Petrov-Galerkin weighting are strongly direction-dependent because they depend on the equation's flow direction. Symmetric schemes, such as the FDM or the usual Galerkin methods with symmetric weighting functions, are unstable or only first-order accurate [4, 1]. Researchers propose many ways to overcome these difficulties. However, if we are looking for a reliable and direction-independent discretisation, none of the available methods seems appropriate. An essential challenge in the numerical solution of the singular perturbation problem is the different approximations required in the smooth part of the solution and the boundary and/or interior layers.

This discrepancy has encouraged researchers to develop parameter-uniform numerical methods in which the discretisation error and the order of convergence are independent of the perturbation parameter. In addition, layer-adapted meshes appear promising in the discretisation of such equations [5], leading to a growing interest in adaptive mesh refinement techniques. Adaptive mesh refinement techniques automatically increase the mesh resolution in regions where it is needed most, such as near steep gradients or boundary layers, while maintaining coarser grids in smoother areas [1, 5]. The adaptive approach not only enhances the accuracy of the solution, but also reduces computational costs by concentrating computational resources where they are most needed. As a result, adaptive meshes enable more efficient and accurate simulations of singularly perturbed systems, making them indispensable tools for researchers and practitioners studying these complex phenomena [5, 1]. Researchers often classify these meshes into a priori meshes and posterior meshes. A priori mesh refinement typically relies on analytical considerations or prior knowledge of the problem's characteristics,

such as the location and width of the layers. These meshes are particularly useful when the problem's features are well understood or when computational resources are limited. A posteriori mesh refinement, on the other hand, involves dynamically adjusting the mesh resolution during or after the solution process based on error estimates or solution properties. Initially proposed by Bakhvalov [107], these meshes have since been extensively studied, particularly in the context of convection-diffusion problems. Notable contributions include Shishkin's piecewise equidistant meshes [5], meshes employing the equidistribution principle [108, 109, 110], Gartland-type meshes [111], Bakhvalov-Shishkin meshes [111], and Vulanović improved Shishkin meshes [112]. Further advances have led to the development of layer-adapted meshes through recursive formulations, such as Gartland-Shishkin meshes and graded meshes analysed in various studies [113, 114, 115, 116, 117, 118, 119, 120] and references therein.

In 1968, Pearson [121] was the first to develop a three-point difference scheme on a uniform mesh for one-dimensional singularly perturbed boundary value problems (SPBVPs). The approach involved identifying mesh locations where the difference between the computed solution and its neighbouring value exceeded a predetermined threshold value. An iterative procedure was used to increase the concentration of mesh points at these locations and smoothing was applied to prevent loss of accuracy due to abrupt changes in mesh spacing. The Gauss elimination method was applied to solve the linear algebraic equations formed by the difference scheme. The numerical results obtained indicate that the computed solution converges to the exact solution. Later, this method was extended to solve a class of nonlinear problems [122]. In this case, the algebraic equations formed by the difference scheme were solved using the Newton-Raphson iterative method. These methods require strict constraints on the spacing of the mesh to maintain stability when the perturbation parameter is very small [123]. The authors in [124] introduced an upwind scheme to overcome this stability issue. In this scheme, the first derivative is replaced by a one-sided difference (forward or backward) instead of the central difference. The choice of forward or backward difference depends on the sign of the coefficients of the convection term at a particular mesh point. This scheme is known as the Il'in-Allen-Southwell scheme [125]. The upwind scheme provides stability and exhibits better convergence compared to the central difference scheme. The scheme under consideration is widely recognised as the first fitted operator scheme. However, it is important to note that it exhibits only a first-order uniform convergence in the outer region.

In [126], a class of singularly perturbed problems is solved using an upwind FDM. The author compared the asymptotic behaviour of the solution obtained from the difference scheme with the exact solution. Later, the authors extended this method to solve second-order ODEs [127]. They obtained elementary estimates for the solution and its derivatives using the maximum principle [128]. In [129], the upwind method is further refined and used to solve a singularly perturbed system of equations. In this method, a parameter was introduced in the difference equation, and it was chosen in such a way that an accurate approximation for the reduced problem is obtained in the interior region as well. Later, this method was extended to solve singular perturbation problems with internal turning points [130]. The author in [131] applied three-point difference schemes to singular perturbation problems without turning points. They used three finite difference operators L_h^1, L_h^2, and L_h^3 on a uniform mesh to

approximate the solution [132, 130, 124]. The operator L_h^1 achieves first-order accuracy with an error of order h. The error bounds for L_h^2 and L_h^3 include a term $\frac{h^2}{(h+\varepsilon)}$. This term shows that the convergence order drops by one as ε approaches zero. These methods show second-order convergence in the outer region, but only first-order convergence in the layer region.

In [133], the exponential box scheme was introduced to solve singularly perturbed convection-diffusion problems. This scheme combined the exponential difference operator with the Keller box scheme [134] to achieve a stable and second-order accurate approximation of the solution. In [135], the authors proved that applying the exponential difference scheme [133] on a uniform mesh yields uniform second-order accurate results for convection-diffusion problems. Their findings demonstrated that the exponential box scheme maintains consistent second-order accuracy across the entire domain. In [136], the authors modified the upwind scheme to enhance its precision for convection-dominated diffusion problems. This modified scheme achieved second-order accuracy, similar to the central difference scheme, while preserving the stability properties of the upwind scheme. This modification improved the accuracy of the solution and provided better convergence properties.

In [137], the author introduced a scheme based on the integral interpolation method [138] to solve singular perturbation problems involving ordinary and parabolic differential equations. He developed the scheme on a mesh similar to the Bakhvalov mesh. He demonstrated third-order pointwise convergence for ODEs and first-order convergence for parabolic PDEs. In the same year, in [139], the authors extended the Bakhvalov mesh for the discretisation of one-dimensional nonlinear singularly perturbed reaction-diffusion problems. His generalisation enabled the mesh to handle nonlinear problems effectively and achieved uniform second-order convergence, thereby improving the accuracy of the numerical solution. In [140], the author developed a family of uniformly accurate FDMs for singularly perturbed convection-diffusion problems using high-order differences within the identity expansion framework proposed in [141] and [142]. Their error analysis relies on the stability results of an earlier study [143]. Theoretical analysis demonstrates that uniform convergence of any order could be achieved, depending on the smoothness of the input data. However, the numerical results showed a fourth-order uniform convergence. It is important to note that achieving such higher-order convergence requires additional evaluations of the problem data.

In [144], the author demonstrated that, for convection-diffusion problems, a fitted finite-difference operator is necessary only in the layer region. The standard fitted operator accurately approximates the solution in the outer region, improving computational efficiency by reducing the cost outside the layer. In [145], the author investigated a variety of FDMs to derive sufficient conditions for uniform convergence. These conditions are satisfied not only by uniformly convergent schemes but also by a more general class of upwind schemes. In [111], an exponentially graded mesh was employed for singularly perturbed two-point boundary value problems. The mesh divides the computational domain into three regions: an inner region with a highly refined mesh, a transition region where the mesh grading transitions from fine to coarse, and an outer region with a uniform mesh. The number of mesh points in the inner region was significantly greater than in the outer region. However, the construction of such graded meshes proved complex, making it difficult to extend them to higher dimensions. To

address this limitation, Shishkin [146] proposed a simpler and more adaptable mesh, now known as the Shishkin mesh. For convection-diffusion problems, he introduced a piecewise uniform mesh with a transition point τ defined as $\tau = \min(1/2, \varepsilon\tau_0 \ln N)$, where $\tau_0 \geq p/\alpha$ and p characterise the order of convergence of the numerical scheme. The mesh $\bar{\Omega}^N = \{x_i\}_{i=0}^N$ is constructed by dividing the domain into two subintervals, $[0,\tau]$ and $[\tau,1]$, each with $N/2$ equally spaced points, assuming a boundary layer near the left endpoint. If $\varepsilon\tau_0 \ln N > 1/2$ (that is, for sufficiently large N relative to $1/\varepsilon$), the mesh becomes uniform. Similarly, if the boundary layer occurs near the right endpoint, we divide the domain into two subintervals $[0,1-\tau]$ and $[1-\tau,1]$, each with equally spaced points $N/2$, yielding a uniform mesh in parts. For reaction-diffusion problems, the transition parameter τ is defined as $\tau = \min(1/4, \sqrt{\varepsilon}\tau_0 \ln N)$, where $\tau_0 \geq p/\beta$. In this case, the domain $\bar{\Omega} = [0,1]$ is divided into three subintervals $[0,\tau]$, $[\tau,1-\tau]$, and $[1-\tau,1]$, with mesh points $N/4$, $N/2$, and $N/4$, respectively. It is important to note that a key limitation of the Shishkin mesh is its reliance on prior knowledge of the location and width of the boundary layers. In [147], the author analysed a defect correction method for one-dimensional convection-diffusion problems without turning points and demonstrated that the kth approximation converges uniformly at a rate of $\mathscr{O}((\varepsilon_0-\varepsilon)^k + h^2)$, where $\varepsilon_0 = \mathscr{O}(h)$ in the outer region, although the error deteriorates to $\mathscr{O}(1)$ in the inner layers.

In [148], the authors introduced a spline difference scheme on a nonuniform mesh for singularly perturbed self-adjoint reaction-diffusion problems. The scheme offers flexibility and accuracy through spline interpolation for problems with unknown or complex layer structures. In [149], the authors proposed a two-level nonlinear difference scheme to solve semilinear parabolic problems with parabolic boundary layers. Using a specially designed nonuniform mesh, they achieved uniform convergence across the entire domain. In [150], the authors developed an exponentially fitted difference scheme for singularly perturbed fourth-order elliptic boundary value problems. In [151], the authors applied quadratic splines on a piecewise Shishkin-type mesh to discretise reaction-diffusion problems and achieved near-second-order accuracy in the discrete maximum norm. In [152], the authors addressed stability issues in singular perturbation problems by employing a Bakhvalov-type nonuniform mesh with a cubic spline difference scheme. They achieve second-order uniform convergence with results superior to those obtained using the Shishkin mesh. The same year, the author in [153] developed a second-order optimal spline difference scheme using exponential cubic splines for two-point self-adjoint SPBVPs. In [154], a nonlinear problem is the subject of investigation. The authors employed a quasi-linearisation technique to linearise the nonlinear equation. They used a cubic spline difference scheme on a variable mesh to approximate the linear equations. Continuing their work, the authors in [155] developed an exponentially fitted difference scheme using a compression spline to solve singularly perturbed two-point boundary value problems.

In [156], the authors proposed an improved numerical method for singularly perturbed two-point boundary value problems with Neumann boundary conditions by incorporating asymptotic approximations into a finite-difference framework. They have provided uniform error estimates accompanied by rigorous theoretical analysis. In [157], they extended their work to singularly perturbed turning point problems with twin boundary layers. They combined exponentially fitted difference schemes with classical numerical methods to improve computational efficiency and accuracy. In [158], the author

introduced an a posteriori mesh that does not require prior information on the width or location of the solution layers. The method first computes an approximate solution on an arbitrary mesh. Then, it uses an error estimate based on the derivatives of this solution to determine a monitoring function. This monitor function facilitates mesh equidistribution. The authors in [159] proposed a monitor function that combines a constant term with a suitable power of the second-order derivative of the singular component of the solution. An arc-length monitor function is used in [160, 161] to achieve mesh equidistribution for convection-diffusion problems. In [162], the author presented numerical methods based on exponential finite difference approximations with h^4 accuracy for one-dimensional and two-dimensional convection-diffusion problems. In [163], the author presented a survey on layer-adapted meshes for convection-diffusion problems, emphasising the importance of using appropriate grids to achieve uniform convergence.

In [164], the authors considered a one-dimensional steady-state convection-diffusion problem with Robin boundary conditions. To discretise the problem, they use standard upwind finite-difference operators on Shishkin meshes. Furthermore, the authors in [165] developed an FDM to solve a one-dimensional time-dependent convection-diffusion problem with initial boundary conditions. They employed the classical Euler implicit method for time discretisation and the simple upwind scheme on a Shishkin mesh for spatial discretisation. In [166], the authors present an adaptive FDM to solve singularly perturbed convection-diffusion problems. The authors combined a first-order upwind scheme with a second-order central difference scheme to achieve higher-order convergence. In [167], the author discretised a singularly perturbed convection-diffusion problem using a simple first-order upwind difference scheme on general meshes. He derived an expression of the error of the scheme, which enables uniform error bounds concerning the perturbation parameter in the discrete maximum norm for both defect correction methods and the Richardson extrapolation technique. In [168], the authors considered a class of singularly perturbed self-adjoint two-point boundary value problems. They employ a fitted FDM on a Shishkin mesh to solve the problem by reducing it to a normal form. The authors in [169] proposed a nonstandard FDM to solve self-adjoint SPBVPs using Micken's FDM. In [170], the authors combine a simple upwind scheme and the central difference scheme on a Shishkin mesh. The proposed scheme exhibited higher-order convergence compared to the simple upwind scheme alone.

In [171], the authors used a compression spline to generate second-order and fourth-order uniformly convergent numerical techniques for SPBVP. To deal with Robin-type boundary conditions, the authors in [172] applied the central difference method on the regular region and cubic splines in the layer region. In [173], the authors investigated the effect of Richardson extrapolation on two fitted operator FDM, namely FOFDM-I [168] and FOFDM-II [169]. They found that FOFDM-I achieved fourth-order accuracy for moderate values of the perturbation parameter, while it is second-order accurate for small values of the perturbation parameter. Further, it was observed that Richardson extrapolation did not improve the order of convergence for FOFDM-I. However, for FOFDM-II, which is uniformly second-order convergent, one can enhance the order of convergence to the order of four. In [174], the author proposed a compact fourth-order FDM for singularly perturbed reaction-diffusion problems on a Shishkin mesh. The authors in [175] applied exponential splines to generate an almost second-order uniformly convergent difference scheme on a Shishkin mesh for semi-linear reaction-diffusion problems. The

method exhibits a uniform convergence of almost second order in the discrete maximum norm. Later, they devised an exponential spline difference method on a piecewise uniform Shishkin mesh [176].

In [177], the authors proposed a numerical method to solve singularly perturbed time-dependent convection-diffusion problems in one spatial dimension. They employed a semi-discretisation technique followed by the backward Euler method in the temporal direction. To discretise the resulting set of ODEs, they utilised the midpoint upwind FDM on a nonuniform mesh of Shishkin type in the spatial direction. In [178], the authors proposed a method that combines domain decomposition with higher-order difference discretisation to solve singularly perturbed two-point convection-diffusion problems. In [179], the authors used the same scheme combination as in [172] on an equidistributed grid. Their approximation scheme uses cubic splines for the mixed-boundary conditions and the classical central scheme elsewhere. In [180], the authors considered a singularly perturbed reaction-diffusion problem dependent on time. They employ the classical backward Euler method to discretise the problem in time and a fitted operator FDM in space. In [181], the authors proposed a classical upwind FDM on layer-adapted nonuniform meshes to solve the singularly perturbed parabolic convection-diffusion problem. In [182], the authors proposed a uniformly convergent FDM for a coupled system of singularly perturbed problems. The proposed discrete operator satisfies the stability property in the maximum norm. In [183], the authors proposed an adaptive FDM using the central difference scheme on a layer-adapted mesh for a linear second-order SPBVP. The proposed method has fourth-order convergence. In [184], the authors considered singularly perturbed degenerate parabolic convection-diffusion problems in two dimensions. They used an alternating-direction implicit FDM to discretise the time derivative and an upwind FDM to discretise the spatial derivative.

In [185], the authors introduced a hybrid difference scheme to solve singularly perturbed convection-diffusion problems. Their scheme combined the upwind scheme on the coarse part of the Shishkin mesh with the central difference method on the fine part. In [186], the authors considered a singularly perturbed fourth-order differential equation with a turning point. A classical FDM on an appropriate piecewise uniform Shishkin mesh is used to solve the problem. In [187], the authors proposed a second-order uniformly convergent numerical method for a singularly perturbed parabolic convection-diffusion problem in two dimensions. They used a fractional step method in the time direction, while FDM was used in the spatial direction. In [188], a higher-order Richardson extrapolation scheme is presented to solve a singularly perturbed system of parabolic convection-diffusion problems. In [189], the authors proposed a uniformly convergent FDM to solve singularly perturbed time-dependent convection-diffusion problems. The method uses FOFDM to discretise the spatial derivatives, followed by the Crank–Nicolson method for the time derivative. Moreover, Richardson extrapolation is performed in space to improve the accuracy of the method. In [190], a linear singularly perturbed parabolic reaction-diffusion problem with incompatible initial and boundary data is considered. The method combines the computational solution of a classical finite-difference operator on a tensor product of two piecewise-uniform Shishkin meshes with an analytical function that captures the local nature of the incompatibility. In [191], the authors proposed a parameter-uniform numerical method for the viscous Burgers equation. To find a numerical approximation, they linearised the equation to obtain a sequence of linear PDEs. The linear PDES are then solved using FDM, which involves a backward FDM for the

time derivative and the upwind FDM for the spatial derivatives. In [192], the authors considered a system of singularly perturbed reaction-diffusion problems. In [193], the authors deal with linear parabolic singularly perturbed systems of convection-diffusion type in two dimensions. The numerical method combined two main techniques. It used the upwind FDM to discretise the problem in space. For time discretisation, the fractional implicit Euler method was applied. Furthermore, the method employed a split approach by direction and component of the reaction-convection-diffusion operator to improve efficiency and accuracy.

In [194], a hybrid higher-order FDM is presented for a class of singularly perturbed linear convection-diffusion problems in one dimension. However, in [195], the authors presented a hybrid scheme to solve singularly perturbed parabolic problems with Robin-type boundary conditions. The scheme is a combination of the FOFDM in space and the backward Euler method in time. They also proposed FDM to solve the Volterra integro-differential equation with a small parameter. The proposed scheme used a nonstandard FDM to solve the differential part and Simpson's rule to solve the integral part. The Richardson extrapolation is used to increase the order of convergence to two. In [196], the authors proposed a second-order FDM to solve a singularly perturbed Volterra integro-differential equation. In [108], the author proposes a higher-order numerical scheme to solve singularly perturbed reaction-diffusion problems. The proposed scheme is a combination of a fourth-order numerical difference method and a classical central difference method. In [197], the authors presented a parameter-uniform numerical method on equidistributed meshes for solving singularly perturbed parabolic problems with Robin boundary conditions. The discretisation consists of a modified Euler scheme in time, a central difference scheme in space, and a special FDM for the Robin boundary conditions.

In [198], the authors presented a second-order robust method for the singularly perturbed Burgers equation. A singularly perturbed parabolic convection-diffusion problem is the subject matter of [199]. The problem was discretised using the backward Euler scheme in the temporal direction and the upwind scheme on a harmonic mesh in the spatial direction. In [200], the authors introduced a high-order convergent numerical method for singularly perturbed time-dependent problems using mesh equidistribution. The discretisation relies on the backward Euler scheme in time and a high-order nonmonotone scheme in space. In [201], numerical approximations are computed for the solution of a system of two reaction-convection-diffusion equations using FDM on a fitted mesh. In [202], the authors investigated an initial boundary value problem for a singularly perturbed system comprising two convection-diffusion equations. They proposed a numerical method that integrates a spline-based scheme and uses a Shishkin mesh. The spline-based scheme offers a robust approach to approximating the solution. Through convergence analysis, the authors demonstrated that the proposed numerical technique achieves nearly second-order uniform convergence. In a separate study [203], the authors introduced a uniformly convergent numerical method for a singularly perturbed time-dependent system of two reaction-diffusion equations. The technique employs the Crank–Nicolson scheme on a uniform mesh for temporal discretisation and a quadratic B-spline collocation technique on an exponentially graded mesh for spatial discretisation. In [204], the authors addressed singularly perturbed convection-diffusion equations in two dimensions. They applied an upwind difference scheme on a modified exponentially graded Bakhvalov mesh for discretisation. The authors in [205]

analysed a higher-order numerical method for a class of two-dimensional parabolic singularly perturbed convection-diffusion problems, specifically for cases where the convection coefficient vanishes within the domain. They used the Peaceman-Rachford scheme for time discretisation on a uniform mesh and a hybrid scheme on a Bakhvalov-Shishkin mesh for spatial discretisation. In [206], the authors studied singularly perturbed one-dimensional parabolic systems involving convection-diffusion equations, where a small positive parameter of different magnitudes influences the diffusion term of each equation.

In [207], the authors proposed a parameter-uniform numerical method to address singularly perturbed Robin-type parabolic convection-diffusion problems characterised by boundary turning points. The authors employed the implicit Euler method for temporal discretisation and used a nonstandard FDM on a uniform mesh for spatial discretisation. Furthermore, the Robin boundary conditions were approximated using the nonstandard scheme to maintain consistency and accuracy. In [208], the author surveyed nonstandard FDMs. In [209], the authors investigated a singularly perturbed convection-diffusion problem in two dimensions with steady-state perturbations subject to Robin boundary conditions. Their study contributed to the broader understanding of boundary layer behaviour in such systems. In a related contribution [210], the authors developed a domain decomposition method for a class of singularly perturbed parabolic reaction-diffusion problems, also incorporating Robin boundary conditions. The technique involved partitioning the computational domain into three subdomains- two employing fine meshes and one employing a coarse mesh. The governing equations were discretised within each subdomain using standard FDMs. In addition, they employed a specially constructed FDM to accurately approximate Robin boundary conditions. In [211], the author examined a class of time-fractional singularly perturbed convection-diffusion problems. The authors applied the classical $L1$ FDM for the temporal component on a graded mesh to discretise the fractional derivative of time. In [212], the authors solved a second-order Volterra integro-differential equation using FDM on a Shishkin mesh adapted to the layer, demonstrating the convergence and reliability of the approach. In a separate work [213], the author presented a fitted mesh FDM to solve a singularly perturbed Fredholm integro-differential equation, further contributing to the development of robust numerical techniques in this domain.

In [214], the authors developed a collocation method that used polynomials and tension splines to solve a singularly perturbed two-point boundary value problem. Their findings indicated that tension splines offered better approximations in boundary layers, while polynomials were more accurate in outer regions. The authors of [215] explored adaptive splines for singularly perturbed initial and boundary value problems. Subsequently, in [216], the authors implemented a spline collocation method. They demonstrated that an appropriate choice of the fitting factor maintains convergence and stability. In [217], the author proposed a technique employing tension splines for singularly perturbed self-adjoint boundary value problems, achieving second-order convergence between grid points and $O(h\min(h,\sqrt{\varepsilon}))$ at grid points. In [218], the author addressed similar problems using exponential splines. The method reduces to a quadratic spline collocation technique in the limiting case. The method is computationally more efficient than other exponential-type methods.

In [219], the author used cubic spline collocation on nonuniform meshes with minimal defect to

approximate solutions for singular perturbation problems. Two years later, the authors of [220] introduced a spline-in-tension collocation method that exhibited linear convergence with suitable tension parameters. In [221], the authors improved the cubic spline collocation method by transitioning the collocation points from a Shishkin mesh to Gauss–Legendre points. B-spline collocation methods were proposed for problems involving twin boundary layers and a turning point, as well as self-adjoint problems and two-parameter problems [222, 223, 224, 225]. In [226], the author presented a quadratic spline collocation method for problems involving two small parameters using error analysis based on barrier functions. In [227, 228], the authors addressed nonlinear SPBVPs using B-spline collocation methods. In [229], the authors presented a quadratic spline collocation method for a convection–diffusion–reaction problem with two small parameters, establishing error bounds and showing convergence of $\mathscr{O}(N^{-2}\ln^2 N)$ in the boundary layer and second order elsewhere. In [230], the authors introduced artificial viscosity in a B-spline collocation method to capture exponential features on a uniform mesh. In [231], the authors developed a FEM that integrates cubic B-spline collocation on a nonuniform Shishkin mesh, achieving fourth-order convergence using Newton's method. In [232], the authors examined a semi-linear singularly perturbed problem using exponential splines on a Shishkin mesh. A numerical scheme that uses Bessel collocation for singularly perturbed two-point problems can be found in [233], and a generalised scheme using non-polynomial sextic splines in [234]. The B-spline method for fourth-order problems without order reduction achieved second-order convergence [235]. They extended this approach to linear and nonlinear problems on a Shishkin mesh and obtained fourth-order convergence [236].

In [237], the authors recognised the need for special approaches to address singular perturbation problems using finite element analysis. They developed a FEM approach analogous to the upwind scheme by incorporating upwinding into the test function. Contributions, such as [238, 239, 240], highlighted the limitations of standard Galerkin methods in handling dominant convective effects and laid the foundation for Petrov–Galerkin formulations that improved stability and accuracy. In [241], the author proposed a FEM using piecewise polynomials of degrees less than or equal to k. He used an irregular mesh and obtained uniform error estimates of order $\mathscr{O}(h^{k+1})$, for $k \geq 2$. In a series of papers [242, 243, 244], the authors introduced the concept of symmetrisation and established general error bounds for a Petrov-Galerkin method. They investigated choices of test space which either exactly or approximately symmetrise the associated bilinear form and retain the optimal character of the approximate solution. Choosing an appropriate test space is crucial to achieve high accuracy, superconvergence, and optimal recovery techniques. In [245], the author combined FEM and FDM with the method of characteristics to treat a parabolic problem. Optimal order error estimates in L^2 and $W^{1,2}$ are derived for the finite element procedure. These schemes have significantly smaller time-truncation errors compared to those of standard methods. In [246], the author introduced a piecewise linear hybrid finite element incorporating characteristics and perturbation techniques. Subsequent work [247, 248, 249] advanced the FEM theory on layer-adapted meshes, achieving uniform convergence regarding the perturbation parameter. In [249], the authors proved that, on an equidistant mesh, polynomial schemes cannot reach a high order of convergence, which is uniform in the perturbation parameter. Then, they constructed a piecewise polynomial Galerkin finite-element method on a Shishkin mesh. The past two decades have

seen significant progress in superconvergence [250, 251, 252] and adaptive mesh refinement [116, 253, 254, 117] and references therein, while novel methods like weak Galerkin FEM [255, 256, 257, 258, 259, 260] and dual FEM [261] have emerged to address problems with multiple small parameters or discontinuous coefficients. In [262], the author constructed a FVM on a Shishkin mesh to solve a singularly perturbed reaction-diffusion problem. The stability of the method was established in the energy norm. In [263], the author developed a nonsymmetric discontinuous Galerkin FEM with interior penalties for singularly perturbed convection-diffusion problems featuring a turning point. A standard Shishkin mesh was employed to handle boundary layers, while a generalised Shishkin-type mesh was used to address interior layers of the cusp type. Uniform error estimates were obtained in the L_2-norm and the DG-norm. For a complete overview of recent advances, see [99, 98, 264] and references therein.

1.6 Plan of the Thesis

In this thesis, we study, analyse and develop adaptive numerical schemes to solve singularly perturbed boundary and initial boundary value problems of varying complexity. The adaptive discretisation techniques we present can handle problems with diverse physical and dynamic characteristics by adjusting the resolution, order, and type of discretisation. The techniques are used in conjunction with adaptive numerical methods to balance the accuracy of the solution with the associated computational cost. Choosing an appropriate numerical method and a suitable discretisation strategy is essential to solving the problem and improving convergence. With this in mind, the thesis presents several numerical methods designed to address SPBVPs of varying levels of complexity.

The thesis is organised as follows: Chapter 1 provides an overview of the fundamentals of singular perturbation theory, key concepts, and a historical overview of the related literature. It also includes a detailed review of various state-of-the-art techniques developed in the past. In addition, the chapter outlines the aims and objectives of the present work.

Chapter 2 presents a higher-order adaptive hybrid difference scheme to solve a system of singularly perturbed reaction-diffusion problems with Dirichlet boundary conditions given as

$$\begin{cases} \mathbf{L}\mathbf{y}(x) := & -\varepsilon \mathbf{y}''(x) + \mathbf{B}\mathbf{y}(x) = \mathbf{g}(x),\ x \in \Omega = (0,1), \\ & \mathbf{y}(0) = \boldsymbol{\phi}, \quad \mathbf{y}(1) = \boldsymbol{\psi}, \end{cases} \tag{1.6.1}$$

where $0 < \varepsilon \ll 1$ is the perturbation parameter, $\mathbf{y}(x) = (y_1(x), y_2(x))^T$ and $\mathbf{B} = (b_{mj}(x))_{2\times 2}$ is an L_0-matrix. The source vector $\mathbf{g}(x) = (g_1(x), g_2(x))^T$ and the given data $b_{mj}(\cdot)$ are sufficiently smooth functions defined in $\bar{\Omega}$. Besides, for every m and j

$$b_{mm} > 0,\ \sum_{\substack{j=1 \\ j\neq m}}^{2} \left\| \frac{b_{mj}(x)}{b_{mm}(x)} \right\| < 1 \text{ and } b_{mj} \leq 0\ \forall\ m \neq j,\ \ m, j = 1, 2.$$

where $||.||$ represents the maximum norm in Ω. The proposed scheme integrates a nonmonotone

fourth-order Hermite difference method with the classical central difference method on a layer-adapted equidistributed grid. The adaptive grid is constructed by equidistributing a nonnegative monitor function. This monitor function automatically detects the thickness and steepness of boundary layers in the solution, eliminating the need for prior knowledge of the analytical behaviour of the solution. Numerical experiments support the theoretical error analysis of the proposed hybrid difference discretisation and demonstrate parameter-uniform fourth-order convergence on the layer-adapted grid.

Chapter 3 presents a uniformly accurate difference approximation for solving a system of singularly perturbed reaction-diffusion equations with a small delay. The problem reads

$$\begin{cases} \mathbf{L}\mathbf{y}(x) := & -\varepsilon\mathbf{y}''(x)+\mathbf{A}\mathbf{y}(x)+\mathbf{B}\mathbf{y}(x-\delta)=\mathbf{g}(x),\ x\in\Omega=(0,1), \\ & \mathbf{y}(x)=\boldsymbol{\rho}(x),\ x\in[-\delta,0], \quad \mathbf{y}(1)=\mathbf{l}, \end{cases} \tag{1.6.2}$$

where $0<\varepsilon\ll 1$ is the perturbation parameter and δ denotes the small shift of order $o(\varepsilon)$. Here, $\mathbf{y}(x)=(y_1(x),y_2(x))^T$, $\mathbf{A}=(a_{mj}(x))_{2\times 2}$ is an L_0-matrix, $\mathbf{B}=diag(b_1(x),b_2(x))$ is a diagonal matrix. The source vector $\mathbf{g}(x)=(g_1(x),g_2(x))^T$ and the given data $a_{mj}(\cdot)$, $b_m(\cdot)$ and $\boldsymbol{\rho}(x)=(\rho_1(x),\rho_2(x))^T$ are sufficiently smooth functions defined on $\bar{\Omega}$. Besides, for every m and j

$$a_{mm}>0,\ b_m>0,\ \min\left\{\left\|\frac{a_{mj}}{a_{mm}+b_m}\right\|,\left\|\frac{a_{mj}}{\delta b_m}\right\|\right\}<1 \text{ and } a_{mj}\le 0\ \forall\, m\neq j,\ \ m,j=1,2.$$

The proposed method uses an appropriate combination of exponential and cubic spline difference schemes. It employs grid equidistribution to address the challenges posed by the multiscale nature of these systems, which often feature sharp gradients and boundary layers. The grid is generated based on the equidistribution of a positive monitor function, a linear combination of a constant floor and a power of the second derivative of the solution. Using adaptive mesh generation and a spline difference method, the approach enhances the accuracy of numerical solutions while maintaining computational efficiency. Numerical experiments validate the uniform convergence and theoretical findings, demonstrating the method's robustness irrespective of the perturbation parameter size.

Chapter 4 presents a semi-analytical approach to solving a coupled system of singularly perturbed differential equations with mixed shifts. The problem we consider reads

$$\begin{cases} \mathbf{L}\tilde{\mathbf{y}} := & \boldsymbol{\varepsilon}\tilde{\mathbf{y}}''+\mathbf{B}\tilde{\mathbf{y}}'+\boldsymbol{\varsigma}\tilde{\mathbf{y}}(x-\tau)+\mathbf{A}\tilde{\mathbf{y}}+\boldsymbol{\rho}\tilde{\mathbf{y}}(x+\mu)=\tilde{\mathbf{g}}(x),\ x\in\Omega=(0,1) \\ & \tilde{\mathbf{y}}(x)=\boldsymbol{\phi}(x), \quad x\in[-\tau,0] \\ & \tilde{\mathbf{y}}(x)=\boldsymbol{\psi}(x), \quad x\in[1,1+\mu] \end{cases} \tag{1.6.3}$$

where $0<\varepsilon_i\ll 1$ for $i=1,2,...m$ denotes the perturbation parameters, $\boldsymbol{\varepsilon}=diag(\varepsilon_1,\varepsilon_2,...\varepsilon_m)$, $\boldsymbol{\rho}=diag(\rho_1,\rho_2,...,\rho_m)$, $\boldsymbol{\varsigma}=diag(\varsigma_1,\varsigma_2,...,\varsigma_m)$, $\tilde{\mathbf{y}}=(\tilde{y}_1,\tilde{y}_2,...\tilde{y}_m)^T\in(C(\Omega)\cap(C^2(\Omega))^m$ and τ and μ represents small shifts of $o(\varepsilon)$, respectively. Moreover, let us assume that $\mathbf{B}=diag(b_1,b_2,...b_m)$ the convection matrix, $\mathbf{A}=(a_{ij})_{m\times m}$ the coupling matrix, $\tilde{\mathbf{g}}=(\tilde{g}_1,\tilde{g}_2,...\tilde{g}_m)^T$ the source vector, and the given data $\boldsymbol{\phi}(x)=(\phi_1,\phi_2,\ldots,\phi_m)^T$, $\boldsymbol{\psi}(x)=(\psi_1,\psi_2,\ldots,\psi_m)^T$ are sufficiently smooth on $\bar{\boldsymbol{\Omega}}$. Besides, for every i and j, $b_i-\tau\varsigma_i+\mu\rho_i>0$, $\varsigma_i+a_{ii}+\rho_i\le 0$ and $a_{ij}\ge 0\ \forall\, i\neq j$. The solution to the problem

manifests a distinctive multiscale nature, characterised by localised narrow regions where the solution undergoes exponential changes. Beyond these regions, the solutions exhibit smooth variations. We employ a factorisation approach to address intricate multiscale characteristics, splitting the given coupled system into two explicit systems. The first, a degenerate system, captures the smooth solution outside the boundary layers through initial value problems. The second, addressing solutions within boundary layers, uses stretching transformations to form a set of boundary value problems. Even though this factorisation seems straightforward, the solutions obtained from these simplified systems capture the essential characteristics of the given system. The Runge–Kutta method is employed to solve the degenerate system of initial value problems, while the system of boundary value problems is solved analytically using asymptotic expansions. We establish the stability and consistency of the proposed method. The method converges uniformly with higher-order accuracy. The proposed method is easy to implement and does not require an adaptive mesh generation procedure. The numerical results and illustrations underscore the effectiveness and potential of the approach.

Chapter 5 presents a novel hybrid difference approximation for time-dependent reaction-diffusion equations with shifts and integral boundary conditions. The model problem reads

$$\begin{cases} Ly(x,t) & = y_t(x,t) - \varepsilon y_{xx}(x,t) + a(x,t)y(x,t) + b(x,t)y(x-\delta,t) = g(x,t),\ (x,t) \in \mathfrak{D}, \\ y(x,0) & = \phi_0(x) \text{ on } \Gamma_0 := \{(x,0) : x \in \bar{\Omega}\}, \\ \kappa_1 y(x,t) & = y(x,t) - \varepsilon \int_0^1 f_1(x,t)y(x,t)dx = \phi_l(x,t) \text{ on } \Gamma_l := \{(x,t) : -\delta \le x \le 0, t \in \Lambda\}, \\ \kappa_2 y(x,t) & = y(1,t) - \varepsilon \int_0^1 f_2(x,t)y(x,t)dx = \phi_r(1,t) \text{ on } \Gamma_r := \{(1,t) : t \in \Lambda\}, \end{cases} \tag{1.6.4}$$

where $0 < \varepsilon \ll 1$ and $\delta = o(\varepsilon)$ denotes the perturbation parameter and shift, respectively. The given functions $a(x,t)$, $b(x,t)$, $g(x,t)$, $\phi_0(x,0)$, $\phi_l(x,t)$, and $\phi_r(1,t)$ are sufficiently smooth and $a(x,t) \ge \eta > 0$, $b(x,t) \le \rho < 0$ and $a(x,t) + b(x,t) \ge \rho > 0$ for all $(x,t) \in \bar{\mathfrak{D}}$. The problem is singularly perturbed from a mathematical perspective and exhibits multiscale behaviour. The proposed approach employs a backward difference discretisation in time on a uniform temporal mesh. A key component of the method is the construction of an adaptive moving mesh in the spatial direction. The mesh we generate relies on the equidistribution principle. The numerical scheme comprises a cubic spline difference method within the boundary layer region and an exponential spline difference method outside the layer region. This strategy improves the accuracy of the numerical solution while maintaining computational efficiency. The chapter presents a comprehensive theoretical analysis, numerical results, and illustrations for model problems. The numerical experiments demonstrate parameter-uniform convergence and corroborate the theoretical findings.

Chapter 6 concludes the work with a summary that highlights its significant contributions. It provides insight into the author's thoughts on the future direction of the research and the challenging steps towards analysing more complicated problems.

Chapter 2

System of Reaction-Diffusion Equations

2.1 Introduction

Singularly perturbed systems of reaction-diffusion equations frequently arise in modelling complex phenomena involving multiple interacting components that diffuse and react over space or time. Such systems appear in a wide range of scientific and engineering applications. For example, in chemical kinetics, they model the rapid spread of substances and their interaction [10]; in ecology, they describe the spatial distribution of competing species[265, 266]; in physiology, they are used to study nerve impulse propagation [267, 27]; and in materials science, they help to understand phase transitions and pattern formation [268]. These systems feature small perturbation parameters that multiply the highest-order derivatives, resulting in sharp gradients or boundary layers within the solution. The coupling between equations further increases complexity, as the dynamics of one variable directly affect others, producing intricate solution behaviours.

The numerical analysis of such systems is particularly challenging due to their inherent stiffness and multiscale features. Standard numerical methods often fail to resolve steep gradients in the layer regions and require extremely fine meshes to maintain accuracy [3, 4]. This requirement leads to high computational costs and numerical instability near boundary layers. This limitation leads to the development of specialised numerical techniques based on adaptive mesh refinement to give stable and accurate results for all values of the perturbation parameter [5]. The articles [50, 51, 269, 52] present a systematic survey of earlier developments in numerical methods for a wide range of problems.

In recent years, adaptive mesh generation has become an essential tool for the numerical solution of singular perturbation problems [192, 270]. In [271], the authors conducted a comprehensive numerical study using FEMs for such systems. The study aimed to identify higher-order methods that converge exponentially, independent of perturbation parameters, even when boundary layers overlap. In [272], the authors introduced a nonsymmetric discontinuous Galerkin method with interior penalties (NIPG) on a Shishkin mesh. They proved uniform convergence in the $(\varepsilon - \mu)$-weighted discontinuous Galerkin norm and demonstrated the method's effectiveness through numerical experiments. In [273], researchers considered a system of coupled singularly perturbed reaction-diffusion equa-

tions. They discretised the problem using a weak Galerkin FEM (WG-FEM) on Shishkin mesh. In [274], the authors employed a FEM using piecewise quadratic splines to solve a system of linear coupled reaction-diffusion equations. Numerical methods based on adaptive mesh generation using the equidistribution principle have been effectively used to solve singular perturbation problems [275, 276, 277, 278]. In [279], the authors proposed a hybrid FDM of higher order for nonlinear systems with distinct perturbation parameters. They proposed a hybrid FDM over a layer adaptive mesh, for which they derived an a posteriori error estimate in the maximum norm. The layer-adapted meshes use the equidistribution principle. In a similar study, the authors in [280] provide optimal error estimates using the mesh equidistribution technique for a class of singularly perturbed systems of reaction-diffusion equations. An analysis of the robust uniformly convergent method for a singularly perturbed linear system of reaction-diffusion equations having nonsmooth data was presented in [281]. A classical FDM is combined with Shishkin and graded Bakhvalov meshes. Their method accounted for interior layers near discontinuities, resulting in second-order uniform convergence. While [282] presents a uniformly convergent method on a piecewise uniform Shishkin mesh for boundary value problems involving a system of two singularly perturbed coupled reaction-diffusion equations. In [283], the authors consider a similar system with discontinuous source terms. In another study [284], the authors developed a hybrid numerical method combining cubic spline methods in fine mesh regions and central difference methods in coarse mesh regions. They achieved uniform stability and second-order convergence.

These studies demonstrate that careful selection of discretisation and mesh adaptation strategies leads to robust numerical methods capable of accurately solving systems of singularly perturbed reaction-diffusion equations. Many articles focus on singularly perturbed boundary value problems. In contrast, the results for boundary value problems involving a system of singularly perturbed reaction-diffusion equations are limited and require further study. This chapter presents a higher-order hybrid difference method to solve a coupled system of singularly perturbed reaction-diffusion equations on an equidistributed mesh. The hybrid method effectively captures the multiscale behaviour of the solution and improves the accuracy of the numerical results while preserving computational efficiency. Furthermore, the chapter provides a rigorous theoretical error analysis and presents numerical experiments for some model problems to validate the theoretical estimates.

2.2 Continous Problem

Consider the system of singularly perturbed reaction-diffusion equations given below

$$\begin{cases} \mathbf{L}\mathbf{y}(x) := & -\varepsilon \mathbf{y}''(x) + \mathbf{B}\mathbf{y}(x) = \mathbf{g}(x),\ x \in \Omega = (0,1) \\ & \mathbf{y}(0) = \boldsymbol{\phi}, \quad \mathbf{y}(1) = \boldsymbol{\psi} \end{cases} \tag{2.2.1}$$

where $0 < \varepsilon \ll 1$ is the perturbation parameter, $\mathbf{y}(x) = (y_1(x), y_2(x))^T$ and $\mathbf{B} = (b_{mj}(x))_{2\times 2}$ is an L_0-matrix. The source vector $\mathbf{g}(x) = (g_1(x), g_2(x))^T$ and the given data $b_{mj}(\cdot)$ are sufficiently smooth

functions defined in $\bar{\Omega}$. Besides, for every m and j

$$b_{mm} > 0,\ \sum_{\substack{j=1 \\ j\neq m}}^{2} \left\| \frac{b_{mj}(x)}{b_{mm}(x)} \right\| < 1 \text{ and } b_{mj} \leq 0 \,\forall\, m \neq j,\ \ m, j = 1,2. \tag{2.2.2}$$

where $||.||$ represents the maximum norm on Ω. The above hypotheses ensure that (2.2.1) admits a unique solution $\mathbf{y} = (y_1, y_2)^T \in \left(C^2(\Omega) \cap C(\bar{\Omega})\right)$ [5].

2.3 Properties of the Solution

In this section, we begin our analysis by studying some analytical properties of the solution $\mathbf{y}$ that can be derived from the maximum principle and establish the stability of the differential operator [128]. The differential operator $\mathbf{L} = (L_1, L_2)^T$ satisfies the maximum principle [285].

Lemma 2.3.1. If $\mathbf{Ly} \geq 0$ on Ω and $\mathbf{y}(0) \geq 0$, $\mathbf{y}(1) \geq 0$. Then $\mathbf{y}(x) \geq 0$ on $\bar{\Omega}$.

Proof. Let $p, q \in \Omega$ be such that $y_1(p) = \min_{x\in\bar{\Omega}}\{y_1(x)\}$ and $y_2(q) = \min_{x\in\bar{\Omega}}\{y_2(x)\}$. Without loss of generality, assume that $y_1(p) \leq y_2(q)$ and let $y_1(p) < 0$. Clearly $p \neq \{0,1\}$, $y_1'(p) = 0$, and $y_1''(p) \geq 0$. Then

$$\begin{aligned} L_1\mathbf{y}(p) &\equiv -\varepsilon y_1''(p) + b_{11}y_1(p) + b_{12}y_2(p) \\ &= -\varepsilon y_1''(p) + (b_{11} + b_{12})y_1(p) + b_{12}(y_2(p) - y_1(p)) < 0. \end{aligned}$$

A contradiction to the assumption, and hence it follows that $\mathbf{y}(x) \geq 0,\ \forall\, x \in \bar{\Omega}$. □

We can directly derive the following estimate as an immediate consequence of the maximum principle.

Lemma 2.3.2. Let $\mathbf{y}(x)$ be any smooth function. Then

$$\|\mathbf{y}(x)\| \leq \max\{\|\mathbf{y}(0)\|, \|\mathbf{y}(1)\|, \max_{x\in\bar{\Omega}} \|L_1\mathbf{y}\|, \max_{x\in\bar{\Omega}} \|L_2\mathbf{y}\|\},\ \forall\, x \in \bar{\Omega}. \tag{2.3.1}$$

Using the stability property of the scalar differential operator, we now estimate the stability of the operator $\boldsymbol{L}$ in the next lemma.

Lemma 2.3.3. Let $\mathbf{y}$ be the solution of (2.2.1) and (2.2.2) hold on $\bar{\Omega}$. Then $\mathbf{y}$ satisfies the following stability estimate:

$$\|y_m\| \leq \sum_{j=1}^{2} (\boldsymbol{\Upsilon}^{-1})_{mj} \left\| \frac{g_j}{b_{jj}} \right\|,\ m = 1,2$$

where $\boldsymbol{\Upsilon} := \boldsymbol{\Upsilon}(\boldsymbol{B}) = (\gamma_{mj})_{2\times 2}$ such that $\gamma_{mm} = 1$ and $\gamma_{mj} = -\left\| \frac{b_{mj}}{b_{mm}} \right\|$ for $m \neq j$.

Proof. Let $\mathbf{y} := \mathbf{u} + \mathbf{v}$ where the components $\mathbf{u}$ and $\mathbf{v}$ satisfy

$$-\varepsilon u_m'' + b_{mm}u_m = g_m \text{ on } \Omega,\ u_m(0) = y_m(0),\ u_m(1) = y_m(1) \text{ and}$$

$$-\varepsilon v_m'' + b_{mm} v_m = -\sum_{\substack{j=1 \\ j\neq m}}^{2} b_{mj} y_j \text{ on } \Omega,\ v_m(0) = 0, v_m(1) = 0.$$

Lemma 2.3.2 and the triangle inequality lead to

$$\|u_m\| \leq \left\| \frac{g_m}{b_{mm}} \right\|, \text{ and}$$

$$\|v_m\| \leq \sum_{\substack{j=1 \\ j\neq m}}^{2} \left\| \frac{b_{mj}}{b_{mm}} \right\| \|y_j\|, \text{ for } m = 1,2.$$

Since, $\|y_m\| \leq \|u_m\| + \|v_m\|$, we get

$$\|y_m\| - \sum_{\substack{j=1 \\ j\neq m}}^{2} \left\| \frac{b_{mj}}{b_{mm}} \right\| \|y_j\| \leq \left\| \frac{g_m}{b_{mm}} \right\|,\ m = 1,2.$$

Since, matrix $\boldsymbol{B}$ satisfies (2.2.2), the matrix $\boldsymbol{\Upsilon} = \boldsymbol{\Upsilon}(\boldsymbol{B})$ is a diagonally dominant L_0-matrix. Hence, $\boldsymbol{\Upsilon}$ is inverse monotone and

$$\|y_m\| \leq \sum_{j=1}^{2} (\boldsymbol{\Upsilon}^{-1})_{mj} \left\| \frac{g_j}{b_{jj}} \right\|,\ m = 1,2.$$

□

The stability of the differential operator $\boldsymbol{L}$ established in Lemma 2.3.3, coupled with the standard maximum principle in Lemma 2.3.1, guarantees the existence of a unique solution $\mathbf{y} \in C^4(\bar{\Omega})^2$. To facilitate the analysis of the numerical discretisation of (2.2.1), we establish a priori bounds on the derivatives of the solution $\boldsymbol{y}$ as follows.

Lemma 2.3.4. Let $\mathbf{y}$ be the solution of (2.2.1) and $\omega \in (0,1) \subset \mathbb{R}$ be such that $\sum_{\substack{j=1 \\ j\neq m}}^{2} \left\| \frac{b_{mj}}{b_{mm}} \right\| < \omega < 1$ for $m = 1,2$. Then, for $k = 0, \ldots, 4$

$$|y_m^{(k)}(x)| \leq C\left(1 + \varepsilon^{-\frac{k}{2}} \left(e^{\left(-x\sqrt{\frac{\rho}{\varepsilon}}\right)} + e^{\left(-(1-x)\sqrt{\frac{\rho}{\varepsilon}}\right)} \right)\right),\ \forall\, x \in \bar{\Omega}, \tag{2.3.2}$$

where $\rho = \rho(\omega) := (1-\omega) \min\limits_{m=1,2} \min\limits_{x\in[0,1]} (b_{mm}(x)) > 0$.

Proof. We establish (2.3.2) by induction on k, the case $k = 0$ being immediate from Lemma 2.3.3. For $k > 1$, differentiate (2.2.1) k-times to get

$$-\varepsilon \mathbf{y}^{(k+2)} + \boldsymbol{B}\mathbf{y}^{(k)} = \boldsymbol{g}^{(k)} - \sum_{s=0}^{k-1} \binom{k}{s} \boldsymbol{B}^{(k-s)} \mathbf{y}^{(s)} = \boldsymbol{f}_k,$$

where $\boldsymbol{f}_k = (f_{k,1}, f_{k,2})^T$. Let $|y_m^{(s)}(x)| \leq C\left(1 + \varepsilon^{-\frac{k}{2}} \left(e^{\left(-x\sqrt{\frac{\rho}{\varepsilon}}\right)} + e^{\left(-(1-x)\sqrt{\frac{\rho}{\varepsilon}}\right)} \right)\right) := \hat{\mathscr{B}}_k$ for all $s \leq k-1$. Consequently, $|f_{k,m}(x)| \leq C\hat{\mathscr{B}}_{k-1}(x)$ for $m = 1,2$. For $x \in \bar{\Omega}$, define $\hat{\mathbf{y}}(x) := \frac{\mathbf{y}^{(k)}(x)}{\hat{\mathscr{B}}_k(x)}$. Using Lemma

2.3.2 along with the M-matrix criterion [286], we obtain $\|\hat{\mathbf{y}}\| \leq C$. Hence, from the definition of $\hat{\mathbf{y}}$, it follows that

$$|y_m^{(k)}(x)| \leq C\left(1+\varepsilon^{-\frac{k}{2}}\left(e^{\left(-x\sqrt{\frac{p}{\varepsilon}}\right)}+e^{\left(-(1-x)\sqrt{\frac{p}{\varepsilon}}\right)}\right)\right),\ \forall\, x\in\bar{\Omega}.$$

□

2.4 Solution Decomposition

The standard decomposition of the solution plays a crucial role in the convergence analysis of numerical methods for singularly perturbed problems. Therefore, we decompose the solution of (2.2.1) into smooth and layer parts as $\mathbf{y}=\mathbf{u}+\mathbf{v}$. where the smooth component $\mathbf{u}=(u_1,u_2)^T$ satisfy

$$\mathbf{L}\mathbf{u}(x)=\mathbf{g}(x),\ \ x\in\Omega;\ \ \mathbf{u}(0)=\mathbf{B}(0)^{-1}\mathbf{g}(0),\ \ \mathbf{u}(1)=\mathbf{B}(1)^{-1}\mathbf{g}(1), \tag{2.4.1}$$

and the layer part $\mathbf{v}=(v_1,v_2)^T$ satisfies

$$\mathbf{L}\mathbf{v}(x)=0,\ \ x\in\Omega;\ \ \mathbf{v}(0)=\mathbf{y}(0)-\mathbf{u}(0),\ \ \mathbf{v}(1)=\mathbf{y}(1)-\mathbf{u}(1). \tag{2.4.2}$$

Following this, we use a proposition from [107] stated below and a standard factorisation to estimate precise bounds on the components and their derivatives.

Proposition 2.4.1. Let $\mu>0$ and $I=[\chi,\chi+\mu]$ be an arbitrary interval. If $F\in C^2(I)$, then

$$\|F'\|_I \leq \frac{2}{\mu}\|F\|_I+\frac{\mu}{2}\|F''\|_I.$$

Lemma 2.4.1. Let $\mathbf{y}=\mathbf{u}+\mathbf{v}$ be the solution of (2.2.1) where $\mathbf{u}$ and $\mathbf{v}$ satisfy (2.4.1) and (2.4.2), respectively. Then, the smooth part $\mathbf{u}=(u_1,u_2)^T$ satisfies

$$\left\|u_m^{(k)}\right\| \leq C\left(1+\varepsilon^{\frac{(2-k)}{2}}\right),\ \ k=0,\ldots,4,\ \ m=1,2,$$

and the layer component $\mathbf{v}=(v_1,v_2)^T$ satisfies

$$\left\|v_m^{(k)}\right\| \leq C\varepsilon^{-\frac{k}{2}}\left(e^{\left(-x\sqrt{\frac{p}{\varepsilon}}\right)}+e^{\left(-(1-x)\sqrt{\frac{p}{\varepsilon}}\right)}\right),\ \ k=0,\ldots,4,\ \ m=1,2,\ \text{and}\ x\in\overline{\Omega}.$$

Proof. Writing $\mathbf{u}(x)$ as an asymptotic series expansion that reads

$$\mathbf{u}(x)=\mathbf{u}_0(x)+\varepsilon\mathbf{u}_1(x)+\varepsilon^2\mathbf{u}_2^*(x)=\left(u_{0,1}(x)+\varepsilon u_{1,1}(x)+\varepsilon^2u_{2,1}^*(x),u_{0,2}(x)+\varepsilon u_{1,2}(x)+\varepsilon^2u_{2,2}^*(x)\right)^T.$$

Substituting $\mathbf{u}(x)$ in (2.2.1) and equating coefficients of like powers of ε, we get

$$\begin{aligned}
&\mathbf{B}(x)\mathbf{u}_0(x) = \mathbf{g}(x) \Rightarrow \begin{cases} b_{11}(x)u_{0,1}(x) + b_{12}(x)u_{0,2}(x) = g_1(x), \\ b_{21}(x)u_{0,1}(x) + b_{22}(x)u_{0,2}(x) = g_2(x), \end{cases} \\
&\mathbf{B}(x)\mathbf{u}_1(x) = \mathbf{u}_0''(x), \\
&\mathbf{L}\mathbf{u}_2^*(x) = \mathbf{u}_1''(x),\ \ \mathbf{u}_2^*(0) = 0,\ \ \mathbf{u}_2^*(1) = 0.
\end{aligned}$$

Then, from Lemma 2.3.3, it follows

$$\left\| u_m^{(k)} \right\| \leq C, \quad k = 0,1,2, \quad m = 1,2.$$

Next, differentiate $\mathbf{L}\mathbf{u} = \mathbf{g}$ twice to obtain $\left\| u_m^{(iv)} \right\| \leq C\varepsilon^{-1}$, $m = 1,2$. Then, for $I \subseteq [0,1]$, Proposition 2.4.1 with $F = u_m''$ and $\mu = \varepsilon^{\frac{1}{2}}$ yields $\|u_m'''\| \leq C\varepsilon^{-\frac{1}{2}}$, $m = 1,2$.

Now, to obtain bounds on the layer part $\mathbf{v}$, it is further decomposed as $\mathbf{v}(x) = \mathbf{v}^-(x) + \mathbf{v}^+(x)$ where the left layer part $\mathbf{v}^-(x) = (v_1^-(x), v_2^-(x))^T$ satisfy

$$\mathbf{L}\mathbf{v}^-(x) = 0,\ \ x \in \Omega,\ \ \mathbf{v}^-(0) = \mathbf{v}(0),\ \ \mathbf{v}^-(1) = 0, \tag{2.4.3}$$

and the right layer part $\mathbf{v}^+(x) = (v_1^+(x), v_2^+(x))^T$ satisfy

$$\mathbf{L}\mathbf{v}^+(x) = 0,\ \ x \in \Omega;\ \ \mathbf{v}^+(0) = 0,\ \ \mathbf{v}^+(1) = \mathbf{v}(1). \tag{2.4.4}$$

Using the method of asymptotic expansions, we get

$$v_m^-(x) = \sum_{s=0}^{2p+1} \varepsilon^{\frac{s}{2}} v_{s,m}^-(x) + \varepsilon^{p+1} v_{2(p+1),m}^{*-},\ \ m = 1,2,\ \text{and} \tag{2.4.5}$$

$$v_m^+(x) = \sum_{s=0}^{2p+1} \varepsilon^{\frac{s}{2}} v_{s,m}^+(x) + \varepsilon^{p+1} v_{2(p+1),m}^{*+},\ \ m = 1,2. \tag{2.4.6}$$

For the left boundary layer $\mathbf{v}^-$, stretch the variable using the coordinate transformation $\xi = \dfrac{x}{\sqrt{\varepsilon}}$ and using Taylor series expansion of $\mathbf{B}(\sqrt{\varepsilon}\xi)$ to define $\widehat{\mathbf{L}} = -\dfrac{d^2}{d\xi^2} + \mathbf{B}(0)I$. Then, from (2.4.3)

$$\widehat{\mathbf{L}}\mathbf{v}_0^-(\xi) = 0,\ \mathbf{v}_0^-(0) = -\mathbf{u}_0^-(0) \text{ and } \lim_{\xi\to\infty} \mathbf{v}_0^-(\xi) = 0,$$

$$\begin{cases} \widehat{\mathbf{L}}\mathbf{v}_s^-(\xi) = -\sum_{j=1}^{s} \frac{\xi^j}{j!}\mathbf{B}^j(0)v_{s-j}^-(\xi), \\ \mathbf{v}_s^- = -\mathbf{u}_s^-(0),\ \lim\limits_{\xi\to\infty} \mathbf{v}_s^-(\xi) = 0,\ s = 1,...,2k+1 \end{cases}$$

and

$$\begin{cases} \mathbf{L}\mathbf{v}_{2p+2}^{*-}(x) = -\varepsilon^{-(p+1)}\mathbf{L}\left(\mathbf{v}_0^- + \cdots + \varepsilon^{\frac{(2p+1)}{2}}\mathbf{v}_{2p+1}^-\right)(x), \\ \mathbf{v}_{2p+2}^{*-}(0) = 0,\ \mathbf{v}_{2p+2}^{*-}(1) = -\varepsilon^{-(p+1)}\left(\mathbf{v}_0^- + \cdots + \varepsilon^{\frac{(2p+1)}{2}}\mathbf{v}_{2p+1}^-\right)(1). \end{cases}$$

Thus, from Lemma 2.3.3, it follows that v_m^- satisfies

$$\left|v_m^-(0)\right| < C,\ \left|v_m^-(1)\right| < Ce^{\left(-\sqrt{\frac{\rho}{\varepsilon}}\right)},\ \text{and}\ \left|(v_m^-)^{(k)}(x)\right| \leq C\varepsilon^{-\frac{k}{2}}e^{\left(-\sqrt{\frac{\rho}{\varepsilon}}x\right)},\ m=1,2.$$

Similarly, we can establish the derivative bounds for the right layer part v_m^+ to complete the proof. □

2.5 Mesh Structure

The development of the adaptive numerical method relies on an adaptive mesh generation algorithm that automatically identifies the basic characteristics of the boundary layers through an equidistribution principle. Following [276, 277], we consider a positive monitor function

$$M = \beta + \left|v_1''\right|^{\frac{1}{4}} + \left|v_2''\right|^{\frac{1}{4}}, \tag{2.5.1}$$

where v_1 and v_2 are the layer parts of the solution $\mathbf{y} = (y_1, y_2)^T$ and β is a positive constant. Earlier work [110, 119, 278, 287] shows that one should choose the least value of the monitor function with caution to improve convergence. By choosing an appropriate floor value β, the mesh prevents the clustering of points within the layers and ensures the proper distribution of the mesh points outside the layers.

Using the derivative bound of $v(x)$ in Lemma 2.4.1 yields an approximation of $v_m''(x)$, $m = 1,2$ given by

$$v_m''(x) \approx \begin{cases} \dfrac{\alpha_0}{\varepsilon}e^{\left(-x\sqrt{\frac{\rho}{\varepsilon}}\right)}, & x \in \left[0, \frac{1}{2}\right], \\ \dfrac{\alpha_1}{\varepsilon}e^{\left(-(1-x)\sqrt{\frac{\rho}{\varepsilon}}\right)}, & x \in \left(\frac{1}{2}, 1\right], \end{cases}$$

where α_0 and α_1 are constants. Imitating the analysis from [277, 287, 278], we have

$$\int_0^1 \left(\left|v_1''(x)\right|^{\frac{1}{2}} + \left|v_2''(x)\right|^{\frac{1}{2}}\right) dx \equiv \Psi \approx \frac{4}{\sqrt[4]{\rho}}\left(|\alpha_0|^{\frac{1}{4}} + |\alpha_1|^{\frac{1}{4}}\right). \tag{2.5.2}$$

Now using (2.5.1) to obtain a map

$$\frac{\beta}{\Psi}x(\xi) + \mu_0\left(1 - e^{\left(-\frac{x(\xi)}{4}\sqrt{\frac{\rho}{\varepsilon}}\right)}\right) = \xi\left(\frac{\beta}{\Psi} + 1\right),\ x(\xi) \leq \frac{1}{2}, \tag{2.5.3}$$

and

$$\frac{\beta}{\Psi}(1 - x(\xi)) + \mu_1\left(1 - e^{\left(-\frac{(1-x(\xi))}{4}\sqrt{\frac{\rho}{\varepsilon}}\right)}\right) = (1-\xi)\left(\frac{\beta}{\Psi} + 1\right),\ x(\xi) > \frac{1}{2},$$

where $\mu_0 = \dfrac{|\alpha_0|^{\frac{1}{4}}}{|\alpha_0|^{\frac{1}{4}} + |\alpha_1|^{\frac{1}{4}}}$ and $\mu_1 = \dfrac{|\alpha_1|^{\frac{1}{4}}}{|\alpha_0|^{\frac{1}{4}} + |\alpha_1|^{\frac{1}{4}}} = 1 - \mu_0$.

Given the relation between uniform mesh $\left\{\xi_i = \dfrac{i}{N}\right\}_{i=0}^{N}$ and adaptive mesh $\{x_i\}_{i=0}^{N}$, the required

nonuniform mesh is given by

$$\frac{\beta}{\Psi}x_i+\mu_0\left(1-e^{\left(-\frac{x_i}{4}\sqrt{\frac{\rho}{\varepsilon}}\right)}\right)=\frac{i}{N}\left(\frac{\beta}{\Psi}+1\right),\ x_i\le\frac{1}{2}, \tag{2.5.4}$$

and

$$\frac{\beta}{\Psi}(1-x_i)+\mu_1\left(1-e^{\left(-\frac{(1-x_i)}{4}\sqrt{\frac{\rho}{\varepsilon}}\right)}\right)=\left(1-\frac{i}{N}\right)\left(\frac{\beta}{\Psi}+1\right),\ x_i>\frac{1}{2}. \tag{2.5.5}$$

Next, for an appropriate β, we examine the structure of the generated mesh and illustrate its distribution.

Lemma 2.5.1. Let $\beta=\Psi$. Then

$$x_{k_l}<4\sqrt{\frac{\varepsilon}{\rho}}\log N<x_{k_{l+1}},\quad\text{and}\quad x_{k_r-1}<1-4\sqrt{\frac{\varepsilon}{\rho}}\log N<x_{k_r},$$

where

$$k_l=\left[\frac{\mu_0}{2}(N-1)+2\sqrt{\frac{\varepsilon}{\rho}}N\log N\right],$$
$$k_r=\left[N-\left(\frac{\mu_1}{2}(N-1)+2\sqrt{\frac{\varepsilon}{\rho}}N\log N\right)\right]+1,$$

Here, $[\cdot]$ represents the integral part of the term. Furthermore,

$$e^{\left(-\frac{x_i}{4}\sqrt{\frac{\rho}{\varepsilon}}\right)}\le CN^{-1},\quad i\ge k_l-1,\quad x_i\le\frac{1}{2},$$
$$e^{\left(-\frac{(1-x_i)}{4}\sqrt{\frac{\rho}{\varepsilon}}\right)}\le CN^{-1},\quad i\le k_r,\quad x_i>\frac{1}{2}.$$

Proof. Substitute $x_i=4\sqrt{\frac{\varepsilon}{\rho}}\log N$ in (2.5.4) and solve for i to find k_l. Using (2.5.5) we can similarly compute k_r. □

Setting $\beta=\Psi$ aligns the equidistributed mesh with some features of a priori mesh. However, exponential stretching within layers reduces discretisation error, enhancing accuracy [288, 277]. Next, we obtain bounds on the mesh width in the layer region $\left(\{x_i\}_{i=0}^{k_l-1}\text{ and }\{x_i\}_{i=k_r+1}^{N}\right)$ and the outer region $(\{x_i\}_{i=k_l}^{k_r})$.

Lemma 2.5.2. For $i=1,\ldots,k_l\cup i=k_r+1,\ldots,N$, the mesh width in the boundary layer part satisfies $h_i<4C\sqrt{\frac{\varepsilon}{\rho}}$. Furthermore

$$\left|h_{i+1}-h_i\right|\le\begin{cases}Ch_i^2, & i=1,\ldots,k_l-1,\\ Ch_{i+1}^2, & i=k_r+1,\ldots,N-1.\end{cases}$$

Proof. We prove the result for the left layer region. The result for the right layer region follows analogously. Imitating the steps from [[278], Lemma 3.2] we use (2.5.4) to $\overline{x_i}>x_i$ such that

$$e^{\left(-\frac{\overline{x_i}}{4}\sqrt{\frac{\rho}{\varepsilon}}\right)}=1-\frac{2i}{\mu_0 N}.$$

A rearrangement of terms yields

$$x_i < \overline{x_i} = -4\sqrt{\frac{\varepsilon}{\rho}}\log\left(1-\frac{2i}{\mu_0 N}\right).$$

Using $\overline{x_i}$ into (2.5.4) to compute

$$x_i > \underline{x_i} = -4\sqrt{\frac{\varepsilon}{\rho}}\log\left(1-\frac{1}{\mu_0}\left(\frac{2i}{N}+4\sqrt{\frac{\varepsilon}{\rho}}\log\left(1-\frac{2i}{\mu_0 N}\right)\right)\right).$$

Thus, for $i = 1,\ldots,k_l$

$$h_i = x_i - x_{i-1} < \overline{x_i} - \underline{x_{i-1}} = 4\sqrt{\frac{\varepsilon}{\rho}}\log\left(1+\frac{2+4\sqrt{\frac{\varepsilon}{\rho}}N\log\left(\frac{\mu_0 N}{\mu_0 N-2(t-1)}\right)}{\mu_0 N-2t}\right) < 4C\sqrt{\frac{\varepsilon}{\rho}}.$$

Moreover, note that

$$\frac{|h_{i+1}-h_i|}{h_i^2} \le \frac{2\left|x_{\xi\xi}\left(\theta_i^{(1)}\right)\right|}{\left(x_\xi\left(\theta_i^{(2)}\right)\right)^2}, \quad \text{where} \quad \theta_i^{(1)} \in (\xi_{i-1},\xi_{i+1}) \quad \text{and} \quad \theta_i^{(2)} \in (\xi_{i-1},\xi_i).$$

Then, from (2.5.3) and $\beta = \Psi$, we obtain

$$x_\xi(\theta) = \frac{8\sqrt{\frac{\varepsilon}{\rho}}}{4\sqrt{\frac{\varepsilon}{\rho}}+\mu_0 e^{\left(-\frac{x(\theta)}{4}\sqrt{\frac{\rho}{\varepsilon}}\right)}}, \text{ and } x_{\xi\xi}(\theta) = \frac{16\mu_0\sqrt{\frac{\varepsilon}{\rho}}e^{\left(-\frac{x(\theta)}{4}\sqrt{\frac{\rho}{\varepsilon}}\right)}}{\left(4\sqrt{\frac{\varepsilon}{\rho}}+\mu_0 e^{\left(-\frac{x(\theta)}{4}\sqrt{\frac{\rho}{\varepsilon}}\right)}\right)^3}.$$

This implies that

$$\frac{|h_{i+1}-h_i|}{h_i^2} \le \frac{\mu_0\sqrt{\frac{\rho}{\varepsilon}}\left(4\sqrt{\frac{\rho}{\varepsilon}}+\mu_0 e^{\left(-\frac{x_{i-1}}{4}\sqrt{\frac{\rho}{\varepsilon}}\right)}\right)^2}{4\left(4\sqrt{\frac{\rho}{\varepsilon}}+\mu_0 e^{\left(-\frac{x_{i+1}}{4}\sqrt{\frac{\rho}{\varepsilon}}\right)}\right)^3} \le C.$$

□

The following lemma generalises the bounds on h_i across the entire domain.

Lemma 2.5.3. For $i = 1,\ldots,N$, the width of the adaptive mesh satisfies $h_i \le CN^{-1}$.

Proof. Use (2.5.1) and (2.5.2) with $\beta = \Psi$ to obtain $\int_0^1 M(x,y(x))dx \le C\beta$. Finally, the equidistribution principle yields $\beta h_i \le \int_{x_{i-1}}^{x_i} M(x,y(x))dx = \frac{1}{N}\int_0^1 M(x,y(x))dx \le C\beta N^{-1}$. □

2.6 The Difference Method

We now describe the difference approximation of (2.2.1) on the adaptive mesh $\bar{\Omega}_E^N \equiv \{0 = x_0 < x_1 < \cdots < x_N = 1\}$. We employ the fourth-order Hermite difference method for discretising the boundary layer region of the mesh and the central difference method for the outer layer region. Then, the discrete

problem corresponding to (2.2.1) takes the following form.

$$\begin{aligned}\left[\mathbf{L}^N\mathbf{Y}\right]_i \equiv -\varepsilon\left[\delta_x^2\mathbf{Y}\right]_i + \left[\Gamma(\mathbf{B}\mathbf{Y})\right]_i = [\Gamma\mathbf{g}]_i, \quad i = 1,...,N-1,\\ \mathbf{Y}_0 = \boldsymbol{\phi}, \quad \mathbf{Y}_N = \boldsymbol{\psi}\end{aligned}$$

where,

$$\begin{aligned}\left[\delta_x^2\mathbf{f}\right] &= \frac{2}{h_i+h_{i+1}}\left(\frac{\mathbf{f}_{i+1}-\mathbf{f}_i}{h_{i+1}} - \frac{\mathbf{f}_i-\mathbf{f}_{i-1}}{h_i}\right), \text{ and}\\ [\Gamma\mathbf{f}] &= q_i^-\mathbf{f}_{i-1} + q_i^c\mathbf{f}_t + q_i^+\mathbf{f}_{i+1}.\end{aligned}$$

By rearranging the terms, the tri-diagonal form of the hybrid difference approximation is as follows

$$\begin{aligned}&\left[\mathbf{L}^N\mathbf{Y}\right]_i = [\Gamma\mathbf{g}]_i\\ &\Leftrightarrow \begin{cases} \left[L_1^N\mathbf{Y}\right]_i \equiv r_{1,i}^- Y_{1,i-1} + r_{1,i}^c Y_{1,i} + r_{1,i}^+ Y_{1,i+1} + q_i^- b_{12,i-1}Y_{2,i-1} + \\ \qquad q_i^c b_{12,i}Y_{2,i} + q_i^+ b_{12,i+1}Y_{2,i+1} = q_i^- g_{1,i-1} + q_i^c g_{1,i} + q_i^+ g_{1,i+1}, \\ \left[L_2^N\mathbf{Y}\right]_i \equiv r_{2,i}^- Y_{2,i-1} + r_{2,i}^c Y_{2,i} + r_{2,i}^+ Y_{2,i+1} + q_i^- b_{21,i-1}Y_{1,i-1} + \\ \qquad q_i^c b_{21,i}Y_{1,i} + q_i^+ b_{21,i+1}Y_{1,i+1} = q_i^- g_{2,i-1} + q_i^c g_{2,i} + q_i^+ g_{2,i+1}, \\ \qquad\qquad\qquad\qquad\qquad\qquad \text{for } i = 1,\ldots,N-1, \\ Y_{1,0} = \phi_1,\ Y_{1,N} = \psi_1,\ Y_{2,0} = \phi_2,\ Y_{2,N} = \psi_2, \end{cases}\end{aligned} \tag{2.6.1}$$

where $\mathbf{L}^N = (L_1, L_2)^N$, $\mathbf{Y} = (Y_1, Y_2)^T$, $\mathbf{g}_i = (g_{1,i}, g_{2,i})^T$ and $[\Gamma(g_m)]_i = q_i^- g_{m,i-1} + q_i^c g_{m,i} + q_i^+ g_{m,i+1}$. The coefficients $r_{m,i}^*$, $m = 1,2$, $i = 1,\ldots,N-1$, $* = -,c,+$ are given by

$$\begin{cases} r_{m,i}^- = \dfrac{-2\varepsilon}{h_i(h_{i+1}+h_i)} + q_i^- b_{mm}(x_{i-1}), \qquad r_{m,i}^c = \dfrac{2\varepsilon}{h_{i+1}h_i} + q_i^c b_{mm}(x_i), \\ r_{m,i}^+ = \dfrac{-2\varepsilon}{h_{i+1}(h_{i+1}+h_i)} + q_i^+ b_{mm}(x_{i+1}), \end{cases} \tag{2.6.2}$$

The coefficients of the fourth-order Hermite difference method satisfy the normalisation condition $q_i^- + q_i^c + q_i^+ = 1$ to ensure that the method is exact for polynomials up to degree four. Thus, based on the location of the mesh points x_i which partition the domain $[0,1]$, the coefficients q_i^*, $i = 1,\ldots,N-1$, $* = -,c,+$ are given as follows:

1. In boundary layer region of the mesh, the coefficients q_i^*, $* = -,c,+$, $i = \{1,\ldots,k_l-1\}$ and $i = \{k_r+1,\ldots,N-1\}$ are given by

$$q_i^- = \frac{h_i^2 + h_ih_{i+1} - h_{i+1}^2}{6h_i(h_{i+1}+h_i)}, \quad q_i^c = \frac{h_i^2 + 3h_ih_{i+1} + h_{i+1}^2}{6h_ih_{i+1}}, \quad q_i^+ = \frac{h_{i+1}^2 + h_ih_{i+1} - h_i^2}{6h_{i+1}(h_{i+1}+h_i)}. \tag{2.6.3}$$

2. In the outer layer region of the mesh, the coefficients q_i^*, $* = -,c,+$, $i = \{k_l,\ldots,k_r\}$ depend on the relation between $h_{\max}$ and ε, such that for a positive constant k independent of N and ε, we have

   - If $kh_{\max}^2\|b_{mm}\|_\infty > \varepsilon$, the central difference method is used and the coefficients q_i^*, $* =$

$-, c, +$, $i = \{k_l, \ldots, k_r\}$ are given by

$$q_i^- = 0, \quad q_i^c = 1, \quad q_i^+ = 0. \tag{2.6.4}$$

- If $kh_{\max}^2 \|b_{mm}\|_\infty \leq \varepsilon$, the fourth-order Hermite difference method is used and the coefficients q_i^*, $* = -, c, +$, $i = \{k_l, \ldots, k_r\}$ are given by the relation (2.6.3).

The following lemma establishes that the associated coefficient matrix of the discrete hybrid operator $\mathbf{L}^N$ satisfies the M-matrix criteria.

Lemma 2.6.1. Let N_0 be the smallest positive integer such that

$$\frac{8\|b_{mm}\|_\infty}{\rho} < 3(\zeta N_0)^2, \tag{2.6.5}$$

where $\zeta = \min\{\mu_0, \mu_1\}$. Then, for every $N \geq N_0$, the coefficients of the discrete hybrid operator $\mathbf{L}^N$ in (2.6.1) satisfy

$$r_{m,i}^c > 0, \quad r_{m,i}^- < 0, \quad r_{m,i}^+ < 0, \quad r_{m,i}^c + r_{m,i}^- + r_{m,i}^+ > 0, \ i = 1, \ldots, N-1, \ m = 1, 2.$$

Proof. 1. In the boundary layer part $\left(\{x_i\}_{i=1}^{k_l-1}$ and $\{x_i\}_{i=k_r+1}^{N-1}\right)$, the coefficients of the fourth-order Hermite difference method are given by (2.6.2)–(2.6.3). Using Lemma 2.5.2 and (2.6.5), we have

$$\begin{cases} r_{m,i}^c &= \dfrac{2\varepsilon}{h_i h_{i+1}} + \dfrac{h_i^2 + 3h_i h_{i+1} + h_{i+1}^2}{6h_i h_{i+1}} b_{mm}(x_i) > 0, \\ r_{m,i}^- &= \dfrac{-2\varepsilon}{h_i(h_i + h_{i+1})} + \dfrac{h_i^2 + h_i h_{i+1} - h_{i+1}^2}{6h_i(h_i + h_{i+1})} b_{mm}(x_{i-1}) \\ &= \dfrac{1}{h_i(h_i + h_{i+1})} \left(-2\varepsilon + \dfrac{h_i^2 + h_i h_{i+1} - h_{i+1}^2}{6} b_{mm}(x_{i-1}) \right) \\ &< \dfrac{1}{h_i(h_i + h_{i+1})} \left(-2\varepsilon + \dfrac{16C^2}{6} \left(\dfrac{\varepsilon}{\rho} \right) \|b_{mm}\|_\infty \right) \\ &< \dfrac{1}{h_i(h_i + h_{i+1})} \left(-2\varepsilon + C^2 \varepsilon (\zeta N_0)^2 \right) < 0. \end{cases}$$

Similarly, $r_{m,i}^+ < 0$. Moreover, under the influence of assumption $b_{mm} \geq \rho > 0$, for $m = 1, 2$, the

row sum is given as

$$\begin{aligned}
r^c_{m,i}+r^-_{m,i}+r^+_{m,i} &= \frac{h_i^2+h_ih_{i+1}-h_{i+1}^2}{6h_i\left(h_{i+1}+h_i\right)}b_{mm}(x_{i-1})+\frac{h_i^2+3h_ih_{i+1}+h_{i+1}^2}{6h_ih_{i+1}}b_{mm}(x_i)\\
&\quad+\frac{h_{i+1}^2+h_ih_{i+1}-h_i^2}{6h_{i+1}\left(h_{i+1}+h_i\right)}b_{mm}(x_{i+1})\\
&\geq \frac{h_i^2+3h_ih_{i+1}+h_{i+1}^2}{6h_ih_{i+1}}\rho\\
&\quad+\frac{\rho}{6\left(h_i+h_{i+1}\right)}\left(\frac{h_i^2h_{i+1}+h_ih_{i+1}^2-h_{i+1}^3+h_ih_{i+1}^2+h_i^2h_{i+1}-h_i^3}{h_ih_{i+1}}\right)\\
&= \frac{h_i^2+3h_ih_{i+1}+h_{i+1}^2}{6h_ih_{i+1}}\rho+\frac{\rho}{3}-\frac{h_i^2-h_ih_{i+1}+h_{i+1}^2}{6h_ih_{i+1}}\rho\\
&= \frac{4h_ih_{i+1}}{6h_ih_{i+1}}\rho+\frac{\rho}{3}=\frac{2\rho}{3}+\frac{\rho}{3}=\rho>0.
\end{aligned}$$

2. In the outer layer $\left(\{x_i\}_{i=k_l}^{k_r}\right)$, the coefficients of hybrid difference discretisation are defined on the basis of a relation between $h_{\max}$ and ε such that

   - If $kh_{\max}^2\|b_{mm}\|_\infty > \varepsilon$, then the coefficients of central difference approximation given by 2.6.2 and 2.6.4 satisfy

     $$r^c_{m,i}>0,\ \ r^-_{m,i}<0,\quad \text{and}\quad r^+_{m,i}<0.$$

     Also,

     $$\begin{aligned}
     r^-_{m,i}+r^c_{m,i}+r^+_{m,i} &= \frac{-2\varepsilon}{h_i\left(h_{i+1}+h_i\right)}+\frac{2\varepsilon}{h_{i+1}h_i}+b_{mm}\left(x_i\right)+\frac{-2\varepsilon}{h_{i+1}\left(h_{i+1}+h_i\right)}\\
     &= b_{mm}(x_i)\geq\rho>0.
     \end{aligned}$$

   - If $kh_{\max}^2\|b_{mm}\|_\infty \leq \varepsilon$, the application of fourth-order Hermite method whose coefficients are given by 2.6.2 and 2.6.3, we have

     $$\begin{aligned}
     r^-_{m,i} &= \frac{-2\varepsilon}{h_i\left(h_i+h_{i+1}\right)}+\frac{h_i^2+h_ih_{i+1}-h_{i+1}^2}{6h_i\left(h_i+h_{i+1}\right)}b_{mm}(x_{i-1})\\
     &= \frac{1}{h_i\left(h_i+h_{i+1}\right)}\left(-2\varepsilon+\frac{h_i^2+h_ih_{i+1}-h_{i+1}^2}{6}b_{mm}(x_{i-1})\right).
     \end{aligned}$$

     Using $h_i\leq h_{\max}$, $h_{i+1}\leq h_{\max}$ and $b_{mm}(x_{i-1})\leq\|b_{mm}\|_\infty$, we get

     $$\begin{aligned}
     r^-_{m,i} &< \frac{1}{h_i\left(h_i+h_{i+1}\right)}\left(-2\varepsilon+\frac{h_{\max}^2\|b_{mm}\|_\infty}{6}\right)\\
     &< \frac{1}{h_i\left(h_i+h_{i+1}\right)}(-2\varepsilon+\varepsilon)<0.
     \end{aligned}$$

     Similarly, $r^c_{m,i}<0$, $r^+_{m,i}<0$ and $r^-_{m,i}+r^c_{m,i}+r^+_{m,i}\geq\rho>0$.

□

As a result, we conclude that the coefficient matrix associated with the hybrid difference discretisation

(2.6.1) satisfies the M-matrix criterion. Consequently, the hybrid difference operator $\mathbf{L}^N$ satisfies the discrete maximum principle as follows.

Lemma 2.6.2. Assume that the mesh function $\mathbf{J} = (J_1, J_2)^T$ satisfies $\mathbf{J}(x_0) \geq 0$ and $\mathbf{J}(x_N) \geq 0$. If $\mathbf{L}^N\mathbf{J}(x_i) \geq 0, \forall\, i = 1, \ldots, N-1$ then $\mathbf{J}(x_i) \geq 0, \forall\, i = 0, \ldots, N$.

Proof. Let $\min\limits_{m=1,2}\left\{J_m(x_k)\right\} = \min\limits_{m=1,2}\left(\min\limits_{k}\left\{J_m(x_k)\right\}\right) < 0$ for some k. Without loss of generality, assume that $J_1(x_k) \leq J_2(x_k)$. Certainly, $k \notin \{0, N\}$. Subsequently, $r^-_{1,k} < 0, r^+_{1,k} < 0$ and $q^-_k > 0, q^c_k > 0, q^+_k > 0$, hence

$$L^N_1\mathbf{J}(x_k) \equiv r^-_{1,k}J_{1,k-1} + r^c_{1,k}J_{1,k} + r^+_{1,k}J_{1,k+1} + q^-_k b_{12}(x_{k-1})J_{2,k-1} + q^c_k b_{12}(x_k)J_{2,k} + q^+_k b_{12}(x_{k+1})J_{2,k+1} < 0,$$

A contradiction to the assumption, and hence it follows that $\mathbf{J}(x_i) \geq 0, 0 \leq i \leq N$. □

Next, we verify the stability of the discrete hybrid operator $\mathbf{L}^N$ using the discrete maximum principle.

Lemma 2.6.3. Assume that the mesh function $\mathbf{J} = (J_1, J_2)^T$ satisfies $J_0 = J_N = 0$. Then

$$\|J\|_{\overline{\Omega}^N_E} \leq C\left\|L^N J\right\|_{\overline{\Omega}^N_E}.$$

Proof. Set $C_1 = C\left\|L^N\mathbf{J}\right\|_{\overline{\Omega}^N_E}$ to obtain the barrier functions $\mathbf{J}^\pm_i = \left(J^\pm_{1,i}, J^\pm_{2,i}\right)^T$ defined as $J^\pm_{m,i} = C_1 \pm J_{m,i}$ $\forall\, i = 0, \ldots, N$, $m = 1, 2$. Then, for $i = 1, \ldots, N-1$, $\mathbf{J}^\pm_0 \geq 0$, $\mathbf{J}^\pm_N \geq 0$ and

$$\begin{aligned} L^N\mathbf{J}^\pm_i = L^N\begin{pmatrix} C_1 \pm J_{1,i} \\ C_1 \pm J_{2,i} \end{pmatrix} &= C_1\begin{pmatrix} b_{11} + b_{12} \\ b_{21} + b_{22} \end{pmatrix} \pm L^N\begin{pmatrix} J_{1i} \\ J_{2i} \end{pmatrix} \\ &\geq C\begin{pmatrix} b_{11} + b_{12} \\ b_{21} + b_{22} \end{pmatrix}\left\|L^N\mathbf{J}\right\|_{\overline{\Omega}^N_E} - \left|L^N\mathbf{J}_i\right| \geq 0. \end{aligned}$$

Then, for $i = 1, \ldots, N-1$, $\mathbf{J}^\pm_i \geq 0$. □

2.7 Error Analysis

In this section, we investigate the order of accuracy of the proposed hybrid difference discretisation of (2.2.1) on the adaptive generated mesh. As in Section 2.4, we decompose the discrete approximate solution $\mathbf{Y}$ of (2.2.1) into smooth and layer part as $\mathbf{Y} = \mathbf{U} + \mathbf{V}$, where the smooth component $\mathbf{U}$ satisfies

$$\left[\mathbf{L}^N\mathbf{U}\right]_i = [\Gamma\mathbf{g}]_i, \quad i = 1, \ldots, N-1, \quad \text{where} \quad \mathbf{U}_0 = \mathbf{u}(0), \quad \text{and} \quad \mathbf{U}_N = \mathbf{u}(1),$$

while the layer part $\mathbf{V}$ satisfies

$$\left[\mathbf{L}^N\mathbf{V}\right]_i = 0, \quad i = 1, \ldots, N-1, \quad \text{where} \quad \mathbf{V}_0 = \mathbf{v}(0), \quad \text{and} \quad \mathbf{V}_N = \mathbf{v}(1).$$

Then, at each x_i, the error associated $\mathbf{Y}_i$ satisfies

$$\left\|\mathbf{Y}_i - \mathbf{y}(x_i)\right\| \leq \left\|\mathbf{U}_i - \mathbf{u}(x_i)\right\| + \left\|\mathbf{V}_i - \mathbf{v}(x_i)\right\|. \tag{2.7.1}$$

Thus, the consistency error estimation of the numerical solution can be done by estimating the errors associated with the smooth and layer parts. We begin the analysis with the smooth part.

Lemma 2.7.1. The smooth component $\mathbf{u}$ of the solution $\mathbf{y}$ and its discrete approximation $\mathbf{U}$ satisfies

$$\left\|\mathbf{L}^N(\mathbf{U}-\mathbf{u})(x_i)\right\| \leq CN^{-4}, \quad i=1,\ldots,N-1.$$

Proof. 1. When $i=\{1,\ldots,k_l-1\}$ and $i=\{k_r+1,\ldots,N-1\}$, for $m=1,2$, the hybrid difference approximation is obtained using the fourth-order Hermite difference method. Then, the Taylor expansion yields

$$\begin{aligned}\left\|L_m^N(\mathbf{U}-\mathbf{u})(x_i)\right\| &= \left|\left(L_m-L_m^N\right)\mathbf{u}(x_i)\right|, \quad m=1,2,\\ &\leq C\varepsilon\left|h_{i+1}-h_i\right|\left(h_i+h_{i+1}\right)^2\left\|u_m^{(v)}(x)\right\|_{[x_{i-1},x_{i+1}]}\\ &\quad + C\varepsilon\left(h_i^4+h_{i+1}^4\right)\left\|u_m^{(vi)}(x)\right\|_{[x_{i-1},x_{i+1}]}\\ &\leq C\varepsilon^{1/2}|h_{i+1}-h_i|\left(h_i+h_{i+1}\right)^2+C\left(h_i^4+h_{i+1}^4\right).\end{aligned}$$

Using the bounds of Lemmas 2.4.1, 2.5.2 and 2.5.3 with the assumption that $\sqrt{\varepsilon}\ll N^{-1}$, we get

$$\left\|L_m^N(\mathbf{U}-\mathbf{u})(x_i)\right\| \leq CN^{-4}, m=1,2.$$

2. When $i=\{k_l,\ldots,k_r\}$, the hybrid difference approximation depends on a relation between $h_{\max}$ and the parameter ε such that

   - When $kh_{\max}^2\|b_{mm}\|_\infty > \varepsilon$, using the central difference method to approximate the solution, the Taylor expansion with integral remainder yields

   $$\left\|L_m^N(\mathbf{U}-\mathbf{u})(x_i)\right\| = \left|\left(L_m-L_m^N\right)\mathbf{u}(x_i)\right| \leq C\varepsilon h_i^2\left\|u_m^{(iv)}(x)\right\|_{[x_{i-1},x_{i+1}]}, \; m=1,2.$$

   Using Lemmas 2.4.1 and 2.5.3 and the assumption that $\sqrt{\varepsilon}\ll N^{-1}$, we obtain

   $$\left\|\mathbf{L}^N(\mathbf{U}-\mathbf{u})(x_i)\right\| \leq CN^{-4}, \quad m=1,2, \;\; i=k_l,\ldots,k_r.$$

   - When $kh_{\max}^2\|b_{mm}\|_\infty \leq \varepsilon$, using fourth-order Hermite difference method to approximate the solution. Then, the Taylor expansion combined with the bounds of Lemma 2.4.1 and Lemma 2.5.3 yields

   $$\left\|L_m^N(\mathbf{U}-\mathbf{u})(x_i)\right\| = \left|\left(L_m-L_m^N\right)\mathbf{u}(x_i)\right| \leq C\varepsilon h_i^2\left\|u_m^{(iv)}(x)\right\|_{[x_{i-1},x_{i+1}]} \leq CN^{-4}.$$

□

Lemma 2.7.2. The layer component $\mathbf{v}$ of the solution $\mathbf{y}$ and its discrete approximation $\mathbf{V}$ satisfies

$$\left\|\mathbf{L}^N(\mathbf{V}-\mathbf{v})(x_i)\right\| \leq CN^{-4}, \quad i=1,\ldots,N-1.$$

Proof. 1. When $i=\{1,\ldots,k_l-1\}$ and $i=\{k_r+1,\ldots,N-1\}$, for the left segment of the boundary

layer region, Taylor expansions yield

$$\begin{aligned}\left\|L_m^N(\mathbf{V}-\mathbf{v})\right\| &= \left|\left(L_m - L_m^N\right)\mathbf{v}(x_i)\right| \\ &\leq C\varepsilon\left|h_{i+1}-h_i\right|\left(h_i+h_{i+1}\right)^2\left\|v_m^{(v)}(x)\right\|_{[x_{i-1},x_{i+1}]} \\ &\quad + C\varepsilon\left(h_i^4+h_{i+1}^4\right)\left\|v_m^{(vi)}(x)\right\|_{[x_{i-1},x_{i+1}]} \\ &\leq C\varepsilon h_i^4\left\|v_m^{(v)}(x)\right\|_{[x_{i-1},x_{i+1}]} + C\varepsilon h_i^4\left\|v_m^{(vi)}(x)\right\|_{[x_{i-1},x_{i+1}]}\end{aligned}$$

Now, using Lemma 2.4.1, Lemma 2.5.2, we get

$$\begin{aligned}\left|L_m^N(\mathbf{V}-\mathbf{v})(x_i)\right| &\leq C\varepsilon^{-\frac{3}{2}}h_i^4 e^{\left(-x_i\sqrt{\frac{\rho}{\varepsilon}}\right)} + C\varepsilon^{-2}h_i^4 e^{\left(-x_i\sqrt{\frac{\rho}{\varepsilon}}\right)} \\ &\leq C\varepsilon^{-1/2}\Psi^4 N^4 + C^{-1}\varepsilon^{-1}\Psi^4 N^{-4} \leq CN^{-4}.\end{aligned}$$

Similarly, we can estimate the result for the right segment of the boundary layer region, and the desired result follows immediately.

2. When $i = \{k_l,\ldots,k_r\}$, the hybrid difference method depends on a relation between $h_{\max}$ and the perturbation parameter ε such that

   - When $kh_{\max}^2\|b_{mm}\|_\infty > \varepsilon$, Taylor expansion with integral remainder yield

   $$\left\|L_m^N(\mathbf{V}-\mathbf{v})(x_i)\right\| = \left|\left(L_m - L_m^N\right)\mathbf{v}(x_i)\right| \leq C\varepsilon\left\|v_m''(x)\right\|_{[x_{i-1},x_{i+1}]},\ m=1,2.$$

   Now the derivative bounds derived in Lemma 2.4.1 yield

   $$\left\|\mathbf{L}^N(\mathbf{V}-\mathbf{v})(x_i)\right\| \leq C\begin{cases} e^{\left(-x_{i-1}\sqrt{\frac{\rho}{\varepsilon}}\right)}, & x_i \leq \dfrac{1}{2}, \\ e^{\left(-(1-x_{i+1})\sqrt{\frac{\rho}{\varepsilon}}\right)}, & x_i > \dfrac{1}{2}. \end{cases}$$

   For $i \geq k_l - 1$ and $x_i \leq \frac{1}{2}$, Lemma 2.5.1 suggests

   $$\begin{aligned}\left\|\mathbf{L}^N(\mathbf{V}-\mathbf{v})(x_i)\right\| &\leq Ce^{\left(-x_{k_l-1}\sqrt{\frac{\rho}{\varepsilon}}\right)} \\ &= C\left(e^{\left(-\frac{x_{k_l-1}}{4}\sqrt{\frac{\rho}{\varepsilon}}\right)}\right)^2 \leq CN^{-4}.\end{aligned}$$

   - When $kh_{\max}^2\|b_{mm}\|_\infty \leq \varepsilon$, Taylor expansion with the bounds of Lemma 2.4.1 and Lemma 2.5.3 yields

   $$\left\|L_m^N(\mathbf{V}-\mathbf{v})(x_i)\right\| = \left|\left(L_m - L_m^N\right)\mathbf{v}(x_i)\right| \leq C\varepsilon\left\|v_m''(x)\right\|_{[x_{i-1},x_{i+1}]} \leq CN^{-4}.$$

   Similarly, the bounds for $i \leq k_r$ and $x_i > \frac{1}{2}$ can be established. Thus, combining the various estimates completes the proof.

□

We now summarise all the previously derived error estimates to present the main convergence result.

The proof follows directly from Lemma 2.7.1, Lemma 2.7.2 and the triangle inequality (2.7.1).

Theorem 2.7.1. Let $\mathbf{y}$ be the solution of the problem (2.2.1) and $\mathbf{Y}$ be the solution of the problem (2.6.1). Then, there exists a positive constant C independent of N and ε such that

$$\left\|\mathbf{y}-\mathbf{Y}\right\|_{\bar{\Omega}_E^N} \leq CN^{-4}.$$

2.8 Numerical Experiments

In this section, we examine the performance of the method using three model problems and present numerical findings. When an exact solution to the problem is not available, we estimate the error $E_{m,\varepsilon}^N$ using the double mesh principle [5], given by:

$$E_{m,\varepsilon}^N = \max_{0\leq i\leq N} |Y_m^N(x_i) - \hat{Y}_m^{2N}(\hat{x}_{2i})|,\ m = 1,2.$$

However, if the exact solution is available, we evaluate the maximum pointwise errors using the formula:

$$E_{m,\varepsilon}^N = \max_{0\leq i\leq N} |Y_m^N(x_i) - y_m(x_i)|,\ m = 1,2.$$

Here, $y_m(x_i)$ represents the exact solution, and $Y_m^N(x_i)$ denotes the numerical solution obtained at the mesh points x_i of the adaptive mesh with N number of intervals. Moreover, we estimate the uniform errors using $E_m^N = \max_{\varepsilon\in K} E_{m,\varepsilon}^N$ where $K = \{\varepsilon | \varepsilon = 2^0, 2^{-2}, ..., 2^{-40}\}$ and compute the order of convergence and parameter-uniform orders of convergence using

$$p_{m,\varepsilon}^N = log_2\left(\frac{E_{m,\varepsilon}^N}{E_{m,\varepsilon}^{2N}}\right), \text{ and } p_m^N = log_2\left(\frac{E_m^N}{E_m^{2N}}\right).$$

In the adaptive mesh generation process, we choose $Q = 1.3$. Tables 2.1 and 2.2 compares the uniform errors and corresponding orders of convergence for the solution component Y_1 and Y_2, respectively, obtained using the hybrid fourth-order compact difference method on the equidistributed mesh where the test results clearly indicate that the nodal errors converge uniformly at the rate of $O(N^{-4})$ with the solution on piecewise uniform Shishkin mesh where the errors have almost third-order uniform convergence. This further demonstrates the suitability of the equidistributed mesh in comparison to the piecewise uniform Shishkin mesh. Utilising the transition parameter to construct the Shishkin mesh by dividing $\bar{\Omega} = [0,1]$ into into three segments: $[0,\sigma]$, $[\sigma, 1-\sigma]$ and $[1-\sigma, 1]$. The segments $[0,\sigma]$ and $[1-\sigma,1]$ are each subdivided into $\frac{N}{4}$ mesh intervals, while the segment $[\sigma, 1-\sigma]$ contains $\frac{N}{2}$ mesh intervals. In Examples 2.8.1 and 2.8.2, we set $\rho = 0.9$ for the Shishkin mesh construction. For Example 2.8.2, Table 2.3 compares the maximum pointwise error and order of convergence using the proposed method and methods in [289, 290]. Similarly, for Example 2.8.3, Table 2.4 compares the maximum pointwise error and order of convergence using the proposed method and methods in [289, 291].

Figures 2.1 and 2.5 illustrate the numerical solution of a system of second-order reaction-diffusion

Table 2.1: Comparison of errors E_m^N and orders of convergence p_m^N in approximations Y_m for Example 2.8.1 with $\varepsilon = 2^{-32}$ on the equidistributed mesh and shishkin mesh.

Mesh		$N=64$	$N=128$	$N=256$	$N=512$	$N=1024$	$N=2048$
Equidistributed	E_1^N	1.065e−03	6.512e−05	3.919e−06	2.358e−07	1.349e−08	7.511e−10
Mesh	p_1^N	4.03	4.05	4.05	4.12	4.16	
	E_2^N	8.761e−04	5.232e−05	3.104e−06	1.784e−07	1.003e−08	5.395e−10
	p_2^N	4.06	4.07	4.12	4.15	4.21	
Shishkin	E_1^N	8.184e−03	1.051e−03	1.295e−04	1.554e−05	1.832e−06	2.017e−10
Mesh	p_1^N	2.96	3.02	3.05	3.08	3.18	
	E_2^N	4.030e−03	5.108e−04	6.201e−05	7.479e−06	8.623e−07	9.400e−10
	p_2^N	2.97	3.04	3.05	3.11	3.19	

equations for Example 2.8.1 with $N = 128$ and for Example 2.8.2 with $N = 160$, computed using the proposed hybrid compact difference method. The plot shows the behaviour of the numerical solution across the domain. The boundary layer effect is evident, highlighting the method's ability to capture steep gradients near the boundary. Figures 2.2 and 2.6 depict a log-log plot of the maximum point-wise errors against the number of mesh intervals for Example 2.8.1 and 2.8.2, respectively. The plot illustrates the error convergence rates for the two components of the solution. The linear behaviour in the log-log plot indicates fourth-order convergence, validating the theoretical error estimates provided in the paper.

Example 2.8.1. Consider the following system of second-order reaction diffusion equation for $x \in \Omega = (0,1)$

$$-\varepsilon \mathbf{y}''(x) + \begin{pmatrix} 10+e^{-x} & -6x^2 \\ -x^4|x| & 7+2x^3 \end{pmatrix} \mathbf{y}(x) = \begin{pmatrix} 6+5x^2 \\ 5+x^3 \end{pmatrix},$$

where $\mathbf{y}(0) = (-e/2, 0)$ and $\mathbf{y}(1) = (0, -0.2)$.

Example 2.8.2. Consider the following system of second-order reaction diffusion equation for $x \in \Omega = (0,1)$

$$-\varepsilon \mathbf{y}''(x) + \begin{pmatrix} 2(x+1)^2 & -(1+x^3) \\ -2\cos\left(\frac{\pi x}{4}\right) & (1+\sqrt{2})e^{1-x} \end{pmatrix} \mathbf{y}(x) = \begin{pmatrix} 2e^x \\ 10x+1 \end{pmatrix},$$

where $\mathbf{y}(0) = 0$ and $\mathbf{y}(1) = 0$.

Example 2.8.3. Consider the following system of second-order reaction diffusion equation for $x \in \Omega = (0,1)$

$$-\varepsilon \mathbf{y}''(x) + \begin{pmatrix} 1 & -0.5 \\ -2 & 4 \end{pmatrix} \mathbf{y}(x) = \mathbf{g}(x),$$

where $\mathbf{y}(0) = (3,0)$ and $\mathbf{y}(1) = (3,0)$. Here, the function $\mathbf{g}(x) = (g_1(x), g_2(x))^T$ is choosen such that the exact solution of the problem reads

$$y_1(x) = \frac{e^{-\frac{x}{\sqrt{\varepsilon}}} + e^{-\frac{(1-x)}{\sqrt{\varepsilon}}}}{1+e^{-\frac{1}{\sqrt{\varepsilon}}}} + \frac{e^{-\frac{2x}{\sqrt{\varepsilon}}} + e^{-\frac{2(1-x)}{\sqrt{\varepsilon}}}}{1+e^{-\frac{2}{\sqrt{\varepsilon}}}} - x + x^2 + \cos^2(\pi x),$$

$$y_2(x) = \frac{e^{-\frac{x}{\sqrt{\varepsilon}}} + e^{-\frac{(1-x)}{\sqrt{\varepsilon}}}}{1+e^{-\frac{1}{\sqrt{\varepsilon}}}} - \frac{e^{-\frac{2x}{\sqrt{\varepsilon}}} + e^{-\frac{2(1-x)}{\sqrt{\varepsilon}}}}{1+e^{-\frac{2}{\sqrt{\varepsilon}}}} + \sin(\pi x).$$

Table 2.2: Comparison of errors E_m^N and orders of convergence p_m^N in approximations Y_m for Example 2.8.2 with $\varepsilon = 2^{-32}$ on the equidistributed mesh and shishkin mesh.

Mesh		$N=64$	$N=128$	$N=256$	$N=512$	$N=1024$	$N=2048$
Equidistributed	E_1^N	8.412e−04	5.067e−05	3.015e−06	1.742e−07	1.005e−08	5.632e−10
Mesh	p_1^N	4.05	4.07	4.11	4.11	4.15	
	E_2^N	7.212e−04	4.291e−05	2.489e−06	1.415e−07	7.860e−09	4.253e−10
	p_2^N	4.07	4.10	4.13	4.17	4.20	
Shishkin	E_1^N	8.239e−03	1.215e−04	1.513e−05	1.859e−06	2.241e−07	2.659e−08
Mesh	p_1^N	2.76	3.00	3.02	3.05	3.07	
	E_2^N	4.382e−03	6.168e−04	7.709e−05	9.493e−06	1.145e−06	1.357e−07
	p_2^N	2.82	3.00	3.02	3.05	3.07	

Table 2.3: Comparison of errors E_m^N and orders of convergence p_m^N for the proposed method with [289], [290] for Example 2.8.2 with $\varepsilon = 2^{-32}$.

Method		$N=64$	$N=128$	$N=256$	$N=512$	$N=1024$
Proposed	E_1^N	8.412e−04	5.067e−05	3.015e−06	1.742e−07	1.005e−08
Method	p_1^N	4.05	4.07	4.11	4.11	
Method	E_ε^N	7.20e-03	8.81e-04	1.01e-04	1.07e-05	1.06e-06
in [289]	p_ε^N	3.03	3.12	3.24	3.34	
Method	E_ε^N	2.43e-01	9.88e-02	3.63e-02	1.28e-02	4.18e-03
in [290]	p_ε^N	1.30	1.44	1.50	1.62	

Table 2.4: Comparison of errors E_m^N and orders of convergence p_m^N for Example 2.8.3 for the proposed method with [291], [289] with $\varepsilon = 2^{-12}$.

Method		$N=64$	$N=128$	$N=256$	$N=512$	$N=1024$
Proposed	E_1^N	1.397e-05	1.077e-06	7.195e-08	4.575e-09	2.874e-10
Method	p_1^N	3.69	3.90	3.97	3.99	
	E_2^N	4.681e-06	3.284e-07	2.123e-08	1.338e-09	8.376e-11
	p_2^N	3.83	3.95	3.98	3.99	
Method	E_1^N	1.201e-1	3.127e-2	1.263e-2	3.427e-3	7.212e-4
in [291]	p_1^N	1.942	1.308	1.882	2.248	
	E_2^N	2.300e-1	6.308e-2	2.540e-2	6.938e-3	1.489e-3
	p_2^N	1.867	1.312	1.872	2.220	
Method	E_ε^N	7.20e-03	8.81e-04	8.82e-05	5.55e-06	3.47e-07
in [289]	p_ε^N	3.03	3.32	3.99	4.00	

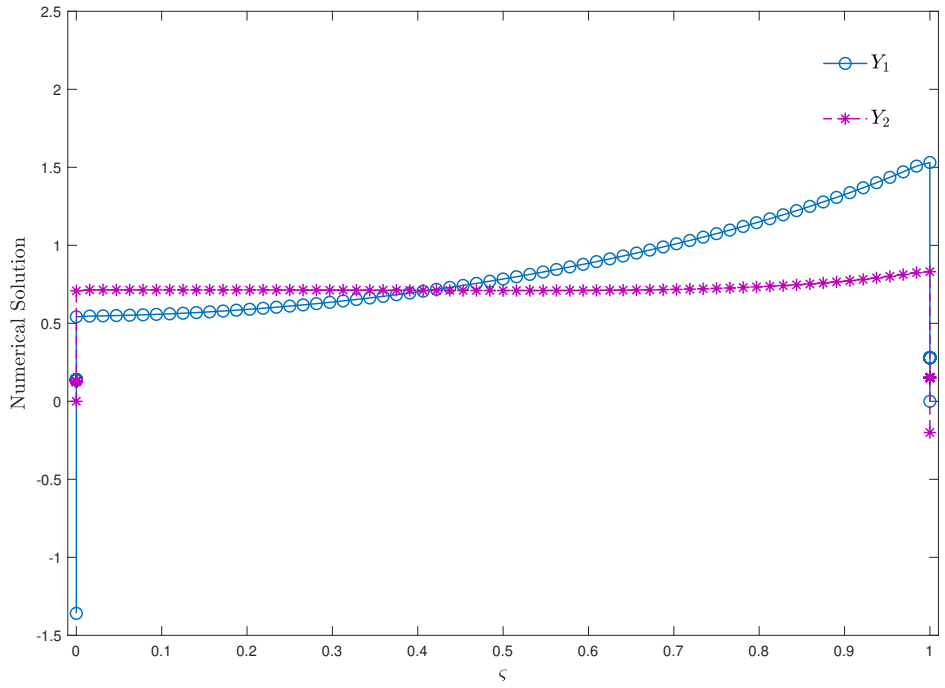

Fig. 2.1: Numerical solution for Example 2.8.1 with $N = 128$ and $\varepsilon = 2^{-36}$.

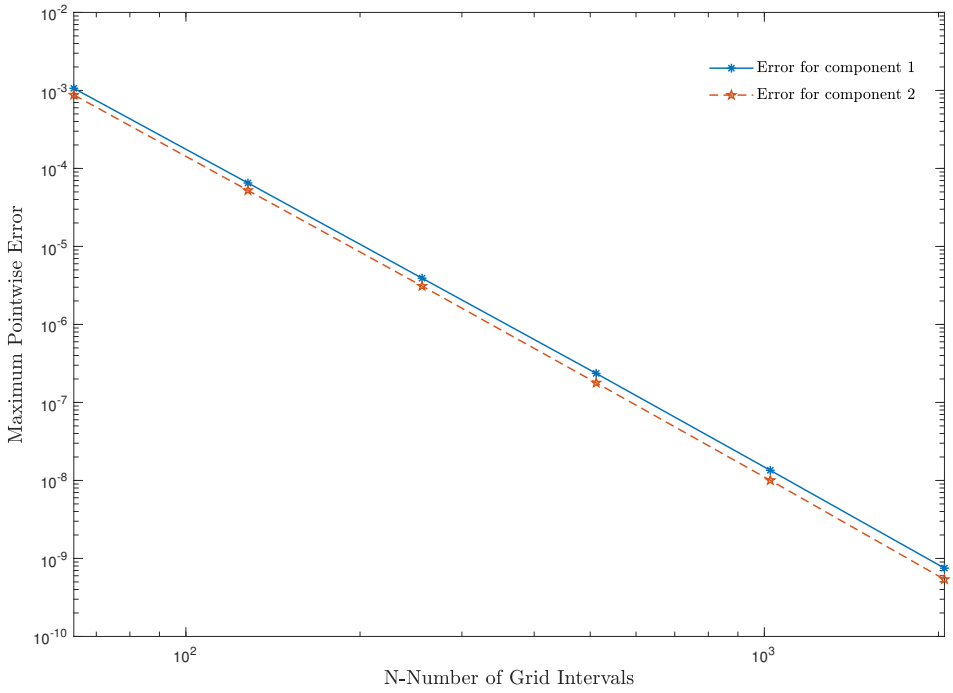

Fig. 2.2: Loglog plot of maximum pointwise errors for Example 2.8.1.

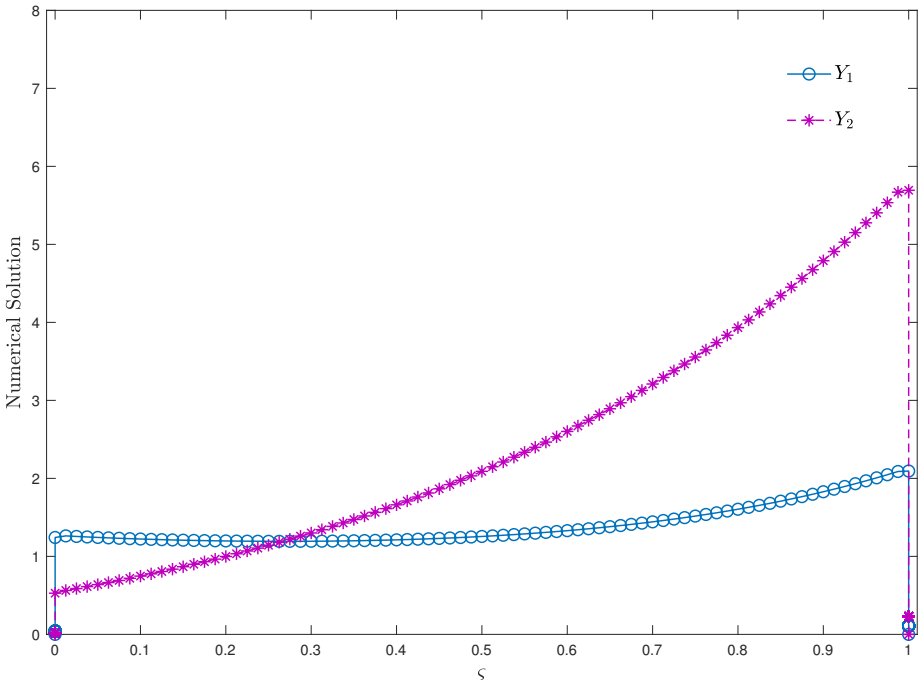

Fig. 2.3: Numerical solution for Example 2.8.2 with $N = 160$ and $\varepsilon = 10^{-12}$.

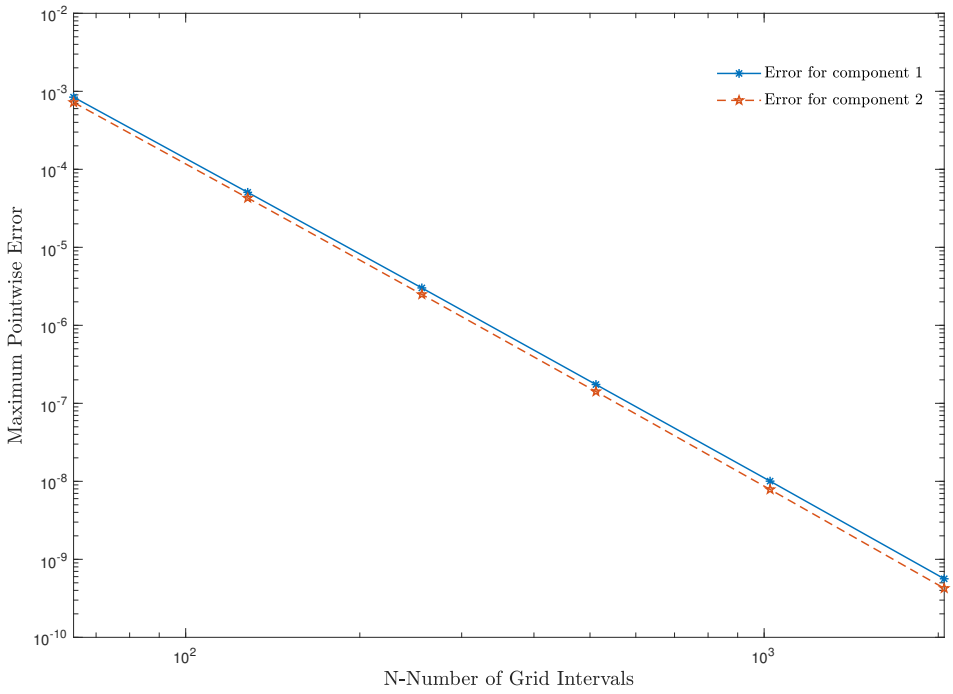

Fig. 2.4: Loglog plot of maximum pointwise errors for Example 2.8.2.

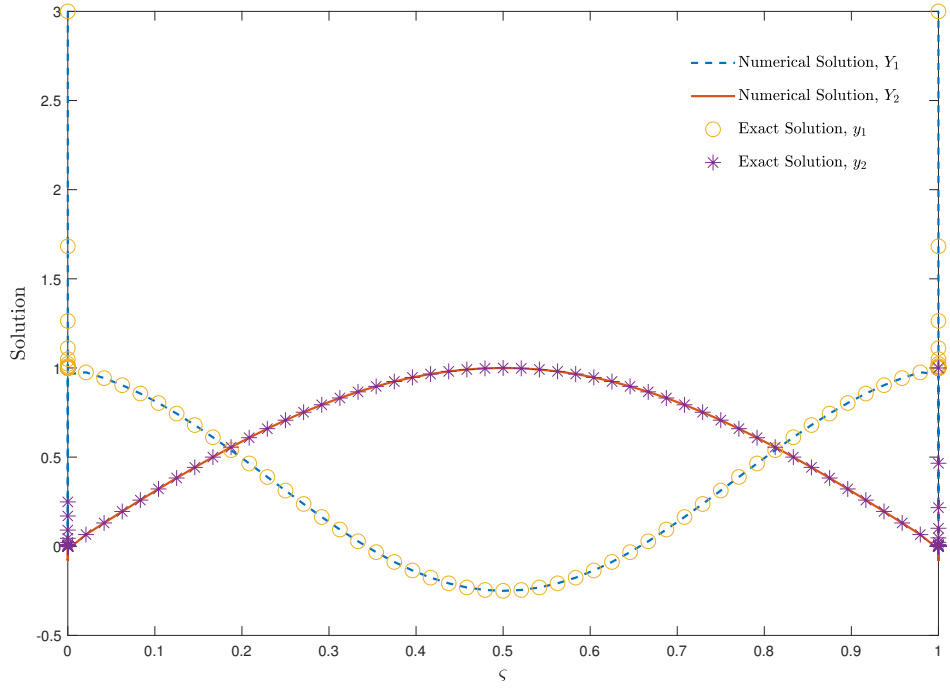

Fig. 2.5: Numerical and exact solution for Example 2.8.3 with $N = 96$ and $\varepsilon = 10^{-12}$.

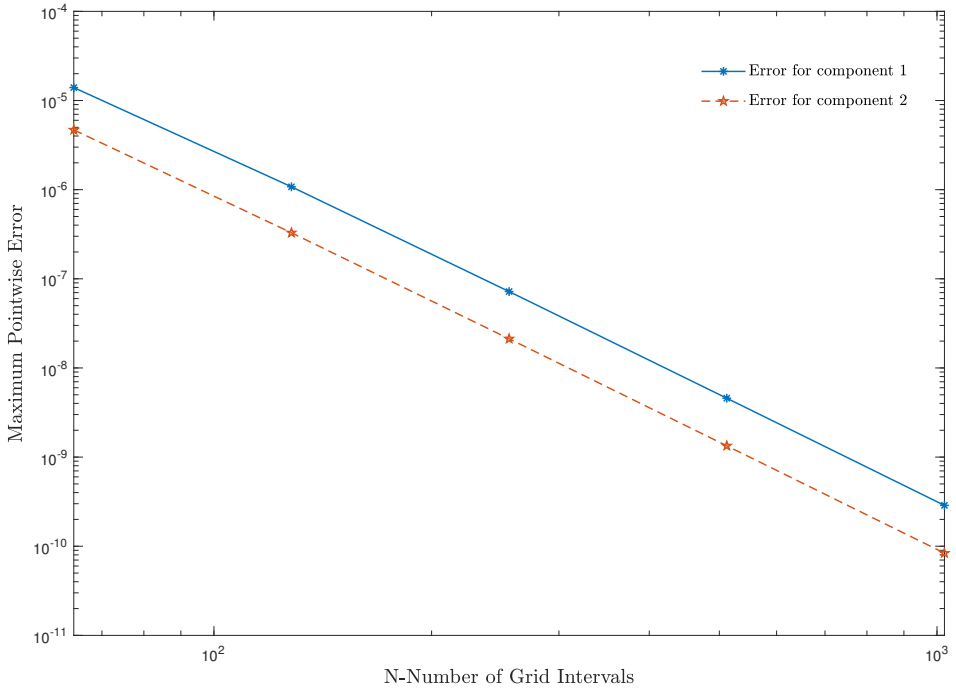

Fig. 2.6: Loglog plot of maximum pointwise errors for Example 2.8.3.

2.9 Conclusion

A singularly perturbed system of reaction-diffusion equations with Dirichlet boundary conditions is solved numerically using a higher-order hybrid method over an equidistributed mesh. The proposed method combines a fourth-order Hermite difference method with the classical central difference method over a layer-adapted mesh. The adaptive mesh is constructed by equidistributing a nonnegative monitor function that takes advantage of the derivatives of the singular component of the solution. The mesh generation procedure does not require a priori information about the analytical behaviour of the solution. The theoretical and numerical analysis of the method confirms parameter-uniform convergence of almost fourth order while maintaining unconditional stability. The comparative study of numerical results further suggests that the method is superior to many adaptive methods available in the literature.

Chapter 3

System of Reaction-Diffusion Equations with Shifts

3.1 Introduction

A singularly perturbed system of reaction-diffusion equations represents a class of mathematical models that describe the dynamics of phenomena where diffusion and reaction processes occur simultaneously but at significantly different rates. These systems are characterised by having one or more small parameters relative to others, resulting in multiscale behaviour. In such systems, the diffusion term dominates at one scale, while the reaction term dominates at another, leading to intricate phenomena such as boundary layer formation and sharp transition regions [3, 5]. Singularly perturbed systems find applications in various fields, including biology [266], chemistry [10], physics [25, 26], and engineering [7, 9, 24], where understanding the intricate interplay between diffusion and reaction is crucial to accurately predict system behaviour.

The analysis and solution of these systems often require specialised mathematical techniques, such as asymptotic analysis and numerical methods tailored to handle stiffness and boundary layer phenomena. Although asymptotic and numerical methods offer valuable tools for tackling singularly perturbed systems of reaction-diffusion equations, they also have limitations [89, 5]. Asymptotic methods, such as matched asymptotic expansions, can struggle to provide accurate solutions in regions where multiple lengths or time scales interact [58]. This leads to challenges in identifying appropriate asymptotic expansions or neglecting important terms. Additionally, these methods often rely on analytical approximations, which may not fully capture the system's behaviour. Numerical methods also have limitations when applied on uniform meshes [5]. The numerical methods on uniform meshes require excessively fine meshes to accurately capture the behaviour within the boundary layers, leading to computationally expensive simulations [5, 4]. Adaptive mesh refinement techniques address this challenge by automatically increasing the mesh resolution in regions where it is needed most, such as near steep gradients or boundary layers, while maintaining coarser meshs in smoother areas [6]. As a result, adaptive meshes enable more efficient and accurate simulations of singularly perturbed systems, making them

indispensable tools for researchers and practitioners studying these complex phenomena [5, 1].

Many authors have made efforts to develop numerically accurate techniques to solve systems involving reaction-diffusion equations [292, 203]. In [291], the authors consider a coupled system of singularly perturbed reaction-diffusion equations and present a higher-order method based on differential identity expansion defined on a Shishkin mesh. The discrete operator satisfies the maximum principle and the method converges uniformly. In [293], the authors use a similar technique to solve a coupled system of singularly perturbed initial value problems. In addition, the paper addresses a system of interconnected first-order nonlinear differential equations. The nonlinear system of equations is linearised using a quasi-linearisation process, resulting in a series of linear equations. The resultant linear equations are then solved using a higher-order differential identity expansion method (HODIE). In [282], one can find a first-order uniform method based on the central difference method on a Shishkin mesh. The authors in [290, 294] demonstrate that the central difference method is almost second-order accurate. In [295], the author dealt with a relatively simple situation involving a system of two equations. In [296], the authors present an overview of methods for solving a system of two equations. In [297], the authors consider a system of two equations and employ the HODIE technique to achieve uniform higher-order convergence. However, only in [297] does the order of convergence exceed two for the system of reaction-diffusion equations. In [298], the author presents a hybrid FDM to solve a system of reaction-diffusion equations with a negative shift. In [299], the author proposed a parameter-uniform method for a similar system with integral boundary conditions.

The analysis of special methods for the coupled system of singularly perturbed differential equations with shifts based on equidistributed meshs has seen limited development and lacks attention. Researchers have applied algorithms based on equidistribution principles to many practical problems, but have conducted little theoretical analysis to explain their success. The reason is primarily due to the inherent nonlinear nature of adaptive methods. This chapter presents a higher-order hybrid approximation using splines over an adaptive mesh generated by the equidistribution of a positive monitor function. Additionally, the chapter presents rigorous theoretical analysis, establishes parameter-uniform error estimates, and provides insight into the convergence behaviour of equidistributed meshs. Numerical results and illustrations for model problems support the theoretical projections.

3.2 Continous Problem

Consider the system of singularly perturbed reaction-diffusion equations with a shift given below

$$\begin{cases} \mathbf{L}\mathbf{y}(x) := & -\varepsilon \mathbf{y}''(x) + \mathbf{A}\mathbf{y}(x) + \mathbf{B}\mathbf{y}(x-\delta) = \mathbf{g}(x),\ x \in \Omega = (0,1) \\ & \mathbf{y}(x) = \boldsymbol{\rho}(x),\ x \in [-\delta, 0], \quad \mathbf{y}(1) = \mathbf{l} \end{cases} \tag{3.2.1}$$

where $0 < \varepsilon \ll 1$ is the perturbation parameter and δ denotes the small shift of order $o(\varepsilon)$. Here, $\mathbf{y}(x) = (y_1(x), y_2(x))^T$, $\mathbf{A} = (a_{mj}(x))_{2\times 2}$ is an L_0-matrix, $\mathbf{B} = diag(b_1(x), b_2(x))$ is a diagonal matrix. The source vector $\mathbf{g}(x) = (g_1(x), g_2(x))^T$ and the given data $a_{mj}(\cdot)$, $b_m(\cdot)$ and $\boldsymbol{\rho}(x) = (\rho_1(x), \rho_2(x))^T$

are sufficiently smooth functions defined on $\bar{\Omega}$. Besides, for every m and j

$$a_{mm} > 0,\ b_m > 0,\ \min\left\{\left\|\frac{a_{mj}}{a_{mm}+b_m}\right\|, \left\|\frac{a_{mj}}{\delta b_m}\right\|\right\} < 1 \text{ and } a_{mj} \leq 0\ \forall\, m \neq j,\ \ m,j = 1,2. \tag{3.2.2}$$

Since δ is of order $o(\varepsilon)$, the Taylor's series expansion of $\mathbf{y}(x-\delta)$ after neglecting the higher order derivative terms in (3.2.1) leads to

$$\begin{cases} \mathbf{L}\mathbf{y}(x) := & -\varepsilon \mathbf{y}''(x) - \delta \mathbf{B}\mathbf{y}'(x) + (\mathbf{A}+\mathbf{B})\mathbf{y}(\mathbf{x}) = \mathbf{g}(\mathbf{x}) \\ & \mathbf{y}(0) = \boldsymbol{\rho}(0) = \boldsymbol{\rho}, \quad \mathbf{y}(1) = \mathbf{l} \end{cases} \tag{3.2.3}$$

where $||.||$ represents the maximum norm on Ω. The above hypotheses ensure that the problem (3.2.1) admits a unique solution $\mathbf{y} = (y_1, y_2)^T \in \left(C^2(\Omega) \cap C(\bar{\Omega})\right)$ [5].

3.3 Properties of the Solution

In this section, we begin our analysis by studying some analytical properties of the solution $\boldsymbol{y}$ that can be deduced from the standard maximum principle as shown in [128] and establish the stability of the differential operator. The differential operator $\mathbf{L} = (L_1, L_2)^T$ satisfies the maximum principle [285].

Lemma 3.3.1. Let $\mathbf{L}\mathbf{y} \geq 0$ on Ω and $\mathbf{y}(0) \geq 0$, $\mathbf{y}(1) \geq 0$. Then $\mathbf{y}(x) \geq 0$ on $\bar{\Omega}$.

Proof. Let $p, q \in \Omega$ be such that $y_1(p) = \min\limits_{x\in\bar{\Omega}}\{y_1(x)\}$ and $y_2(q) = \min\limits_{x\in\bar{\Omega}}\{y_2(x)\}$. Without loss of generality, assume that $y_1(p) \leq y_2(q)$ and let $y_1(p) < 0$. Clearly $p \neq \{0,1\}$, $y_1'(p) = 0$ and $y_1''(p) \geq 0$. Then

$$\begin{aligned} L_1\mathbf{y}(p) &\equiv -\varepsilon y_1''(p) - \delta b_1 y_1' + (a_{11}+b_1)y_1(p) + a_{12}y_2(p) \\ &= -\varepsilon y_1''(p) + (a_{11}+b_1+a_{12})y_1(p) + a_{12}(y_2(p) - y_1(p)) < 0. \end{aligned}$$

A contradiction to the assumption, and hence it follows that $\mathbf{y}(x) \geq 0$ for all $x \in \bar{\Omega}$. □

As an immediate consequence of the maximum principle, it is straightforward to obtain the following estimate.

Lemma 3.3.2. Let $\mathbf{y}(x)$ be any smooth function. Then

$$\|\mathbf{y}(x)\| \leq \max\{\|\mathbf{y}(0)\|, \|\mathbf{y}(1)\|, \max_{x\in\bar{\Omega}}\|L_1\mathbf{y}\|, \max_{x\in\bar{\Omega}}\|L_2\mathbf{y}\|\},\ \forall\, x \in \bar{\Omega}. \tag{3.3.1}$$

Using the stability property of the scalar differential operator, we proceed to estimate the stability of the operator $\mathbf{L}$ in the following lemma.

Lemma 3.3.3. Let $\mathbf{y}$ be the solution of (3.2.1) and (3.2.2) hold on $\bar{\Omega}$. Then

$$\|y_m\| \leq \sum_{j=1}^{2} (\boldsymbol{\Upsilon}^{-1})_{mj} \min\left\{\left\|\frac{g_j}{a_{jj}+b_j}\right\|, \left\|\frac{g_j}{\delta b_j}\right\|\right\},\ m = 1,2$$

where $\Upsilon = (\gamma_{mj})_{2\times 2}$ such that $\gamma_{mm} = 1$ and $\gamma_{mj} = -\min\left\{\left\|\frac{a_{mj}}{a_{mm}+b_m}\right\|, \left\|\frac{a_{mj}}{\delta b_m}\right\|\right\}$ for $m \neq j$.

Proof. Let $\mathbf{y} := \mathbf{u} + \mathbf{v}$ where the components $\mathbf{u}$ and $\mathbf{v}$ satisfy

$$-\varepsilon u_m'' - \delta b_m u_m' + (a_{mm}+b_m)u_m = g_m \text{ on } \Omega,\ u_m(0) = \rho_m,\ u_m(1) = l_m \text{ and}$$

$$-\varepsilon v_m'' - \delta b_m v_m' + (a_{mm}+b_m)v_m = -\sum_{\substack{j=1\\ j\neq m}}^{2} a_{mj}y_j \text{ on } \Omega, v_m(0) = 0, v_m(1) = 0.$$

Lemma 3.3.2 and the triangle inequality lead to

$$\|y_m\| - \sum_{\substack{j=1\\ j\neq m}}^{2} \min\left\{\left\|\frac{a_{mj}}{a_{mm}+b_m}\right\|, \left\|\frac{a_{mj}}{\delta b_m}\right\|\right\}\|y_j\| \leq \min\left\{\left\|\frac{g_m}{a_{mm}+b_m}\right\|, \left\|\frac{g_m}{\delta b_m}\right\|\right\},\ m = 1,2.$$

Since, matrix $\mathbf{A}$ and $\mathbf{B}$ satisfies (3.2.2), the matrix $\Upsilon = (\gamma_{mj})_{2\times 2}$ is a diagonally dominant L_0-matrix. Hence, Υ is inverse monotone and

$$\|y_m\| \leq \sum_{j=1}^{2} (\Upsilon^{-1})_{mj} \min\left\{\left\|\frac{g_j}{a_{jj}+b_j}\right\|, \left\|\frac{g_j}{\delta b_j}\right\|\right\},\ m = 1,2.$$

□

The stability of the differential operator $\mathbf{L}$ as established in Lemma 3.3.3, coupled with the standard maximum principle in Lemma 3.3.1, guarantees the existence of a unique solution $\mathbf{y} \in C^4(\bar{\Omega})^2$. To facilitate the analysis of the numerical discretisation of (3.2.1), we establish a priori bounds on the derivatives of the solution $\mathbf{y}$ as follows.

Lemma 3.3.4. Let $\mathbf{y}$ be the solution of (3.2.1) and $\omega \in (0,1) \subset \mathbb{R}$ be such that

$$\sum_{\substack{j=1\\ j\neq m}}^{2} \min\left\{\left\|\frac{a_{mj}}{a_{mm}+b_m}\right\|, \left\|\frac{a_{mj}}{\delta b_m}\right\|\right\} < \omega < 1 \text{ for } m = 1,2.$$

Then, for $k = 0,\ldots,4$

$$|y_m^{(k)}(x)| \leq C\left(1 + \varepsilon^{-\frac{k}{2}}\left(e^{\left(-x\sqrt{\frac{\rho}{\varepsilon}}\right)} + e^{\left(-(1-x)\sqrt{\frac{\rho}{\varepsilon}}\right)}\right)\right),\ \forall\, x \in \bar{\Omega}, \tag{3.3.2}$$

where $\rho = \rho(\omega) := (1-\omega)\min\limits_{m=1,2}\min\limits_{x\in[0,1]}(a_{mm}(x)+b_m(x)) > 0$.

Proof. We establish (3.3.2) by induction on k, the case $k = 0$ being immediate from Lemma 3.3.3. For $k > 1$, differentiate (3.2.1) k-times to get

$$-\varepsilon \mathbf{y}^{(k+2)} + \mathbf{A}\mathbf{y}^{(k)} + \mathbf{b}\mathbf{y}^{(k)} = \mathbf{g}^{(k)} - \sum_{l=0}^{k-1}\binom{k}{s}(\mathbf{A}^{(k-s)} + \mathbf{b}^{(k-s)})\mathbf{y}^{(s)} = \mathbf{f}_k,$$

where $\mathbf{f}_k = (f_{k,1}, f_{k,2})^T$. Let $|y_m^{(s)}(x)| \leq C\left(1+\varepsilon^{-\frac{k}{2}}\left(e^{\left(-x\sqrt{\frac{p}{\varepsilon}}\right)}+e^{\left(-(1-x)\sqrt{\frac{p}{\varepsilon}}\right)}\right)\right) := \hat{\mathscr{A}_k}$ for all $s \leq k-1$. Consequently, $|f_{k,m}(x)| \leq C\hat{\mathscr{A}_{k-1}}(x)$ for $m = 1,2$. For $x \in \bar{\Omega}$, define $\hat{\mathbf{y}}(x) := \frac{\mathbf{y}^{(k)}(x)}{\hat{\mathscr{A}_k}(x)}$. After careful manipulations, as outlined in [286] and using Lemma 3.3.2 along with the M-matrix criterion, we obtain the inequality $\|\hat{\mathbf{y}}\| \leq C$. Hence, from the definition of $\hat{\mathbf{y}}$, it follows that

$$|y_m^{(k)}(x)| \leq C\left(1+\varepsilon^{-\frac{k}{2}}\left(e^{\left(-x\sqrt{\frac{p}{\varepsilon}}\right)}+e^{\left(-(1-x)\sqrt{\frac{p}{\varepsilon}}\right)}\right)\right), \forall\, x \in \bar{\Omega}.$$

□

3.4 Solution Decomposition

The standard decomposition of the solution plays a crucial role in the convergence analysis of numerical methods for singularly perturbed problems. Therefore, we decompose the solution of (3.2.1) into smooth and layer parts as $\mathbf{y} = \mathbf{u} + \mathbf{v}$, where the smooth component $\mathbf{u} = (u_1, u_2)^T$ satisfy

$$\mathbf{L}\mathbf{u}(x) = \mathbf{g}(x),\ x \in \Omega;\ \mathbf{u}(0) = \mathbf{u}_0(0),\ \mathbf{u}(1) = \mathbf{u}_0(1) \tag{3.4.1}$$

and the layer part $\mathbf{v} = (v_1, v_2)^T$ satisfy

$$\mathbf{L}\mathbf{v}(x) = 0,\ x \in \Omega;\ \mathbf{v}(0) = \rho - \mathbf{u}_0(0),\ \mathbf{v}(1) = \mathbf{l} - \mathbf{u}_0(1). \tag{3.4.2}$$

Following this, we utilise a proposition from [300] stated below and the standard factorisation to estimate precise bounds on the components and their derivatives.

Proposition 3.4.1. Let $\mu > 0$ and $I = [\chi, \chi+\mu]$ be an arbitrary interval. If $F \in C^2(I)$, then

$$\|F'\|_I \leq \frac{2}{\mu}\|F\|_I + \frac{\mu}{2}\|F''\|_I.$$

Lemma 3.4.1. Let $\mathbf{y} := \mathbf{u} + \mathbf{v}$ be the solution of (3.2.1) where $\mathbf{u}$ and $\mathbf{v}$ satisfy (3.4.1) and (3.4.2), respectively. Then, the smooth part $\mathbf{u} = (u_1, u_2)^T$ satisfies

$$\|u_m^{(k)}\| \leq C\left(1+\varepsilon^{\frac{(2-k)}{2}}\right),\ k = 0,...,4,\ m = 1,2,$$

and the layer part $\mathbf{v} = (v_1, v_2)^T$ satisfies

$$\|v_m^k\| \leq C\left(1+\varepsilon^{-\frac{k}{2}}\left(e^{\left(-x\sqrt{\frac{p}{\varepsilon}}\right)}+e^{\left(-(1-x)\sqrt{\frac{p}{\varepsilon}}\right)}\right)\right),\ k = 0,...,4,\ m = 1,2 \text{ and } \rho \in \bar{\Omega}.$$

Proof. Writing $\mathbf{u}(x)$ as an asymptotic series expansion that reads

$$\mathbf{u}(x) = \mathbf{u}_0(x) + \varepsilon\mathbf{u}_1(x) + \varepsilon^2\mathbf{u}_2^*(x) = (u_{0,1}(x) + \varepsilon u_{1,1}(x) + \varepsilon^2 u_{2,1}^*(x), u_{0,2}(x) + \varepsilon u_{1,2}(x) + \varepsilon^2 u_{2,2}^*(x))^T.$$

Substitute $\mathbf{u}(x)$ into (3.2.1) and equate coefficients of like powers of ε to obtain

$$\begin{aligned}
&\mathbf{A}(x)\mathbf{u}_0(x)+\mathbf{b}(x)\mathbf{u}_0(x-\delta)=\mathbf{g}(x)\\
&\mathbf{A}(x)\mathbf{u}_1(x)+\mathbf{b}(x)\mathbf{u}_1(x-\delta)=\mathbf{u}_0''(x),\\
&\mathbf{L}\mathbf{u}_2^*(x)=\mathbf{u}_1''(x),\ \mathbf{u}_2^*(0)=\mathbf{u}_2^*(1)=0.
\end{aligned}$$

Then, from Lemma (3.3.4), it follows that

$$\|u_m^{(k)}\|\leq C,\ k=0,1,2\ \text{ and }\ m=1,2.$$

Next, we differentiate $\mathbf{Lu}=\mathbf{g}$ twice to obtain $\|u_m^{(iv)}\|\leq C\varepsilon^{-1}$, $m=1,2$. Finally, for $\mathbf{I}\subseteq\Omega$, Proposition (3.4.1) with $F=u_m''$ and $\mu=\varepsilon^{\frac{1}{2}}$ yields $\|u_m'''\|=C\varepsilon^{-\frac{1}{2}}$, $m=1,2$.

To find bounds on $\mathbf{v}(x)=(\mathbf{v}_1(x),\mathbf{v}_2(x))^T$ and its derivatives, we factorise it further as $\mathbf{v}(x)=\mathbf{v}^-(x)+\mathbf{v}^+(x)$, where $\mathbf{v}^-(x)=(\mathbf{v}_1^-(x),\mathbf{v}_2^-(x))^T$ satisfy

$$\mathbf{L}\mathbf{v}^-(x)=0,\ x\in\Omega,\ \mathbf{v}^-(0)=\mathbf{v}(0),\ \mathbf{v}^-(1)=0, \tag{3.4.3}$$

and $\mathbf{v}^+(x)=(\mathbf{v}_1^+(x),\mathbf{v}_2^+(x))^T$ satisfy

$$\mathbf{L}\mathbf{v}^+(x)=0,\ x\in\Omega,\ \mathbf{v}^+(0)=0,\ \mathbf{v}^+(1)=\mathbf{v}(1). \tag{3.4.4}$$

Using the method of the matched asymptotic expansions, we find that

$$\mathbf{v}_m^-(x)=\sum_{s=0}^{2p+1}\varepsilon^{\frac{s}{2}}v_{s,m}^-(x)+\varepsilon^{p+1}v_{2(p+1),m}^{*-},\ m=1,2\text{ and} \tag{3.4.5}$$

$$\mathbf{v}_m^+(x)=\sum_{s=0}^{2p+1}\varepsilon^{\frac{s}{2}}v_{s,m}^+(x)+\varepsilon^{p+1}v_{2(p+1),m}^{*+},\ m=1,2. \tag{3.4.6}$$

For $\mathbf{v}^-$, stretch the variable using the coordinate transformation $\xi=\frac{x}{\sqrt{\varepsilon}}$ and using Taylor's series expansion of $\mathbf{A}(\sqrt{\varepsilon}\xi)$ to define $\hat{\mathbf{L}}=-\frac{d^2}{d\xi^2}-\delta\mathbf{b}(0)I$. Then, from (3.4.3)

$$\hat{\mathbf{L}}\mathbf{v}_0^-(\xi)=0,\ \mathbf{v}_0^-=\rho-\mathbf{u}_0^-(0)\text{ and }\lim_{\xi\to\infty}\mathbf{v}_0^-(\xi)=0,$$

$$\begin{cases}
\hat{\mathbf{L}}\mathbf{v}_s^-(\xi)=-\sum_{j=1}^{s}\Big(-\frac{\xi^j}{j!}\delta\mathbf{b}^j(0)\mathbf{v}_{s-j}'^-(\xi)+\frac{\xi}{(j-1)!}(\mathbf{A}^{j-1}(0)+\mathbf{b}^{j-1}(0))\mathbf{v}_{s-j}^-(\xi)\Big)\\
\mathbf{v}_s^-=-\mathbf{u}_s^-(0),\ \lim_{\xi\to\infty}\mathbf{v}_s^-(\xi)=0,\ s=1,...,2k+1
\end{cases}$$

and

$$\begin{cases}
\mathbf{L}\mathbf{v}_{2p+2}^{*-}(x)=-\varepsilon^{-(p+1)}\mathbf{L}(\mathbf{v}_0^-+\cdots+\varepsilon^{\frac{(2p+1)}{2}}\mathbf{v}_{2p+1}^-)(x),\\
\mathbf{v}_{2p+2}^{*-}(0)=0,\ \mathbf{v}_{2p+2}^{*-}(1)=-\varepsilon^{-(p+1)}\mathbf{L}(\mathbf{v}_0^-+\cdots+\varepsilon^{\frac{(2p+1)}{2}}\mathbf{v}_{2p+1}^-)(1).
\end{cases}$$

Thus, from Lemma (3.3.4), it follows that v_m^- satisfies

$$|v_m^-(0)| < C,\ |v_m^-(1)| < Ce^{\left(-\sqrt{\frac{\rho}{\varepsilon}}\right)},\ \text{and}\ |v_m^-(k)| < C\varepsilon^{-\frac{k}{2}}e^{\left(-x\sqrt{\frac{\rho}{\varepsilon}}\right)},\ m = 1,2.$$

Similarly, we can establish the derivative bounds for v_m^+ to complete the proof. □

3.5 Mesh Structure

To construct an adaptive mesh, we propose a mesh generation algorithm based on the mesh equidistribution principle. The algorithm begins with a uniform mesh and then refines it into a layer-adapted mesh by equidistributing a nonnegative monitor function. This function helps improve the mesh structure by estimating the error bound on the computed approximation. In singularly perturbed differential equations, these estimates account for sudden changes in solution behaviour due to steep boundary layers.

For a suitable monitor function $M(y(\varkappa),\varkappa) > 0$, the equidistribution principle defines a mapping $x = x(\xi)$ that relates the physical coordinate $\varkappa \in [0,1]$ to the numerical coordinate $\xi \in [0,1]$ using the relation

$$\int_0^{x(\xi)} M(y(\varkappa),\varkappa)d\varkappa = \xi \int_0^1 M(y(\varkappa),\varkappa)d\varkappa. \tag{3.5.1}$$

Thus, a nonuniform mesh $\bar{\Omega}^N$ is generated using the relation

$$\int_{x_{i-1}}^{x_i} M(y(\varkappa),\varkappa)d\varkappa = \frac{1}{N}\int_0^1 M(y(\varkappa),\varkappa)d\varkappa.$$

We consider the following monitor function

$$M = \beta + |v_1''|^{\frac{1}{2}} + |v_2''|^{\frac{1}{2}} \tag{3.5.2}$$

where v_1 and v_2 are the layer components of the solution $\boldsymbol{y} = (y_1, y_2)^T$ and β is a positive constant. Earlier work [108, 287, 278] shows that one should choose the least value of the monitor function with caution to improve convergence. Therefore, setting an appropriate floor value β, the mesh prevents point clustering within layers and ensures a proper distribution of mesh points outside layers.

The leading term in the expression (3.4.5) and (3.4.6) yields an approximation of $v_m''(x)$, $m = 1,2$ given by

$$v_m''(x) = \begin{cases} \dfrac{\alpha_0}{\varepsilon}e^{\left(-x\sqrt{\frac{\rho}{\varepsilon}}\right)}, & x \in [0, \frac{1}{2}], \\ \dfrac{\alpha_1}{\varepsilon}e^{\left(-(1-x)\sqrt{\frac{\rho}{\varepsilon}}\right)}, & x \in \left(\frac{1}{2}, 1\right], \end{cases}$$

where α_0 and α_1 are the constants. Imitating the analysis from [277, 287, 278], we have

$$\int_0^1 (|v_1''|^{\frac{1}{2}} + |v_2''|^{\frac{1}{2}})dx \equiv \Psi \approx \frac{2}{\sqrt{\rho}}(|\alpha_0|^{\frac{1}{2}} + |\alpha_1|^{\frac{1}{2}}). \tag{3.5.3}$$

Now, using (3.5.2) and (3.5.1) to obtain a map

$$\frac{\beta}{\Psi}x(\xi)+\mu_0\Big(1-e^{\Big(-\frac{x(\xi)}{2}\sqrt{\frac{\rho}{\varepsilon}}\Big)}\Big)=\xi\Big(\frac{\beta}{\Psi}+1\Big),\ x(\xi)\leq\frac{1}{2} \tag{3.5.4}$$

and

$$\frac{\beta}{\Psi}(1-x(\xi))+\mu_1\Big(1-e^{\Big(-\frac{(1-x(\xi))}{2}\sqrt{\frac{\rho}{\varepsilon}}\Big)}\Big)=(1-\xi)\Big(\frac{\beta}{\Psi}+1\Big),\ x(\xi)>\frac{1}{2} \tag{3.5.5}$$

where $\mu_0=\dfrac{|\alpha_0|^{\frac{1}{2}}}{|\alpha_0|^{\frac{1}{2}}+|\alpha_1|^{\frac{1}{2}}}$ and $\mu_1=\dfrac{|\alpha_1|^{\frac{1}{2}}}{|\alpha_0|^{\frac{1}{2}}+|\alpha_1|^{\frac{1}{2}}}=1-\mu_0$.

Given the relation between adaptive mesh $\{x_i\}_{i=0}^N$ and uniform mesh $\Big\{\xi_i=\dfrac{i}{N}\Big\}_{i=0}^N$, the required nonuniform mesh is given by

$$\frac{\beta}{\Psi}x_i+\mu_0\left(1-e^{\left(-\frac{x_i}{2}\sqrt{\frac{\rho}{\varepsilon}}\right)}\right)=\frac{i}{N}\left(\frac{\beta}{\Psi}+1\right),\ x_i\leq\frac{1}{2} \tag{3.5.6}$$

and

$$\frac{\beta}{\Psi}(1-x_i)+\mu_1\left(1-e^{\left(-\frac{(1-x_i)}{2}\sqrt{\frac{\rho}{\varepsilon}}\right)}\right)=\left(1-\frac{i}{N}\right)\left(\frac{\beta}{\Psi}+1\right),\ x_i>\frac{1}{2}. \tag{3.5.7}$$

Next, for an appropriate β, we examine the structure of the generated mesh, some of its associated properties, and illustrate its distribution.

Lemma 3.5.1. Let $\beta=\Psi$. Then

$$x_{k_l}<2\sqrt{\frac{\varepsilon}{\rho}}logN<x_{k_{l+1}}\text{ and }x_{k_{r-1}}<1-2\sqrt{\frac{\varepsilon}{\rho}}logN<x_{k_r}$$

where

$$k_l=\left[\frac{\mu_0}{2}(N-1)+\sqrt{\frac{\varepsilon}{\rho}}NlogN\right]\text{ and }k_r=\left[N-\left(\frac{\mu_1}{2}(N-1)+\sqrt{\frac{\varepsilon}{\rho}}NlogN\right)\right]+1.$$

Here, $[\cdot]$ represents the integral part of the term. Moreover,

$$e^{\left(-\frac{x_i}{2}\sqrt{\frac{\rho}{\varepsilon}}\right)}\leq CN^{-1},\ i\geq k_l-1,\ x_i\leq\frac{1}{2}\text{ and }e^{\left(-\frac{(1-x_i)}{2}\sqrt{\frac{\rho}{\varepsilon}}\right)}\leq CN^{-1},\ i\leq k_r,\ x_i>\frac{1}{2}.$$

Proof. Put $x_i=2\sqrt{\frac{\varepsilon}{\rho}}\log N$ in (3.5.6) and solve for i to find k_l. Using (3.5.7) we can similarly compute k_r. □

Setting $\beta=\Psi$ aligns the equidistributed mesh with some features of the a priori mesh. However, exponential stretching within layers reduces discretisation errors, enhancing precision [288]. Next, we obtain bounds on the width of the mesh in the layer region $\Big(\{x_i\}_{i=0}^{k_l-1}$ and $\{x_i\}_{i=k_r+1}^{N}\Big)$ and the outer region $\Big(\{x_i\}_{i=k_l}^{k_r}\Big)$.

Lemma 3.5.2. For $i = \{1,...,k_l\} \cup \{k_r+1,...,N\}$, $h_i := h_i - h_{i-1} < 2C\sqrt{\frac{\varepsilon}{\rho}}$. Moreover

$$|h_{i+1} - h_i| \leq \begin{cases} Ch_i^2, & i = 1,...,k_l - 1, \\ Ch_{i+1}^2, & i = k_r+1,...,N-1. \end{cases}$$

Proof. We prove the result for the left layer region. The result for the right layer region follows analogously. Imitating the steps from [278, Lemma 3.2] we use (3.5.6) to obtain $\bar{x}_i > x_i$ such that

$$e^{\left(-\frac{x_i}{2}\sqrt{\frac{\rho}{\varepsilon}}\right)} = 1 - \frac{2i}{\mu_0 N}.$$

A rearrangement of terms yields

$$x_i < \bar{x}_i = -2\sqrt{\frac{\varepsilon}{\rho}} log\left(1 - \frac{2i}{\mu_0 N}\right).$$

Using $\bar{x}_i$ into (3.5.6) to compute

$$x_i > \underline{x_i} = -2\sqrt{\frac{\varepsilon}{\rho}} log\left(1 - \frac{1}{\mu_0}\left(\frac{2i}{N} + 2\sqrt{\frac{\varepsilon}{\rho}} log\left(1 - \frac{2i}{\mu_0 N}\right)\right)\right).$$

Thus, for $i = 1,...,k_l$

$$h_i = x_i - x_{i-1} < \bar{x}_i - x_{i-1} = 2\sqrt{\frac{\varepsilon}{\rho}} log\left[1 + \frac{2 + 2\sqrt{\frac{\rho}{\varepsilon}} N log\left(\frac{\mu_0 N}{\mu_0 N - 2(i-1)}\right)}{\mu_0 N - 2i}\right] < 2C\sqrt{\frac{\varepsilon}{\rho}}.$$

Moreover, note that

$$\frac{|h_{i+1} - h_i|}{h_i^2} \leq \frac{2\left|x_{\xi\xi}\left(\theta_i^{(1)}\right)\right|}{\left(x_\xi\left(\theta_i^{(2)}\right)\right)^2} \text{ where } \theta_i^{(1)} \in (\xi_{i-1}, \xi_{i+1}) \text{ and } \theta_i^{(2)} \in (\xi_{i-1}, \xi_i).$$

Then, from (3.5.4) and $\beta = \Psi$, we obtain

$$x_\xi(\theta) = \frac{4\sqrt{\frac{\varepsilon}{\rho}}}{\sqrt{2\frac{\varepsilon}{\rho}} + \mu_0 e^{\left(-\frac{x(\theta)}{2}\sqrt{\frac{\rho}{\varepsilon}}\right)}} \text{ and } x_{\xi\xi}(\theta) = \frac{8\mu_0\sqrt{\frac{\varepsilon}{\rho}} e^{\left(-\frac{x(\theta)}{2}\sqrt{\frac{\rho}{\varepsilon}}\right)}}{\left(2\frac{\varepsilon}{\rho} + \mu_0 e^{\left(-\frac{x(\theta)}{2}\sqrt{\frac{\rho}{\varepsilon}}\right)}\right)^3}.$$

This implies that

$$\frac{|h_{i+1} - h_i|}{h_i^2} \leq \frac{\mu_0\sqrt{\frac{\rho}{\varepsilon}}\left(2\frac{\rho}{\varepsilon} + \mu_0 e^{\left(-\frac{x(\theta)}{2}\sqrt{\frac{\rho}{\varepsilon}}\right)}\right)^2}{2\left(2\frac{\rho}{\varepsilon} + \mu_0 e^{\left(-\frac{x(\theta)}{2}\sqrt{\frac{\rho}{\varepsilon}}\right)}\right)^3} \leq C.$$

□

The following lemma generalises the bounds on h_i across the entire domain.

Lemma 3.5.3. For $i = 1,...,N$, the width of the adaptive mesh satisfies $h_i \leq CN^{-1}$.

Proof. Use (3.5.2) and (3.5.3) with $\beta = \Psi$ to obtain

$$\int_0^1 M(x,y(x))dx \leq C\beta.$$

Finally, the equidistribution principle leads to

$$\beta h_i \leq \int_{x_{i-1}}^{x_i} M(x,y(x))dx = \frac{1}{N}\int_0^1 M(x,y(x))dx \leq C\beta N^{-1}.$$

□

3.6 The Difference Method

We now describe the difference approximation of (3.2.1) on the adaptive mesh $\bar{\Omega}_E^N \equiv \{0 = x_0 < x_1 < \cdots < x_N = 1\}$. We employ the cubic spline difference method for discretising the boundary layer and the exponential spline difference method for the outer layer. To begin with, the cubic spline difference method, let us introduce the cubic spline polynomial $S_m(x)$ for $m = 1,2$, on the nonuniform mesh $\{0 = x_0 < x_1 < \cdots < x_N = 1\}$ where $h_i = x_i - x_{i-1}$. For the given values $Y_m(x_0), Y_m(x_1), ..., Y_m(x_N)$ of the polynomial $y_m(x)$, $m = 1,2$, at $x_0, x_1, ..., x_N$, the polynomial $S_m(x)$ satisfies for $m = 1,2$,

1. $S_m(x) \in C^2[0,1]$,

2. On each sub-interval $[x_{i-1}, x_i]$, $S_m(x)$ is a polynomial of degree 3, $i = 1,\ldots,N$ and

3. $S_m(x_i) = Y_m(x_i)$, $i = 0,1,...,N$.

The polynomials $S_m(x)$ for $m = 1,2$, are determined by solving $D^4 S_m(x) = 0$, for all $x \in [x_{i-1}, x_i]$, $i = 1,2,\ldots N$ such that $S_m(x_{i-1}) = Y_m(x_{i-1})$, $S_m(x_i) = Y_m(x_i)$, $S_m''(x_{i-1}) = Y_m''(x_{i-1})$ and $S_m''(x_i) = Y_m''(x_i)$. Now, using $S_m''(x_i) = \mathscr{M}_{m,i}$, $i = 0,\ldots,N$, the solution of the above boundary value problem reads

$$\begin{aligned} S_m(x) &= \frac{(x_i - x)^3}{6h_i}\mathscr{M}_{m,i-1} + \frac{(x - x_{i-1})^3}{6h_i} + \left(Y_m(x_{i-1}) - \frac{h_i^2}{6}\mathscr{M}_{m,i-1}\right)\frac{(x_i - x)}{h_i} \\ &\quad + \left(Y_m(x_i) - \frac{h_i^2}{6}\mathscr{M}_{m,i}\right)\frac{(x - x_{i-1})}{h_i}. \end{aligned} \tag{3.6.1}$$

To determine $\mathscr{M}_{m,i}$, we use the continuity constraint of $S_m'(x)$ at the internal nodes x_i, where $i = 1,...,N-1$. This leads us to the following system of equations

$$\frac{h_i}{6}\mathscr{M}_{m,i-1} + \left(\frac{h_i + h_{i+1}}{3}\right)\mathscr{M}_{m,i} + \frac{h_{i+1}}{6}\mathscr{M}_{m,i+1} = \frac{Y_m(x_{i+1}) - Y_m(x_i)}{h_{i+1}} - \frac{Y_m(x_i) - Y_m(x_{i-1})}{h_i}. \tag{3.6.2}$$

To obtain second order approximation for $Y_m'(x)$, we use Taylor's series expansion of Y_m about x_i to write

$$Y_m(x_{i+1}) \approx Y_m(x_i) + h_{i+1}Y_m'(x_i) + \frac{h_{i+1}^2}{2}Y_m''(x_i) \text{ and}$$

$$Y_m(x_{i-1}) \approx Y_m(x_i) - h_iY_m'(x_i) + \frac{h_i^2}{2}Y_m''(x_i),\ m = 1,2.$$

Consequently, for $m = 1,2$, we obtain

$$Y_m'(x_i) \approx \frac{h_i^2Y_m(x_{i+1}) + (h_{i+1}^2 - h_i^2)Y_m(x_i) - h_{i+1}^2Y_m(x_{i-1})}{h_{i+1}h_i(h_{i+1}+h_i)} \text{ and}$$
$$Y_m''(x_i) \approx \frac{2(h_iY_m(x_{i+1}) - (h_{i+1}+h_i)Y_m(x_i) + h_{i+1}Y_m(x_{i-1}))}{h_{i+1}h_i(h_{i+1}+h_i)}.$$

A substitution in $Y_m'(x_{i+1}) \approx Y_m'(x_i) + h_{i+1}Y_m''(x_i)$ and $Y_m'(x_{i-1}) \approx Y_m'(x_i) - h_iY_m''(x_i)$ leads to

$$Y_m'(x_{i+1}) \approx \frac{(h_i^2 + 2h_{i+1}h_i)Y_m(x_{i+1}) - (h_{i+1}+h_i)^2Y_m(x_i) + h_{i+1}^2Y_m(x_{i-1})}{h_{i+1}h_i(h_{i+1}+h_i)} \text{ and}$$
$$Y_m'(x_{i-1}) \approx \frac{2(-h_i^2Y_m(x_{i+1}) + (h_{i+1}+h_i)^2Y_m(x_i) - (h_{i+1}^2 + 2h_{i+1}h_i)Y_m(x_{i-1}))}{h_{i+1}h_i(h_{i+1}+h_i)},\ m = 1,2.$$

Substitute $\mathscr{M}_{m,i}$ from

$$-\varepsilon\mathscr{M}_{1,j} - \delta b_1(x_j)Y_1'(x_j) + (a_{11}(x_j) + b_1(x_j))Y_1(x_j) + a_{12}(x_j)Y_2(x_j) = g_1(x_j),\ j = i, i\pm1,$$
$$-\varepsilon\mathscr{M}_{2,j} - \delta b_2(x_j)Y_2'(x_j) + a_{21}(x_j)Y_1(x_j) + (a_{22}(x_j) + b_2(x_j))Y_2(x_j) = g_2(x_j),\ j = i, i\pm1$$

in (3.6.2) to obtain the following linear system of equations for $i = 1,\ldots N-1$, $m = 1,2$

$$\left(\frac{-\varepsilon}{h_i(h_{i+1}+h_i)} + \frac{h_i}{6(h_{i+1}+h_i)}(a_{mm}(x_{i-1}) + b_m(x_{i-1})) + \frac{h_{i+1}+2h_i}{6(h_{i+1}+h_i)^2}\delta b_m(x_{i-1}) + \right.$$
$$\left.\frac{h_{i+1}}{3h_i(h_{i+1}+h_i)}\delta b_m(x_i) - \frac{(h_{i+1})^2}{6h_i(h_{i+1}+h_i)^2}\delta b_m(x_{i+1})\right)Y_{m,i-1} +$$
$$\left(\frac{\varepsilon}{h_{i+1}h_i} + \frac{(a_{mm}(x_i) + b_m(x_i))}{3} - \frac{1}{6h_{i+1}}\delta b_m(x_{i-1}) - \frac{(h_{i+1}-h_i)}{3h_{i+1}h_i}\delta b_m(x_i) + \frac{1}{6h_i}\delta b_m(x_{i+1})\right)Y_{m,i} +$$
$$\left(\frac{-\varepsilon}{h_{i+1}(h_{i+1}+h_i)} + \frac{h_{i+1}}{6(h_{i+1}+h_i)}(a_{mm}(x_{i+1}) + b_m(x_{i+1})) + \frac{(h_i)^2}{6(h_{i+1}+h_i)^2}\delta b_m(x_{i-1}) - \right.$$
$$\left.\frac{h_i}{3h_{i+1}(h_{i+1}+h_i)}\delta b_m(x_i) - \frac{(h_i+2h_{i+1})}{6(h_{i+1}+h_i)^2}\delta b_m(x_{i+1})\right)Y_{m,i+1} +$$
$$\left(\frac{h_i}{6(h_{i+1}+h_i)}a_{m(3-m)}(x_{i-1})\right)Y_{(3-m),i-1} + \left(\frac{a_{m(3-m)}(x_i)}{3}\right)Y_{(3-m),i} +$$
$$\left(\frac{h_{i+1}}{6(h_{i+1}+h_i)}a_{m(3-m)}(x_{i+1})\right)Y_{(3-m),i+1} = \frac{h_i}{6(h_{i+1}+h_i)}g_m(x_{i-1}) + \frac{g_m(x_i)}{3} + \frac{h_{i+1}}{6(h_{i+1}+h_i)}g_m(x_{i+1}). \tag{3.6.3}$$

The difference method (3.6.3) ceases to be uniformly stable in the outer layer region. It does not satisfy the discrete maximum principle. Hence, we resort to using exponential splines outside the layers. The exponential spline is determined as the solution to the boundary value problem:

$$\begin{cases} (D^4 - p_{m,i}^2 D^2)T_m = 0,\ \forall x \in [x_{i-1}, x_i],\ m = 1,2,\ i = 1,...,N, \\ T_m(x_{i-1}) = Y_m(x_{i-1}),\ T_m(x_i) = Y_m(x_i),\ T_m''(x_{i-1}) = T_{m,i-1}'',\ T_m''(x_i) = T_{m,i}'' \end{cases} \tag{3.6.4}$$

where $p_{m,i}$ are nonnegative tension parameters and $T_{m,i}''$ are yet to be determined. Notably, the differential equation (3.6.4) reduces to $D^4 T_m = 0$ whenever the tension parameter $p_{m,i} \to 0$, thus yielding a cubic spline. A rigorous analysis reveals that $\{1, x, e^{p_{m,i}x}, e^{-p_{m,i}x}\}$ spans the solution space of (3.6.4) [277]. As in our earlier derivation, we employ continuity constraints to derive a system of equations representing the exponential spline relation

$$\begin{cases} e_{m,i} T_{m,i-1}'' + (d_{m,i} + d_{m,i+1}) T_{m,i}'' + e_{m,i+1} T_{m,i+1}'' = \dfrac{Y_m(x_{i+1}) - Y_m(x_i)}{h_{i+1}} - \dfrac{Y_m(x_i) - Y_m(x_{i-1})}{h_i}, \\ e_{m,i} = \dfrac{s_{m,i} - p_{m,i} h_i}{p_{m,i}^2 s_{m,i} h_i},\ d_{m,i} = \dfrac{p_{m,i} h_i c_{m,i} - s_{m,i}}{p_{m,i}^2 s_{m,i} h_i}, \\ s_{m,i} = \sinh(p_{m,i} h_i),\ c_{m,i} = \cosh(p_{m,i} h_i). \end{cases} \tag{3.6.5}$$

Now substitute $T_{m,i}''$ from

$$\begin{aligned} &-\varepsilon T_{1,j}'' - \delta b_1(x_j) Y_1'(x_j) + (a_{11}(x_j) + b_1(x_j)) Y_1(x_j) + a_{12}(x_j) Y_2(x_j) = g_1(x_j),\ j = i, i \pm 1, \\ &-\varepsilon T_{2,j}'' - \delta b_2(x_j) Y_2'(x_j) + a_{21}(x_j) Y_1(x_j) + (a_{22}(x_j) + b_2(x_j)) Y_2(x_j) = g_2(x_j),\ j = i, i \pm 1 \end{aligned}$$

into (3.6.5), we get the following system of equations for $i = 1,\dots N-1$, $m = 1,2$

$$
\begin{aligned}
&\left(\frac{-\varepsilon}{h_i(h_{i+1}+h_i)} + \frac{e_{m,i}}{h_{i+1}+h_i}(a_{mm}(x_{i-1}) + b_m(x_{i-1})) + \frac{e_{m,i}(h_{i+1}+2h_i)}{h_i(h_{i+1}+h_i)^2}\delta b_m(x_{i-1}) + \right.\\
&\left.\frac{(d_{m,i}+d_{m,i+1})h_{i+1}}{h_i(h_{i+1}+h_i)^2}\delta b_m(x_i) - \frac{e_{m,i+1}h_{i+1}}{h_i(h_{i+1}+h_i)^2}\delta b_m(x_{i+1})\right)Y_{m,i-1} +\\
&\left(\frac{\varepsilon}{h_{i+1}h_i} + \left(\frac{d_{m,i}+d_{m,i+1}}{h_{i+1}+h_i}\right)(a_{mm}(x_i) + b_m(x_i)) - \frac{e_{m,i}}{h_{i+1}h_i}\delta b_m(x_{i-1}) - \right.\\
&\left.\frac{(d_{m,i}+d_{m,i+1})(h_{i+1}-h_i)}{h_{i+1}h_i(h_{i+1}+h_i)}\delta b_m(x_i) + \frac{e_{m,i+1}}{h_{i+1}h_i}\delta b_m(x_{i+1})\right)Y_{m,i} +\\
&\left(\frac{-\varepsilon}{h_{i+1}(h_{i+1}+h_i)} + \frac{e_{m,i+1}}{h_{i+1}+h_i}(a_{mm}(x_{i+1}) + b_m(x_{i+1})) + \frac{e_{m,i}h_i}{h_{i+1}(h_{i+1}+h_i)^2}\delta b_m(x_{i-1}) - \right.\\
&\left.\frac{(d_{m,i}+d_{m,i+1})h_i}{h_{i+1}(h_{i+1}+h_i)^2}\delta b_m(x_i) - \frac{e_{m,i+1}(h_i+2h_{i+1})}{h_{i+1}(h_{i+1}+h_i)^2}\delta b_m(x_{i+1})\right)Y_{m,i+1} +\\
&\frac{e_{m,i}}{h_{i+1}+h_i}a_{m(3-m)}(x_{i-1})Y_{(3-m),i-1} +\\
&\left(\frac{d_{m,i}+d_{m,i+1}}{h_{i+1}+h_i}\right)a_{m(3-m)}(x_i)Y_{(3-m),i} + \frac{e_{m,i+1}}{h_{i+1}+h_i}a_{m(3-m)}(x_{i+1})Y_{(3-m),i+1} =\\
&\frac{e_{m,i}}{h_{i+1}+h_i}g_m(x_{i-1}) + \left(\frac{d_{m,i}+d_{m,i+1}}{h_{i+1}+h_i}\right)g_m(x_i) + \frac{e_{m,i+1}}{h_{i+1}+h_i}g_m(x_{i+1}).
\end{aligned}
\tag{3.6.6}
$$

Therefore, in the outer layer region, the proposed method mitigates the nonmonotonic behaviour of the cubic spline difference method by incorporating exponential splines. Consequently, the associated problem for the system (3.2.1) takes the form: Find $\mathbf{Y} = (Y_1, Y_2)^T$ such that

$$
\begin{aligned}
&[\mathbf{L}^N\mathbf{Y}]_i = [\Gamma\mathbf{g}]_i\\
&\iff \begin{cases}
[L_1^N\mathbf{Y}] \equiv r_{1,i}^- Y_{1,i-1} + r_{1,i}^c Y_{1,i} + r_{1,i}^+ Y_{1,i+1} + q_{m,i}^- a_{12,i-1}Y_{2,i-1} + \\
\qquad q_{m,i}^c a_{12,i}Y_{2,i} + q_{m,i}^+ a_{12,i+1}Y_{2,i+1} = q_{m,i}^- g_{1,i-1} + q_{m,i}^c g_{1,i} + q_{m,i}^+ g_{1,i+1},\\
[L_2^N\mathbf{Y}] \equiv r_{2,i}^- Y_{2,i-1} + r_{2,i}^c Y_{2,i} + r_{2,i}^+ Y_{2,i+1} + q_{m,i}^- a_{21,i-1}Y_{1,i-1} + \\
\qquad q_{m,i}^c a_{21,i}Y_{1,i} + q_{m,i}^+ a_{21,i+1}Y_{1,i+1} = q_{m,i}^- g_{2,i-1} + q_{m,i}^c g_{2,i} + q_{m,i}^+ g_{2,i+1},\\
Y_{1,0} = y_1(0),\ Y_{1,N} = y_1(1),\ Y_{2,0} = y_2(0),\ Y_{2,N} = y_2(1)
\end{cases}
\end{aligned}
\tag{3.6.7}
$$

where $[\Gamma(g_m)]_i = q_{m,i}^- g_{m,i-1} + q_{m,i}^c g_{m,i} + q_{m,i}^+ g_{m,i+1}$, $\mathbf{L}^N = (L_1, L_2)^N$ and $\mathbf{g}_i = (g_{1,i}, g_{2,i})^T$.

The values of the coefficients $r_{m,i}^*$ and $q_{m,i}^*$, where $m = 1,2$, $i = 1,...,N-1$ and $* = -,c,+$, are determined based on the location of the mesh points x_i that partition the domain $[0,1]$ of $\mathbf{L}^N$. The coefficients are given as follows:

1. When x_i lies within the boundary layer part of the mesh, i.e. $i \in \{1,...k_l-1\} \cup \{k_r+1,...,N-1\}$,

the cubic spline difference method employed to determine the coefficients reads

$$\begin{cases} r^{-}_{m,i} &= \dfrac{-\varepsilon}{h_i(h_{i+1}+h_i)} + q^{-}_{m,i}(a_{mm}(x_{i-1}) + b_m(x_{i-1})) + \dfrac{(h_{i+1}+2h_i)}{6(h_{i+1}+h_i)^2}\delta b_m(x_{i-1}) + \\ & \dfrac{h_{i+1}}{3h_i(h_{i+1}+h_i)}\delta b_m(x_i) - \dfrac{(h_{i+1})^2}{6h_i(h_{i+1}+h_i)^2}\delta b_m(x_{i+1}), \\ r^{c}_{m,i} &= \dfrac{\varepsilon}{h_{i+1}h_i} + q^{c}_{m,i}(a_{mm}(x_i) + b_m(x_i)) - \dfrac{1}{6h_{i+1}}\delta b_m(x_{i-1}) - \dfrac{(h_{i+1}-h_i)}{3h_{i+1}h_i}\delta b_m(x_i) + \\ & \dfrac{1}{6h_i}\delta b_m(x_{i+1}), \\ r^{+}_{m,i} &= \dfrac{-\varepsilon}{h_i(h_{i+1}+h_i)} + q^{+}_{m,i}(a_{mm}(x_{i+1}) + b_m(x_{i+1})) + \dfrac{(h_i)^2}{6(h_{i+1}+h_i)^2}\delta b_m(x_{i-1}) - \\ & \dfrac{h_i}{3h_{i+1}(h_{i+1}+h_i)}\delta b_m(x_i) - \dfrac{(h_i+2h_{i+1})}{6(h_{i+1}+h_i)^2}\delta b_m(x_{i+1}), \end{cases} \tag{3.6.8}$$

$$q^{-}_{m,i} = \frac{h_i}{6(h_{i+1}+h_i)}, \quad q^{c}_{m,i} = \frac{1}{3}, \quad q^{+}_{m,i} = \frac{h_{i+1}}{6(h_{i+1}+h_i)}. \tag{3.6.9}$$

2. When x_i lies outside layers, i.e. $i \in \{k_l, \ldots, k_r\}$, the coefficients associated with the exponential spline difference method reads

$$\begin{cases} r^{-}_{m,i} &= \dfrac{-\varepsilon}{h_i(h_{i+1}+h_i)} + q^{-}_{m,i}(a_{mm}(x_{i-1}) + b_m(x_{i-1})) + \dfrac{e_{m,i}(h_{i+1}+2h_i)}{h_i(h_{i+1}+h_i)^2}\delta b_m(x_{i-1}) + \\ & \dfrac{(d_{m,i}+d_{m,i+1})h_{i+1}}{h_i(h_{i+1}+h_i)^2}\delta b_m(x_i) - \dfrac{e_{m,i+1}h_{i+1}}{h_i(h_{i+1}+h_i)^2}\delta b_m(x_{i+1}), \\ r^{c}_{m,i} &= \dfrac{\varepsilon}{h_{i+1}h_i} + q^{c}_{m,i}(a_{mm}(x_i) + b_m(x_i)) - \dfrac{e_{m,i}}{h_{i+1}h_i}\delta b_m(x_{i-1}) - \\ & \dfrac{(d_{m,i}+d_{m,i+1})(h_{i+1}-h_i)}{h_{i+1}h_i(h_{i+1+h_i})}\delta b_m(x_i) + \dfrac{e_{m,i+1}}{h_{i+1}h_i}\delta b_m(x_{i+1}), \\ r^{+}_{m,i} &= \dfrac{-\varepsilon}{h_i(h_{i+1}+h_i)} + q^{+}_{m,i}(a_{mm}(x_{i+1}) + b_m(x_{i+1})) + \dfrac{e_{m,i}h_i}{h_{i+1}(h_{i+1}+h_i)^2}\delta b_m(x_{i-1}) - \\ & \dfrac{(d_{m,i}+d_{m,i+1})h_i}{h_{i+1}(h_{i+1}+h_i)^2}\delta b_m(x_i) - \dfrac{e_{m,i+1}(h_i+2h_{i+1})}{h_{i+1}(h_{i+1}+h_i)^2}\delta b_m(x_{i+1}), \end{cases} \tag{3.6.10}$$

$$q^{-}_{m,i} = \frac{e_{m,i}}{h_{i+1}+h_i}, \quad q^{+}_{m,i} = \frac{e_{m,i+1}}{h_{i+1}+h_i}, \quad q^{c}_{m,i} = \frac{d_{m,i}}{h_{i+1}+h_i} + \frac{d_{m,i+1}}{h_{i+1}+h_i}. \tag{3.6.11}$$

A thorough analysis indicates that the coefficient matrix does not meet the **M**-matrix criterion outside the layer region [277]. However, for a specific choice of the tension parameter

$$p_m = \min_{i=k_l,\ldots k_r}\{p_{m,i}\} = \max_{i=k_l,\ldots k_r}\left\{\sqrt{\frac{a_{mm}(x_i)+b_m(x_i)}{\varepsilon}}, \sqrt{\frac{\delta b_m(x_i)}{\varepsilon}}\right\}$$

a systematic application of the exponential spline difference method results in a uniformly stable numerical discretisation. Consequently, the associated coefficient matrix of the discrete hybrid operator $\mathbf{L}^N$ is an **M**-matrix with positive diagonal and nonpositive off-diagonal entries [287, 278].

3.7 Error Analysis

In this section, we investigate the order of accuracy of the proposed hybrid spline difference discretisation of (3.2.1) over the adaptive mesh generated. As in section 3.4, we decompose the discrete

approximate solution $\mathbf{Y}$ of (3.2.1) into smooth and layer parts as $\mathbf{Y} := \mathbf{U} + \mathbf{V}$, where the smooth component $\mathbf{U}$ satisfies

$$[\mathbf{L}^N\mathbf{U}] = [\Gamma\mathbf{g}]_i,\ i = 1,...,N-1;\ \mathbf{U}_0 = \mathbf{u}(0),\ \mathbf{U}_N = \mathbf{u}(1)$$

and the boundary layer part $\mathbf{V}$ satisfies

$$[\mathbf{L}^N\mathbf{V}] = 0,\ i = 1,...,N-1;\ \mathbf{V}_0 = \mathbf{v}(0),\ \mathbf{V}_N = \mathbf{v}(1).$$

Then, at each x_i, the error associated with $\mathbf{Y}_i$ satisfies

$$\|\mathbf{Y}_i - \mathbf{y}(x_i)\| \leq \|\mathbf{U}_i - \mathbf{u}(x_i)\| + \|\mathbf{V}_i - \mathbf{v}(x_i)\|. \tag{3.7.1}$$

Next, we calculate the consistency error for regular and singular components separately. Then, we combine both results and estimate the error. We begin our analysis with the smooth component.

Lemma 3.7.1. The smooth component $\mathbf{u}$ of the solution $\boldsymbol{y}$ and its discrete approximation $\mathbf{U}$ satisfies

$$\|\mathbf{L}^N(\mathbf{U} - \mathbf{u})(x_i)\| \leq CN^{-2},\ i = 1,...,N-1.$$

Proof. 1. When $i \in \{1,\ldots,k_l-1\} \cup \{k_r+1,\ldots,N-1\}$, the spline difference approximation is obtained using cubic splines. Then, for $m = 1,2$, the Taylor's expansion yields

$$\begin{aligned}\|\mathbf{L}_m^N(\mathbf{U} - \mathbf{u})(x_i)\| &= |(L_m - L_m^N)\mathbf{u}(x_i)|,\\ &\leq C\varepsilon|h_{i+1} - h_i|\|u_m'''(x)\|_{[x_{i-1},x_{i+1}]} + C\varepsilon(h_{i+1}^2 + h_i^2)\|u_m^{(iv)}(x)\|_{[x_i,x_{i+1}]}\\ &\leq C\varepsilon h_i^2(1+\varepsilon^{\frac{-1}{2}}) + C(h_{i+1}^2 + h_i^2) \leq C(h_{i+1}^2 + h_i^2).\end{aligned}$$

The required estimate follows immediately from Lemma 3.4.1, Lemma 3.5.2 and Lemma 3.5.3.

2. When $i \in \{k_l,\ldots,k_r\}$, the spline difference approximation is obtained using exponential splines. Then, it is easy to follow that

$$\|\mathbf{L}_m^N(\mathbf{U} - \mathbf{u})(x_i)\| = |(L_m - L_m^N)\mathbf{u}(x_i)| \leq C\varepsilon h_i^2 p^2\|u_m''(x)\|_{[x_{i-1},x_{i+1}]},\ m = 1,2.$$

For $p_m = \min\limits_{i=k_l,\ldots,k_r}\{p_{m,i}\} = \max\limits_{i=k_l,\ldots,k_r}\left\{\sqrt{\dfrac{a_{mm}(x_i)+b_m(x_i)}{\varepsilon}}, \sqrt{\dfrac{\delta b_m(x_i)}{\varepsilon}}\right\}$, it follows from Lemma 3.4.1 and Lemma 3.5.3 that

$$\|\mathbf{L}^N(\mathbf{U} - \mathbf{u})(x_i)\| \leq CN^{-2},\ i = k_l,\ldots,k_r.$$

□

Lemma 3.7.2. The layer component $\mathbf{v}$ of the solution $\boldsymbol{y}$ and its discrete approximation $\mathbf{V}$ satisfies

$$\|\mathbf{L}^N(\mathbf{V} - \mathbf{v})(x_i)\| \leq CN^{-2},\ i = 1,\ldots,N-1.$$

Proof. 1. When $i \in \{1,\ldots,k_l-1\} \cup \{k_r+1,\ldots,N-1\}$, for the left segment of the boundary layer

region, Taylor's expansion yields

$$\|\mathbf{L}_m^N(\mathbf{V}-\mathbf{v})(x_i)\| = |(L_m - L_m^N)\mathbf{v}(x_i)| = \varepsilon \frac{|h_{i+1}^2 v_m'''(\theta_i^{(2)}) - h_i^2 v_m'''(\theta_i^{(1)})|}{3(h_{i+1}+h_i)},\ m = 1,2$$

where $\theta_i^{(2)} \in (x_i, x_{i+1})$ and $\theta_i^{(1)} \in (x_{i-1}, x_i)$. Moreover,

$$\begin{aligned}|h_{i+1}^2 v_m'''(\theta_i^{(2)}) - h_i^2 v_m'''(\theta_i^{(1)})| &\leq |h_{i+1}^2 - h_i^2\|v_m'''(\theta_i^{(2)})| + h_i^2|v_m'''(\theta_i^{(2)}) - v_m'''(\theta_i^{(1)})| \\ &\leq C(|h_{i+1}^2 - h_i^2\|v_m'''(x_i)| + h_i^2|h_{i+1}+h_i\|v_m^{(iv)}(x_i)|)\end{aligned}$$

where $|\theta_i^{(2)} - \theta_i^{(1)}| < (h_{i+1}+h_i)$. Now, using Lemma 3.4.1, Lemma 3.5.2 and (3.5.1) to compute

$$\begin{aligned}|\mathbf{L}^N(\mathbf{V}-\mathbf{v})(x_i)| &\leq C\varepsilon^{\frac{-1}{2}} h_i^2 e^{\left(-x_i\sqrt{\frac{\rho}{\varepsilon}}\right)} + C\varepsilon^{-1} h_i^2 e^{\left(-x_i\sqrt{\frac{\rho}{\varepsilon}}\right)} \\ &\leq C(\varepsilon^{\frac{-1}{2}} + \varepsilon^{-1}) \left(\int_{x_{i-1}}^{x_i} e^{\left(-\frac{t}{2}\sqrt{\frac{\rho}{\varepsilon}}\right)} dt\right)^2 \\ &\leq C(\varepsilon^{\frac{-1}{2}} + \varepsilon^{-1}) \left(\sqrt{\varepsilon}\int_{x_{i-1}}^{x_i} M(y(\varkappa),\varkappa) d\varkappa\right)^2 \leq C\Psi^2 N^{-2} \leq CN^{-2}.\end{aligned}$$

Likewise, we can estimate the outcome for the right segment of the boundary layer region, and the desired result follows immediately.

2. When $i \in \{k_l, ..., k_r\}$, Taylor's expansion with integral remainder yields

$$\|\mathbf{L}_m^N(\mathbf{V}-\mathbf{v})(x_i)\| = |(L_m - L_m^N)\mathbf{v}(x_i)| \leq C\varepsilon \|v_m''(x)\|_{[x_{i-1}, x_{i+1}]},\ m = 1,2.$$

Now, the derivative bounds derived in Lemma 3.4.1 yield

$$\|\mathbf{L}_m^N(\mathbf{V}-\mathbf{v})(x_i)\| \leq C \begin{cases} e^{\left(-x_{i-1}\sqrt{\frac{\rho}{\varepsilon}}\right)}, & x_i \leq \frac{1}{2}, \\ e^{\left(-(1-x_{i+1})\sqrt{\frac{\rho}{\varepsilon}}\right)}, & x_i > \frac{1}{2}. \end{cases}$$

For $i \geq k_l - 1$ and $x_i \leq \frac{1}{2}$, Lemma (3.5.1) suggests

$$\begin{aligned}\|\mathbf{L}_m^N(\mathbf{V}-\mathbf{v})(x_i)\| &\leq Ce^{\left(-x_{k_l-1}\sqrt{\frac{\rho}{\varepsilon}}\right)} \\ &= C\left(e^{\left(\frac{-x_{k_l-1}}{2}\sqrt{\frac{\rho}{\varepsilon}}\right)}\right)^2 \leq CN^{-2}.\end{aligned}$$

The bounds for $i \leq k_r$ and $x_i > \frac{1}{2}$ can be easily established in a similar manner. Thus, combining the various estimates completes the proof. □

We can now present the main convergence result by summarising the error estimates derived thus far. The proof of this result follows from Lemma 3.7.1, Lemma 3.7.2 and the triangle inequality.

Theorem 3.7.1. Let $\mathbf{y}$ be the solution of the continuous problem (3.2.1) and $\mathbf{Y}$ be the solution of the discrete problem (3.6.7) on the equidistributed mesh defined by (3.5.6)-(3.5.7).Then, there exists a

positive constant C independent of N and ε such that

$$\|\mathbf{y}-\mathbf{Y}\|_{\bar{\Omega}_E^N} \leq CN^{-2}.$$

3.8 Numerical Experiments

In this section, we examine the performance of the proposed method and numerically verify the theoretical estimates. We consider four test problems for numerical computations. If the exact solution of the problem is unknown, we estimate the maximum pointwise errors using the double mesh principle [5], given by:

$$E_{m,\varepsilon}^N = \max_{0\leq i\leq N} |Y_m^N(x_i) - \hat{Y}_m^{2N}(\hat{x}_{2i})|,\ m = 1,2.$$

However, if the exact solution is available, we evaluate the maximum pointwise errors using the formula:

$$E_{m,\varepsilon}^N = \max_{0\leq i\leq N} |Y_m^N(x_i) - y_m(x_i)|,\ m = 1,2.$$

Here, $y_m(x_i)$ represents the exact solution, and $Y_m^N(x_i)$ denotes the numerical solution obtained at the mesh points x_i of the adaptive mesh with N number of intervals. Taking the maximum over a wide range of ε say $K = \{\varepsilon | \varepsilon = 2^0, 2^{-2}, ..., 2^{-40}\}$, the uniform errors are estimated by $E_m^N = \max_{\varepsilon\in K} E_{m,\varepsilon}^N$. To compute the corresponding orders of convergence and the parameter-uniform orders of convergence, we utilise the following standard formulas:

$$p_{m,\varepsilon}^N = log_2\left(\frac{E_{m,\varepsilon}^N}{E_{m,\varepsilon}^{2N}}\right), \text{ and } p_m^N = log_2\left(\frac{E_m^N}{E_m^{2N}}\right).$$

In the adaptive mesh generation process, we choose $Q = 1.3$. Tables 3.1-3.4 list the uniform errors and corresponding order of convergence for the proposed method applied to Examples 3.8.1 and 3.8.2. The uniform errors decrease consistently as the number of mesh intervals increases, and the orders of convergence are approximately two, confirming the second-order accuracy of the method. The results align with the theoretical predictions, reinforcing the method's effectiveness across different examples. For Example 3.8.3, Table 3.5 compares the maximum pointwise error and the order of convergence using the proposed method and a hybrid finite difference method on a Shiskin mesh [298].

Figures 3.1 and 3.3 illustrate the numerical solution of a system of second-order delay reaction-diffusion equations for Example 3.8.1 with $N = 160$ and for Example 3.8.2 with $N = 128$, computed using the proposed hybrid spline difference method. The plot shows the behaviour of the numerical solution across the domain. The boundary layer effect is evident, highlighting the method's ability to capture steep gradients near the boundary. The solution remains stable and accurate, reflecting the robustness of the proposed method in handling the system of reaction-diffusion equations with delay terms. Figures 3.2 and 3.4 show the distribution of mesh points for Example 3.8.1 with $N = 160$ and for Example 3.8.2 with $N = 128$ highlighting areas with higher density. The density of the mesh is higher near the boundary layer, indicating that the adaptive algorithm effectively places more points where

the solution requires a higher resolution. This adaptive mesh ensures better accuracy and efficiency in solving the problem. Figures 3.5 and 3.6 depict a log-log plot of the maximum pointwise errors against the number of mesh intervals for Examples 3.8.1 and 3.8.2, respectively. The plot illustrates the error convergence rates for the two components of the solution. The linear behaviour in the log-log plot indicates second-order convergence, validating the theoretical error estimates provided in the paper. Figure 3.7 compares the maximum pointwise errors for various values of the perturbation parameter in Example 3.8.1. The plot shows how the error varies with different values of the perturbation parameter ε. The consistent pattern indicates the robustness of the method to changes in ε, maintaining second-order accuracy across a range of perturbation sizes. In contrast, Figure 3.8 compares the maximum pointwise error of the proposed method with a hybrid finite difference method over a Shiskin mesh for Example 3.8.3. The comparison demonstrates the superiority of the proposed hybrid spline difference method, which achieves lower maximum pointwise errors, particularly in resolving boundary layers. Finally, Figure 3.9 shows the comparison between the exact and numerical solutions for Example 3.8.4. The numerical solution closely matches the exact solution within and outside the boundary layer. This visual confirmation underscores the accuracy and reliability of the method.

Example 3.8.1. Consider the following system of second-order delay reaction diffusion equation for $x \in \Omega = (0,1)$

$$-\varepsilon \mathbf{y}''(x) + \begin{pmatrix} x^2 + e^{-2x} & -12x^2 \\ -x^3 & 4(1+x^4) \end{pmatrix} \mathbf{y}(x) + \begin{pmatrix} 2x^4 & 0 \\ 0 & xe^{-x} \end{pmatrix} \mathbf{y}(x-\delta) = \begin{pmatrix} x^4 \\ 2e^x \end{pmatrix},$$

where $\mathbf{y}(x) = \left(-\frac{\cos x}{2}, x-1\right)^T$ for $x \in [-\delta, 0]$ and $\mathbf{y}(1) = \left(-\frac{1}{2}, -1\right)^T$.

Example 3.8.2. Consider the following system of second-order delay reaction diffusion equation for $x \in \Omega = (0,1)$

$$-\varepsilon \mathbf{y}''(x) + \begin{pmatrix} (x+1)^2 & -(1+x^3) \\ -2\cos\left(\frac{\pi x}{4}\right) & 3e^{-x} \end{pmatrix} \mathbf{y}(x) + \begin{pmatrix} x^2 & 0 \\ 0 & 10x \end{pmatrix} \mathbf{y}(x-\delta) = \begin{pmatrix} e^{x-1} \\ 4x \end{pmatrix},$$

where $\mathbf{y}(x) = \left(-\frac{\sin x}{2}, x\right)^T$ for $x \in [-\delta, 0]$ and $\mathbf{y}(1) = (0,0)^T$.

Example 3.8.3. Consider the following system of second-order delay reaction diffusion equation

$$-\varepsilon \mathbf{y}''(x) + \begin{pmatrix} 11 & 0 \\ 0 & 16 \end{pmatrix} \mathbf{y}(x) + \begin{pmatrix} -(x^2+1) & -(x+1) \\ -x & -x \end{pmatrix} \mathbf{y}(x-1) = \begin{pmatrix} e^x \\ e^x \end{pmatrix},$$

where $\mathbf{y}(x) = (1,1)^T$ for $x \in [-1, 0]$ and $\mathbf{y}(1) = (1,1)^T$.

Example 3.8.4. Consider the following system of second-order delay reaction diffusion equation for $x \in \Omega = (0,1)$

$$-\varepsilon \mathbf{y}''(x) + \begin{pmatrix} 2(x+1)^2 & -x^2 \\ -\sin(\pi x) & e^{1-x} \end{pmatrix} \mathbf{y}(x) + \begin{pmatrix} x^2 & 0 \\ 0 & x \end{pmatrix} \mathbf{y}(x-\delta) = \mathbf{g}(x),$$

where $\mathbf{y}(x) = (x, \sin(x))^T$ for $x \in [-\delta, 0]$ and $\mathbf{y}(1) = \left(e^{-1} - 1, 0\right)^T$. Here, the function $\mathbf{g}(x) = (g_1(x), g_2(x))^T$ is choosen such that the exact solution of the problem reads

$$y_1(x) = (x-1)e^{-\frac{2x}{\varepsilon+\delta}} - xe^{-\frac{2(1-x)}{\varepsilon+\delta}} + e^{-x}, \quad y_2(x) = (x-1)e^{-\frac{x}{\varepsilon+\delta}} - xe^{-\frac{1-x}{\varepsilon+\delta}} + 1.$$

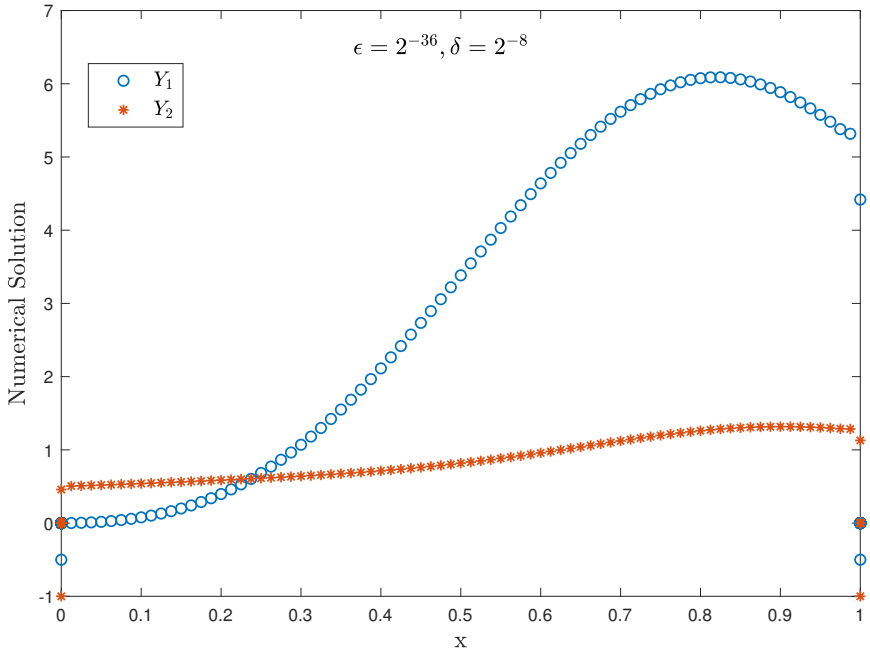

Fig. 3.1: Numerical solution for Example 3.8.1 with $N = 160$.

Table 3.1: The errors E_m^N and orders of convergence p_m^N in approximations Y_m for Example 3.8.1 with $\varepsilon = 2^{-4}$, $\delta = 2^{-6}$ and $m = 1, 2$.

	N=32	N=64	N=128	N=256	N=512	N=1024
E_1^N	8.372e-04	2.207e-04	5.768e-05	1.481e-05	3.757e-06	8.789e-07
p_1^N	1.96	1.98	1.99	1.99	1.99	
E_2^N	6.131e-03	1.546e-03	3.874e-04	9.689e-05	2.423e-05	6.057e-06
p_2^N	1.98	1.99	1.99	1.99	2.00	

3.9 Conclusion

A singularly perturbed system of reaction-diffusion equations with a shift is solved numerically using a higher-order hybrid approximation over an adaptive mesh. The equidistribution of a positive monitor function generates the mesh. The difference method combines an exponential spline difference method for the outer layer and a cubic spline difference method for the boundary layer on the adaptive mesh generated. This innovative approach improves the accuracy of numerical solutions while maintaining computational efficiency. The proposed numerical method is consistent, stable, and converges regardless of the size of the perturbation parameter. The numerical results and illustrations support the theoretical findings.

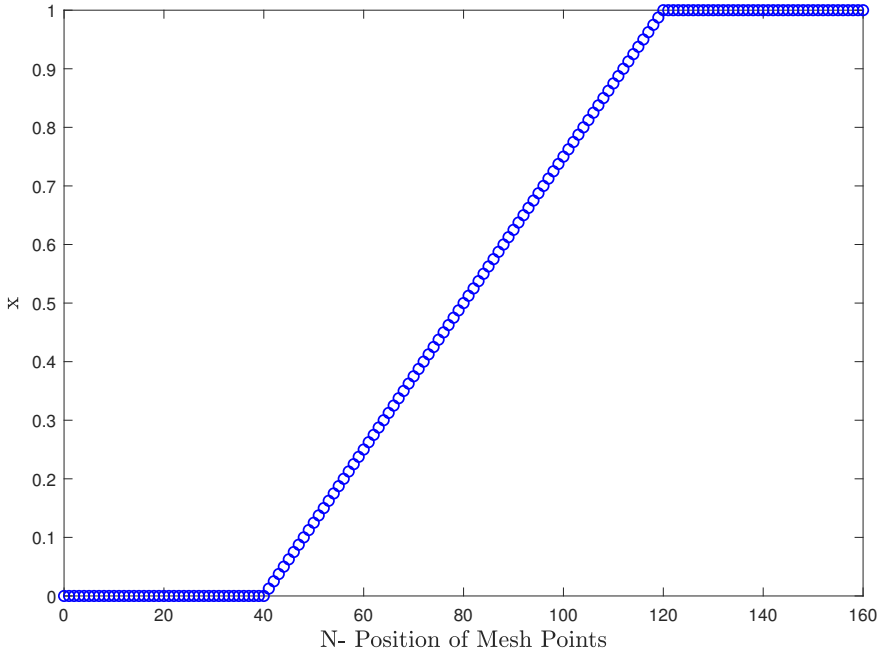

Fig. 3.2: Density of mesh points for Example 3.8.1 with $N = 160$.

Table 3.2: The errors E_m^N in approximations Y_m for Example 3.8.1 for different values of ε and N with $\delta = 0.03$ and $m = 1, 2$.

$\varepsilon \downarrow$		N=32	N=64	N=128	N=256	N=512
0.01	E_1^N	1.160e-02	1.472e-03	3.727e-04	9.334e-05	2.353e-05
	E_2^N	5.057e-02	1.018e-02	2.411e-03	6.049e-04	1.514e-04
0.05	E_1^N	1.072e-03	2.777e-04	7.222e-05	1.852e-05	4.697e-06
	E_2^N	7.637e-03	1.931e-03	4.841e-04	1.211e-04	3.028e-05
0.09	E_1^N	5.642e-04	1.521e-04	3.998e-05	1.028e-05	2.609e-06
	E_2^N	4.273e-03	1.075e-03	2.691e-04	6.729e-05	1.682e-05

Table 3.3: The errors E_m^N and orders of convergence p_m^N in approximations Y_m for Example 3.8.2 with $\varepsilon = 2^{-4}$, $\delta = 2^{-6}$ and $m = 1, 2$.

	N=32	N=64	N=128	N=256	N=512	N=1024
E_1^N	1.147e-03	2.856e-04	7.133e-05	1.783e-05	4.456e-06	1.114e-06
p_1^N	2.00	2.00	2.00	2.00	2.00	
E_2^N	4.315e-03	1.094e-03	2.743e-04	6.864e-05	1.716e-05	4.292e-06
p_2^N	1.97	1.99	1.99	2.00	1.99	

Table 3.4: The errors E_m^N in approximations Y_m for Example 3.8.2 for different values of ε and N with $\delta = 0.03$ and $m = 1, 2$.

$\varepsilon \downarrow$		N=32	N=64	N=128	N=256	N=512
0.01	E_1^N	1.065e-02	1.928e-03	4.464e-04	1.115e-04	2.786e-05
	E_2^N	3.405e-02	7.115e-03	1.704e-03	4.283e-04	1.072e-04
0.05	E_1^N	1.435e-03	3.571e-04	8.916e-05	2.228e-05	5.571e-06
	E_2^N	5.367e-03	1.365e-03	3.428e-04	8.580e-05	2.146e-05
0.09	E_1^N	7.954e-04	1.983e-04	4.953e-05	1.238e-05	3.095e-06
	E_2^N	3.014e-03	7.606e-04	1.906e-04	4.767e-05	1.192e-05

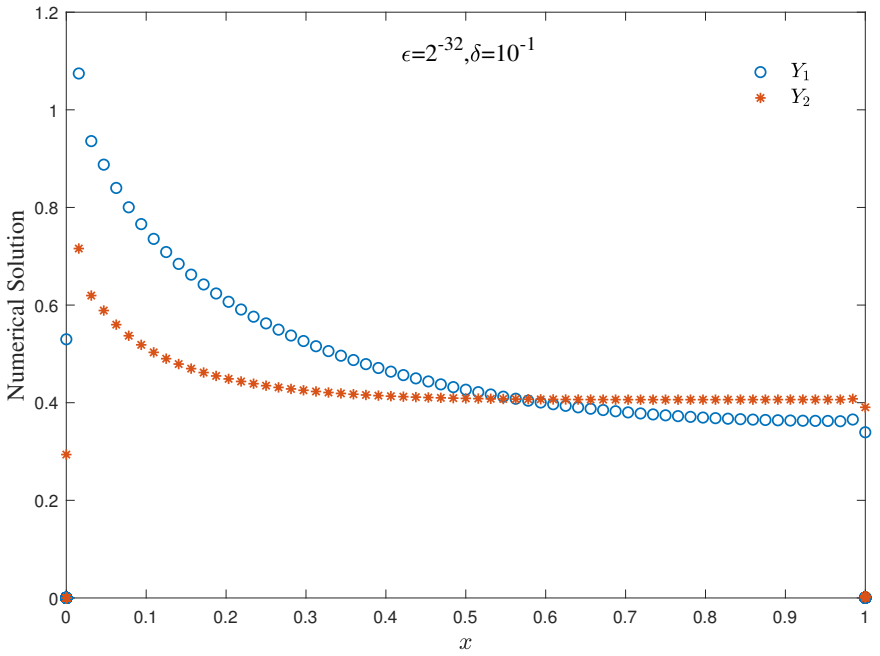

Fig. 3.3: Numerical solution for Example 3.8.2 with $N = 128$.

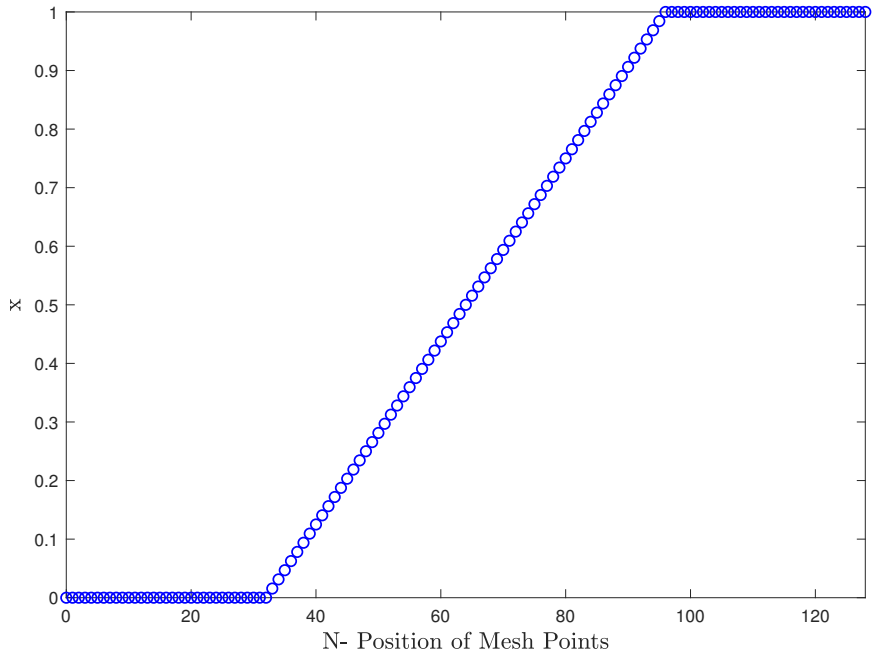

Fig. 3.4: Density of mesh points for Example 3.8.2 with $N = 128$.

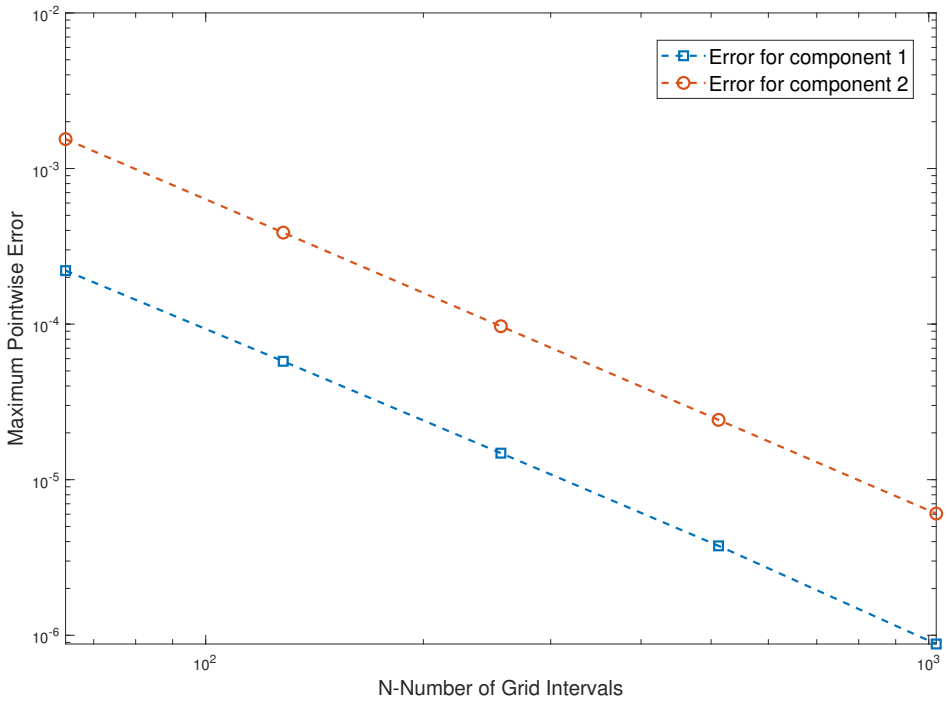

Fig. 3.5: Loglog plot of maximum pointwise errors for Example 3.8.1.

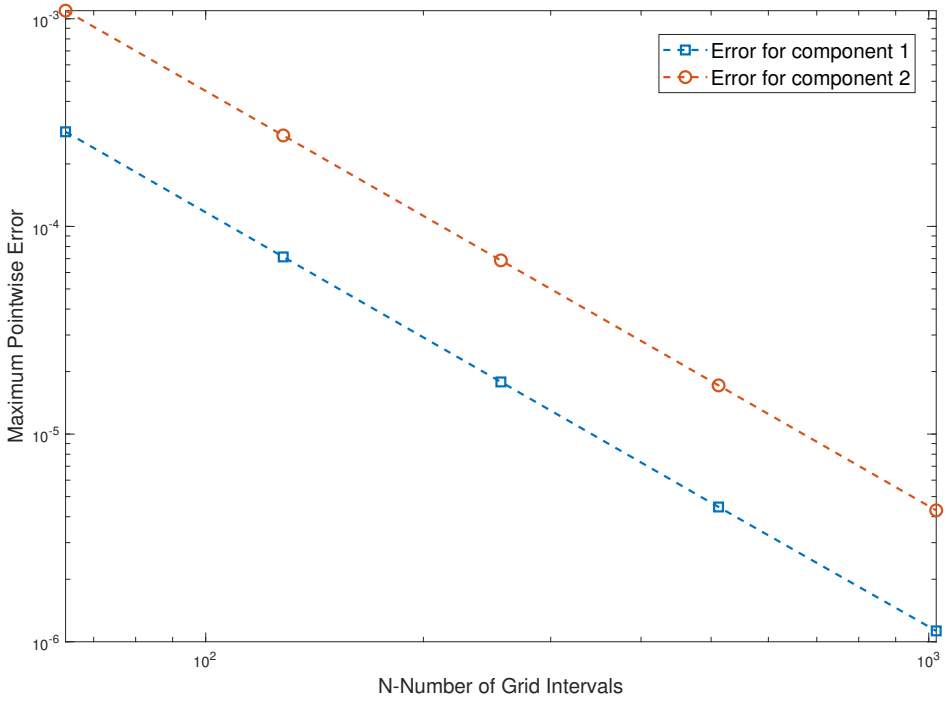

Fig. 3.6: Loglog plot of maximum pointwise errors for Example 3.8.2.

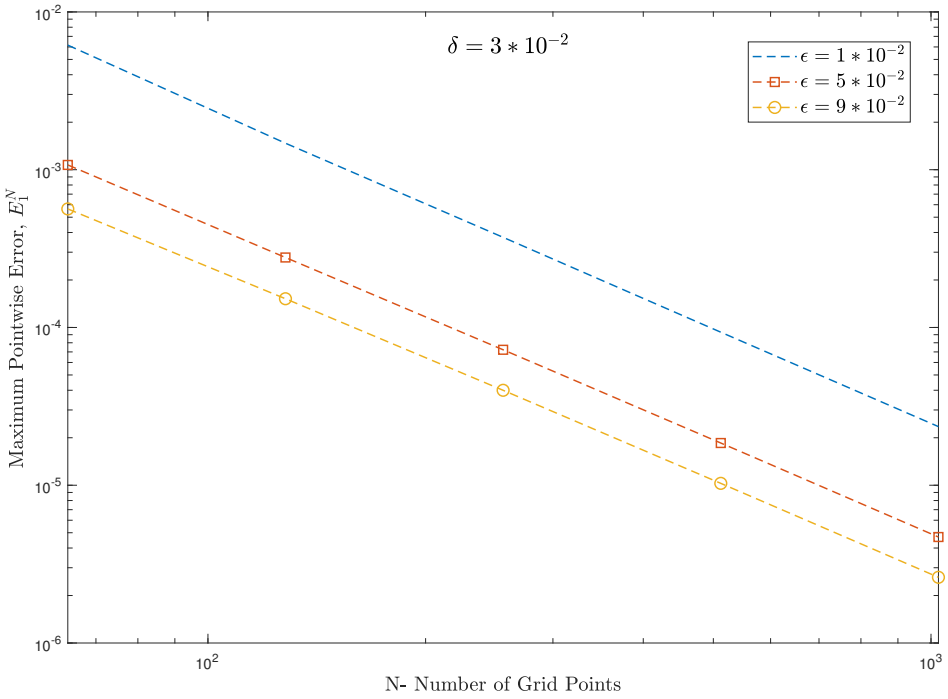

Fig. 3.7: Comparison of maximum pointwise errors, E_1^N for Example 3.8.1 for different values of ε.

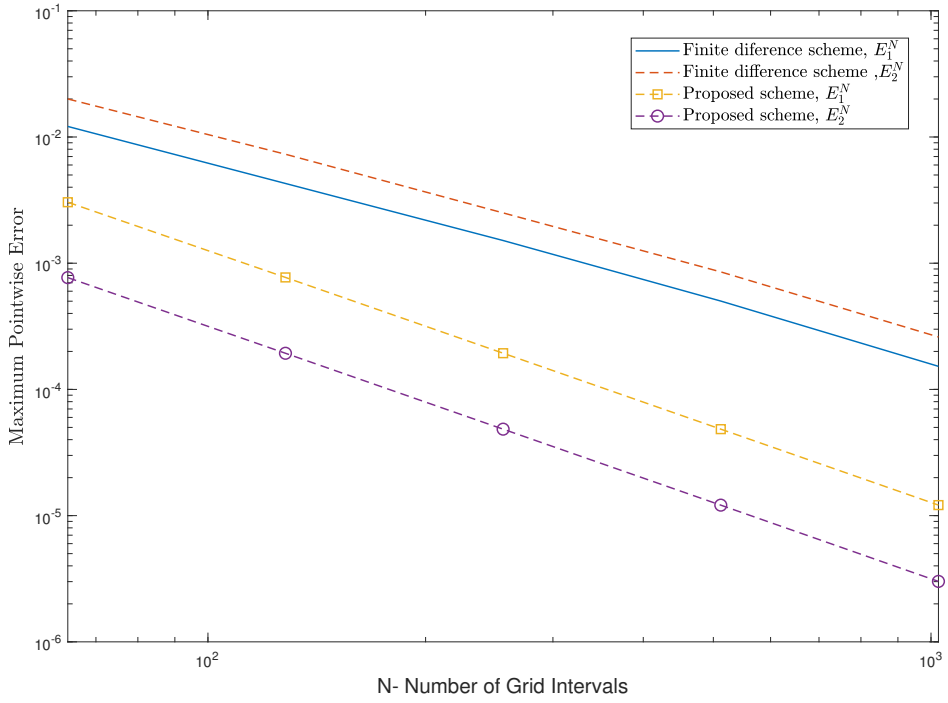

Fig. 3.8: Comparison of maximum pointwise errors for Example 3.8.3 for proposed method with a finite difference method defined over a piece-wise uniform Shiskin mesh.

Table 3.5: Comparison of errors E_m^N and order of convergence p_m^N for Example 3.8.3 of the proposed method with a hybrid difference method on a Shiskin mesh [298] with $m = 1, 2$.

N	Method in [298]		Proposed method		Method in [298]		Proposed method	
	E_1^N	p_1^N	E_1^N	p_1^N	E_2^N	p_2^N	E_2^N	p_2^N
32	2.8268e-2	1.2217	1.154e-02	1.9240	4.4596e-2	1.1560	3.002e-03	1.9650
64	1.2121e-2	1.5008	3.041e-03	1.9788	2.0012e-2	1.4547	7.689e-04	1.9912
128	4.2829e-3	1.5013	7.715e-04	1.9945	7.3012e-3	1.5440	1.934e-04	1.9976
256	1.5128e-3	1.5937	1.936e-04	1.9988	2.5038e-3	1.5529	4.843e-05	1.9997
512	5.0124e-4	1.7179	4.844e-05	1.9996	8.5338e-4	1.7106	1.211e-05	2.0074
1024	1.5237e-4		1.212e-05		2.6074e-4		3.012e-06	

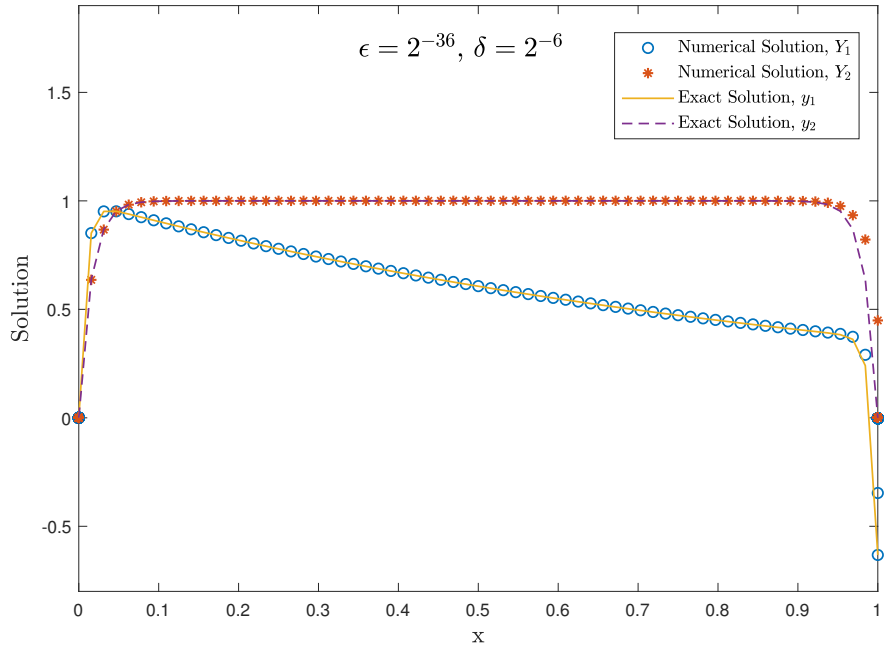

Fig. 3.9: Comparison of numerical solution with the exact solution for Example 3.8.4 with $N = 128$.

Chapter 4

System of Convection-Diffusion Equations with Shifts

4.1 Introduction

A singularly perturbed system of convection-diffusion equations constitutes a class of mathematical models that involves simultaneous interactions of convection and diffusion phenomena. A small parameter characterises them, which multiplies the highest-order derivative term in the governing equations. This small parameter induces a significant disparity in the scales of convection and diffusion processes. The solution of these equations exhibits a multiscale character, since the corresponding degenerate system fails to satisfy the given boundary data. There are narrow regions in which the solution changes rapidly, with the gradient growing exponentially and showing layer behaviour [1]. Coupled systems of equations with shifts have garnered significant attention due to their diverse applications in neuroscience [267, 27], ecology [1], control theory [26], and population dynamics [266], among others [9, 24, 25, 268]. These systems often arise where the dynamics of interconnected processes are influenced by instantaneous and delayed interactions and singular perturbation parameters, leading to rich and complex dynamics that defy straightforward analysis. Understanding the behaviour of singularly perturbed coupled systems with shifts is crucial to predicting system stability, identifying critical thresholds, and designing effective control strategies [3, 5]. However, the inherent complexity of these systems poses significant challenges in analytical treatment, which requires the development of advanced mathematical techniques and computational tools [6].

Many researchers have tried to provide a consistent numerical approximation to singularly perturbed systems involving convection-diffusion equations with shifts. In [301], the author explores a system of convection-diffusion equations that are weakly coupled and feature a discontinuous source. The system under consideration is singularly perturbed, and overlapping boundaries and interior layers characterise the solution to the problem. The paper presents a uniformly convergent numerical approach based on finite differences on a piecewise uniform Shishkin mesh. In addition, [302] deals with a similar system of convection-diffusion equations, but with integral boundary conditions, and proposes

an almost first-order convergent method. In the paper [303], the author proposes a numerical method to solve a system of two convection-diffusion equations with discontinuous coefficients and source terms. The hybrid parameter-uniform approach uses FDM on piecewise uniform Shishkin meshes to handle interior layers. These layers arise from discontinuities in the solution. In the study described in [304], the author deals with a system of weakly coupled convection-diffusion equations that exhibit multiple scales. The author uses sharp estimates for the first-order derivatives obtained in [305] to analyse an upwind FDM on a Shishkin mesh. This analysis leads to sharp bounds for second-order derivatives. Moreover, the study provides the first robust convergence result for the Galerkin FEM on modified Shishkin meshes.

On the other hand, the research presented in [306] introduces an algorithm to approximate solutions to a coupled system of singularly perturbed convection-diffusion problems. This method involves constructing a zero-order asymptotic approximate solution, which leads to the formation of two systems: one with a known analytical solution for the boundary layer and another for the reduced terminal value system. The latter was solved analytically using an improved residual power series approach. Moreover, in [307], the author proposes a fitted numerical method for solving coupled systems of singularly perturbed convection-diffusion delay differential equations. This method presents a novel approach to addressing complex systems, utilising a cubic spline in tension on a uniform mesh. However, these works only analyse systems that have two equations. In reference [308], the author discusses a system of strongly coupled singularly perturbed convection-diffusion problems. They discretise the system using an upwind FDM on a nonuniform mesh, derive a posteriori error estimation in the maximum norm, and design an adaptive mesh algorithm based on this estimation. The algorithm employs a mesh generation procedure using a monitor function based on the arc length. Similarly, reference [309] focuses on a system of weakly coupled singularly perturbed convection-diffusion equations, discretising them using an upwind FDM. They also design an adaptive mesh generation algorithm using a posteriori error estimates in the maximum norm. This algorithm establishes a first-order convergence rate independent of the perturbation parameters. In the article [310], they investigate a system of singularly perturbed convection-diffusion equations with Robin boundary conditions in a unit interval. They transform the problem into a system of first-order singularly perturbed initial value problems and discretise it using the backward Euler formula on a nonuniform mesh. Besides, they develop a posteriori error estimation in the maximum norm for mesh generation and determine the initial values by solving a nonlinear optimisation problem using the Nelder-Mead simplex method. In [280], the authors explore adaptive mesh generation for a coupled system of reaction-diffusion equations. They utilise a central difference method on adaptively generated meshes derived from an equidistribution principle. The method provides a priori and a posteriori error estimates, facilitating second-order parameter uniform convergence, albeit relying on prior knowledge of boundary layer characteristics. For some other earlier works, the reader is referred to [311, 312, 313, 314, 296, 292].

Over the last few decades, the authors have extensively developed various numerical methods for singular perturbation problems. However, most computational studies focus solely on second-order differential equations. The results are notably limited for systems of differential equations or higher-order differential equations. In recent scholarly works, non-classical techniques have emerged as

a powerful tool for diverse systems of singularly perturbed differential equations. The development of special methods for singularly perturbed systems of convection-diffusion equations is a growing area of research that has yet to receive significant attention in the literature. This chapter presents one such method for a system of singularly perturbed convection-diffusion equations with shifts. A careful factorisation handles complex multiscale systems by splitting them into two explicit parts: one capturing smooth solutions and the other addressing boundary layer solutions. Despite its simplicity, this approach effectively captures all essential characteristics of the system. The method utilises the Runge-Kutta method for smooth solutions and asymptotic expansions for boundary layer solutions, ensuring stability and higher-order accuracy. The method is easy to implement, does not require adaptive mesh generation, and avoids logarithmic terms. The numerical results and illustrations support the theoretical results.

4.2 Continous Problem

Let $m \geq 2$ be an integer and consider a system of m-coupled convection-diffusion equations with shifts of mixed type

$$\begin{cases} \mathbf{L}\tilde{\mathbf{y}} := & \boldsymbol{\varepsilon}\tilde{\mathbf{y}}'' + \mathbf{B}\tilde{\mathbf{y}}' + \boldsymbol{\varsigma}\tilde{\mathbf{y}}(x-\tau) + \mathbf{A}\tilde{\mathbf{y}} + \boldsymbol{\rho}\tilde{\mathbf{y}}(x+\mu) = \tilde{\mathbf{g}}(x),\ x \in \Omega = (0,1) \\ & \tilde{\mathbf{y}}(x) = \boldsymbol{\phi}(x), \quad x \in [-\tau, 0] \\ & \tilde{\mathbf{y}}(x) = \boldsymbol{\psi}(x), \quad x \in [1, 1+\mu] \end{cases} \tag{4.2.1}$$

where $0 < \varepsilon_i \ll 1$ for $i = 1,2,...m$ denotes the perturbation parameters, $\boldsymbol{\varepsilon} = diag(\varepsilon_1, \varepsilon_2, ...\varepsilon_m)$, $\boldsymbol{\rho} = diag(\rho_1, \rho_2, ..., \rho_m)$, $\boldsymbol{\varsigma} = diag(\varsigma_1, \varsigma_2, ..., \varsigma_m)$, $\tilde{\mathbf{y}} = (\tilde{y}_1, \tilde{y}_2, ...\tilde{y}_m)^T \in (C(\Omega) \cap (C^2(\Omega))^m$ and τ and μ represents small shifts of $o(\varepsilon)$, respectively. Moreover, let us assume that $\mathbf{B} = diag(b_1, b_2, ...b_m)$ the convection matrix, $\mathbf{A} = (a_{ij})_{m\times m}$ the coupling matrix, $\tilde{\mathbf{g}} = (\tilde{g}_1, \tilde{g}_2, ...\tilde{g}_m)^T$ the source vector, and the given data $\boldsymbol{\phi}(x) = (\phi_1, \phi_2, \ldots, \phi_m)^T$, $\boldsymbol{\psi}(x) = (\psi_1, \psi_2, \ldots, \psi_m)^T$ are sufficiently smooth on $\bar{\Omega}$. Besides, for every i and j

$$b_i - \tau\varsigma_i + \mu\rho_i > 0,\ \varsigma_i + a_{ii} + \rho_i \leq 0 \,\text{and}\, a_{ij} \geq 0\ \forall\ i \neq j.$$

Since τ and μ are of $o(\varepsilon)$, the Taylor series approximation of $\tilde{\mathbf{y}}(x-\tau)$ and $\tilde{\mathbf{y}}(x+\mu)$ after neglecting higher order terms in (4.2.1) leads to

$$\begin{cases} \boldsymbol{\varepsilon}\tilde{\mathbf{y}}'' + (\mathbf{B} - \tau\boldsymbol{\varsigma} + \mu\boldsymbol{\rho})\tilde{\mathbf{y}}'(x) + (\boldsymbol{\varsigma} + \mathbf{A} + \boldsymbol{\rho})\tilde{\mathbf{y}}(x) = \tilde{\mathbf{g}}(x) \\ \tilde{\mathbf{y}}(0) = \boldsymbol{\phi}(0) = \boldsymbol{\phi}, \quad \tilde{\mathbf{y}}(1) = \boldsymbol{\psi}(1) = \boldsymbol{\psi}. \end{cases} \tag{4.2.2}$$

In general, one can assume homogeneous boundary conditions by subtracting from $\tilde{\mathbf{y}}(x)$ a smooth function $\boldsymbol{\wp}(x)$ that satisfies the original boundary conditions [4]. For example, given Drichlet boundary conditions $\tilde{\mathbf{y}}(0) = \boldsymbol{\phi}$ and $\tilde{\mathbf{y}}(1) = \boldsymbol{\psi}$, take

$$\boldsymbol{\wp}(x) = \boldsymbol{\phi}(1-x) + \boldsymbol{\psi}x$$

and set $\mathbf{y}(x) = \tilde{\mathbf{y}}(x) - \wp(x)$. Then $\mathbf{y}$ is the solution of a differential equation of the same type but with homogeneous boundary conditions

$$\begin{cases} \boldsymbol{\varepsilon}\mathbf{y}'' + (\mathbf{B} - \tau\boldsymbol{\varsigma} + \mu\boldsymbol{\rho})\mathbf{y}'(x) + (\boldsymbol{\varsigma} + \mathbf{A} + \boldsymbol{\rho})\mathbf{y}(x) = \mathbf{g}(x) \\ \mathbf{y}(0) = 0, \quad \mathbf{y}(1) = 0 \end{cases} \tag{4.2.3}$$

where $\mathbf{g}(x) := \tilde{\mathbf{g}}(x) - (\mathbf{B} - \tau\boldsymbol{\varsigma} + \mu\boldsymbol{\rho})(\boldsymbol{\psi} - \boldsymbol{\phi}) - (\boldsymbol{\varsigma} + \mathbf{A} + \boldsymbol{\rho})((1-x)\boldsymbol{\phi} + x\boldsymbol{\psi})$.

For $i = 1, 2, \ldots, m$, the i^{th} equation of (5.2.2) satisfies

$$\begin{cases} \varepsilon_i y_i'' + (b_i(x) - \tau\varsigma_i(x) + \mu\rho_i(x))y_i' + (\varsigma_i(x) + \rho_i(x))y_i + \sum_{j=1}^{m} a_{ij}(x)y_j = g_i(x),\ x \in \Omega \\ y_i(0) = 0, y_i(1) = 0. \end{cases} \tag{4.2.4}$$

Rewriting (4.2.4) as

$$\begin{cases} \varepsilon_i y_i'' + (b_i - \tau\varsigma_i + \mu\rho_i)y_i' + (\varsigma_i + a_{ii} + \rho_i)y_i = g_i - \sum\limits_{\substack{j=1 \\ j\neq i}}^{m} a_{ij}y_j \\ y_i(0) = 0, y_i(1) = 0 \end{cases}$$

and from [5, pp. 64], it follows that

$$\|y_i\| + \sum_{\substack{j=1 \\ j\neq i}}^{m} \gamma_{ij}\|y_j\| \leq \min\left\{\left\|\frac{g_i}{\varsigma_i + a_{ii} + \rho_i}\right\|, \left\|\frac{g_i}{b_i - \tau\varsigma_i + \mu\rho_i}\right\|\right\},\ i = 1, 2, \ldots, m.$$

where $\gamma = (\gamma_{ij})_{m\times m}$ is a constant matrix defined as

$$\gamma_{ii} = 1,\ \ \gamma_{ij} = -\min\left\{\left|\left|\frac{a_{ij}}{\varsigma_i + a_{ii} + \rho_i}\right|\right|, \left|\left|\frac{a_{ij}}{b_i - \tau\varsigma_i + \mu\rho_i}\right|\right|\right\} \text{ for } i \neq j$$

and $\|.\|$ is the maximum norm over Ω.

4.3 Properties of the Solution

Imitating the analysis of [305], the stability of the differential operator and uniqueness of the solution follow from the following estimates from [5, Theorem 3.51 and Corollary 3.52].

Theorem 4.3.1. Let $\tilde{\mathbf{A}} := \boldsymbol{\varsigma} + \mathbf{A} + \boldsymbol{\rho}$ be a matrix with its entries in $C[0,1]$ and γ is inverse monotone. Then

$$\|y_i\| \leq \sum_{j=1}^{m} (\gamma^{-1})_{ij} \min\left\{\left|\left|\frac{(\mathscr{L}y)_j}{\varsigma_j + a_{jj} + \rho_j}\right|\right|, \left|\left|\frac{(\mathscr{L}y)_j}{b_j - \tau\varsigma_j + \mu\rho_j}\right|\right|\right\},\ i = 1, \ldots, m$$

for any function $\mathbf{y} = (y_1, y_2, ..., y_m)^T \in \Omega$ with $\mathbf{y}(0) = \mathbf{y}(1) = 0$. The first term in $min\{\ldots\}$ should be omitted if $\varsigma_i + a_{ii} + \rho_i = 0$ for any $x \in \Omega$.

Corollary 4.3.2. Under the hypotheses of Theorem (4.3.1), the solution $\mathbf{y}$ of (5.2.2) is unique and satisfies $\|\mathbf{y}\| \leq C\|\mathbf{g}\|$ for some constant C.

The derivatives of the solution grow exponentially across overlapping boundary layers [4]. Consequently, sharper estimates will be needed to bound the solution derivative.

Theorem 4.3.3. Let $\mathbf{y} = (y_1, y_2, ..., y_m)^T$ be the solution of (5.2.2). Then

$$\|y_i^{(k)}\| = \begin{cases} \mathscr{O}(\varepsilon_i^{-k}) & \text{if } k = 1,2 \\ \mathscr{O}(\varepsilon_p^{-k}) & \text{if } k \geq 3 \end{cases}$$

for $i = 1, 2, \ldots, m$ and $\varepsilon_p := \min\limits_{1 \leq i \leq m} \varepsilon_i$.

Proof. The problem (4.2.4) can be written as:

$$\varepsilon_i y_i'' + (b_i(x) - \tau\varsigma_i(x) + \mu\rho_i(x))y_i' = g_i - (\varsigma_i(x) + \rho_i(x))y_i + \sum_{j=1}^{m} a_{ij}(x)y_j = h_i(x).$$

Multiplying both sides by $e^{\frac{1}{\varepsilon_i}\int_0^x (b_i(t) - \tau\varsigma_i(t) + \mu\rho_i(t))dt}$ and integrating both sides within the limits 0 to x, we get

$$y_i'(x) = \int_0^x \frac{1}{\varepsilon_i} e^{-\frac{1}{\varepsilon_i}\int_s^x (b_i(t) - \tau\varsigma_i(t) + \mu\rho_i(t))dt} h ds + y_i'(0) e^{-\frac{1}{\varepsilon_i}\int_0^x (b_i(t) - \tau\varsigma_i(t) + \mu\rho_i(t))dt}. \tag{4.3.1}$$

Again integrating within the limits 0 to x and using the boundary conditions at $x = 0$, we obtain

$$y_i(x) - \kappa_i = \int_0^x \int_0^\xi \frac{1}{\varepsilon_i} e^{-\frac{1}{\varepsilon_i}\int_s^\xi (b_i(t) - \tau\varsigma_i(t) + \mu\rho_i(t))dt} h ds d\xi + y_i'(0) \int_0^x e^{-\frac{1}{\varepsilon_i}\int_0^\xi (b_i(t) - \tau\varsigma_i(t) + \mu\rho_i(t))dt} d\xi.$$

Let $x = 1$, we get

$$y_i'(0) = \frac{\lambda_i - \kappa_i - \int_0^x \int_0^\xi \frac{1}{\varepsilon_i} e^{-\frac{1}{\varepsilon_i}\int_s^\xi (b_i(t) - \tau\varsigma_i(t) + \mu\rho_i(t))dt} h ds d\xi}{\int_0^1 e^{-\frac{1}{\varepsilon_i}\int_0^\xi (b_i(t) - \tau\varsigma_i(t) + \mu\rho_i(t))dt} d\xi}.$$

This implies

$$|y_i'(0)| \leq \frac{|\lambda_i| + |\kappa_i| + |\int_0^x \int_0^\xi \frac{1}{\varepsilon_i} e^{-\frac{1}{\varepsilon_i}\int_s^\xi (b_i(t) - \tau\varsigma_i(t) + \mu\rho_i(t))dt} h ds d\xi|}{|\int_0^1 e^{-\frac{1}{\varepsilon_i}\int_0^\xi (b_i(t) - \tau\varsigma_i(t) + \mu\rho_i(t))dt} d\xi|} \leq C_2 \varepsilon_i^{-1}.$$

Then equation (4.3.1) gives

$$\begin{aligned} \|y_i'\| &\leq \frac{1}{\underline{(b_i - \tau\varsigma_i + \mu\rho_i)}} (1 - e^{-\underline{(b_i - \tau\varsigma_i + \mu\rho_i)}\frac{x}{\varepsilon_i}}) + |y_i'(0)| e^{-\frac{1}{\varepsilon_i}\int_0^x (b_i(t) - \tau\varsigma_i(t) + \mu\rho_i(t))dt} \\ &\leq C\{1 + \varepsilon_i^{-1} e^{-\underline{(b_i - \tau\varsigma_i + \mu\rho_i)}\frac{x}{\varepsilon_i}}\}. \end{aligned}$$

Now for $k=2$, differentiate (4.2.4) to obtain

$$\begin{aligned}\|y_i''\| &\leq \frac{(b_i-\tau\varsigma_i+\mu\rho_i)}{\varepsilon_i}\|y_i'\|+\frac{\|g_i\|}{\varepsilon_i}+\frac{\|\varsigma_i+\rho_i\|}{\varepsilon_i}\|y_i\|+\sum_{j=1}^{m}\frac{\|a_{ij}\|}{\varepsilon_i}\|y_j\|\\ &\leq C_1\varepsilon_i^{-2}+C_2\varepsilon_i^{-1}+C_3\varepsilon_i^{-1}+C_4\varepsilon_i^{-1}\\ &\leq C\varepsilon_i^{-2}.\end{aligned}$$

For $k=3$, differentiating (4.2.4) to get

$$\begin{aligned}\|y_i'''\| &\leq \frac{\|b_i-\tau\varsigma_i+\mu\rho_i\|}{\varepsilon_i}\|y_i''\|+\frac{\|b_i-\tau\varsigma_i+\mu\rho_i\|}{\varepsilon_i}\|y_i'\|+\frac{\|g_i'\|}{\varepsilon}+\frac{\|\varsigma_i+\rho_i\|}{\varepsilon_i}\|y_i\|+\frac{\|\varsigma_i+\rho_i\|}{\varepsilon_i}\|y_i'\|\\ &\quad+\sum_{j=1}^{m}\Big(\frac{\|a_{ij}\|}{\varepsilon_i}\|y_j\|+\frac{\|a_{ij}\|}{\varepsilon_i}\|y_j'\|\Big)\\ &\leq C\Big(\varepsilon_i^{-3}+\varepsilon_i^{-2}+\varepsilon_i^{-1}+\varepsilon_i^{-1}+\varepsilon_i^{-2}+\sum_{j=1}^{m}\big(\varepsilon_i^{-1}+\varepsilon_i^{-1}\varepsilon_j^{-1}\big)\Big)\\ &\leq C\Big(\varepsilon_p^{-3}+\varepsilon_p^{-2}+\varepsilon_p^{-1}+\varepsilon_p^{-1}+\varepsilon_p^{-2}+\sum_{j=1}^{m}\big(\varepsilon_p^{-1}+\varepsilon_p^{-1}\varepsilon_j^{-1}\big)\Big)\\ &\leq C\varepsilon_p^{-3},\end{aligned}$$

where $\varepsilon_p := \min\limits_{1\leq i\leq m}\varepsilon_i$. For $k>3$, the required result follows from the successive differentiation. □

Remark 4.3.1. The solution of the problem exhibits interacting/overlapping layers of width $\mathscr{O}(\varepsilon_i\, ln\varepsilon_i)$ near $x=0$ for small perturbation parameters. We can obtain similar estimates for problems with condensing layers near $x=1$ simply by replacing $x\mapsto 1-x$.

4.4 Analysis of the Method

Let us write the solution ($\mathbf{y}$) as the sum of a regular ($\mathbf{u}$) and singular ($\mathbf{v}$) parts, $\mathbf{y}:=\mathbf{u}+\mathbf{v}$. Next, we expand $\mathbf{u}$ as an asymptotic series expansion that reads

$$\mathbf{u}=\mathbf{u}_0+\boldsymbol{\epsilon}\mathbf{u}_1+\boldsymbol{\epsilon}^2\mathbf{u}_2+\cdots+\boldsymbol{\epsilon}^k\mathbf{u}_k+\boldsymbol{\epsilon}^{k+1}\mathbf{U}(x,\boldsymbol{\epsilon}) \tag{4.4.1}$$

where $\mathbf{u_i}=(u_{i1},u_{i2},\ldots,u_{im})^T$ for $i=0,1,...,k$. The components $\mathbf{u}_i$ satisfies

$$\begin{cases}(\mathbf{B}-\tau\boldsymbol{\varsigma}+\mu\boldsymbol{\rho})\mathbf{u}_0'+(\boldsymbol{\varsigma}+\mathbf{A}+\boldsymbol{\rho})\mathbf{u}_0=\mathbf{g}\\ \mathbf{u}_0(1)=0\end{cases} \tag{4.4.2}$$

$$\begin{cases}(\mathbf{B}-\tau\boldsymbol{\varsigma}+\mu\boldsymbol{\rho})\mathbf{u}_i'+(\boldsymbol{\varsigma}+\mathbf{A}+\boldsymbol{\rho})\mathbf{u}_i=-\mathbf{u}_{i-1}''\\ \mathbf{u}_i(1)=0\end{cases} \tag{4.4.3}$$

for each $i = 1, 2, \ldots, k$ and

$$\begin{cases} \boldsymbol{\varepsilon}\mathbf{U}'' + (\mathbf{B} - \tau\boldsymbol{\varsigma} + \mu\boldsymbol{\rho})\mathbf{U}' + (\boldsymbol{\varsigma} + \mathbf{A} + \boldsymbol{\rho})\mathbf{U} = -\mathbf{u}_k'' \\ \mathbf{U}(0) = 0, \quad \mathbf{U}(1) = 0. \end{cases} \tag{4.4.4}$$

On the other hand, the singular part $\mathbf{v}$ satisfies

$$\begin{cases} \boldsymbol{\varepsilon}\mathbf{v}'' + (\mathbf{B} - \tau\boldsymbol{\varsigma} + \mu\boldsymbol{\rho})\mathbf{v}' + (\boldsymbol{\varsigma} + \mathbf{A} + \boldsymbol{\rho})\mathbf{v} = 0 \\ \mathbf{v}(0) = -\mathbf{u}(0), \quad \mathbf{v}(1) = 0. \end{cases} \tag{4.4.5}$$

4.4.1 Outer solution

Let $h := 1/N$, $N \in \mathbb{N}$ and define $\bar{\boldsymbol{\Omega}}^N = \{x_i : x_i = ih,\ i = 0, 1, \ldots, N\}$. In this section, we present a higher-order approximation of the smooth part of the solution using the q-stage Runge-Kutta method and estimate the error.

The matrices $(\mathbf{B} - \tau\boldsymbol{\varsigma} + \mu\boldsymbol{\rho})$, $(\boldsymbol{\varsigma} + \mathbf{A} + \boldsymbol{\rho})$ and $\mathbf{g}$ are continuous on $\bar{\boldsymbol{\Omega}}$ and $\|(\mathbf{B} - \tau\boldsymbol{\varsigma} + \mu\boldsymbol{\rho})\| \neq 0$. Thus, the initial value problem (4.4.2) becomes

$$\mathbf{u}_0' = -(\mathbf{B} - \tau\boldsymbol{\varsigma} + \mu\boldsymbol{\rho})^{-1}[(\boldsymbol{\varsigma} + \mathbf{A} + \boldsymbol{\rho})\mathbf{u}_0 - \mathbf{g}] := \mathbf{G}_0(x, \mathbf{u}_0),\ \mathbf{u}_0(1) = 0 \tag{4.4.6}$$

where $\mathbf{G}_0 : \boldsymbol{\Omega} \times \mathbb{R}^m \to \mathbb{R}^m$. Note that its contribution to the solution is only for values near $x = 1$. The q-stage Runge-Kutta method applied to (4.4.6) leads to

$$\begin{cases} (\mathbf{u}_0)_{n+1} = (\mathbf{u}_0)_n - h\psi(x_n, (\mathbf{u}_0)_n, h), \\ \psi(x_n, (\mathbf{u}_0)_n, h) = \sum\limits_{r=1}^{q} w_r^0 \mathbf{k}_r^0, \\ \mathbf{k}_r^0 = \mathbf{G}_0(x_n - \kappa_r^0(\mathbf{u}_0)_n - h\sum\limits_{s=1}^{q} \lambda_{rs}^0 \mathbf{k}_s^0), \\ \lambda_{rs}^0 = 0 \text{ for } s \geq r \text{ and } \sum\limits_{s=1}^{q} \lambda_{rs}^0 = \kappa_r^0 \text{ for } 1 \leq r \leq q. \end{cases}$$

The corresponding determinantal equation is $\rho(\zeta) = \zeta - 1$, and the root condition $\rho(1) = 0$ is satisfied by the polynomial. In addition, we assume that $\sum\limits_{r=1}^{q} w_r^0 = 1$ to ensure the stability and consistency of the Runge-Kutta approach [315]. Thus, an application of the Lax-Richtmyer theorem leads to convergence [315]. Also, it follows from [316] that

$$\|\mathbf{u}_0(x_n) - (\mathbf{u}_0)_n\| = \mathscr{O}(h^{p_0});\ p_0 \leq q.$$

For $\mathbf{u}_1$, set $i = 1$ in (4.4.3), we get

$$\mathbf{u}_1' = -(\mathbf{B} - \tau\boldsymbol{\varsigma} + \mu\boldsymbol{\rho})^{-1}(\boldsymbol{\varsigma} + \mathbf{A} + \boldsymbol{\rho})\mathbf{u}_1 - (\mathbf{B} - \tau\boldsymbol{\varsigma} + \mu\boldsymbol{\rho})^{-1}\mathbf{u}_0''$$

substitute value of $\mathbf{u}_0''$ from (4.4.6) in equation above to write

$$\begin{cases} \mathbf{u}_1' = -(\mathbf{B}-\tau\boldsymbol{\varsigma}+\mu\boldsymbol{\rho})^{-1}(\boldsymbol{\varsigma}+\mathbf{A}+\boldsymbol{\rho})\mathbf{u}_1 + (\mathbf{B}-\tau\boldsymbol{\varsigma}+\mu\boldsymbol{\rho})^{-1}(((\mathbf{B}-\tau\boldsymbol{\varsigma}+\mu\boldsymbol{\rho})^{-1}(\boldsymbol{\varsigma}+\mathbf{A}+\boldsymbol{\rho}))' \\ \qquad -((\mathbf{B}-\tau\boldsymbol{\varsigma}+\mu\boldsymbol{\rho})^{-1}(\boldsymbol{\varsigma}+\mathbf{A}+\boldsymbol{\rho}))^2)\mathbf{u}_0 + \mathbf{B}^{-1}((\mathbf{B}-\tau\boldsymbol{\varsigma}+\mu\boldsymbol{\rho})^{-1}(\boldsymbol{\varsigma}+\mathbf{A}+\boldsymbol{\rho})) \\ \qquad (((\mathbf{B}-\tau\boldsymbol{\varsigma}+\mu\boldsymbol{\rho}))^{-1}\mathbf{g}) - (\mathbf{B}-\tau\boldsymbol{\varsigma}+\mu\boldsymbol{\rho})^{-1}((\mathbf{B}-\tau\boldsymbol{\varsigma}+\mu\boldsymbol{\rho})^{-1}\mathbf{g})' \\ \mathbf{u}_1(1) = 0. \end{cases} \tag{4.4.7}$$

From (4.4.6) and (4.4.7) it follows that

$$\mathbf{u}_{01}' = \mathbf{G}_1(x, \mathbf{u}_{01}); \quad \mathbf{u}_{01}(1) = \boldsymbol{\eta_1} \tag{4.4.8}$$

where $\mathbf{G}_1 : \boldsymbol{\Omega} \times \mathbb{R}^{2m} \to \mathbb{R}^{2m}$, $\mathbf{u}_{01} : \boldsymbol{\Omega} \to \mathbb{R}^{2m}$ and $\boldsymbol{\eta_1}$ are given by

$$\mathbf{G}_1(x, \mathbf{u}_{01}) = \begin{bmatrix} \mathbf{C}_{11} & 0 \\ \mathbf{C}_{21} & \mathbf{C}_{22} \end{bmatrix} \begin{bmatrix} \mathbf{u}_0 \\ \mathbf{u}_1 \end{bmatrix} + \begin{bmatrix} \mathbf{D}_1 \\ \mathbf{D}_2 \end{bmatrix}, \ \mathbf{u}_{01} = \begin{bmatrix} \mathbf{u}_0 \\ \mathbf{u}_1 \end{bmatrix}, \ \boldsymbol{\eta_1} = \begin{bmatrix} 0 \\ 0 \end{bmatrix}$$

and

$$\begin{aligned} \mathbf{C}_{11} &= -(\mathbf{B}-\tau\boldsymbol{\varsigma}+\mu\boldsymbol{\rho})^{-1}(\boldsymbol{\varsigma}+\mathbf{A}+\boldsymbol{\rho}), \\ \mathbf{C}_{21} &= (\mathbf{B}-\tau\boldsymbol{\varsigma}+\mu\boldsymbol{\rho})^{-1}(((\mathbf{B}-\tau\boldsymbol{\varsigma}+\mu\boldsymbol{\rho})^{-1}(\boldsymbol{\varsigma}+\mathbf{A}+\boldsymbol{\rho}))' - ((\mathbf{B}-\tau\boldsymbol{\varsigma}+\mu\boldsymbol{\rho})^{-1}(\boldsymbol{\varsigma}+\mathbf{A}+\boldsymbol{\rho}))^2), \\ \mathbf{C}_{22} &= -(\mathbf{B}-\tau\boldsymbol{\varsigma}+\mu\boldsymbol{\rho})^{-1}\mathbf{A}, \\ \mathbf{D}_1 &= (\mathbf{B}-\tau\boldsymbol{\varsigma}+\mu\boldsymbol{\rho})^{-1}\mathbf{g}, \\ \mathbf{D}_2 &= (\mathbf{B}-\tau\boldsymbol{\varsigma}+\mu\boldsymbol{\rho})^{-1}((\mathbf{B}-\tau\boldsymbol{\varsigma}+\mu\boldsymbol{\rho})^{-1}(\boldsymbol{\varsigma}+\mathbf{A}+\boldsymbol{\rho}))((\mathbf{B}-\tau\boldsymbol{\varsigma}+\mu\boldsymbol{\rho})^{-1}\mathbf{g}), \\ &\quad -(\mathbf{B}-\tau\boldsymbol{\varsigma}+\mu\boldsymbol{\rho})^{-1}((\mathbf{B}-\tau\boldsymbol{\varsigma}+\mu\boldsymbol{\rho})^{-1}\mathbf{g})'. \end{aligned}$$

Again, (4.4.8) leads to

$$\begin{cases} (\mathbf{u}_{01})_{n+1} = (\mathbf{u}_{01})_n - h\boldsymbol{\psi}(x_n, (\mathbf{u}_{01})_n, h), \\ \boldsymbol{\psi}(x_n, (\mathbf{u}_{01})_n, h) = \sum\limits_{r=1}^{q} w_r^1 \mathbf{k}_r^1, \\ \mathbf{k}_r^1 = \mathbf{G}_1(x_n - \kappa_r^1, (\mathbf{u}_{01})_n - h\sum\limits_{s=1}^{q} \lambda_{rs}^1 \mathbf{k}_s^1), \\ \lambda_{rs}^1 = 0 \text{ for } s \geq r \text{ and } \sum\limits_{s=1}^{q} \lambda_{rs}^1 = \kappa_r^1 \text{ for } 1 \leq r \leq q. \end{cases}$$

As earlier, we assume that $\sum\limits_{r=1}^{q} w_r^1 = 1$ and obtain

$$\|\mathbf{u}_{01}(x_n) - (\mathbf{u}_{01})_n\| = \mathscr{O}(h^{p_1}); \quad p_1 \leq q.$$

Finally, set $i = k$ in (4.4.3), and then from (4.4.6), (4.4.7), we obtain

$$\mathbf{u}_k' = \sum_{i=0}^{k} \mathbf{P}_i \mathbf{u}_i + \mathbf{Q}_i; \quad \mathbf{u}_k(1) = 0 \tag{4.4.9}$$

where $\mathbf{P}_i$ and $\mathbf{Q}_i$ depend continuously on the given data and the coefficient matrices. For $i = 0, 1, \ldots, k$, we now examine the following system of first-order initial value problems

$$\mathbf{u}_{0i}' = \mathbf{G}_i(x, \mathbf{u}_{0i}); \quad \mathbf{u}_{0i}(1) = \boldsymbol{\eta_i} \tag{4.4.10}$$

where $\mathbf{u}_{0i} : \boldsymbol{\Omega} \to \mathbb{R}^{im}$, $\mathbf{G}_i : \boldsymbol{\Omega} \times \mathbb{R}^{im} \to \mathbb{R}^{im}$ and $\boldsymbol{\eta_i}$ reads

$$\mathbf{u}_{0i} = \begin{bmatrix} \mathbf{u}_0 \\ \mathbf{u}_1 \\ \mathbf{u}_2 \\ \vdots \\ \mathbf{u}_i \end{bmatrix}, \mathbf{G}_i(x, \mathbf{u}_{0i}) = \begin{bmatrix} \mathbf{C}_{11} & 0 & 0 & \ldots & 0 \\ \mathbf{C}_{21} & \mathbf{C}_{22} & 0 & \ldots & 0 \\ \mathbf{C}_{31} & \mathbf{C}_{32} & \mathbf{C}_{33} & \ldots & 0 \\ \vdots & \vdots & \vdots & \vdots & \vdots \\ \mathbf{C}_{i1} & \mathbf{C}_{i2} & \mathbf{C}_{i3} & \ldots & \mathbf{C}_{ii} \end{bmatrix} \begin{bmatrix} \mathbf{u}_0 \\ \mathbf{u}_1 \\ \mathbf{u}_2 \\ \vdots \\ \mathbf{u}_i \end{bmatrix} + \begin{bmatrix} \mathbf{D}_1 \\ \mathbf{D}_2 \\ \mathbf{D}_3 \\ \vdots \\ \mathbf{D}_i \end{bmatrix}, \boldsymbol{\eta_i} = \begin{bmatrix} 0 \\ 0 \\ 0 \\ \vdots \\ 0 \end{bmatrix}.$$

Here, $\mathbf{C}_{rs}$ are matrices of order $m \times m$ and $\mathbf{D}_r$ are the vectors of order $m \times 1$ that depend on the given data and the coefficient matrices. For $i = 2, 3, \ldots, k$, again we solve (4.4.10) using the q-stage Runge-Kutta approach that reads

$$\begin{cases} (\mathbf{u}_{0i})_{n+1} = (\mathbf{u}_{0i})_n - h\boldsymbol{\psi}(x_n, (\mathbf{u}_{0i})_n, h), \\ \boldsymbol{\psi}(x_n, (\mathbf{u}_{0i})_n, h) = \sum\limits_{r=1}^{q} w_r^i \mathbf{k}_r^i, \\ \mathbf{k}_r^i = \mathbf{G}_i(x_n - \kappa_r^i, (\mathbf{u}_{0i})_n - h \sum\limits_{s=1}^{q} \lambda_{rs}^i \mathbf{k}_s^i), \\ \lambda_{rs}^i = 0 \text{ for } s \geq r \text{ and } \sum\limits_{s=1}^{q} \lambda_{rs}^i = \kappa_r^i \text{ for } 1 \leq r \leq q. \end{cases}$$

As earlier, for $i = 2, 3, \ldots, k$, we assume that $\sum\limits_{r=1}^{q} w_r^i = 1$ and obtain

$$\|\mathbf{u}_{0i}(x_n) - (\mathbf{u}_{0i})_n\| = \mathscr{O}(h^{p_i}), \quad p_i \leq q. \tag{4.4.11}$$

Hence, for $i = 1, 2, \ldots, k$, we get

$$\|\mathbf{u}_i(x_n) - (\mathbf{u}_i)_n\| = \mathscr{O}(h^p), \quad p := \min(p_0, p_1, \ldots, p_i) \leq q. \tag{4.4.12}$$

Using (4.4.9) into (4.4.4) to get

$$\begin{cases} \epsilon \mathbf{U}'' + (\mathbf{B} - \tau\boldsymbol{\varsigma} + \mu\boldsymbol{\rho})\mathbf{U}' + (\boldsymbol{\varsigma} + \mathbf{A} + \boldsymbol{\rho})\mathbf{U} = -\big(\sum\limits_{i=0}^{k} \mathbf{P}_i u_i + \mathbf{Q}_i\big) \\ \mathbf{U}(0) = 0, \quad \mathbf{U}(1) = 0. \end{cases}$$

Then, Corollary (4.3.2) asserts that $\mathbf{U}$ is bounded. Consequently, it follows that

$$\|\mathbf{u}(x_n) - (\mathbf{u})_n\| \leq \sum_{i=0}^{k} \|\boldsymbol{\epsilon}^i(\mathbf{u}_i(x_n) - (\mathbf{u}_i)_n\| + \|\boldsymbol{\epsilon}^{k+1}\mathbf{U}\|. \tag{4.4.13}$$

Next, we combine (4.4.12) and (4.4.13) to obtain the error estimate, summarised below.

Theorem 4.4.1. For $i = 0,1,\ldots,k$, let $(\mathbf{u}_i)_n$ be the approximation to $\mathbf{u}_i$. Then

$$\|\mathbf{u}(x_n) - (\mathbf{u})_n\| = \mathscr{O}(h^p); \quad p \le q. \tag{4.4.14}$$

4.4.2 Inner solution

The singular part $\mathbf{v} = (v_1, v_2, \ldots, v_m)^T$ satisfies (4.4.5). For $i = 1,2,\ldots,m$, we rewrite (4.4.5) as

$$\begin{cases} \varepsilon_i v_i'' + (b_i(x) - \tau\varsigma_i(x) + \mu\rho_i(x))v_i' + (\varsigma_i(x) + \rho_i(x))v_i + \sum\limits_{j=1}^{m} a_{ij}(x)v_j = 0 \\ v_i(0) = -\sum\limits_{j=0}^{k} \varepsilon_i^j u_{ji}(0),\ v_i(1) = 0. \end{cases} \tag{4.4.15}$$

Using the coordinate transform $t_i = x/\varepsilon_i$, $i = 1,2,\ldots,m$, to write

$$\begin{cases} v_i''(t_i) + (b_i(t_i\varepsilon_i) - \tau\varsigma_i(t_i\varepsilon_i) + \mu\rho_i(t_i\varepsilon_i))v_i'(t_i) + (\varsigma_i(t_i\varepsilon_i) + \rho_i(t_i\varepsilon_i))v_i(t_i) \\ \qquad +\varepsilon_i \sum\limits_{j=1}^{m} a_{ij}(t_i\varepsilon_i)v_j(t_j) = 0 \\ v_i(0) = -\sum\limits_{j=0}^{k} \varepsilon_i^j u_{ji}(0),\ \lim\limits_{t_i\to\infty} v_i(t_i) = 0. \end{cases} \tag{4.4.16}$$

For each i, (4.4.16) preserves the order of the original problem and is regularly perturbed from a mathematical perspective. Hence, we can induce a perturbation expansion

$$v_i(t_i) = v_{0i}(t_i) + \varepsilon_i v_{1i}(t_i) + \varepsilon_i^2 v_{2i}(t_i) + \cdots + \varepsilon_i^k v_{ki}(t_i), \quad k \to \infty$$

where $v_{ri} = (v_{r1}, v_{r2}, \ldots, v_{rm})^T$ for $r = 0,1,\ldots,k$. Consequently, from (4.4.16) we get

$$\begin{cases} v_{0i}''(t_i) + (b_i(0) - \tau\varsigma_i(0) + \mu\rho_i(0))v_{0i}'(t_i) = 0 \\ v_{0i} = -u_{0i}(0),\ \lim\limits_{t_i\to\infty} v_{0i}(t_i) = 0 \end{cases} \tag{4.4.17}$$

and

$$\begin{cases} v_{ri}''(t_i) + (b_i(0) - \tau\varsigma_i(0) + \mu\rho_i(0))v_{ri}'(t_i) = -\sum\limits_{n=1}^{r} \left(\dfrac{b_i^n(0) - \tau\varsigma_i^n(0) + \mu\rho_i^n(0)}{n!} t_i^n v_{r-n,i}' \right. \\ \qquad \left. + \left(\dfrac{\varepsilon_j}{\varepsilon_i}\right)^{r-n} \dfrac{(\varsigma_i(0) + \rho_i(0))^{n-1}}{(n-1)!} t_i v_{r-n,i}(t_i) \right) + \sum\limits_{j=1}^{m} \left(\dfrac{\varepsilon_j}{\varepsilon_i}\right)^{r-n} \dfrac{a_{ij}^{n-1}(0)}{(n-1)!} t_i v_{r-n,j}(t_j) \\ v_{ri}(0) = -u_{ri}(0),\ \lim\limits_{t_i\to\infty} v_{ri}(t_i) = 0 \end{cases} \tag{4.4.18}$$

for $r = 1,2,\ldots,k$ and $i = 1,2,\ldots,m$. Note that the solution of (4.4.17) is

$$v_{0i}(x) = -u_{0i}(0)e^{-(b_i(0) - \tau\varsigma_i(0) + \mu\rho_i(0))\frac{x}{\varepsilon_i}}.$$

Let $(v_{0i})_n$ denote the approximation of $v_{0i}(x)$ subject to q-stage Runge-Kutta approximation $(u_{0i})_N$ of the regular component u_{0i} obtained in the previous section. Then, at $x = x_n$, we have

$$(v_{0i})_n = -(u_{0i})_N e^{-(b_i(0)-\tau\varsigma_i(0)+\mu\rho_i(0))\frac{x_n}{\varepsilon_i}}.$$

Then, for $i = 1, 2, \ldots, m$, we compute

$$\|v_{0i}(x_n) - (v_{0i})_n\| \quad = \quad \|(u_{0i}(0) - (u_{0i})_N)\| e^{-(b_i(0)-\tau\varsigma_i(0)+\mu\rho_i(0))\frac{x_n}{\varepsilon_i}}\| = \|(u_{0i}(0) - (u_{0i})_N)\|.$$

If $(v_0)_n$ is the approximation of v_0, then the above expression with (4.4.11) yields

$$\|v_0(x_n) - (v_0)_n\| = \mathscr{O}(h^{p_0}); \quad p_0 \leq q.$$

Taking $r = 1$ in (4.4.18), we get

$$\begin{cases} v''_{1i}(t_i) + (b_i(0) - \tau\varsigma_i(0) + \mu\rho_i(0))v'_{1i}(t_i) = -\Big(\dfrac{b'_i(0) - \tau\varsigma'_i(0) + \mu\rho'_i(0)}{1!} t_i v'_{0i}(t_i) \\ \qquad + \dfrac{\varsigma_i(0) + \rho_i(0)}{0!} v_{0i}(t_i) + \displaystyle\sum_{j=1}^{m} \frac{a_{ij}(0)}{0!} v_{0j}(t_j)\Big) \\ v_{1i}(0) = -u_{1i}(0), \ \lim\limits_{t_i \to \infty} v_{ri}(t_i) = 0. \end{cases} \tag{4.4.19}$$

The exact solution v_{1i} of (4.4.19) is obtained as

$$\begin{aligned} v_{1i}(x) = &-\left(\frac{(b'_i(0) - \tau\varsigma'_i(0) + \mu\rho'_i(0))u_{0i}(0)}{(b_i(0) - \tau\varsigma_i(0) + \mu\rho_i(0))^2} + u_{1i}(0)\right) e^{-(b_i(0)-\tau\varsigma_i(0)+\mu\rho_i(0))\frac{x}{\varepsilon_i}} \\ &- \sum_{\substack{j=1 \\ j\neq i}}^{m} \frac{a_{ij}(0)u_{0j}(0)e^{-(b_i(0)-\tau\varsigma_i(0)+\mu\rho_i(0))\frac{x}{\varepsilon_i}}}{(b_j(0) - \tau\varsigma_j(0) + \mu\rho_j(0)\frac{\varepsilon_i}{\varepsilon_j})^2 - (b_i(0) - \tau\varsigma_i(0) + \mu\rho_i(0))(b_j(0) - \tau\varsigma_j(0) + \mu\rho_j(0))\frac{\varepsilon_i}{\varepsilon_j}} \\ &+ u_{0i}(0)\left((b'_i(0) - \tau\varsigma'_i(0) + \mu\rho'_i(0))\left(\frac{x^2}{2\varepsilon_i^2} + \frac{x}{(b_i(0) - \tau\varsigma_i(0) + \mu\rho_i(0))\varepsilon_i} + \frac{1}{(b_i(0) - \tau\varsigma_i(0) + \mu\rho_i(0))^2}\right)\right. \\ &\left. - \frac{\varsigma_i(0) + a_{ii}(0) + \rho_i(0)}{b_i(0) - \tau\varsigma_i(0) + \mu\rho_i(0)}\frac{x}{\varepsilon_i}\right) e^{-(b_i(0)-\tau\varsigma_i(0)+\mu\rho_i(0))\frac{x}{\varepsilon_i}} \\ &+ \sum_{\substack{j=1 \\ j\neq i}}^{m} \frac{a_{ij}(0)u_{0j}(0)e^{-(b_j(0)-\tau\varsigma_j(0)+\mu\rho_j(0))\frac{x}{\varepsilon_j}}}{(b_j(0) - \tau\varsigma_j(0) + \mu\rho_j(0))\frac{\varepsilon_i}{\varepsilon_j})^2 - (b_i(0) - \tau\varsigma_i(0) + \mu\rho_i(0))(b_j(0) - \tau\varsigma_j(0) + \mu\rho_j(0))\frac{\varepsilon_i}{\varepsilon_j}}. \end{aligned} \tag{4.4.20}$$

Now, if $(v_{1i})_n$ denotes the approximation of $v_{1i}(x)$ at $x = x_n$, we obtain

$$
\begin{aligned}
(v_{1i})_n = & \Big(- \frac{(b_i'(0) - \tau\varsigma_i'(0) + \mu\rho_i'(0))(u_{0i})_N}{(b_i(0) - \tau\varsigma_i(0) + \mu\rho_i(0))^2} - (u_{1i})_N \Big) e^{-(b_i(0)-\tau\varsigma_i(0)+\mu\rho_i(0))\frac{x_n}{\varepsilon_i}} \\
& - \sum_{\substack{j=1 \\ j\neq i}}^{m} \frac{a_{ij}(0)(u_{0j})_N e^{-(b_i(0)-\tau\varsigma_i(0)+\mu\rho_i(0))\frac{x_n}{\varepsilon_i}}}{((b_j(0) - \tau\varsigma_j(0) + \mu\rho_j(0))\frac{\varepsilon_i}{\varepsilon_j})^2 - (b_i(0) - \tau\varsigma_i(0) + \mu\rho_i(0))(b_j(0) - \tau\varsigma_j(0) + \mu\rho_j(0))\frac{\varepsilon_i}{\varepsilon_j}} \\
& + (u_{0i})_N \Big((b_i'(0) - \tau\varsigma_i'(0) + \mu\rho_i'(0)) \Big(\frac{x_n^2}{2\varepsilon_i^2} + \frac{x_n}{(b_i(0)-\tau\varsigma_i(0)+\mu\rho_i(0))\varepsilon_i} + \frac{1}{(b_i(0) - \tau\varsigma_i(0) + \mu\rho_i(0))^2} \Big) \\
& - \frac{\varsigma_i(0) + a_{ii}(0) + \rho_i(0)}{b_i(0) - \tau\varsigma_i(0) + \mu\rho_i(0)} \frac{x_n}{\varepsilon_i} \Big) e^{-(b_i(0)-\tau\varsigma_i(0)+\mu\rho_i(0))\frac{x_n}{\varepsilon_i}} \\
& + \sum_{\substack{j=1 \\ j\neq i}}^{m} \frac{a_{ij}(0)(u_{0j})_N e^{-(b_j(0)-\tau\varsigma_j(0)+\mu\rho_j(0))\frac{x_n}{\varepsilon_j}}}{((b_j(0) - \tau\varsigma_j(0) + \mu\rho_j(0))\frac{\varepsilon_i}{\varepsilon_j})^2 - (b_i(0) - \tau\varsigma_i(0) + \mu\rho_i(0))(b_j(0) - \tau\varsigma_j(0) + \mu\rho_j(0))\frac{\varepsilon_i}{\varepsilon_j}}.
\end{aligned}
\tag{4.4.21}
$$

Therefore, from (4.4.20) and (4.4.21), the error for v_{1i} satisfies

$$
\begin{aligned}
\|v_{1i}(x_n) - (v_{1i})_n\| \leq & \Big(\Big| - \frac{b_i'(0) - \tau\varsigma_i'(0) + \mu\rho_i'(0)}{(b_i(0) - \tau\varsigma_i(0) + \mu\rho_i(0))^2} \Big| |u_{0i}(0) - (u_{0i})_N| + |u_{1i}(0) - (u_{1i})_N| \Big) \\
& \|e^{-(b_i(0)-\tau\varsigma_i(0)+\mu\rho_i(0))\frac{x_n}{\varepsilon_i}}\| \\
& + |b_i'(0) - \tau\varsigma_i'(0) + \mu\rho_i'(0)||u_{0i}(0) - (u_{0i})_N| \Big(\frac{1}{2} \Big| \Big| \frac{x_n^2}{\varepsilon_i^2} e^{-(b_i(0)-\tau\varsigma_i(0)+\mu\rho_i(0))\frac{x_n}{\varepsilon_i}} \Big| \Big| \\
& + \Big| \frac{1}{b_i(0) - \tau\varsigma_i(0) + \mu\rho_i(0)} \Big| \Big| \Big| \frac{x_n}{\varepsilon_i} e^{-(b_i(0)-\tau\varsigma_i(0)+\mu\rho_i(0))\frac{x_n}{\varepsilon_i}} \Big| \Big| \\
& + \Big| \frac{1}{(b_i(0) - \tau\varsigma_i(0) + \mu\rho_i(0))^2} \Big| \Big| \Big| \frac{x_n}{\varepsilon_i} e^{-(b_i(0)-\tau\varsigma_i(0)+\mu\rho_i(0))\frac{x_n}{\varepsilon_i}} \Big| \Big| \Big) \\
& + \sum_{j=1}^{m} \Big| \frac{a_{ij}(0)}{b_i(0) - \tau\varsigma_i(0) + \mu\rho_i(0)} \Big| |u_{0i}(0) - (u_{0i})_N| \Big| \Big| \frac{x_n}{\varepsilon_i} e^{-(b_i(0)-\tau\varsigma_i(0)+\mu\rho_i(0))\frac{x_n}{\varepsilon_i}} \Big| \Big| \\
& + \Big| \frac{\varsigma_i(0) + \rho_i(0)}{b_i(0) - \tau\varsigma_i(0) + \mu\rho_i(0)} \Big| |u_{0i}(0) - (u_{0i})_N| \Big| \Big| \frac{x_n}{\varepsilon_i} e^{-(b_i(0)-\tau\varsigma_i(0)+\mu\rho_i(0))\frac{x_n}{\varepsilon_i}} \Big| \Big| \\
& + \sum_{\substack{j=1 \\ j\neq i}}^{m} \frac{|a_{ij}(0)||u_{0j}(0) - (u_{0j})_N|}{|((b_j(0)-\tau\varsigma_j(0)+\mu\rho_j(0))\frac{\varepsilon_i}{\varepsilon_j})^2 - (b_i(0)-\tau\varsigma_i(0)+\mu\rho_i(0))(b_j(0)-\tau\varsigma_j(0)+\mu\rho_j(0))\frac{\varepsilon_i}{\varepsilon_j}|} \\
& (\|e^{-(b_i(0)-\tau\varsigma_i(0)+\mu\rho_i(0))\frac{x_n}{\varepsilon_i}}\| + \|e^{-(b_j(0)-\tau\varsigma_j(0)+\mu\rho_j(0))\frac{x_n}{\varepsilon_j}}\|), \ \ i = 1, 2, \ldots, m.
\end{aligned}
\tag{4.4.22}
$$

Also, for $n \in \mathbb{N}$, note that

$$
\|e^{-(b_i(0)-\tau\varsigma_i(0)+\mu\rho_i(0))\frac{x_n}{\varepsilon_i}}\|_{\bar{\Omega}} = 1, \ \Big| \Big| \frac{x^n}{\varepsilon_i^n} e^{-(b_i(0)-\tau\varsigma_i(0)+\mu\rho_i(0))\frac{x}{\varepsilon_i}} \Big| \Big|_{\bar{\Omega}} = \Big(\frac{ne^{-1}}{b_i(0) - \tau\varsigma_i(0) + \mu\rho_i(0)} \Big)^n.
\tag{4.4.23}
$$

Using (4.4.11), (4.4.23) and (4.4.22) to estimate

$$
\|v_{1i}(x_n) - (v_{1i})_n\| = \mathscr{O}(h^p) \text{ for } i = 1, 2, \ldots, m \text{ and } p = \min\{p_0, p_1, \ldots, p_k\} \leq q.
$$

Similarly, we an get estimates for $r = 2,3,\ldots,k$, leading to the following theorem.

Theorem 4.4.2. If $u_{0i}(x_n)$ and $u_{ri}(x_n)$ be the computed solution of (4.4.2) and (4.4.3), respectively. Then

$$\|v_{ri}(x_n) - (v_{ri})_n\| = \mathscr{O}(h^p);\ \ 1 \le r \le k,\ \ 1 \le i \le m,\ \ p \le q$$

where $v_{ri}(x_n)$ and $(v_{ri})_n$ are the exact and approximate solutions of (4.4.17) and (4.4.18).

Let us write the singular component $\mathbf{v}$ in the form of a perturbation series as previously done with the regular component

$$\mathbf{v} = \mathbf{v}_0 + \boldsymbol{\epsilon}\mathbf{v}_1 + \boldsymbol{\epsilon}^2\mathbf{v}_2 + \cdots + \boldsymbol{\epsilon}^k\mathbf{v}_k, \tag{4.4.24}$$

where $\mathbf{v}_r = (v_{r1}, v_{r2}, \ldots, v_{rm})^T$ for $r = 0,1,...,k$. Let

$$(\mathbf{v})_n = (\mathbf{v}_0)_n + \boldsymbol{\epsilon}(\mathbf{v}_1)_n + \boldsymbol{\epsilon}^2(\mathbf{v}_2)_n + \cdots + \boldsymbol{\epsilon}^k(\mathbf{v}_k)_n \tag{4.4.25}$$

where $(\mathbf{v}_r)_n = ((v_{r1})_n, (v_{r2})_n, \ldots, (v_{rm})_n)^T$ denotes the estimated equivalents of $\mathbf{v}_r$ for $r = 0,1,...,k$. Consequently, (4.4.24), (4.4.25) and Theorem 4.4.2 yields

$$\|\mathbf{v}(x_n) - (\mathbf{v})_n\| = \mathscr{O}(h^p). \tag{4.4.26}$$

Let $(\mathbf{y})_n$ be the approximate solution of (5.2.2) and is represented as

$$(\mathbf{y})_n = (\mathbf{u})_n + (\mathbf{v})_n.$$

Then, (4.4.14) and (4.4.26) yields

$$\|\mathbf{y}(x_n) - (\mathbf{y})_n\| = \mathscr{O}(h^p),\ \ p = \min(p_0, p_1, \ldots, p_i) \le q$$

the required estimate.

4.5 Numerical Experiments

To showcase the efficacy of the proposed method, we undertake some test problems and present a comparative analysis of numerical results against well-established numerical methodologies or with the exact analytical solution if available. Notably among the numerical methods are a fitted numerical method based on cubic spline in tension [307], an iterative scheme [317] and a FDM over layer adaptive meshes generated via an entropy production operator [318]. The reduced or degenerate system is numerically solved for the outer solution using the q-stage Runge-Kutta method. For numerical computation, we choose $q = 4$. The inner problem, derived through appropriate coordinate transformations, is addressed analytically. When an exact solution is accessible for comparison, we compute maximum

absolute errors $(E^k_{\varepsilon,N})$ employing the formula

$$E^k_{\varepsilon,N} := \sum_{i=0}^{k} \|(\tilde{y}_i(x_n) - (\tilde{y}_i)_n)\|, \quad k \geq 0.$$

If the exact solution is unavailable, we obtain the maximum absolute error using the double mesh principle [5] given by

$$E^k_{\varepsilon,N} := \sum_{i=0}^{k} \|(\tilde{y}^N_i)_n - (\tilde{y}^{2N}_i)_n\|, \quad k \geq 0.$$

Example 4.5.1. For $x \in \Omega$, consider the boundary value problem

$$\begin{pmatrix} \varepsilon_1 & 0 \\ 0 & \varepsilon_2 \end{pmatrix} \tilde{\mathbf{y}}''(x) + \begin{pmatrix} 1 & 0 \\ 0 & 2 \end{pmatrix} \tilde{\mathbf{y}}'(x) + \begin{pmatrix} 1 & 0 \\ 0 & 1 \end{pmatrix} \tilde{\mathbf{y}}(x-\tau) + \begin{pmatrix} -6 & 2 \\ 1 & -5 \end{pmatrix} \tilde{\mathbf{y}} + \begin{pmatrix} 1 & 0 \\ 0 & 2 \end{pmatrix} \tilde{\mathbf{y}}(x+\mu) = \tilde{\mathbf{g}}(x),$$

where $\tilde{\mathbf{y}}(x) = (\sin x, x)^T$ for $x \in [-\tau, 0]$ and $\tilde{\mathbf{y}}(x) = \left(x-1, \cos\left(\frac{\pi}{2}x\right)\right)^T$ for $x \in [1, 1+\mu]$. Here, $\tilde{\mathbf{g}}(x) = (\tilde{g}_1(x), \tilde{g}_2(x))^T$ is choosen such that

$$\tilde{y}_1(x) = \frac{1 - e^{-\frac{2x}{\varepsilon_2+\mu}}}{1 - e^{-\frac{2}{\varepsilon_2+\mu}}} + \frac{1 - e^{-\frac{x}{\varepsilon_1+\tau}}}{1 - e^{-\frac{1}{\varepsilon_1+\tau}}} - 2x, \quad \tilde{y}_2(x) = \frac{1 - e^{-\frac{2x}{\varepsilon_2+\mu}}}{1 - e^{-\frac{2}{\varepsilon_2+\mu}}} - \sin\left(\frac{\pi}{2}x\right).$$

Example 4.5.2. For $x \in \Omega$, consider the boundary value problem [307, 317]

$$\begin{pmatrix} -\varepsilon_1 & 0 \\ 0 & -\varepsilon_2 \end{pmatrix} \tilde{\mathbf{y}}''(x) + \begin{pmatrix} 11 & 0 \\ 0 & 16 \end{pmatrix} \tilde{\mathbf{y}}'(x) + \begin{pmatrix} -1 & 0 \\ 0 & -1 \end{pmatrix} \tilde{\mathbf{y}}(x-1) + \begin{pmatrix} 6 & -2 \\ -2 & 5 \end{pmatrix} \tilde{\mathbf{y}}(x) + \begin{pmatrix} 0 & 0 \\ 0 & 0 \end{pmatrix} \tilde{\mathbf{y}}(x+1) = \begin{pmatrix} e^x \\ x^2 \end{pmatrix},$$

where $\tilde{\mathbf{y}}(x) = (1+x, \cos(\pi x))^T$ for $x \in [-1, 0]$ and $\tilde{\mathbf{y}}(2) = (1,1)^T$ for $x \in [1, 2]$. The analytical solution of the problem is not known.

Example 4.5.3. For $x \in \Omega$, consider the boundary value problem

$$\begin{pmatrix} \varepsilon_1 & 0 \\ 0 & \varepsilon_2 \end{pmatrix} \tilde{\mathbf{y}}''(x) + \begin{pmatrix} 1 & 0 \\ 0 & 2 \end{pmatrix} \tilde{\mathbf{y}}'(x) + \begin{pmatrix} 1 & 0 \\ 0 & 1 \end{pmatrix} \tilde{\mathbf{y}}(x-\tau) + \begin{pmatrix} -4 & 1 \\ 1 & -6 \end{pmatrix} \tilde{\mathbf{y}}(x) + \begin{pmatrix} 1 & 0 \\ 0 & 2 \end{pmatrix} \tilde{\mathbf{y}}(x+\mu) = \tilde{\mathbf{g}}(x),$$

where $\tilde{\mathbf{y}}(x) = \left(\sin x, x^2\right)^T$ for $x \in [-\tau, 0]$ and $\tilde{\mathbf{y}}(x) = \left(xe^{-x}, \frac{x}{2}(2-x)\right)^T$ for $x \in [1, 1+\mu]$. Here, $\tilde{\mathbf{g}}(x) = (\tilde{g}_1(x), \tilde{g}_2(x))^T$ is choosen such that

$$\tilde{y}_1(x) = \frac{1 - e^{-\frac{x}{\varepsilon_2+\mu}}}{1 - e^{-\frac{1}{\varepsilon_2+\mu}}} + \frac{1 - e^{-\frac{x}{\varepsilon_1+\tau}}}{1 - e^{-\frac{1}{\varepsilon_1+\tau}}} + xe^{-x} - 2x, \quad \tilde{y}_2(x) = \frac{1 - e^{-\frac{x}{\varepsilon_2+\mu}}}{1 - e^{-\frac{1}{\varepsilon_2+\mu}}} + \frac{x}{2} - xe^{(x-1)}.$$

Example 4.5.4. For $x \in \Omega$, consider the boundary value problem

$$\begin{pmatrix} \varepsilon_1 & 0 & 0 \\ 0 & \varepsilon_2 & 0 \\ 0 & 0 & \varepsilon_3 \end{pmatrix} \tilde{\mathbf{y}}''(x) + \begin{pmatrix} -1 & 0 & 0 \\ 0 & -1 & 0 \\ 0 & 0 & -1 \end{pmatrix} \tilde{\mathbf{y}}'(x) + \begin{pmatrix} 1 & 0 & 0 \\ 0 & 1 & 0 \\ 0 & 0 & 2 \end{pmatrix} \tilde{\mathbf{y}}(x-\tau) + \begin{pmatrix} -6 & 1 & 2 \\ 2 & -7 & 2 \\ 4 & 2 & -11 \end{pmatrix} \tilde{\mathbf{y}}(x) + \begin{pmatrix} 1 & 0 & 0 \\ 0 & 1 & 0 \\ 0 & 0 & 2 \end{pmatrix} \tilde{\mathbf{y}}(x+\mu) = \tilde{\mathbf{g}}(x),$$

where $\tilde{\mathbf{y}}(x) = \left(\frac{1-3x}{4}, \frac{1-x^2}{2}, e^{-1}-x\right)^T$ for $x \in [-\tau, 0]$ and $\tilde{\mathbf{y}}(x) = \left(1-x, 0, \frac{x}{2}(1-x)\right)^T$ for $x \in [1, 1+\mu]$. Here, $\tilde{\mathbf{g}}(x) = (\tilde{g}_1(x), \tilde{g}_2(x), \tilde{g}_3(x))^T$ is choosen such that

$$\begin{aligned}
\tilde{y}_1(x) &= \frac{1-e^{-\frac{1-x}{\varepsilon_3}}}{1-e^{-\frac{1}{\varepsilon_3}}} + \frac{1-e^{-\frac{1-x}{\varepsilon_2+\mu}}}{1-e^{-\frac{1}{\varepsilon_2+\mu}}} + \frac{1-e^{-\frac{1-x}{\varepsilon_1+\tau}}}{1-e^{-\frac{1}{\varepsilon_1+\tau}}} + \frac{1-x}{4} - 3(1-x), \\
\tilde{y}_2(x) &= \frac{1-e^{-\frac{1-x}{\varepsilon_3}}}{1-e^{-\frac{1}{\varepsilon_3}}} + \frac{1-e^{-\frac{1-x}{\varepsilon_2+\mu}}}{1-e^{-\frac{1}{\varepsilon_2+\mu}}} + \frac{1-x}{2} - 2\sin\left(\frac{\pi}{2}(1-x)\right), \\
\tilde{y}_3(x) &= \frac{1-e^{-\frac{1-x}{\varepsilon_3}}}{1-e^{-\frac{1}{\varepsilon_3}}} + (1-x)e^{x-1} - (1-x)e^{-x}.
\end{aligned}$$

Table 4.1: Maximum absolute errors for Example 4.5.1 with $\tau = 10^{-2}, \mu = 10^{-8}$ and $\varepsilon_1 = \varepsilon_2 = \varepsilon$.

ε		N=64	N=128	N=256	N=512	N=1024
10^{-5}	$E^0_{\varepsilon,N}$	5.1649e-06	5.1660e-06	5.1662e-06	5.1662e-06	5.1662e-06
	$E^1_{\varepsilon,N}$	1.1585e-08	7.1479e-10	5.6439e-11	5.4915e-11	5.4858e-11
10^{-7}	$E^0_{\varepsilon,N}$	5.0533e-08	5.1591e-08	5.1658e-08	5.1662e-08	5.1662e-08
	$E^1_{\varepsilon,N}$	1.1582e-08	7.1007e-10	4.3955e-11	2.7343e-12	1.7097e-13
10^{-9}	$E^0_{\varepsilon,N}$	1.1697e-08	8.3740e-10	5.1232e-10	5.1635e-10	5.1660e-10
	$E^1_{\varepsilon,N}$	1.1582e-08	7.1007e-10	4.3954e-11	2.7338e-12	1.7064e-13

Table 4.2: Comparison of analytic and approximate solutions for Example 4.5.1 with $N = 100$, $\tau = \mu = 10^{-8}$ and $\varepsilon_1 = \varepsilon_2 = 10^{-10}$.

	$\tilde{y}_1$		$\tilde{y}_2$	
x	Analytic	Approximate	Analytic	Approximate
0.00	0.0000000000	0.0000000000	0.0000000000	0.0000000000
0.02	1.9600000000	1.9599999994	0.9685892409	0.9685892410
0.04	1.9200000000	1.9199999993	0.9372094805	0.9372094806
0.06	1.8800000000	1.8799999992	0.9058916867	0.9058916868
0.08	1.8400000000	1.8399999992	0.8746667664	0.8746667666
0.10	1.8000000000	1.7999999991	0.8435655350	0.8435655351
0.20	1.6000000000	1.5999999988	0.6909830056	0.6909830058
0.40	1.2000000000	1.1999999983	0.4122147477	0.4122147480
0.60	0.8000000000	0.7999999981	0.1909830056	0.1909830059
0.80	0.4000000000	0.3999999985	0.0489434837	0.0489434839
1.00	0.0000000000	0.0000000000	0.0000000000	0.0000000000

For Examples 4.5.1, 4.5.3 and 4.5.4, Figures 4.1, 4.2, 4.3, 4.4, 4.5 and 4.6 illustrate the comparison between analytic and computed solutions for different values of perturbation parameters and shifts,

Table 4.3: Maximum absolute error ($E^1_{\varepsilon,N}$) for Example 4.5.1 with $N = 512$ and $\tau = \mu = 10^{-6}$.

$\varepsilon_1 \downarrow \varepsilon_2 \rightarrow$	10^{-10}	10^{-11}	10^{-12}	10^{-13}	10^{-14}	10^{-15}
10^{-10}	5.5511e-15	2.1088e-11	2.3254e-11	2.3417e-11	2.3417e-11	5.7344e-11
10^{-11}	2.1074e-11	1.7097e-14	2.1787e-12	2.3415e-12	2.3415e-12	2.3415e-12
10^{-12}	2.3182e-11	2.0963e-12	7.1276e-14	2.3404e-13	2.3404e-13	2.3404e-13
10^{-13}	2.3393e-11	2.3059e-12	1.4921e-13	2.3093e-14	2.3093e-14	2.3093e-14
10^{-14}	2.3413e-11	2.3270e-12	1.6165e-13	6.3283e-15	2.2204e-15	2.2204e-15
10^{-15}	2.3416e-11	2.3290e-12	1.6276e-13	6.3283e-15	2.2204e-15	2.2204e-15

Table 4.4: Comparison of maximum absolute errors for Example 4.5.2 for different values of $\varepsilon_1 = \varepsilon_2 = \varepsilon \in \{2^{-6}, 2^{-7}, ..., 2^{-19}, 2^{-20}\}$.

	Method [307]	Method [317]	Present Method	Method [307]	Method [317]	Present Method
N	$E^0_{\varepsilon,N}$	$E^0_{\varepsilon,N}$	$E^0_{\varepsilon,N}$	$E^1_{\varepsilon,N}$	$E^1_{\varepsilon,N}$	$E^1_{\varepsilon,N}$
64	3.0136e–03	5.7577e-3	4.5621e-07	1.8168e–03	4.5703e-3	5.1227e-10
128	1.5232e–03	2.9662e-3	5.1691e-07	9.3052e–04	2.5914e-3	2.9841e-11
256	7.6577e–04	1.4985e-3	5.1732e-07	4.7082e–04	1.4979e-3	1.7409e-12
512	3.8392e–04	7.5187e-4	5.1751e-07	2.3681e–04	8.3942e-4	2.1128e-13
1024	1.9222e–04	3.7640e-4	5.1760e-07	1.1875e–04	4.6870e-4	1.1161e-13
2048	9.6175e–05	1.8828e-4	5.1764e-07	5.9465e–05	2.5666e-4	1.0123e-13

respectively. The Figures confirm that the solution to the problem exhibits layer behaviour. Note that as the perturbation parameter decreases, the problem becomes stiffer from a mathematical perspective, and the layer becomes sharper and sharper. It is clear from Figures that the computed solutions of the system are sufficiently close to the analytic solutions within and outside the boundary layer regions. The maximum absolute errors are tabulated in Tables 4.1, 4.6 and 4.9 for Examples 4.5.1, 4.5.3 and 4.5.4, respectively. In contrast, Tables 4.4 and 4.5 compare the maximum absolute error obtained using the present method with some other state-of-the-art methods [307, 317, 318]. The analytic solution is available for Example, 4.5.1, 4.5.3 and 4.5.4, and Tables 4.2, 4.7, and 4.8 compare the computed solution with the analytic solution. Moreover, Table 4.3 illustrates the maximum absolute error for Example 4.5.1, for the relative values of the perturbation parameters.

4.6 Conclusion

A singularly perturbed coupled system of convection-diffusion equations with shifts is solved numerically using a semi-analytical approach. The strategy involves factorising a coupled system of equations into explicit systems of first-order initial value and second-order boundary problems. The solutions to the degenerate system correspond to the regular component. In contrast, those of the system of boundary value problems represent the singular component. The process combines the regular and singular components to obtain the complete solution. The q-stage Runge-Kutta method computes the outer solution, and an analytical approach derives the inner solution. The proposed method is unconditionally stable and converges independently of the perturbation parameters. Unlike numerical methods, the proposed technique does not require adaptive mesh generation to sustain approximation and consequently has less computational complexity. The process is straightforward and interdisciplinary researchers can quickly adapt the method to solve problems related to chemical

Table 4.5: Comparison of maximum absolute errors for Example 4.5.2 for different values of $\varepsilon_1 = \varepsilon_2 = \varepsilon$ and $N = 23$.

ε	Generated Mesh	Method in [318] $E^0_{\varepsilon,N}$	Present Method $E^0_{\varepsilon,N}$	Method in [318] $E^1_{\varepsilon,N}$	Present Method $E^1_{\varepsilon,N}$
2^{-6}	35	0.00196	3.0231e-05	0.00304	2.2421e-05
2^{-7}	37	0.00193	3.0239e-05	0.00308	2.2439e-05
2^{-8}	39	0.00192	3.0241e-05	0.00309	2.2445e-05
2^{-9}	41	0.00191	3.0242e-05	0.00310	2.2445e-05
2^{-10}	43	0.00192	3.0242e-05	0.00309	2.2446e-05
2^{-11}	45	0.00192	3.0242e-05	0.00310	2.2446e-05
2^{-12}	47	0.00192	3.0242e-05	0.00309	2.2446e-05
2^{-13}	51	0.00192	3.0242e-05	0.00309	2.2446e-05
2^{-14}	53	0.00192	3.0242e-05	0.00309	2.2446e-05
2^{-15}	55	0.00192	3.0242e-05	0.00309	2.2446e-05
2^{-16}	57	0.00192	3.0242e-05	0.00309	2.2446e-05
2^{-17}	59	0.00192	3.0242e-05	0.00309	2.2446e-05
2^{-18}	61	0.00192	3.0242e-05	0.00309	2.2446e-05

Table 4.6: Maximum absolute errors for Example 4.5.3 with $\tau = 10^{-2}, \mu = 10^{-8}$ and $\varepsilon_1 = \varepsilon_2 = \varepsilon$.

ε		N=64	N=128	N=256	N=512	N=1024
10^{-3}	$E^0_{\varepsilon,N}$	7.0481e-04	7.1248e-04	7.1248e-04	7.1271e-04	7.1299e-04
	$E^1_{\varepsilon,N}$	5.0000e-04	5.0000e-04	5.0626e-03	3.0516e-02	5.8581e-02
10^{-5}	$E^0_{\varepsilon,N}$	7.1450e-06	7.2253e-06	7.2649e-06	7.2846e-06	7.2946e-06
	$E^1_{\varepsilon,N}$	5.0000e-06	5.0000e-06	5.0000e-06	5.0000e-06	5.0000e-06
10^{-7}	$E^0_{\varepsilon,N}$	5.5883e-07	5.5883e-07	5.5883e-07	5.5883e-07	5.5883e-07
	$E^1_{\varepsilon,N}$	5.9562e-07	5.9562e-07	5.9562e-07	5.9562e-07	5.9562e-07
10^{-9}	$E^0_{\varepsilon,N}$	5.5883e-07	5.5883e-07	5.5883e-07	5.5883e-07	5.5883e-07
	$E^1_{\varepsilon,N}$	5.5920e-07	5.5920e-07	5.5920e-07	5.5920e-07	5.5920e-07

Table 4.7: Comparison of analytic and approximate solutions for Example 4.5.3 with $N = 100$, $\tau = \mu = 10^{-8}$ and $\varepsilon_1 = \varepsilon_2 = 10^{-10}$.

	$\tilde{y}_1$		$\tilde{y}_2$	
x	Analytic	Approximate	Analytic	Approximate
0.00	0.0000000000	0.0000000000	0.0000000000	0.0000000000
0.02	1.9796039735	1.9795305955	1.0024937780	1.0024694497
0.04	1.9584315776	1.9583578622	1.0046842846	1.0046598507
0.06	1.9365058720	1.9364318844	1.0065623299	1.0065378062
0.08	1.9138493077	1.9137751129	1.0081184767	1.0080938793
0.10	1.8904837418	1.8904094051	1.0093430340	1.0093183791
0.20	1.7637461506	1.7636720899	1.0101342072	1.0101095231
0.40	1.4681280184	1.4680596219	0.9804753456	0.9804520782
0.60	1.1292869817	1.1292317866	0.8978079724	0.8977886185
0.80	0.7594631713	0.7594301914	0.7450153975	0.7450033654
1.00	0.3678800000	0.3678800000	0.5000000000	0.5000000000

Table 4.8: Comparison of analytic and approximate solutions for Example 4.5.4 with $\varepsilon_1 = \varepsilon_2 = \varepsilon_3 = 2^{-8}$, $\tau = \mu = 2^{-4}$ and $N = 100$.

	$\tilde{y}_1$		$\tilde{y}_2$		$\tilde{y}_3$	
x	Analytic	Approximate	Analytic	Approximate	Analytic	Approximate
0.00	0.2500000000	0.2500000000	0.5000000000	0.5000000000	0.3678800000	0.3678800000
0.20	0.8008765479	0.8008765474	0.5000124959	0.5000124961	0.7099226452	0.7099226449
0.40	1.3518369769	1.3518369765	0.6848226346	0.6848226382	0.9336150582	0.9336150580
0.60	1.9025426699	1.9025426695	1.0279171656	1.0279171734	1.0558126200	1.0558126186
0.80	2.4531550579	2.4531550571	1.4859528053	1.4859528155	1.0811615628	1.0811615561
0.90	2.7268792589	2.7268792552	1.7398193355	1.7398193381	1.0549536256	1.0549536198
0.92	2.7777692589	2.7777692476	1.7880982301	1.7880982383	1.0419618912	1.0419618833
0.94	2.8178048465	2.8178048391	1.8263191306	1.8263191367	1.0147509823	1.0147508981
0.96	2.8187617869	2.8187617756	1.8276162685	1.8276162733	0.9391041896	0.9391041732
0.98	2.6733546895	2.6733539567	1.6881064826	1.6881064938	0.6919178562	0.6919178417
1.00	0.0000000000	0.0000000000	0.0000000000	0.0000000000	0.0000000000	0.0000000000

Table 4.9: Maximum absolute errors for Example 4.5.4 with $\tau = \mu = 10^{-10}$ and $\varepsilon_1 = \varepsilon_2 = \varepsilon_3 = \varepsilon$.

ε		N=64	N=128	N=256	N=512	N=1024
10^{-3}	$E^0_{\varepsilon,N}$	4.8922e-04	4.8942e-04	6.9985e-04	1.1683e-02	5.9284e-02
	$E^1_{\varepsilon,N}$	3.9361e-07	3.5393e-07	8.5502e-05	7.1336e-03	3.9073e-02
10^{-5}	$E^0_{\varepsilon,N}$	4.8815e-06	4.8932e-06	4.8947e-06	4.8951e-06	4.8953e-06
	$E^1_{\varepsilon,N}$	5.2448e-08	3.2209e-09	2.4869e-10	1.8337e-10	1.8059e-10
10^{-7}	$E^0_{\varepsilon,N}$	5.1153e-08	4.8141e-08	4.8747e-08	4.8787e-08	4.8791e-08
	$E^1_{\varepsilon,N}$	5.2430e-08	3.1992e-09	2.2594e-10	1.6572e-10	1.6348e-10
10^{-9}	$E^0_{\varepsilon,N}$	5.2377e-08	3.1433e-09	2.8735e-10	3.2381e-10	3.2607e-10
	$E^1_{\varepsilon,N}$	5.2430e-08	3.1992e-09	2.2594e-10	1.6572e-10	1.6348e-10

kinetics, mathematical physics, and biology. The method is highly accurate, free from directional bias, and the estimates are free from logarithmic terms. The results demonstrate that the numerical method outperforms many existing methods.

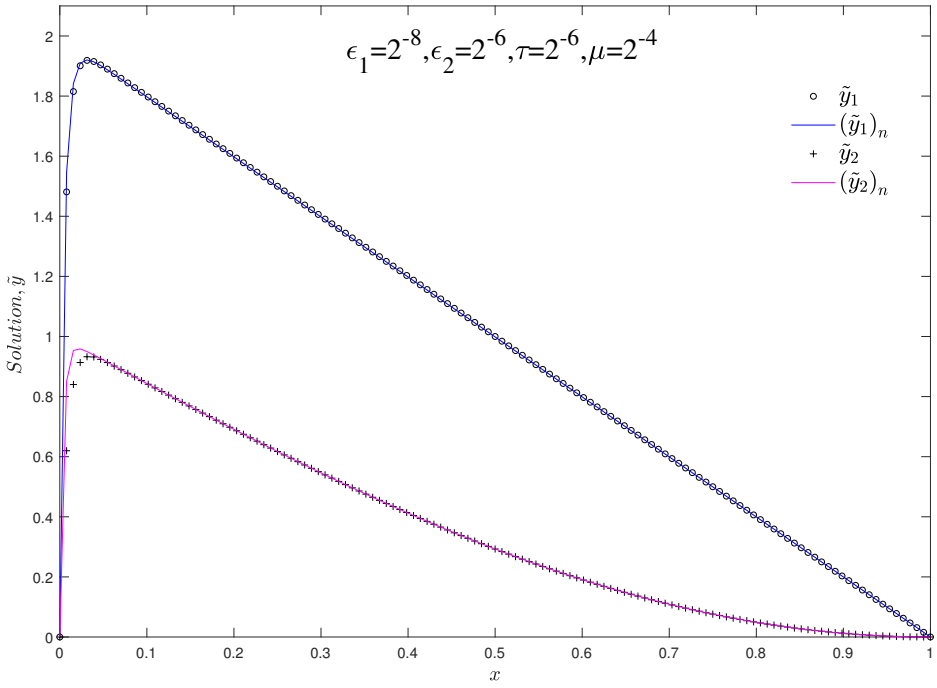

Fig. 4.1: Analytic $(\tilde{y}_i)$ and approximate $((\tilde{y}_i)_n)$ solutions for Example 4.5.1 with $N = 128$.

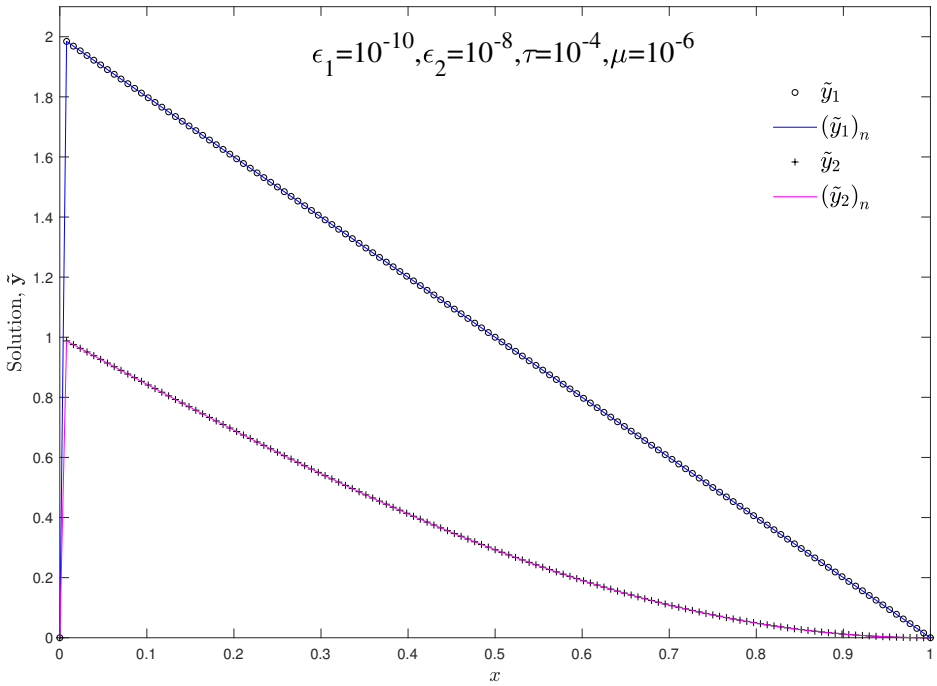

Fig. 4.2: Analytic $(\tilde{y}_i)$ and approximate $((\tilde{y}_i)_n)$ solutions for Example 4.5.1 with $N = 128$.

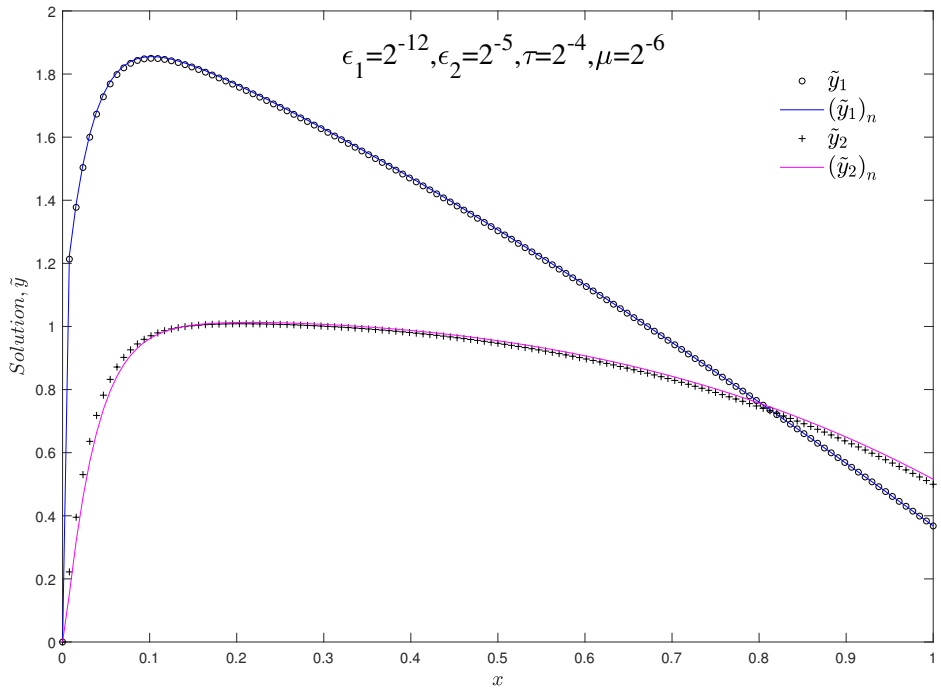

Fig. 4.3: Analytic $(\tilde{y}_i)$ and approximate $((\tilde{y}_i)_n)$ solutions for Example 4.5.3 with $N = 128$.

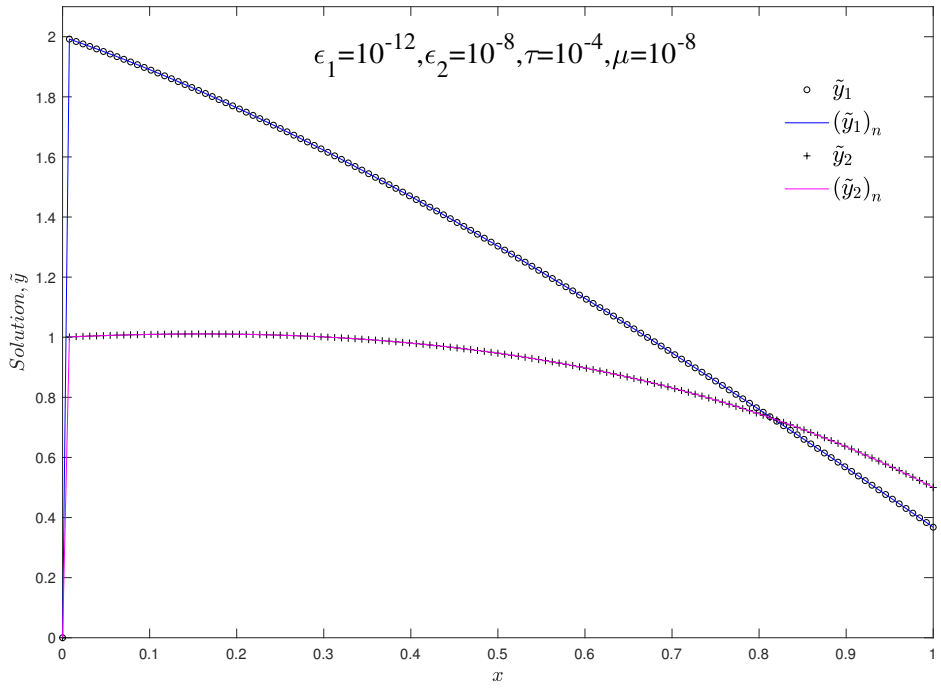

Fig. 4.4: Analytic $(\tilde{y}_i)$ and approximate $((\tilde{y}_i)_n)$ solutions for Example 4.5.3 with $N = 128$.

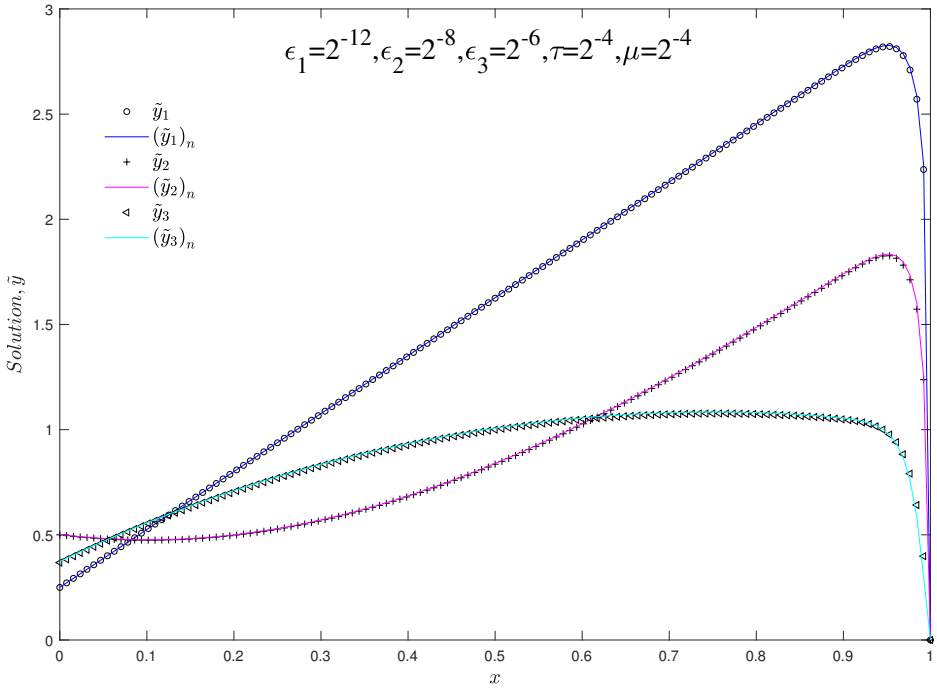

Fig. 4.5: Analytic $(\tilde{y}_i)$ and approximate $((\tilde{y}_i)_n)$ solutions for Example 4.5.4 with $N = 128$.

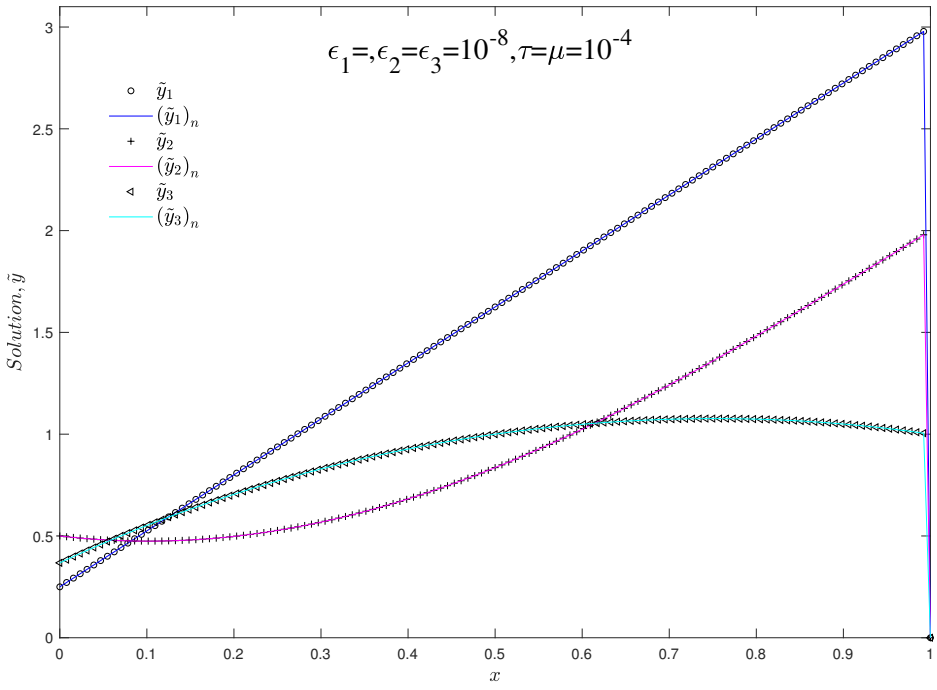

Fig. 4.6: Analytic $(\tilde{y}_i)$ and approximate $((\tilde{y}_i)_n)$ solutions for Example 4.5.4 with $N = 128$.

Chapter 5

Reaction-Diffusion Equation with Shift and Integral Boundary Conditions

5.1 Introduction

Singularly perturbed time-dependent reaction-diffusion problems describe processes involving interactions of reactions and diffusion processes that evolve over time. These problems are prevalent in various scientific and engineering disciplines, including chemistry [10], biology [267, 266], physics [25, 26, 27], and engineering [7, 9, 24], where they model phenomena such as chemical reactions, heat conduction, and population dynamics, to name a few. These problems involve a small perturbation parameter that multiplies the highest-order spatial derivative. This small parameter leads to rapid changes in the solution, especially in thin regions known as boundary or interior layers. The terms involving shifts cause asymmetry or displacement in the diffusion behaviour, making the problem more complex. Additionally, integral boundary conditions, where the boundary values depend on integrals of the solution over the domain, introduce nonlocal effects, reflecting scenarios such as global constraints or memory effects in the system. These features pose significant analytical and numerical challenges that require robust and accurate solution techniques. Effective numerical methods for these problems must balance accuracy and efficiency, often requiring specialised techniques such as adaptive mesh refinement, layer-adapted meshes, and hybrid difference methods.

Recently, there has been a growing emphasis on using adaptively generated meshes. These meshes have been shown to be suitable for capturing boundary layers by automatically increasing mesh resolution near steep gradients or boundary layers while maintaining coarser meshes in smoother areas [6, 108, 117, 111, 319, 116, 253]. Researchers have used a variety of mesh generation algorithms for different classes of problems [320, 160, 159, 204, 254, 113]. In [277], the authors developed a numerical method for solving singularly perturbed reaction-diffusion differential equations with Robin-type boundary conditions. This method employs cubic splines to discretise the Robin boundary conditions. It uses exponential splines to compute the solution at the internal nodes of a layer-adapted mesh generated by equidistributing a positive monitor function. Similarly, the paper [287] introduces a

higher-order parameter-uniform numerical approximation for a fourth-order singularly perturbed boundary value problem on a nonuniform mesh. The authors transform the problem into a coupled system of singularly perturbed differential equations and apply a higher-order hybrid difference method on a nonuniform mesh to discretise the system.

In contrast, the work in [278] proposes a hybrid numerical method for discretising a class of singularly perturbed parabolic reaction-diffusion problems with Robin boundary conditions on an equidistributed mesh. In [321], the author addresses a singularly perturbed mathematical model arising in control theory, where the solution depends on the current state and its history. A robust numerical method utilising mesh equidistribution is applied to solve this problem, although the method is only first-order accurate in the discrete supremum norm. In [119], the authors investigate singularly perturbed parabolic reaction-diffusion problems with a time delay and Robin boundary conditions, employing a moving mesh strategy based on the equidistribution principle. In [110], the authors focus on the approximation of a coupled system of parameterised problems with mixed-type conditions. They employ a triangular splitting-based additive method on an equidistributed mesh to reduce computational costs and achieve second-order accuracy at interior points, maintaining this accuracy for mixed boundary conditions. However, the approach only ensures uniform linear accuracy in time. In [114], the author deals with time-dependent problems where diffusion parameters have varying magnitudes. For further details on such systems of equations, the reader can refer to [179, 322, 323, 108, 324] and related references. Singularly perturbed reaction-diffusion equations with delay and integral boundary conditions are studied in [325]. In [326], the author deals with a singularly perturbed parabolic initial boundary value problem with a negative shift and integral boundary condition. In [327], the authors present an exponentially fitted FDM to solve a similar problem. The reader can find a similar treatment for a parabolic convection-diffusion problem in [328] and for a system of reaction-diffusion equations, see [329].

This chapter further extends the idea of developing higher-order adaptive methods. It presents a hybrid difference method over a moving mesh for the numerical solution of time-dependent reaction-diffusion problems with shift and integral boundary conditions. A key feature is the generation of an adaptive moving mesh, partitioning the spatial domain to leverage the strengths of different discretisation methods. The targeted approach effectively captures the multiscale behaviour of the solution and enhances the accuracy of numerical solutions while maintaining computational efficiency. In addition, the chapter presents a rigorous theoretical error analysis and illustrates numerical results for model problems to support theoretical estimates.

5.2 Continous Problem

Let $\mathfrak{D} = \Omega \times \Lambda := (0,1) \times (0,T]$ and consider the following problem with a shift and integral boundary condition

$$\begin{cases} Ly(x,t) & = y_t(x,t) - \varepsilon y_{xx}(x,t) + a(x,t)y(x,t) + b(x,t)y(x-\delta,t) \\ & = g(x,t),\ (x,t) \in \mathfrak{D}, \\ y(x,0) & = \phi_0(x) \text{ on } \Gamma_0 := \{(x,0) : x \in \bar{\Omega}\}, \\ \kappa_1 y(x,t) & = y(x,t) - \varepsilon \int_0^1 f_1(x,t)y(x,t)dx \\ & = \phi_l(x,t) \text{ on } \Gamma_l := \{(x,t) : -\delta \le x \le 0, t \in \Lambda\}, \\ \kappa_2 y(x,t) & = y(1,t) - \varepsilon \int_0^1 f_2(x,t)y(x,t)dx \\ & = \phi_r(1,t) \text{ on } \Gamma_r := \{(1,t) : t \in \Lambda\}, \end{cases} \tag{5.2.1}$$

where $0 < \varepsilon \ll 1$ and $\delta = o(\varepsilon)$ denotes the perturbation parameter and shift, respectively. The given functions $a(x,t)$, $b(x,t)$, $g(x,t)$, $\phi_0(x,0)$, $\phi_l(x,t)$, and $\phi_r(1,t)$ are sufficiently smooth and

$$a(x,t) \ge \eta > 0,\ b(x,t) \le \rho < 0 \text{ and } a(x,t) + b(x,t) \ge \rho > 0 \text{ for all } (x,t) \in \bar{\mathfrak{D}}. \tag{5.2.2}$$

Also, suppose that $f_1(x,t)$ and $f_2(x,t)$ are nonnegative monotonic functions such that $\int_0^1 f_i(x,t)dx < 1$, $i = 1,2$. Since δ is of order $o(\varepsilon)$, the Taylor series approximation of $y(x-\delta,t)$ after neglecting the terms involving second and higher order derivatives in (5.2.1) leads to

$$\begin{cases} Ly(x,t) & = y_t(x,t) - \varepsilon y_{xx}(x) - \delta b(x,t)y_x(x,t) + (a(x,t) + b(x,t))y(x,t) \\ & = g(x,t),\ (x,t) \in \mathfrak{D}, \\ y(x,0) & = \phi_0(x,0),\ \text{on } \Gamma_0 := \{(x,0) : x \in \bar{\Omega}\}, \\ \kappa_1 y(x,t) & = y(0,t) - \varepsilon \int_0^1 f_1(x,t)y(x,t)dx \\ & = \phi_l(0,t) \text{ on } \Gamma_l := \{(0,t) : t \in \Lambda\}, \\ \kappa_2 y(x,t) & = y(1,t) - \varepsilon \int_0^1 f_2(x,t)y(x,t)dx \\ & = \phi_r(1,t) \text{ on } \Gamma_r := \{(1,t) : t \in \Lambda\}. \end{cases} \tag{5.2.3}$$

Additionally, we assume that the given data satisfies the compatibility conditions

$$\begin{aligned} &\phi_0(0,0) = \phi_l(0,0),\ \phi_0(1,0) = \phi_r(1,0), \\ &\frac{\partial \phi_l(0,0)}{\partial t} - \varepsilon \frac{\partial^2 \phi_0(0,0)}{\partial x^2} - \delta b(0,0) \frac{\partial \phi_0(0,0)}{\partial x} + (a(0,0) + b(0,0))\phi_0(0,0) = g(0,0), \\ &\frac{\partial \phi_r(1,0)}{\partial t} - \varepsilon \frac{\partial^2 \phi_0(1,0)}{\partial x^2} - \delta b(1,0) \frac{\partial \phi_0(1,0)}{\partial x} + (a(1,0) + b(1,0))\phi_0(1,0) = g(1,0) \end{aligned}$$

These conditions ensure the existence of a unique solution [330]. Moreover, it is easy to see that the differential operator satisfies the following maximum principle [128].

Lemma 5.2.1. Let $Ly(x,t) \geq 0$ on $\mathfrak{D}$ and $y(x,t) \geq 0$ on $\partial\mathfrak{D}$. Then $y(x,t) \geq 0$ on $\bar{\mathfrak{D}}$.

If we define two barrier functions as

$$\upsilon^{\pm}(x,t) = \xi^{-1}\|g\| + max\{\phi_0(x,0), max\{\phi_l(x,t), \phi_r(x,t)\}\} \pm y(x,t).$$

Then, Lemma 5.2.1 suggests that

$$|y| \leq \xi^{-1}\|g\| + max\{\phi_0(x,0), max\{\phi_l(x,t), \phi_r(x,t)\}\},\ (x,t) \in \bar{\mathfrak{D}}. \tag{5.2.4}$$

Moreover, if we imitate steps as in Theorem 3 of [330], we can easily obtain the following bounds on the solution y and its derivatives.

Lemma 5.2.2. The derivatives of the unique solution y of problem (5.2.1) satisfy, for all nonnegative integers l, m with $0 \leq l + 2m \leq 4$,

$$\left|\frac{\partial^{l+m} y}{\partial x^l \partial t^m}\right| \leq C\left(1 + \varepsilon^{-\frac{l}{2}}\left(e^{\left(-x\sqrt{\frac{\rho}{\varepsilon}}\right)} + e^{\left(-(1-x)\sqrt{\frac{\rho}{\varepsilon}}\right)}\right)\right).$$

5.3 Solution Decomposition

Let us decompose the solution of (5.2.1) as $y := u + v$, where the smooth part $u := u_0 + \varepsilon u_1 + \varepsilon^2 u_2$. Then, for $(x,t) \in \mathfrak{D}$, u satisfies

$$\begin{cases} u_t(x,t) - \varepsilon u_{xx}(x,t) - \delta b(x,t) u_x + (a(x,t) + b(x,t))u(x,t) = g(x,t), \\ u(x,0) = \phi_0(x,0),\ x \in [0,1], \\ u(0,t) = u_0(0,t),\ u(1,t) = u_0(1,t),\ t \in (0,T] \end{cases} \tag{5.3.1}$$

and the layer part v satisfies

$$\begin{cases} v_t(x,t) - \varepsilon v_{xx}(x,t) - \delta b(x,t) v_x + (a(x,t) + b(x,t))v(x,t) = 0, \\ v(x,0) = 0,\ x \in [0,1], \\ v(0,t) = \phi_l(0,t) - u_0(0,t),\ v(1,t) = \phi_r(1,t) - u_0(1,t),\ t \in (0,T]. \end{cases}$$

Further, the layer part is decomposed as $v = v_l + v_r$, then the left layer part satisfies

$$\begin{aligned} &(v_l)_t(x,t) - \varepsilon(v_l)_{xx}(x,t) - \delta b(x,t)(v_l)_x + (a(x,t) + b(x,t))v_l(x,t) = 0,\ (x,t) \in \mathfrak{D}, \\ &v_l(x,0) = 0,\ x \in [0,1], \\ &v_l(0,t) = \phi_l(0,t) - u_0(0,t),\ v_r(1,t) = 0,\ t \in (0,T] \end{aligned} \tag{5.3.2}$$

and the right layer part satisfies

$$\begin{aligned}
&(v_r)_t(x,t)-\varepsilon(v_r)_{xx}(x,t)-\delta b(x,t)(v_r)_x+(a(x,t)+b(x,t))v_r(x,t)=0,\ (x,t)\in\mathfrak{D},\\
&v_r(x,0)=0,\ x\in[0,1],\\
&v_r(0,t)=0,\ v_r(1,t)=\phi_r(1,t)-u_0(1,t),\ t\in(0,T].
\end{aligned}\tag{5.3.3}$$

Following this, we establish the bounds on the outer and layer parts of the solution and its derivatives as follows.

Lemma 5.3.1. Let y be the solution of (5.2.1). Then, for all nonnegative integers l,m with $0\leq l+2m\leq 4$ the smooth component satisfies (5.3.1) and

$$\left|\frac{\partial^{l+m}u}{\partial x^l\partial t^m}\right|\leq C\left(1+\varepsilon^{1-\frac{l}{2}}\right),$$

while the left layer component satisfies (5.3.2) and

$$\left|\frac{\partial^{l+m}v_l}{\partial x^l\partial t^m}\right|\leq C\left(1+\varepsilon^{-\frac{l}{2}}\left(e^{\left(-x\sqrt{\frac{p}{\varepsilon}}\right)}\right)\right),$$

and the right layer component satisfies (5.3.3) and

$$\left|\frac{\partial^{l+m}v_r}{\partial x^l\partial t^m}\right|\leq C\left(1+\varepsilon^{-\frac{l}{2}}\left(e^{\left(-(1-x)\sqrt{\frac{p}{\varepsilon}}\right)}\right)\right).$$

Proof. The proof imitates steps as in Theorem 4 of [330]. □

5.4 Mesh Structure

The development of the adaptive numerical method is based on an adaptive moving mesh algorithm that automatically identifies the basic characteristics of the boundary layers through an equidistribution principle. Following [278, 287], we consider a nonnegative monitor function

$$M=\beta+|v_{xx}(x,t_i)|^{\frac{1}{2}},\tag{5.4.1}$$

where $v(x,t_i)$ is the layer part of the solution $y(x,t_i)$ at any time level $t=t_i$ and β is a positive constant. Earlier works [110, 119, 278, 287] show that one should choose the least value of the monitor function with caution to improve convergence. Consequently, with an appropriate floor value β, the mesh prevents the clustering of points within the layers and ensures the proper distribution of the mesh points outside the layers.

Using the derivative bound of $v(x,t)$ in Lemma (5.3.1) yields an approximation of $v_{xx}(x,t)$ at $t=t_i$ given by

$$v_{xx}(x,t_i)=\begin{cases}\dfrac{\alpha_0}{\varepsilon}e^{\left(-x\sqrt{\frac{p}{\varepsilon}}\right)}, & x\in\left[0,\frac{1}{2}\right],\\ \dfrac{\alpha_1}{\varepsilon}e^{\left(-(1-x)\sqrt{\frac{p}{\varepsilon}}\right)}, & x\in\left(\frac{1}{2},1\right].\end{cases}$$

where α_0 and α_1 are constants. Imitating the analysis from [278], [108], we have

$$\int_0^1 |v_{xx}(x,t_i)|^{\frac{1}{2}} dx \equiv \Psi \approx \frac{2}{\sqrt{\rho}} \left(|\alpha_0|^{\frac{1}{2}} + |\alpha_1|^{\frac{1}{2}} \right). \tag{5.4.2}$$

Now using (5.4.1) to obtain a map

$$\frac{\beta}{\Psi} x(\xi) + \mu_0 \left(1 - e^{\left(-\frac{x(\xi)}{2} \sqrt{\frac{\rho}{\varepsilon}} \right)} \right) = \xi \left(\frac{\beta}{\Psi} + 1 \right), \ x(\xi) \leq \frac{1}{2}, \tag{5.4.3}$$

and

$$\frac{\beta}{\Psi} (1 - x(\xi)) + \mu_1 \left(1 - e^{\left(-\frac{(1-x(\xi))}{2} \sqrt{\frac{\rho}{\varepsilon}} \right)} \right) = (1 - \xi) \left(\frac{\beta}{\Psi} + 1 \right), \ x(\xi) > \frac{1}{2}, \tag{5.4.4}$$

where $\mu_0 = \dfrac{|\alpha_0|^{\frac{1}{2}}}{|\alpha_0|^{\frac{1}{2}} + |\alpha_1|^{\frac{1}{2}}}$ and $\mu_1 = \dfrac{|\alpha_1|^{\frac{1}{2}}}{|\alpha_0|^{\frac{1}{2}} + |\alpha_1|^{\frac{1}{2}}} = 1 - \mu_0$.

Given the relation between uniform mesh $\left\{ \xi_j = \dfrac{j}{N} \right\}_{j=0}^{N}$ and adaptive mesh $\{x_j^i\}_{j=0}^{N}$ at $t = t_i$, the required nonuniform mesh is given by

$$\frac{\beta}{\Psi} x_j^i + \mu_0 \left(1 - e^{\left(-\frac{x_j^i}{2} \sqrt{\frac{\rho}{\varepsilon}} \right)} \right) = \frac{j}{N} \left(\frac{\beta}{\Psi} + 1 \right), \ x_j^i \leq \frac{1}{2}, \tag{5.4.5}$$

and

$$\frac{\beta}{\Psi} (1 - x_j^i) + \mu_1 \left(1 - e^{\left(-\frac{(1-x_j^i)}{2} \sqrt{\frac{\rho}{\varepsilon}} \right)} \right) = \left(1 - \frac{j}{N} \right) \left(\frac{\beta}{\Psi} + 1 \right), \ x_j^i > \frac{1}{2}. \tag{5.4.6}$$

Next, for an appropriate value of β, we examine the structure of the generated layer-adapted mesh and illustrate its distribution.

Lemma 5.4.1. Let $\beta = \Psi$. Then

$$x_{k_l}^i < 2\sqrt{\frac{\varepsilon}{\rho}} logN < x_{k_{l+1}}^i, \text{ and } x_{k_{r-1}}^i < 1 - 2\sqrt{\frac{\varepsilon}{\rho}} logN < x_{k_r}^i,$$

where

$$k_l = \left[\frac{\mu_0}{2} (N-1) + \sqrt{\frac{\varepsilon}{\rho}} NlogN \right], \text{ and } k_r = \left[N - \left(\frac{\mu_1}{2} (N-1) + \sqrt{\frac{\varepsilon}{\rho}} NlogN \right) \right] + 1,$$

and $[\cdot]$ represents the integral part of the term. Moreover,

$$e^{\left(-\frac{x_j^i}{2} \sqrt{\frac{\rho}{\varepsilon}} \right)} \leq CN^{-1}, \ j \geq k_{l-1}, \ x_j^i \leq \frac{1}{2},$$
$$e^{\left(-\frac{(1-x_j^i)}{2} \sqrt{\frac{\rho}{\varepsilon}} \right)} \leq CN^{-1}, \ j \leq k_r, \ x_j^i > \frac{1}{2}.$$

Proof. Put $x_j^i = 2\sqrt{\frac{\varepsilon}{\rho}} \log N$ in (5.4.5) and solve for j to find k_l. Using (5.4.6) we can similarly compute k_r. □

Setting $\beta = \Psi$ aligns the equidistributed mesh with some features of the a priori mesh. However,

exponential stretching within layers reduces discretisation errors, enhancing accuracy [288].

Lemma 5.4.2. For $j = \{1,...k_l - 1\} \cup \{k_r + 1,...,N-1\}$, the mesh width in the boundary layer part satisfies $h_j^i < 2C\sqrt{\frac{\varepsilon}{\rho}}$. Furthermore,

$$|h_{j+1}^i - h_j^i| \leq \begin{cases} C(h_j^i)^2, & j = 1,...k_l - 1, \\ C(h_{j+1}^i)^2, & j = k_r + 1,...,N-1. \end{cases}$$

Proof. We establish the estimate for the left layer. The estimate for the right layer follows analogously. Then, using (5.5.4) to obtain $\bar{x_j^i} > x_j^i$ such that $e^{\left(-\frac{\bar{x_j^i}}{2}\sqrt{\frac{\rho}{\varepsilon}}\right)} = 1 - \frac{2j}{\mu_0 N}$. A rearrangement of terms yields $x_j^i < \bar{x_j^i} = -2\sqrt{\frac{\varepsilon}{\rho}} log\left(1 - \frac{2j}{\mu_0 N}\right)$. Using $\bar{x_j^i}$ in (5.5.4) again, we get

$$x_j^i > \underline{x_j^i} = -2\sqrt{\frac{\varepsilon}{\rho}} log\left(1 - \frac{1}{\mu_0}\left(\frac{2j}{N} + 2\sqrt{\frac{\varepsilon}{\rho}} log\left(1 - \frac{2j}{\mu_0 N}\right)\right)\right).$$

Thus, for $j = 1,...,k_l$

$$h_j^i = x_j^i - x_{j-1}^i < \bar{x_j^i} - x_{j-1}^i = 2\sqrt{\frac{\rho}{\varepsilon}} log\left[1 + \frac{2 + 2\sqrt{\frac{\rho}{\varepsilon}} N log\left(\frac{\mu_0 N}{\mu_0 N - 2(j-1)}\right)}{\mu_0 N - 2j}\right] < 2C\sqrt{\frac{\rho}{\varepsilon}}.$$

Moreover, note that

$$\frac{|h_{j+1}^i - h_j^i|}{(h_j^i)^2} \leq \frac{2x_{\xi\xi}^i(\theta_j^{(1)})}{(x_\xi^i(\theta_j^{(2)}))^2}, \text{ where } \theta_j^{(1)} \in (\xi_{j-1}, \xi_{j+1}) \text{ and } \theta_j^{(2)} \in (\xi_{j-1}, \xi_j).$$

Then, from (5.4.3) with $\beta = \Psi$, we obtain

$$x_\xi^i(\theta) = \frac{4\sqrt{\frac{\rho}{\varepsilon}}}{\sqrt{2\frac{\rho}{\varepsilon}} + \mu_0 e^{\left(-\frac{x(\theta)}{2}\sqrt{\frac{\rho}{\varepsilon}}\right)}}, \text{ and } x_{\xi\xi}^i(\theta) = \frac{8\mu_0\sqrt{\frac{\rho}{\varepsilon}} e^{\left(-\frac{x^i(\theta)}{2}\sqrt{\frac{\rho}{\varepsilon}}\right)}}{\left(2\frac{\rho}{\varepsilon} + \mu_0 e^{\left(-\frac{x^i(\theta)}{2}\sqrt{\frac{\rho}{\varepsilon}}\right)}\right)^3}.$$

This implies that $\frac{|h_{j+1}^i - h_j^i|}{(h_j^i)^2} \leq \frac{\mu_0\sqrt{\frac{\rho}{\varepsilon}}\left(2\frac{\rho}{\varepsilon} + \mu_0 e^{\left(-\frac{x^i(\theta)}{2}\sqrt{\frac{\rho}{\varepsilon}}\right)}\right)^2}{2\left(2\frac{\rho}{\varepsilon} + \mu_0 e^{\left(-\frac{x^i(\theta)}{2}\sqrt{\frac{\rho}{\varepsilon}}\right)}\right)^3} \leq C.$ □

Next, we find the following generalised bounds on h_j^i.

Lemma 5.4.3. For $j = 1,...,N$ and at any time level $t = t_i$, the width of the mesh satisfies $h_j^i \leq CN^{-1}$.

Proof. Use (5.4.1) and (5.4.2) with $\beta = \Psi$ to obtain $\int_0^1 M(x, y(x,t_i))dx \leq C\beta$. Finally, the equidistribution principle leads to

$$\beta h_j^i \leq \int_{x_{j-1}^i}^{x_j^i} M(x, y(x,t_i))dx = \frac{1}{N}\int_0^1 M(x, y(x,t_i))dx \leq C\beta N^{-1}.$$

□

5.5 The Difference Method

We now describe the difference approximation of (5.2.1) on the classical equidistant mesh $\{t_i = i\Delta t, i = 0,1,...,M, \Delta t = T/M\}$ while for the spatial domain at any time level $t = t_i$, we discretise the problem on the adaptive mesh $\{0 = x_0^i < x_1^i < \cdots < x_N^i = 1\}$. To approximate the solution on the mesh $\bar{\mathfrak{D}} = \{(x_j^i, t_i) : 0 \le j \le N, 0 \le i \le M\}$, we employ a cubic spline difference method within the boundary layer region and an exponential spline difference method in the outer layer region. In contrast, we discretised the time derivative using the backward difference method. Defining the modified backward difference operator in time as

$$[\rho_t^* Y] := \frac{Y_j^i - \hat{Y}^{i-1}(x_j^{i-1})}{\Delta t}, \ \forall\, 0 \le j \le N,\ 1 \le i \le M, \tag{5.5.1}$$

where $\hat{Y}^{i-1}(x_j^{i-1})$ symbolises the piecewise linear interpolant of $Y_j^{i-1} = Y((x_j^{i-1}), t_{i-1})$ at time $t = t_{i-1}$.The modified backward difference discretisation of (5.2.1) at time $t = t_i$ for $i = 1,...,M$ and $j = 0,...,N$ is given by

$$\begin{aligned}
&\frac{Y(x_j^i,t_i) - \hat{Y}(x_j^{i-1},t_{i-1})}{\Delta t} - \varepsilon Y_{xx}(x_j^i,t_i) - \delta b(x_j^i,t_i) Y_x(x_j^i,t_i) + (a(x_j^i,t_i) + b(x_j^i,t_i)) Y(x_j^i,t_i) = g(x_j^i,t_i),\\
&Y(x_j,0) = \phi_0(x_j,0),\\
&Y(0,t_i) = \phi_l(0,t_i),\ Y(1,t_i) = \phi_r(1,t_i).
\end{aligned} \tag{5.5.2}$$

To obtain a second-order approximation for $Y'(x_j^i, t_j^i)$, we use Taylor's expansion of Y about (x_j^i, t_i) at any time level $t = t_i$ to write

$$Y(x_{j+1}^i,t_i) \approx Y(x_j^i,t_i) + h_{j+1}^i Y_x(x_j^i,t_i) + \frac{(h_{j+1}^i)^2}{2} Y_{xx}(x_j^i,t_i).$$

$$Y(x_{j-1}^i,t_i) \approx Y(x_j^i,t_i) - h_j^i Y_x(x_j^i,t_i) + \frac{(h_j^i)^2}{2} Y_{xx}(x_j^i,t_i).$$

Consequently, we obtain

$$\begin{aligned}
Y_x(x_j^i,t_i) &\approx \frac{1}{h_{j+1}^i h_j^i (h_{j+1}^i + h_j^i)} ((h_j^i)^2 Y(x_{j+1}^i,t_i) + ((h_{j+1}^i)^2 - (h_j^i)^2) Y(x_j^i,t_i) - (h_{j+1}^i)^2 Y(x_{j-1}^i,t_i)),\\
Y_{xx}(x_j^i,t_i) &\approx \frac{2}{h_{j+1}^i h_j^i (h_{j+1}^i + h_j^i)} (h_j^i Y(x_{j+1}^i,t_i) - (h_{j+1}^i + h_j^i) Y(x_j^i,t_i) + h_{j+1}^i Y(x_{j-1}^i,t_i)).
\end{aligned}$$

A substitution in $Y_x(x_{j+1}^i,t_i) \approx Y_x(x_j^i,t_i) + h_{j+1}^i Y_{xx}(x_j^i,t_i)$ and $Y_x(x_{j-1}^i,t_i) \approx Y_x(x_j^i,t_i) - h_j^i Y_{xx}(x_j^i,t_i)$ leads to

$$Y_x(x^i_{j+1},t_i) \approx \frac{1}{h^i_{j+1}h^i_j(h^i_{j+1}+h^i_j)}(((h^i_j)^2+2h^i_{j+1}h^i_j)Y(x^i_{j+1},t_i)-(h^i_{j+1}+h^i_j)^2Y(x^i_j,t_i)+(h^i_{j+1})^2Y(x^i_{j-1},t_i)),$$
$$Y_x(x^i_{j-1},t_i) \approx \frac{2}{h^i_{j+1}h^i_j(h^i_{j+1}+h^i_j)}(-(h^i_j)^2Y(x^i_{j+1},t_i)+(h^i_{j+1}+h^i_j)^2Y(x^i_j,t_i)-((h^i_{j+1})^2+2h^i_{j+1}h^i_j)Y(x^i_{j-1},t_i)).$$

The cubic spline polynomial $S(x)$ is determined by solving $D^4S(x)=0$, for all $x\in[x^i_{j-1},x^i_j]$, $j=1,2,...N$ at any time level $t=t_i$ such that $S(x^i_{j-1})=Y(x^i_{j-1})$, $S(x^i_j)=Y(x^i_j)$, $S''(x^i_{j-1})=Y''(x^i_{j-1})$, and $S''(x^i_j)=Y''(x^i_j)$. Now, for $j=0,...,N$, we use $S''(x^i_j)=\mathscr{M}^i_j$ to find

$$S(x)=\frac{(x^i_j-x)^3}{6h^i_j}\mathscr{M}_{j-1}+\frac{(x-x^i_{j-1})^3}{6h^i_j}+\left(Y(x^i_{j-1})-\frac{(h^i_j)^2}{6}\mathscr{M}_{j-1}\right)\frac{(x^i_j-x)}{h^i_j}+$$
$$\left(Y(x^i_j)-\frac{(h^i_j)^2}{6}\mathscr{M}^i_j\right)\frac{(x-x^i_{j-1})}{h^i_j}.$$

For fixed i and $j=1,...,N-1$, the continuity constraint of $S'(x)$ at x^i_j leads to the following system for $\mathscr{M}^i_j$

$$\frac{h^i_j}{6}\mathscr{M}^i_{j-1}+\left(\frac{h^i_j+h^i_{j+1}}{3}\right)\mathscr{M}^i_j+\frac{h^i_{j+1}}{6}\mathscr{M}^i_{j+1}=\frac{Y(x^i_{j+1})-Y(x^i_j)}{h^i_{j+1}}-\frac{Y(x^i_j)-Y(x^i_{j-1})}{h^i_j}. \tag{5.5.3}$$

In a similar way, we devise an exponential difference method for the outer solution. The exponential spline is determined by solving

$$\begin{aligned}&(D^i_j-(p^i_j)^2D^2)T=0,\ \forall x\in[x^i_{j-1},x^i_j],\ j=1,...,N,\text{with}\\&T(x^i_{j-1})=Y(x^i_{j-1}),\ T(x^i_j)=Y(x^i_j),\ T''(x^i_{j-1})=\tau^i_{j-1},\ T''(x^i_j)=\tau^i_j,\end{aligned} \tag{5.5.4}$$

where $p^i_j\geq 0$ are the tension parameters. As in our earlier derivation, we employ continuity constraints to find

$$\begin{cases} e^i_j\tau^i_{j-1}+(d^i_j+d^i_{j+1})\tau^i_j+e^i_{j+1}\tau^i_{j+1}=\frac{Y(x^i_{j+1})-Y(x^i_j)}{h^i_{j+1}}-\frac{Y(x^i_j)-Y(x^i_{j-1})}{h^i_j},\\ \text{where } e^i_j=\frac{s^i_j-p^i_jh^i_j}{(p^i_j)^2s^i_jh^i_j},\ d^i_j=\frac{p^i_jh^i_jc^i_j-s^i_j}{(p^i_j)^2s^i_jh^i_j},\ s^i_j=sinh(p^i_jh^i_j),\ \text{and } c^i_j=cosh(p^i_jh^i_j).\end{cases} \tag{5.5.5}$$

Using exponential spline difference discretisation of problem (5.5.2) leads to

$$\frac{Y^i_j-\hat{Y}^{i-1}(x^{i-1}_j)}{\Delta t}-\varepsilon\tau^i_j-\delta b^i_j(Y_x)^i_j+(a^i_j+b^i_j)Y^i_j=g^i_j,\ j=1,...,N-1,\ i=1,...,M.$$

Substitute τ^i_j from the above relation in (5.5.5) at time $t=t_i$, to obtain the following system of equations

for $j = 1,...,N-1$ and $i = 1,...,M$

$$\left\{\begin{array}{l}
\left(\frac{-\varepsilon\Delta t}{h^i_j(h^i_{j+1}+h^i_j)}+\frac{e^i_j}{h^i_{j+1}+h^i_j}((a^i_{j-1}+b^i_{j-1})\Delta t+1)+\frac{e^i_j(h^i_{j+1}+2h^i_j)}{h^i_j(h^i_{j+1}+h^i_j)^2}\delta b^i_{j-1}\Delta t+\right.\\
\left.\frac{(d^i_j+d^i_{j+1})h^i_{j+1}}{h^i_j(h^i_{j+1}+h^i_j)^2}\delta b^i_j\Delta t-\frac{e^i_{j+1}h^i_{j+1}}{h^i_j(h^i_{j+1}+h^i_j)^2}\delta b^i_{j+1}\Delta t\right)Y^i_{j-1}+\\
\left(\frac{\varepsilon\Delta t}{h^i_{j+1}h^i_j}+\left(\frac{d^i_j+d^i_{j+1}}{h^i_{j+1}+h^i_j}\right)((a^i_j+b^i_j)\Delta t+1)-\frac{e^i_j}{h^i_{j+1}h^i_j}\delta b^i_{j-1}\Delta t-\right.\\
\left.\frac{(d^i_j+d^i_{j+1})(h^i_{j+1}-h^i_j)}{h^i_{j+1}h^i_j(h_{j+1}+h_j)}\delta b^i_j\Delta t+\frac{e^i_{j+1}}{h^i_{j+1}h^i_j}b^i_{j+1}\Delta t\right)Y^i_j+\\
\left(\frac{-\varepsilon\Delta t}{h^i_{j+1}(h^i_{j+1}+h^i_j)}+\frac{e^i_{j+1}}{h^i_{j+1}+h^i_j}((a^i_{j+1}+b^i_{j+1})\Delta t+1)+\frac{e^i_jh^i_j}{h^i_{j+1}(h^i_{j+1}+h^i_j)^2}\delta b^i_{j-1}\Delta t-\right.\\
\left.\frac{(d^i_j+d^i_{j+1})h^i_j}{h^i_{j+1}(h^i_{j+1}+h^i_j)^2}\delta b^i_j\Delta t-\frac{e^i_{j+1}(h^i_j+2h^i_{j+1})}{h^i_{j+1}(h^i_{j+1}+h^i_j)^2}\delta b^i_{j+1}\Delta t\right)Y^i_{j+1}=\\
\frac{e^i_j}{h^i_{j+1}+h^i_j}(g^i_{j-1}\Delta t+\hat{Y}^{i-1}_{j-1})+\left(\frac{d_j+d_{j+1}}{h_{j+1}+h_j}\right)(g^i_j\Delta t+\hat{Y}^{i-1}_j)+\frac{e^i_{j+1}}{h^i_{j+1}+h^i_j}(g^i_{j+1}\Delta t+\hat{Y}^{i-1}_{j+1}).
\end{array}\right. \tag{5.5.6}$$

Simultaneously, the cubic splines for the spatial discretisation of (5.5.2) lead to

$$\frac{Y^i_j-\hat{Y}^{i-1}(x^{i-1}_j)}{\Delta t}-\varepsilon.\mathscr{M}^i_j-\delta b^i_j(Y_x)^i_j+(a^i_j+b^i_j)Y^i_j=g^i_j,\ j=1,...,N-1,\ i=1,...,M.$$

Substitute $\mathscr{M}^i_j$ from above relation in (5.5.3) at time $t=t_i$, to obtain the following system of equations for $j = 1,...,N-1$ and $i = 1,...,M$

$$\left\{\begin{array}{l}
\left(\frac{-\varepsilon\Delta t}{h^i_j(h^i_{j+1}+h^i_j)}+\frac{h^i_j}{6(h^i_{j+1}+h^i_j)}((a^i_{j-1}+b^i_{j-1})\Delta t+1)+\frac{h^i_{j+1}+2h^i_j}{6(h^i_{j+1}+h^i_j)^2}\delta b^i_{j-1}\Delta t+\right.\\
\left.\frac{h^i_{j+1}}{3h^i_j(h^i_{j+1}+h^i_j)}\delta b^i_j\Delta t-\frac{(h^i_{j+1})^2}{6h^i_j(h^i_{j+1}+h^i_j)^2}\delta b^i_{j+1}\Delta t\right)Y^i_{j-1}\Delta t+\\
\left(\frac{\varepsilon\Delta t}{h^i_{j+1}h^i_j}+\frac{(a^i_j+b^i_j)\Delta t+1}{3}-\frac{1}{6h^i_{j+1}}\delta b^i_{j-1}\Delta t-\frac{h^i_{j+1}-h^i_j}{3h^i_{j+1}h^i_j}\delta b^i_j\Delta t+\frac{1}{6h^i_j}b^i_{j+1}\Delta t\right)Y^i_j+\\
\left(\frac{-\varepsilon\Delta t}{h^i_{j+1}(h^i_{j+1}+h^i_j)}+\frac{h^i_{j+1}}{6(h^i_{j+1}+h^i_j)}((a^i_{j+1}+b^i_{j+1})\Delta t+1)+\frac{(h^i_j)^2}{6(h^i_{j+1}+h^i_j)^2}\delta b^i_{j-1}\Delta t-\right.\\
\left.\frac{h^i_j}{3h^i_{j+1}(h^i_{j+1}+h^i_j)}\delta b^i_j\Delta t-\frac{(h^i_j+2h^i_{j+1})}{6(h^i_{j+1}+h^i_j)^2}\delta b^i_{j+1}\Delta t\right)Y^i_{j+1}=\\
\frac{h^i_j}{6(h^i_{j+1}+h^i_j)}(g^i_{j-1}\Delta t+\hat{Y}^{i-1}_{j-1})+\frac{g^i_j\Delta t+\hat{Y}^{i-1}_j}{3}+\frac{h^i_{j+1}}{6(h^i_{j+1}+h^i_j)}(g^i_{j+1}\Delta t+\hat{Y}^{i-1}_{j+1}).
\end{array}\right. \tag{5.5.7}$$

Therefore, in the outer layer portion, the proposed method mitigates the nonmontonic behaviour of the cubic spline difference method by incorporating exponential splines. Consequently, the associated problem (5.2.1) takes the form: Find Y such that

$$\begin{cases} [L^{N,M}Y]^i_j := r^-_{j,i}Y(x^i_{j-1},t_i) + r^c_{j,i}Y(x^i_j,t_i) + r^+_{j,i}Y(x^i_{j+1},t_i) = q^-_{j,i}G^i_{j-1} + q^c_{j,i}G^i_j + q^+_{j,i}G^i_{j+1}, \\ \hat{Y}(x_j,0) = \phi_0(x_j,0), \\ Y(0,t_i) = \phi_l(0,t_i),\ Y(1,t_i) = \phi_r(1,t_i). \end{cases} \tag{5.5.8}$$

where $G^i_j = g(x^i_j,t_i) + \hat{Y}(x^{i-1}_j,t_{i-1})$ for all $j = 0,...,N,\ i = 1,...,M$, and $\hat{Y}(x^{i-1}_j,t_{i-1})$ is the linear interpolant of Y^{i-1}_j at any time level $t = t_{i-1}$. The value of the coefficients $r^*_{j,i}$ and $q^*_{j,i}$, where $j = 0,...,N, i = 1,...,M$ and $* = -,c,+$, are determined based on the location of the mesh points x^i_j which partitions the domain $[0,1]\times[0,T]$ of $L^{N,M}$. The coefficients are given as follows:

1. Whenever x^i_j lies within the boundary layer part of the mesh i.e., $j = \{1,...,k_l-1\}\cup\{k_r+1,...,N-1\}, i = 1,...,M$, the cubic spline difference method employed to determine the coefficients reads

$$\begin{cases} r^-_{j,i} &= \dfrac{-\varepsilon\Delta t}{h^i_j(h^i_{j+1}+h^i_j)} + q^-_{j,i}\left(\left(a(x^i_{j-1},t_i)+b(x^i_{j-1},t_i)\right)\Delta t+1\right) + \dfrac{h^i_{j+1}+2h^i_j}{6(h^i_{j+1}+h^i_j)^2}\delta b(x^i_{j-1},t_i)\Delta t + \\ & \dfrac{h^i_{j+1}}{3h^i_j(h^i_{j+1}+h^i_j)}\delta b(x^i_j,t_i)\Delta t - \dfrac{(h^i_{j+1})^2}{6h^i_j(h^i_{j+1}+h^i_j)^2}\delta b(x^i_{j+1},t_i)\Delta t, \\ r^c_{j,i} &= \dfrac{\varepsilon\Delta t}{h^i_{j+1}h^i_j} + q^c_{j,i}\left(\left(a(x^i_j,t_i)+b(x^i_j,t_i)\right)\Delta t+1\right) - \dfrac{1}{6h^i_{j+1}}\delta b(x^i_{j-1},t_i)\Delta t - \\ & \dfrac{(h^i_{j+1}-h^i_j)}{3h^i_{j+1}h^i_j}\delta b(x^i_j,t_i)\Delta t + \dfrac{1}{6h_j}\delta b(x^i_{j+1},t_i)\Delta t, \\ r^+_{j,i} &= \dfrac{-\varepsilon\Delta t}{h^i_j(h^i_{j+1}+h^i_j)} + q^+_{j,i}\left(\left(a(x^i_{j+1},t_i)+b(x^i_{j+1},t_i)\Delta t\right)+1\right) + \dfrac{(h^i_j)^2}{6(h^i_{j+1}+h^i_j)^2}\delta b(x^i_{j-1},t_i)\Delta t - \\ & \dfrac{h^i_j}{3h^i_{j+1}(h^i_{j+1}+h^i_j)}\delta b(x^i_j,t_i)\Delta t - \dfrac{h^i_j+2h^i_{j+1}}{6(h^i_{j+1}+h^i_j)^2}\delta b(x^i_{j+1},t_i)\Delta t, \end{cases} \tag{5.5.9}$$

$$q^-_{j,i} = \frac{h^i_j}{6(h^i_{j+1}+h^i_j)}, \quad q^c_{j,i} = \frac{1}{3}, \quad q^+_{j,i} = \frac{h^i_{j+1}}{6(h^i_{j+1}+h^i_j)}. \tag{5.5.10}$$

2. While x^i_j lies outside layers i.e. $j = \{k_l,...k_r\}, i = 1,...,M$, the coefficients associated with the exponential spline difference method reads

$$
\begin{cases}
r^-_{j,i} &= \dfrac{-\varepsilon\Delta t}{h^i_j(h^i_{j+1}+h^i_j)} + q^-_{j,i}\left(\left(a(x^i_{j-1},t_i)+b(x^i_{j-1},t_i)\right)\Delta t+1\right) + \dfrac{e^i_j(h^i_{j+1}+2h^i_j)}{h^i_j(h^i_{j+1}+h^i_j)^2}\delta b(x^i_{j-1},t_i)\Delta t + \\
& \dfrac{(d^i_j+d^i_{j+1})h^i_{j+1}}{h^i_j(h^i_{j+1}+h^i_j)^2}\delta b(x^i_j,t_i)\Delta t - \dfrac{e^i_{j+1}h^i_{j+1}}{h^i_j(h^i_{j+1}+h^i_j)^2}\delta b(x^i_{j+1},t_i)\Delta t, \\
r^c_{j,i} &= \dfrac{\varepsilon\Delta t}{h^i_{j+1}h^i_j} + q^c_{j,i}\left(\left(a(x^i_j,t_i)+b(x^i_j,t_i)\right)\Delta t+1\right) - \dfrac{e^i_j}{h^i_{j+1}h^i_j}\delta b(x^i_{j-1},t_i)\Delta t - \\
& \dfrac{(d^i_j+d^i_{j+1})(h^i_{j+1}-h^i_j)}{h^i_{j+1}h^i_j(h^i_{j+1}+h^i_j)}\delta b(x^i_j,t_i)\Delta t + \dfrac{e^i_{j+1}}{h^i_{j+1}h^i_j}\delta b(x^i_{j+1},t_i)\Delta t, \\
r^+_{j,i} &= \dfrac{-\varepsilon\Delta t}{h^i_j(h^i_{j+1}+h^i_j)} + q^+_{j,i}\left(\left(a(x^i_{j+1},t_i)+b(x^i_{j+1},t_i)\right)\Delta t+1\right) + \dfrac{e^i_j h^i_j}{h^i_{j+1}(h^i_{j+1}+h^i_j)^2}\delta b(x^i_{j-1},t_i)\Delta t - \\
& \dfrac{(d^i_j+d^i_{j+1})h^i_j}{h^i_{j+1}(h^i_{j+1}+h^i_j)^2}\delta b(x^i_j,t_i)\Delta t - \dfrac{e^i_{j+1}(h^i_j+2h^i_{j+1})}{h^i_{j+1}(h^i_{j+1}+h^i_j)^2}\delta b(x^i_{j+1},t_i)\Delta t,
\end{cases}
\tag{5.5.11}
$$

$$
q^-_{j,i} = \frac{e^i_j}{h^i_{j+1}+h^i_j}, \quad q^+_{j,i} = \frac{e^i_{j+1}}{h^i_{j+1}+h^i_j}, \quad q^c_{j,i} = \frac{d^i_j}{h^i_{j+1}+h^i_j} + \frac{d^i_{j+1}}{h^i_{j+1}+h^i_j}. \tag{5.5.12}
$$

5.6 Error Analysis

At each mesh point $(x^i_j,t_i),\ j=0,...,N,\ i=0,...,M$, let $\eta^i_j = y(x^i_j,t_i) - Y(x^i_j,t_i)$ denotes the error in the numerical solution Y. Then, the consistency error associated with the hybrid spline difference discretisation (5.5.8) is given by

$$
[L^{N,M}\eta]^i_j = L^{N,M}(y(x^i_j,t_i) - Y(x^i_j,t_i)) = \chi^i_{1,j} + \chi^i_{2,j},\ j=0,...,N,\ i=0,...,M, \tag{5.6.1}
$$

where, $\chi^i_{1,j} = (L^{N,M}_1 - L_1)y(x^i_j,t_i)$, $L_1 y := -\varepsilon y_{xx} - \delta b(x,t)y_x + (a(x,t)+b(x,t))y$ and $\chi^i_{2,j} = \rho^*_t y(x^i_j,t_i) - y_t(x^i_j,t_i)$. Now, to examine the order of convergence, we decompose the consistency error as $\eta^i_j = \Phi^i_j + \psi^i_j$, where for each fixed $i=0,...,M$ and $j=1,...,N-1$, Φ^i_j is defined as the solution of

$$
[L^{N,M}_1\Phi]^i_j = \chi^i_{1,j},\ [\kappa^{N,M}_1\Phi]^j_0 = (\kappa^{N,M}_1 - \kappa_1)y(0,t_i),\ [\kappa^{N,M}_2\Phi]^j_N = (\kappa^{N,M}_2 - \kappa_2)y(1,t_i), \tag{5.6.2}
$$

and ψ^i_j is defined as the solution of

$$
\begin{cases}
[L_{N,M}\psi]^i_j = \chi^i_{2,j} - [\rho^*_t\Phi]^i_j, \quad i=0,...,M,\ j=1,...,N-1, \\
[\kappa^{N,M}_1\psi]^i_0 = \rho^*_t y(0,t_i) - y_t(0,t_i) - \rho^*_t\Phi^i_0, \\
[\kappa^{N,M}_2\psi]^i_N = \rho^*_t y(1,t_i) - y_t(1,t_i) - \rho^*_t\Phi^i_N, \\
\psi^0_j = -\Phi^0_j.
\end{cases}
\tag{5.6.3}
$$

Using (5.2.4), (5.6.2) as in [331], we get a bound on Φ given by

$$
\|\Phi^i\| \le C\|\chi^i_1\|, \quad \text{for all } i=0,...,M. \tag{5.6.4}
$$

Lemma 5.6.1. For $i=1,...,M$, the error component Φ^i satisfies $\|\Phi^i\| \le CN^{-2}$.

Proof. Using the standard decomposition of the solution y as $y^i_j = u^i_j + s^i_j$, we have

$$\chi^i_{1,j} = [(L_1^{N,M} - L_1)y]^i_j = [(L_1^{N,M} - L_1)u]^i_j + [(L_1^{N,M} - L_1)s]^i_j.$$

Next, we calculate an error bound for the smooth parts and the layers separately. We begin our analysis with the smooth part, such that

1. When $j = \{1, ...k_l - 1\} \cup \{k_r + 1, ..., N-1\}$, the spline difference approximation is obtained using cubic splines. Then, the Taylor expansions yield

$$\begin{aligned}|[(L_1^{N,M} - L_1)u]^i_j| &\leq C\varepsilon |h^i_{j+1} - h^i_j| ||u'''(x)||_{[x^i_{j-1}, x^i_{j+1}]} + C\varepsilon((h^i_{j+1})^2 + (h^i_j)^2)||u^{(iv)}(x)||_{[x^i_j, x^i_{j+1}]} \\ &\leq C\varepsilon(h^i_j)^2(1 + \varepsilon^{\frac{-1}{2}}) + C((h^i_{j+1})^2 + (h^i_j)^2) \leq C\varepsilon^{\frac{1}{2}}(h^i_j)^2 + C(h^i_j)^2.\end{aligned}$$

   Using Lemmas (5.3.1), (5.4.2) and (5.4.3) along with the assumption that $\sqrt{\varepsilon} \ll N^{-1}$, we obtain

$$|[(L_1^{N,M} - L_1)u]^i_j| \leq CN^{-2}.$$

2. When $j = \{k_l, ..., k_r\}$, the spline difference approximation is obtained using exponential splines. Then, it is easy to follow that

$$|[(L_1^{N,M} - L_1)u]^i_j| \leq C\varepsilon(h^i_j)^2(p^i)^2||u''(x)||_{[x^i_{j-1}, x^i_{j+1}]}.$$

   For $p = \min\limits_{j=k_l,...k_r}\{p_j\} = \max\limits_{j=k_l,...k_r}\left\{\sqrt{\dfrac{a(x^i_j,t_i) + b(x^i_j,t_i) + \frac{1}{\Delta t}}{\varepsilon}}, \sqrt{\dfrac{\delta b(x^i_j,t_i)}{\varepsilon}}\right\}$ it follows from lemmas (5.3.1), (5.4.2) and (5.4.3), that

$$|[(L_1^{N,M} - L_1)u]^i_j| \leq CN^{-2}.$$

Next, to compute the error bound on the layer part, such that

1. When $j = \{1, ...k_l - 1\} \cup \{k_r + 1, ..., N-1\}$, for the left side of the boundary layer portion, Taylor expansions yield

$$\left|\left[\left(L_1^{N,M} - L_1\right)v\right]^i_j\right| \leq \varepsilon \frac{\left|\left(h^i_{j+1}\right)^2 v'''\left(\theta^{(2)}_j, t_i\right) - \left(h^i_j\right)^2 v'''\left(\theta^{(1)}_j, t_i\right)\right|}{3\left(h^i_{j+1} + h^i_j\right)},$$

where $\theta_j^{(2)} \in \left(x_j^i, x_{j+1}^i\right)$ and $\theta_j^{(1)} \in \left(x_{j-1}^i, x_j^i\right)$. Moreover,

$$\begin{aligned}\left|\left(h_{j+1}^i\right)^2 v'''\left(\theta_j^{(2)}, t_i\right) - \left(h_j^i\right)^2 v'''\left(\theta_j^{(1)}, t_i\right)\right| \leq & \left|(h_{j+1}^i)^2 - (h_j^i)^2\right| \left|v'''\left(\theta_j^{(2)}, t_i\right)\right| + \\ & \left(h_j^i\right)^2 \left|v'''\left(\theta_j^{(2)}, t_i\right) - v'''\left(\theta_j^{(1)}, t_i\right)\right| \\ \leq & C\Big(\left|(h_{j+1}^i)^2 - (h_j^i)^2\right| \left|v'''\left(x_j^i, t_i\right)\right| + \\ & \left(h_j^i\right)^2 \left|h_{j+1}^i + h_j^i\right| \left|v^{(iv)}\left(x_j^i, t_i\right)\right| \Big),\end{aligned}$$

Now using Lemma (5.3.1) and Lemma (5.4.2) to compute

$$\begin{aligned}\left|\left[\left(L_1^{N,M} - L_1\right) v\right]_j^i\right| &\leq C\varepsilon^{\frac{-1}{2}} \left(h_j^i\right)^2 e^{\left(-x_j^i \sqrt{\frac{\rho}{\varepsilon}}\right)} + C\varepsilon^{-1} \left(h_j^i\right)^2 e^{\left(-x_j^i \sqrt{\frac{\rho}{\varepsilon}}\right)} \\ &\leq C\left(\varepsilon^{\frac{-1}{2}} + \varepsilon^{-1}\right) \left(\int_{x_{j-1}^i}^{x_j^i} e^{\left(-\frac{x}{2}\sqrt{\frac{\rho}{\varepsilon}}\right)} dx\right)^2 \\ &\leq C\left(\varepsilon^{\frac{-1}{2}} + \varepsilon^{-1}\right) \left(\sqrt{\varepsilon} \int_{x_{j-1}^i}^{x_j^i} M\left(x, y(x, t_i)\right) dx\right)^2 \leq C\Psi^2 N^{-2} \leq CN^{-2}.\end{aligned}$$

Likewise, we can estimate the outcome for the right side of the boundary layer portion, and the desired result follows immediately.

2. When $j = \{k_l, ..., k_r\}$, the taylor expansions with integral remainder yields

$$\left|\left[\left(L_1^{N,M} - L_1\right) v\right]_j^i\right| \leq C\varepsilon ||v''(x)||_{[x_{j-1}^i, x_{j+1}^i]}.$$

Now the derivative bounds derived in Lemma (5.3.1) yield

$$\left|\left[\left(L_1^{N,M} - L_1\right) v\right]_j^i\right| \leq C \begin{cases} e^{\left(-x_{j-1}^i \sqrt{\frac{\rho}{\varepsilon}}\right)}, & x_j^i \leq \frac{1}{2}, \\ e^{\left(-(1-x_{j+1}^i) \sqrt{\frac{\rho}{\varepsilon}}\right)}, & x_j^i > \frac{1}{2}. \end{cases}$$

For $j \geq k_l - 1$ and $x_j^i \leq \frac{1}{2}$, Lemma (5.4.1) suggests

$$\begin{aligned}\left|\left[\left(L_1^{N,M} - L_1\right) v\right]_j^i\right| &\leq Ce^{\left(-x_{k_l-1}^i \sqrt{\frac{\rho}{\varepsilon}}\right)} \\ &= C\left(e^{\left(\frac{-x_{k_l-1}^i}{2} \sqrt{\frac{\rho}{\varepsilon}}\right)}\right)^2 \leq CN^{-2}.\end{aligned}$$

The bounds for $j \leq k_r$ and $x_j^i > \frac{1}{2}$ can easily be established in a similar manner. □

Lemma 5.6.2. For all $j = 1, ..., N-1$ and $i = 1, ..., M$, the error component ψ_j^i satisfies $\psi_j^i \leq C(N^{-2} + \Delta t)$.

Proof. Using (5.6.3) and Lemma (5.2.1), we obtain the following bounds

$$\left|\psi_j^i\right| \leq \left(\max_j\left(\Phi_j^0\right) + \max_{j,i}\left|\chi_{2,j}^i - \rho_t^*\left(\Phi_j^i\right)\right| + \max_i\left(\psi_0^i\right) + \max_i\left(\psi_N^i\right)\right).$$

Now, using Taylor expansions and the time derivative bounds on the solution in Lemma (5.2.2), it is easy to verify that $\left|\chi_{2,j}^i\right| \leq C\Delta t,\ j = 1,...,N-1,\ i = 1,...,M$. Using (5.6.2), (5.6.3) and Lemma (5.6.1) with $i = 0$, we have

$$\left|\psi_j^i\right| \leq C\left(N^{-2} + \Delta t + \max_{j,i}\left|\rho_t^*\left(\Phi_j^i\right)\right| + \max_i\left(\psi_0^i\right) + \max_i\left(\psi_N^i\right)\right).$$

Using (5.6.2) such that for a fixed i, $\rho_t^*\Phi_j^i$ satisfies the following boundary value problem

$$\begin{aligned}
&L_1^{N,M}\rho_t^*\Phi_j^i = \rho_t^*\chi_{1,j}^i - \left(\left(\rho_t^*\left(a_j^i + b_j^i\right)\right)\Phi_j^{i-1}\right),\ j = 1,...,N-1\\
&[\kappa_1^{N,M}\rho_t^*\Phi]_0^j = \rho_t^*(\kappa_1^{N,M} - \kappa_1)y(0,t_i),\ [\kappa_2^{N,M}\rho_t^*\Phi]_N^j = \rho_t^*(\kappa_2^{N,M} - \kappa_2)y(1,t_i).
\end{aligned}$$

Using the piecewise linear interpolant technique on $x_{q-1}^{i-1} \leq x_j^i \leq x_{q-1}^i$, for some q with a fixed i, yields

$$\begin{aligned}
\rho_t^*\chi_{1,j}^i = \frac{\chi_{1,j}^i - \hat{\chi}_1^{i-1}(x_j^{i-1})}{\Delta t} =& \frac{1}{\Delta t}\Big(\left(L_1^{N,M} - L_1\right)u_j^i - \sigma_{q-1}\left(x_j^i\right)\left(\left(L_1^{N,M} - L_1\right)u_{q-1}^{i-1}\right) -\\
&\sigma_q\left(x_j^i\right)\left(\left(L_1^{N,M} - L_1\right)u_q^{i-1}\right)\Big),
\end{aligned}$$

where $\sigma_{q-1}(x) = \dfrac{x_q^{i-1} - x}{x_q^{i-1} - x_{q-1}^{i-1}}$ and $\sigma_q(x) = \dfrac{x - x_{q-1}^{i-1}}{x_q^{i-1} - x_{q-1}^{i-1}}$. As the interpolation error in the space domain is of order $O(N^{-2})$, let $\hat{L}_1 = -\varepsilon\dfrac{\partial^2}{\partial x^2}$ and $\hat{L}_1^{N,M} = -\varepsilon\rho_x^2$, we obtain

$$\rho_t^*\chi_{1,j}^i \leq \frac{1}{\Delta t}\left|\int_{t_{i-1}}^{t_i}\left(\hat{L}_1^{N,M} - \hat{L}_1\right)\frac{\partial y}{\partial t}(x_j^i,t)dt\right| + O(N^{-2})$$

.

Now using Lemma (5.2.2) and Lemma (5.6.1) yields the bound required on $\rho_t^*\chi_{1,j}^i$. Moreover, since $\left|\rho_t^*\left(a_j^i + b_j^i\right)\right| \leq C$, using the bounds of Lemma (5.6.1), we have

$$\max_j\left|\rho_t^*\left(a_j^i + b_j^i\right)\Phi_j^{i-1}\right| \leq C\max_j\left|\Phi_j^{i-1}\right| \leq CN^{-2}.$$

Thus, combining the various estimates completes the proof. □

We now summarise all the previously derived error estimates to present the main convergence result. The proof follows directly from Lemma (5.6.1), Lemma (5.6.2), and the triangle inequality.

Theorem 5.6.1. Let y be the solution of (5.2.1) and Y be the solution of (5.5.9). Then, there exists a positive constant C independent of N, ε and Δt such that

$$\max_{j,i}\left|y(x_j^i,t_i) - Y(x_j^i,t_i)\right| \leq C(\Delta t + N^{-2}).$$

5.7 Numerical Experiments

In this section, we examine the performance of the method using three model problems and present numerical findings. When an exact solution to the problem is not available, we estimate the error $E_\varepsilon^{N,\Delta t}$ using the double mesh principle [5], according to the formula defined in [324, 278]. However, if the exact solution is known, we use

$$E_\varepsilon^{N,\Delta t} = \max_{(x_j^i,t_i)\in\bar{\mathfrak{D}}^{N,M}} \left| y(x_j^i,t_i) - Y^{N,\Delta t}(x_j^i,t_i) \right|.$$

Here, $y(x_j^i,t_i)$ marks the analytic solution and $Y^{N,\Delta t}$ is the numerical approximation on $\bar{\mathfrak{D}}^{N,M}$. Moreover, we estimate uniform errors using $E^{N,\Delta t} = \max_{\varepsilon\in K} E_\varepsilon^{N,\Delta t}$ where $K = \{\varepsilon | \varepsilon = 2^0, 2^{-2}, ..., 2^{-40}\}$ and compute the order of convergence $p_\varepsilon^{N,\Delta t}$ and parameter-uniform order of convergence $p^{N,\Delta t}$ using the formula defined in [119, 324, 278].

Example 5.7.1. Consider the following problem:

$$\begin{cases} y_t(x,t) - \varepsilon y_{xx}(x,t) + (0.1+\sin(\pi x))y(x,t) + (x+10e^{-t})y(x-\delta,t) = g(x,t),\ (x,t)\in(0,1)\times(0,1], \\ y(x,0) = \cos\left(\dfrac{\pi x}{2}\right)\left(1-e^{-x\sqrt{\delta+2/\varepsilon}}\right) + \left(1-e^{-(1-x)\sqrt{\delta+2/\varepsilon}}\right),\ x\in[0,1], \\ y(x,t) = \displaystyle\int_0^1 \frac{1-e^{-\sqrt{\delta+2/\varepsilon}}}{(\delta+2/\varepsilon-2)^{-1}\left(\sqrt{\delta+2/\varepsilon}+2e^{-\sqrt{\delta+2/\varepsilon}}\right) - (\delta+2/\varepsilon)^{-1}\left(1-e^{-\sqrt{\delta+2/\varepsilon}}\right)+1} y(x,t)dx, \\ \qquad\qquad (x,t)\in[-\delta,0]\times[0,1], \\ y(1,t) = \displaystyle\int_0^1 \frac{1}{\cos\left(\frac{\pi x}{2}\right)\left(1-e^{-x\sqrt{\delta+2/\varepsilon}}\right) + \left(1-e^{-(1-x)\sqrt{\delta+2/\varepsilon}}\right)} y(x,t)dx,\ t\in[0,1] \end{cases}$$

where the function $g(x,t)$ is choosen such that

$$y(x,t) = (1-t^3)\left(\cos\left(\frac{\pi x}{2}\right)\left(1-e^{-x\sqrt{\delta+2/\varepsilon}}\right) + \left(1-e^{-(1-x)\sqrt{\delta+2/\varepsilon}}\right)\right).$$

Example 5.7.2. Consider the following problem [332]:

$$\begin{cases} y_t(x,t) - \varepsilon y_{xx}(x,t) + 3y(x,t) - y(x-1,t) = 1,\ (x,t)\in(0,1)\times(0,1], \\ y(x,0) = 0,\ x\in[0,2], \\ y(x,t) = \dfrac{\varepsilon}{6}\displaystyle\int_0^2 y(x,t)dx,\ (x,t)\in[-1,0]\times[0,1], \\ y(2,t) = \displaystyle\int_0^2 \frac{e^{-\sqrt{\delta+1/\varepsilon}}}{2} y(x,t)dx,\ t\in[0,1]. \end{cases}$$

Example 5.7.3. Consider the following problem

$$\begin{cases} y_t(x,t)-\varepsilon y_{xx}(x,t)+\cos(\pi x)y(x,t)+xe^{-t}y(x-\delta,t)=g(x,t),\ (x,t)\in(0,1)\times(0,1], \\ y(x,0)=0,\ x\in[0,1], \\ y(x,t)=\dfrac{1}{\sqrt{2\varepsilon}}\displaystyle\int_0^1 \frac{1-e^{-\sqrt{2/\varepsilon}}}{\sqrt{2/\varepsilon}-1+e^{-\sqrt{2/\varepsilon}}}y(x,t)dx,\ (x,t)\in[-\delta,0]\times[0,1], \\ y(1,t)=\dfrac{1}{\sqrt{2\varepsilon}}\displaystyle\int_0^1 \frac{1-e^{-\sqrt{2/\varepsilon}}}{\sqrt{2/\varepsilon}-1+e^{-\sqrt{2/\varepsilon}}}y(x,t)dx,\ t\in[0,1] \end{cases}$$

where the function $g(x,t)$ is choosen such that

$$y(x,t)=t\left(2-\left(e^{-x\sqrt{2/\varepsilon}}+e^{-(1-x)\sqrt{2/\varepsilon}}\right)\right).$$

Example 5.7.4. Consider the following problem [333]:

$$y_t(x,t)-\varepsilon y_{xx}(x,t)+y(x,t)=g(x,t),\ (x,t)\in\mathfrak{D}=(0,1)\times(0,1]$$

where the source term, initial and boundary conditions are calculated from the exact solution reads

$$\left(t+\frac{x^2}{2\varepsilon}\right)erfc\left(\frac{x}{2\sqrt{\varepsilon t}}\right)-\sqrt{\frac{t}{\pi\varepsilon}}xe^{-x^2/4\varepsilon t}.$$

Table 5.1: The error $E^{N,\Delta t}$ and the order of convergence $p^{N,\Delta t}$ for Example 5.7.1 for different values of ε, N and M with $\delta=0.05$.

ε		N=32 M=8	N=64 M=32	N=128 M=128	N=256 M=512	N=512 M=2048
2^{-1}	$E^{N,\Delta t}$	5.292e-02	1.499e-02	3.690e-03	8.783e-04	2.0811e-04
	$p^{N,\Delta t}$	1.8198	2.0223	2.0708	2.0773	
2^{-2}	$E^{N,\Delta t}$	5.706e-02	1.602e-02	3.927e-03	9.292e-04	2.1879e-04
	$p^{N,\Delta t}$	1.8326	2.0283	2.0793	2.0864	
2^{-3}	$E^{N,\Delta t}$	5.981e-02	1.661e-02	4.046e-03	9.552e-04	2.2546e-04
	$p^{N,\Delta t}$	1.84833	2.0374	2.0826	2.0829	
2^{-4}	$E^{N,\Delta t}$	6.202e-02	1.699e-02	4.105e-03	1.022e-03	2.5129e-04
	$p^{N,\Delta t}$	1.8680	2.0492	2.0059	2.0239	
2^{-5}	$E^{N,\Delta t}$	5.358e-02	1.738e-02	4.391e-03	1.107e-03	2.7359e-04
	$p^{N,\Delta t}$	1.6242	1.9848	1.9878	2.0165	

We choose $Q=1.05$ in the adaptive moving mesh generation process. For Example 5.7.1, Tables 5.1, 5.2, and 5.3 list the parameter uniform error and order of convergence for spatial variables, time variables, and a comparative analysis of the analytical and approximate solutions, respectively. It is evident from Tables 5.1, 5.5 and 5.6 that the method is second-order accurate in the space variable. To demonstrate the global first-order accuracy in the time variable, we balance the contribution of space and time discretisations by doubling the number of mesh points in space and quadrupling the number of time steps defined in [119]. The same is apparent from Table 5.2. Also, Tables 5.2 and 5.5 illustrate parameter uniform error and order of convergence and compare the result of the proposed hybrid method with uniformly convergent difference methods over a Shishkin mesh and equidistributed

Table 5.2: The error $E^{N,\Delta t}$ and the order of convergence $p^{N,\Delta t}$ for Example 5.7.1 for different values of ε, N and M with $\delta = 0.05$.

ε		N=32 M=8	N=64 M=16	N=128 M=32	N=256 M=64	N=512 M=128
2^{-1}	$E^{N,\Delta t}$	5.292e-02	2.858e-02	1.425e-02	6.788e-03	3.3244e-03
	$p^{N,\Delta t}$	0.8888	1.0040	1.0699	1.0298	
2^{-2}	$E^{N,\Delta t}$	5.706e-02	3.055e-02	1.516e-02	7.220e-03	3.5912e-03
	$p^{N,\Delta t}$	0.9013	1.0109	1.0701	1.0075	
2^{-3}	$E^{N,\Delta t}$	5.981e-02	3.168e-02	1.562e-02	7.443e-03	3.7018e-03
	$p^{N,\Delta t}$	0.9168	1.0201	1.0694	1.0076	
2^{-4}	$E^{N,\Delta t}$	6.202e-02	3.240e-02	1.585e-02	7.8211e-3	3.8921e-03
	$p^{N,\Delta t}$	0.9367	1.0315	1.0190	1.0068	
2^{-5}	$E^{N,\Delta t}$	5.358e-02	3.314e-02	1.697e-02	8.678e-03	4.3198e-03
	$p^{N,\Delta t}$	0.6931	0.9655	0.9675	1.0063	

Table 5.3: Comparison of analytic and approximate solution for Example 5.7.1 with $\varepsilon = 10^{-4}$, $\delta = 10^{-2}$, $N = 100$ and $M = 32$.

Analytic Solution						
$x \downarrow / t \rightarrow$	0	0.2	0.4	0.6	0.8	1
0.00	1.0000000000	0.9920000000	0.9360000000	0.7840000000	0.4880000000	0.0000000000
0.30	1.8910065242	1.8758784720	1.7699821066	1.4825491150	0.9228111838	0.0000000000
0.60	1.5877852523	1.5750829703	1.4861669961	1.2448236378	0.7748392031	0.0000000000
0.90	1.1564337437	1.1471822737	1.0824219841	0.9066440551	0.5643396669	0.0000000000
0.92	1.1253210291	1.1163184609	1.0533004833	0.8822516868	0.5491566622	0.0000000000
0.94	1.0939018285	1.0851506138	1.0238921114	0.8576190335	0.5338240923	0.0000000000
0.96	1.0592970352	1.0508226589	0.9915020249	0.8304888756	0.5169369532	0.0000000000
0.98	0.9723050543	0.9645266139	0.9100775308	0.7622871626	0.4744848665	0.0000000000
1.00	0.0000000000	0.0000000000	0.0000000000	0.0000000000	0.0000000000	0.0000000000
Approximate Solution						
$x \downarrow / t \rightarrow$	0	0.2	0.4	0.6	0.8	1
0.00	1.0000000000	0.9920000000	0.9360000000	0.7840000000	0.4880000000	0.0000000000
0.30	1.8910065433	1.8758784800	1.7699821064	1.4825491151	0.9228111839	0.0000000000
0.60	1.5877852635	1.5750829793	1.4861669978	1.2448236380	0.7748392029	0.0000000000
0.90	1.1564337563	1.1471822847	1.0824219833	0.9066440551	0.5643396670	0.0000000000
0.92	1.1253210293	1.1163184633	1.0533004879	0.8822516860	0.5491566623	0.0000000000
0.94	1.0939018296	1.0851506142	1.0238921134	0.8576190332	0.5338240923	0.0000000000
0.96	1.0592970363	1.0508226599	0.9915020251	0.8304888758	0.5169369532	0.0000000000
0.98	0.9723050549	0.9645266143	0.9100775309	0.7622871615	0.4744848665	0.0000000000
1.00	0.0000000000	0.0000000000	0.0000000000	0.0000000000	0.0000000000	0.0000000000

Table 5.4: Comparison of order of convergence $p^{N,\Delta t}$ for Example 5.7.2 for proposed method with a FDM over a piecewise uniform Shishkin mesh.

	ε	N=64 M=32	N=128 M=128	N=256 M=512	N=512 M=2048	N=1024 M=8192
Present Method	2^{-12}					
$E^{N,\Delta t}$		1.655e-02	4.328e-03	1.094e-03	2.744e-04	6.865e-05
$p^{N,\Delta t}$		1.9350	1.9840	1.9952	1.9989	1.9993
Method in [332]						
$p^{N,\Delta t}$		1.3369	1.5402	1.6333	1.6722	1.7052

Table 5.5: The error $E^{N,\Delta t}$ and the order of convergence $p^{N,\Delta t}$ for Example 5.7.3 for different values of ε, N and M with $\delta = 0.05$.

ε		N=32 M=8	N=64 M=32	N=128 M=128	N=256 M=512	N=512 M=2048
2^{-1}	$E^{N,\Delta t}$	2.661e-04	7.388e-05	1.921e-05	4.9860e-06	1.2834e-06
	$p^{N,\Delta t}$	1.8487	1.9433	1.9459	1.9579	
2^{-2}	$E^{N,\Delta t}$	2.512e-04	7.135e-05	1.877e-05	4.8281e-06	1.1919e-06
	$p^{N,\Delta t}$	1.8158	1.9264	1.9589	2.0181	
2^{-3}	$E^{N,\Delta t}$	2.346e-04	6.872e-05	1.837e-05	4.7922e-06	1.1922e-06
	$p^{N,\Delta t}$	1.7714	1.9033	1.9385	2.0070	
2^{-4}	$E^{N,\Delta t}$	2.132e-04	6.518e-05	1.782e-05	4.6821e-06	1.1782e-06
	$p^{N,\Delta t}$	1.7097	1.8709	1.9282	1.9905	
2^{-5}	$E^{N,\Delta t}$	2.697e-04	6.013e-05	1.698e-05	4.5291e-06	1.1490e-06
	$p^{N,\Delta t}$	2.1651	1.8242	1.9065	1.9788	

Table 5.6: Comparison of errors $E^{N,\Delta t}$ and order of convergence $p^{N,\Delta t}$ for Example 5.7.4 for proposed method with a modified backward Euler FDM on layer adapted nonuniform mesh.

	ε	N=16 M=5	N=32 M=20	N=64 M=80	N=128 M=320	N=256 M=1280
Present Method	10^0					
$E^{N,\Delta t}$		8.463e-03	2.245e-03	5.537e-04	1.362e-04	3.326e-05
$p^{N,\Delta t}$		1.9145	2.0195	2.0234	2.0339	
Method in [333]						
$E^{N,\Delta t}$		1.3208e-02	4.8368e-03	1.3771e-03	3.6046e-04	9.2406e-05
$p^{N,\Delta t}$		1.4493	1.8124	1.9337	1.9638	
Present Method	10^{-2}					
$E^{N,\Delta t}$		4.912e-03	1.231e-03	3.018e-04	7.233e-05	1.678e-05
$p^{N,\Delta t}$		1.9965	2.0282	2.0609	2.1079	
Method in [333]						
$E^{N,\Delta t}$		1.6934e-02	5.0200e-03	1.3741e-03	3.6053e-04	9.2542e-05
$p^{N,\Delta t}$		1.7542	1.8693	1.9302	1.9619	

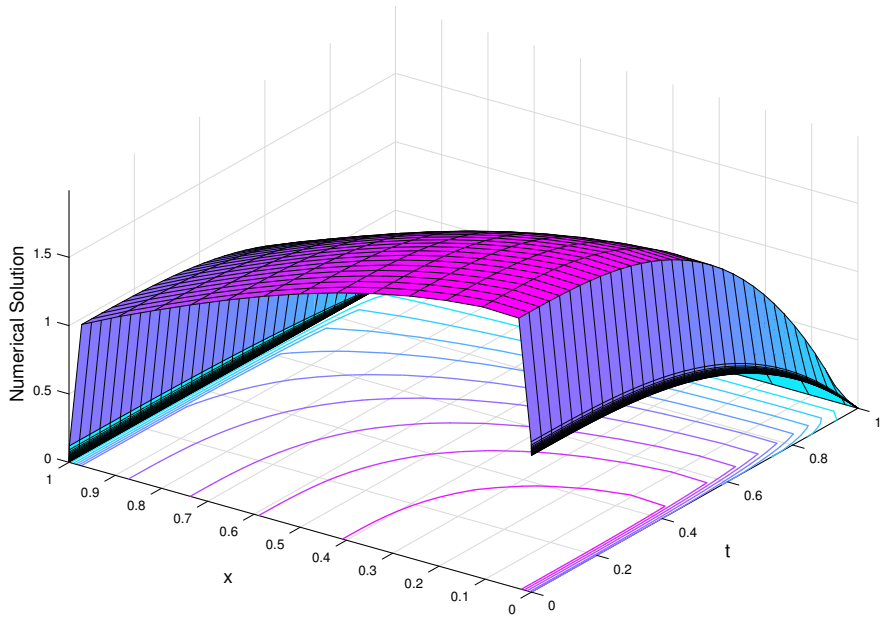

Fig. 5.1: Numerical solution of Example 5.7.1 with $\varepsilon = 10^{-4}$, $\delta = 10^{-2}$, $N = 64$ and $M = 32$.

meshs, respectively, for Examples, 5.7.2 and 5.7.4. Similarly, for Example 5.7.3, the uniform error and the order of convergence are tabulated in Table 3.4.

Figures 5.1, 5.3 and 5.5 illustrate the numerical solution of Examples 5.7.1, 5.7.2 and 5.7.3 for the given values of different parameters. Figures 5.2 depict the solution of Example 5.7.1 at different time levels. In contrast, Figure 5.7 shows the behaviour of the solution of Example 5.7.4 at a given time level for different values of the perturbation parameters. It is evident from the Figures that the solution to the problem exhibits layer behaviour in the neighbourhood of the outflow boundary. In these regions, the solution gradient grows exponentially, giving rise to multiscale character. Moreover, Figures 5.4 and 5.8 represent the log-log plot for the maximum pointwise error for Examples 5.7.2 and 5.7.4, respectively. The straight line in the log-log plot ensures that the error decreases monotonically and that the error satisfies the power function relationship as anticipated by theoretical estimates. Figure 5.6 presents the mesh density for the corresponding example in the spatial direction when $N = 128$. Note that the moving mesh algorithm successfully generates the mesh that remains dense in the layer regions and sparse outside as required.

5.8 Conclusion

A singularly perturbed time-dependent reaction-diffusion problem with shift and integral boundary conditions is solved numerically using a hybrid difference method over a moving mesh. The technique utilises a modified backward difference discretisation in time on a uniform mesh and a suitable combination of the exponential and cubic spline difference methods over a layer adaptive moving mesh in space. The layer-adapted mesh in space is generated by equidistributing a nonnegative monitor

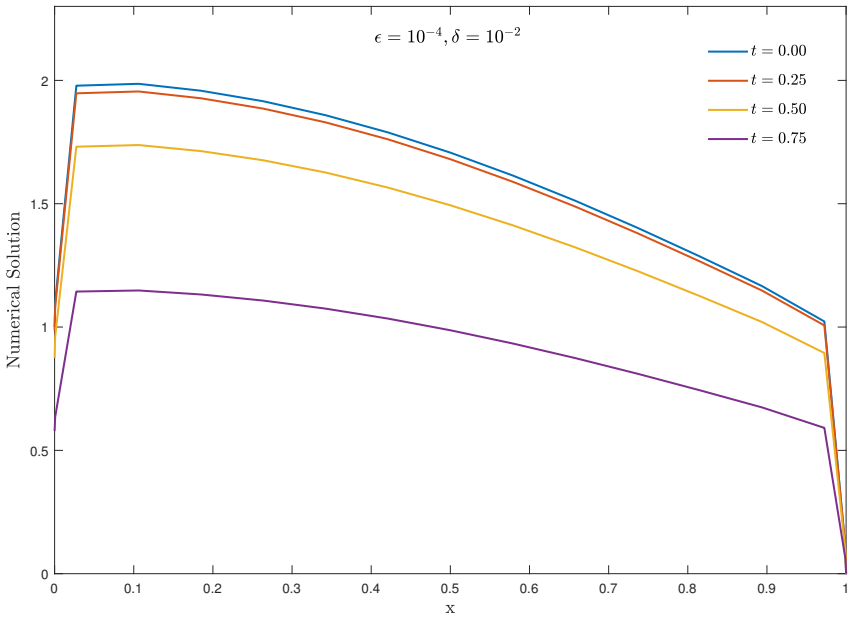

Fig. 5.2: Numerical solution of Example 5.7.1 at different time-levels with $M = 32$ and $N = 64$.

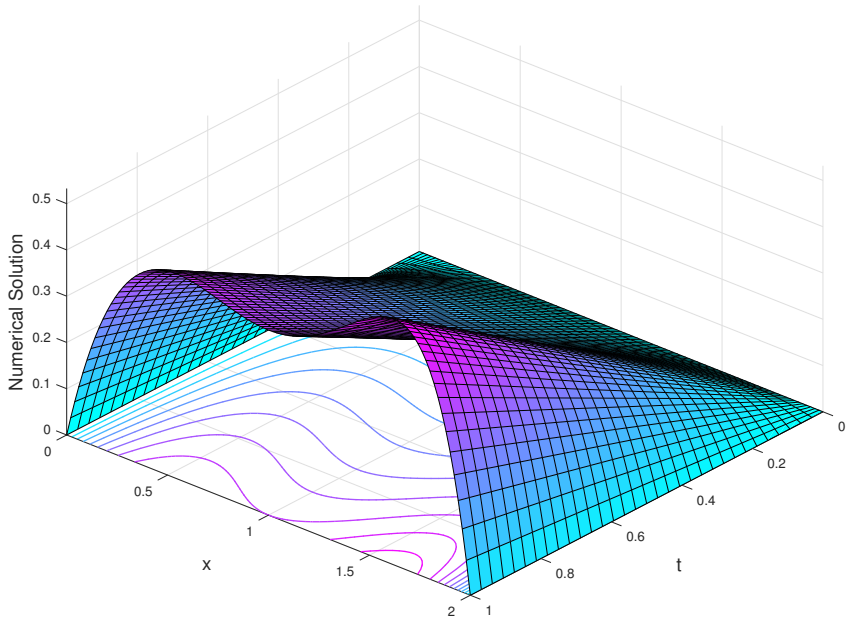

Fig. 5.3: Numerical solution of Example 5.7.2 with $\varepsilon = 2^{-5}$, $\delta = 1$, $N = 100$ and $M = 32$.

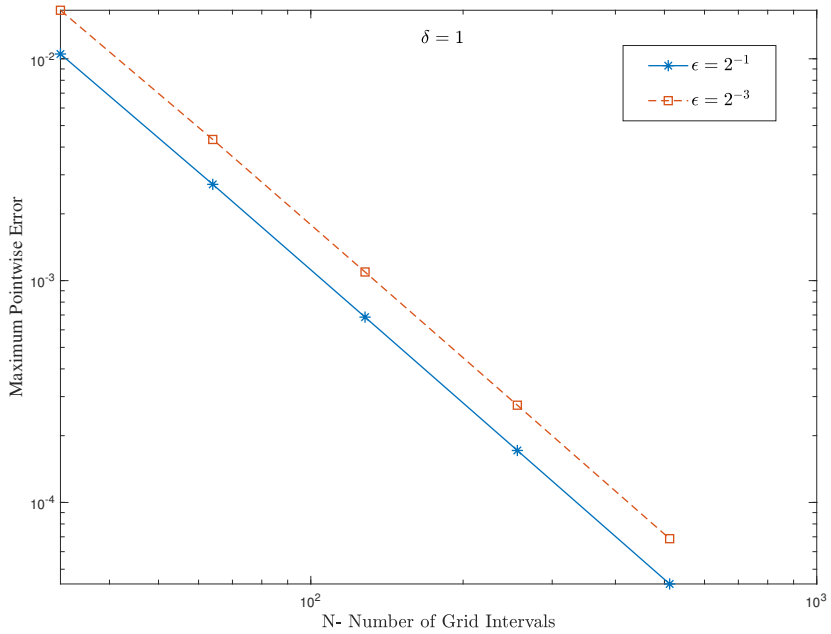

Fig. 5.4: Log-log plot of maximum pointwise errors for Example 5.7.2.

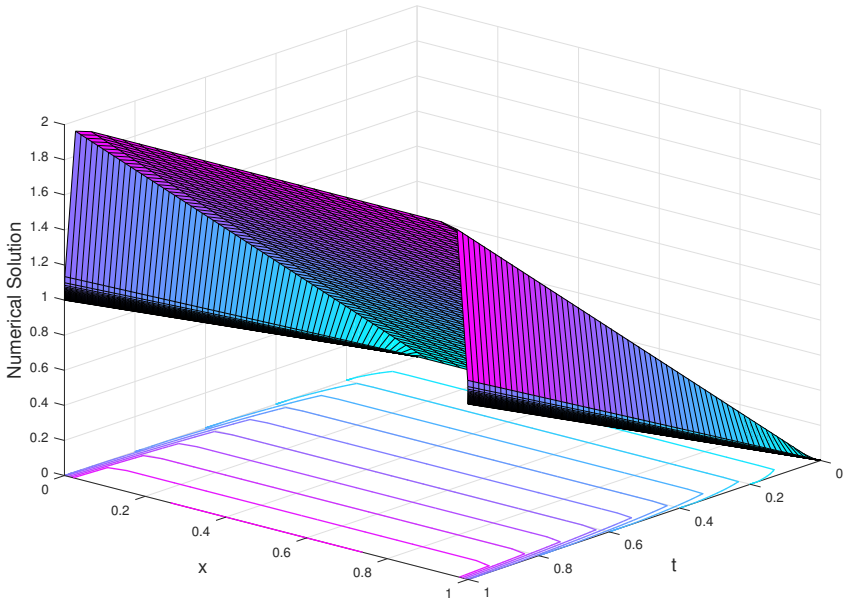

Fig. 5.5: Numerical solution of example 5.7.3 with $\varepsilon = 10^{-4}$, $\delta = 10^{-2}$, $N = 128$ and $M = 64$.

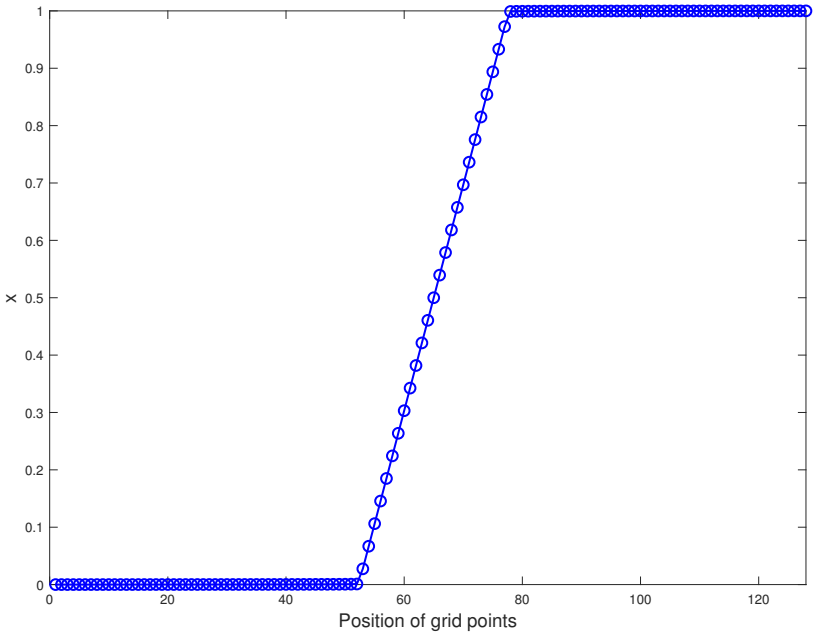

Fig. 5.6: Mesh density for numerical results of Example 5.7.3 with $N = 128$.

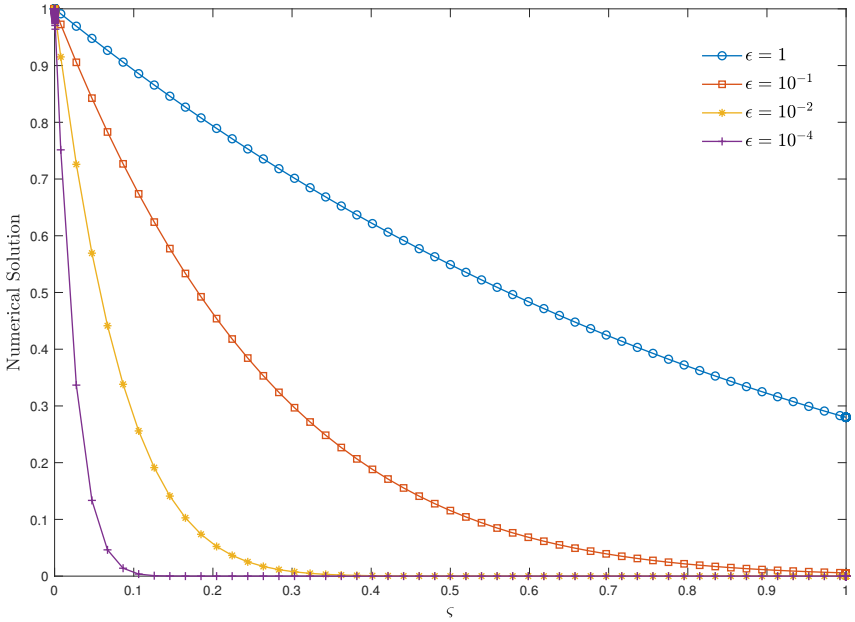

Fig. 5.7: Numerical solution for Example 5.7.4 at $t = 1$, $\delta = 0$ with $N = 256$, $M = 64$ and different values of ε.

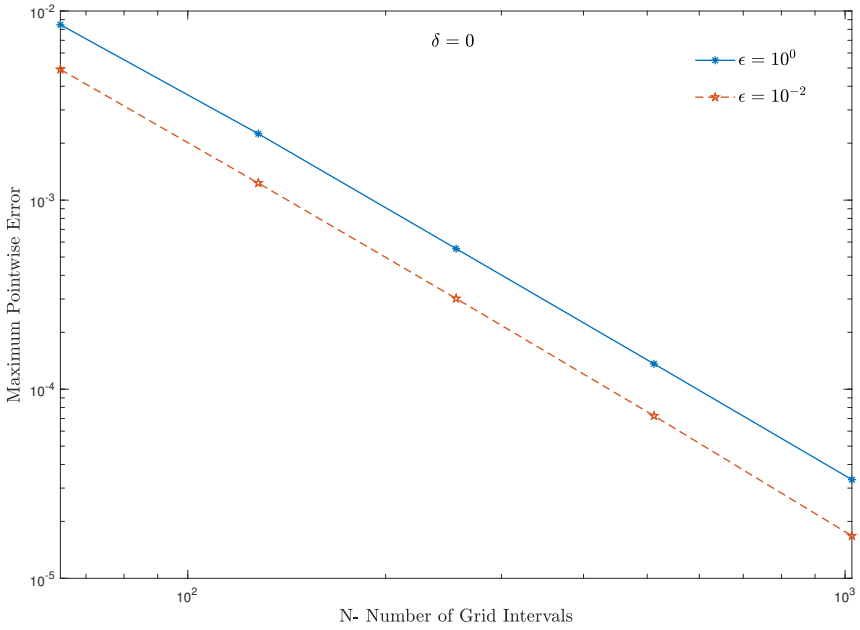

Fig. 5.8: Log-log plot of maximum pointwise errors for Example 5.7.4.

function, and the modified backward difference discretisation ensures alignment with the mesh at each subsequent time level. The presented method demonstrates second-order parameter uniform convergence in space and first-order convergence in time. The method improves the accuracy of numerical solutions while maintaining computational efficiency. The method is unconditionally stable and free from directional bias. The numerical experiments validate the theoretical estimates.

Chapter 6

Summary and Future Scope

6.1 Summary

This chapter summarises the work of the thesis and outlines future research directions with possible extensions of the present work. This thesis contributes to the development of adaptive numerical methods for analysing different classes of singularly perturbed boundary value problems with shifts and integral boundary conditions. The numerical techniques combine a high-order FDM with the adaptive moving mesh refinement strategy or a semi-analytical approach to capture the layer behaviour of the solution. This thesis comprises six chapters. The first chapter presents the introduction, providing the necessary background and motivation for the research. The subsequent four chapters detail the academic contributions to the treatment of four distinct problems. Finally, the sixth chapter offers the conclusion of the thesis and outlines potential directions for future research. The following is a chapter-wise summary of the thesis and its significant contributions.

Chapter 1 recalls an overview of the fundamentals of singular perturbation theory. It also presents concepts and a historical assessment of the related literature. This chapter also provides a detailed literature review of various state-of-the-art techniques developed in the recent past. In addition, the chapter illustrates the aim and objectives of the thesis.

Chapter 2 presents a higher-order adaptive hybrid difference method to solve a singularly perturbed system of reaction-diffusion problems with Dirichlet boundary conditions. The numerical method combines a Hermite difference method with the classical central difference method on a layer-adapted mesh. The equidistribution principle generates the mesh using a nonnegative monitor function. The mesh generation procedure automatically detects the thickness and steepness of any boundary layers present in the solution and does not require prior information about its analytical behaviour. The chapter presents a rigorous theoretical analysis and numerical results for model problems to support theoretical findings. The method is almost fourth-order accurate, converges uniformly, and is unconditionally stable. Moreover, the convergence obtained is optimal, as the estimates are free from any logarithmic term compared to the difference methods over the piecewise uniform Shishkin mesh.

Chapter 3 presents a higher-order hybrid approximation over an adaptive mesh designed to solve a

coupled system of singularly perturbed reaction-diffusion equations with a shift on an equidistributed mesh. The difference method combines an exponential spline difference method for the outer layer and a cubic spline difference method for the boundary layer on the adaptive mesh generated. The mesh relies on the equidistribution principle, a nonnegative monitor function, and the second-order derivatives of the layer components of the solution. The proposed numerical method improves the accuracy of numerical solutions while maintaining computational efficiency. The proposed numerical method is consistent, stable, and converges regardless of the size of the perturbation parameter. The numerical results and illustrations support the theoretical findings.

Chapter 4 presents a semi-analytical approach to solving a system of singularly perturbed convection-diffusion equations with shifts. A careful factorisation handles complex multiscale systems by splitting them into two explicit parts: one capturing smooth solutions and the other addressing boundary layer solutions. The strategy involves factoring a coupled system of equations into explicit systems of first-order initial value problems and second-order boundary value problems. The solutions to the degenerate system correspond to the regular component. In contrast, those of the system of boundary value problems represent the singular component. The process combines the regular and singular components to obtain the complete solution. The q-stage Runge-Kutta method computes the outer solution, and an analytical approach derives the inner solution. The proposed method is unconditionally stable and converges independently of the perturbation parameters. Unlike numerical methods, the proposed technique does not require adaptive mesh generation to sustain approximation and consequently has lower computational complexity. The process is straightforward and interdisciplinary researchers can quickly adapt the method to solve problems related to chemical kinetics, mathematical physics, and biology. The method is highly accurate, free from directional bias, and the estimates are free from logarithmic terms. The results demonstrate that the numerical method outperforms many existing methods.

Chapter 5 presents a highly efficient hybrid difference approximation for a time-dependent singularly perturbed reaction-diffusion equation with shift and integral boundary conditions. The technique utilises a modified backward difference discretisation in time on a uniform mesh and a suitable combination of the exponential and cubic spline difference methods over a layer adaptive moving mesh in space. The layer-adapted mesh in space is generated by equidistributing a nonnegative monitor function, and the modified backward difference discretisation ensures alignment with the mesh at each subsequent time level. The presented method demonstrates second-order spatial uniform convergence and first-order temporal convergence. The method improves the accuracy of numerical solutions while maintaining computational efficiency. The method is unconditionally stable and free from directional bias. The numerical experiments validate the theoretical estimates.

6.2 Future Scope

In this section, we outline some of the interesting problems to which the approach/idea presented in the thesis can be extended. It would be interesting to consider the following problems for future work.

1. Consider a time-dependent reaction-diffusion problem with a fractional temporal derivative

$$\begin{cases} D_t^{\alpha} y(x,t) - \varepsilon \frac{\partial^2 y(x,t)}{\partial x^2} + b(x,t)y(x,t) = g(x,t), \ \ (x,t) \in \Omega = (0,1) \times (0,T], \\ y(x,0) = \phi_0(x,0), \text{ on } \Gamma_0 := \{(x,0) : x \in [0,1]\}, \\ y(0,t) = \phi_l(0,t), \text{ on } \Gamma_l := \{(0,t) : t \in (0,T]\}, \\ y(1,t) = \phi_r(1,t), \text{ on } \Gamma_r := \{(1,t) : t \in (0,T]\}, \end{cases}$$

where $0 < \varepsilon \ll 1$, $0 < \alpha < 1$, $T > 0$, $b(x,t)$ and $g(x,t)$ are sufficiently smooth functions such that $b(x,t) \geq \beta > 0$ on $(x,t) \in \Omega$ and D_t^{α} denotes the Caputo fractional derivative defined by

$$D_t^{\alpha}\{(x,t) := \frac{1}{\Gamma(1-\alpha)} \int_{s=0}^{t} (t-s)^{-\alpha} \frac{\partial \{(x,s)}{\partial s} ds, \quad \text{for } (x,t) \in \mathscr{D}.$$

Such problems model various physical phenomena, particularly in the fields of genetic algorithms, traffic systems, telecommunications, robotic technology, signal processing, and many more.

2. Consider a two-parameter singularly perturbed parabolic convection-diffusion problem with a time delay posed on the domain $\Omega = (0,1) \times (0,T]$, $\Gamma = \bar{\Omega} \backslash \Omega$

$$\begin{cases} \varepsilon \frac{\partial^2 y(x,t)}{\partial x^2} + \mu a \frac{\partial y(x,t)}{\partial x} + by(x,t-\tau) + cy(x,t) - \frac{\partial y(x,t)}{\partial t} = g(x,t), \\ y(x,t) = \phi_0(x,t), \quad x \in (0,1) = \Gamma_0, \ t \in [-\tau, 0), \\ y = \phi_1(t), \ \text{ on } \ \Gamma_l \bigcup \Gamma_r, \end{cases}$$

where $\Gamma_0 = \{(x,0) : 0 \leq x \leq 1\}$, $\Gamma_l = \{(0,t) : 0 \leq t \leq T\}$, and $\Gamma_r = \{(1,t) : 0 \leq t \leq T\}$. Note that $0 < \varepsilon \leq 1$ and $0 < \mu \leq 1$ are perturbation parameters.

These types of problems have several applications in physical, biological and chemical processes, including chemical flow, lubrication theory, and reactor theory.

3. Consider a time dependent singularly perturbed convection-diffusion problem with discontinuity in the initial condition on domain Ω:

$$\begin{cases} \frac{\partial y(x,t)}{\partial t} - \varepsilon \frac{\partial^2 y(x,t)}{\partial x^2} + a(x,t) \frac{\partial y(x,t)}{\partial x} + b(x,t)y(x,t) = g(x,t), \quad (x,t) \in \Omega, \\ y(x,0) = \phi(x), \quad 0 \leq x \leq 1, \quad [\phi](\tilde{d}) \neq 0, 0 < \tilde{d} \leq \mathscr{O}(1) < 1, \\ y(0,t) = y(1,t) = 0, \quad 0 < t \leq T, \\ a(x,t) > \alpha > 0, \quad \forall (x,t) \in D, \quad 0 \leq t \leq T, \quad a, g \in C^{4+\gamma}(\bar{D}), \quad \gamma > 0, \\ \phi^{(i)} \in C^4(((0,1)) \backslash \{\tilde{d}\}) : \phi^{(i)}(0) = \phi^{(i)}(1) = 0, \quad 0 \leq i \leq 4, \\ g^{(i+2j)}(p,0) = 0, \quad 0 \leq i + 2j \leq 4 - 2p, \quad p = 0,1, \\ a_x(\tilde{d},0) = 0, \quad [\phi'](\tilde{d}) = 0, \end{cases}$$

where $\Omega = (0,1) \times (0,T], T > 0$. Here ε is a perturbation parameter such that $0 < \varepsilon \ll 1$ and the coefficients $a(x,t), b(x,t)$ are smooth functions such that $a(x,t) \geq \alpha > 0$, $b(x,t) \geq \beta \geq 0$ on

$\bar{\Omega}$. Moreover, $[\phi]$ denotes the jump in the function ϕ across the point of discontinuity $x = \tilde{d}$, that is, $[\phi](\tilde{d}) = \phi\left(\tilde{d^+}\right) - \phi\left(\tilde{d^-}\right)$.

Such type of problems appear in many fields of science and engineering, including the simulation of oil extraction from underground reservoirs, fluid flows such as water quality problems in river networks and convective heat transport problems with large Peclet numbers.

Bibliography

[1] L. Barbu and G. Moroşanu. *Singularly Perturbed Boundary Value Problems*. Birkhäusar, Basel, 2007.

[2] J.K. Kevorkian and J.D. Cole. *Multiple Scale and Singular Perturbation Methods*. Springer, Berlin, 1996.

[3] R.E. O'Malley. *Introduction to Singular Perturbations*. Academic Press, New York, 1974.

[4] H.G. Roos, M. Stynes, and L. Tobiska. *Robust Numerical Methods for Singularly Perturbed Differential Equations*. Springer, Berlin, 2008.

[5] T. Linß. *Layer Adapted Meshes for Reaction Convection Diffusion Problems*. Springer, Berlin, 2010.

[6] K.K. Sharma and A. Kaushik. "A solution of the discrepancy occurs due to using the fitted mesh approach rather than to the fitted operator for solving singularly perturbed differential equations". In: *Appl. Math. Comput.* 181 (2006), pp. 756–766.

[7] H. Schlichting and K. Gersten. *Boundary Layer Theory*. Springer-Verlag, Berlin, 2003.

[8] L. Prandtl. *Über Flüssigkeitsbewegung bei sehr kleiner Reibung: in Verhandlungen des III Internationalen Mathematiker-Kongresses*. Teubner, Leipzig, 1904.

[9] P.C. Lu. *Introduction to the Mechanics of Viscous Fluids*. Holt-Rinehart & Winston, New York, 1973.

[10] J.J.H. Miller. *Singular Perturbation Problems in Chemical Physics*. John Wiley & Sons, New York, 1997.

[11] S.J. Polak, C. Den Heijer, W.H.A. Schilders, and P. Markowich. "Semiconductor device modelling from the numerical point of view". In: *Int. J. Numer. Methods Eng.* 24 (1987), pp. 763–838.

[12] D. Bahuguna, S. Abbas, and J. Dabas. "Partial functional differential equation with an integral condition and applications to population dynamics". In: *Nonlinear Anal.* 69 (2008), pp. 2623–2635.

[13] R. FitzHugh. "Impulses and physiological states in theoretical models of nerve membrane". In: *Biophysical journal* 1 (1961), pp. 445–466.

[14] H. Baumert, P. Braun, E. Glos, W.D. Müller, and G. Stoyan. "Modelling and computation of water quality problems in river networks". In: *Optimization Techniques: Proceedings of the 9th IFIP Conference on Optimization Techniques Warsaw, September 4-8, 1979*. Springer, 2005, pp. 482–491.

[15] J. Bear and A. Verruijt. *Modelling Groundwater Flow and Pollution*. Springer Science & Business Media, 1987.

[16] C. Huan-wen. "Some application of the singular perturbation methodto the bending problems of thin plates and shells". In: *Appl. Math. Mech.* 5 (1984), pp. 1449–1457.

[17] J.D. Murray. *Lectures on Nonlinear-Differential-Equation Models in Biology*. Clarendon Press, Oxford, 1977.

[18] S.Y. Hahn, J. Bigeon, and J.C. Sabonnadiere. "An upwind finite element method for electromagnetic field problems in moving media". In: *Int. J. Numer. Methods Eng.* 24 (1987), pp. 2071–2086.

[19] J. Black and M. Scholes. "The pricing of options and corporate liabilities". In: *J. Polit. Econ.* 81 (1973), pp. 637–654.

[20] R.B. Stein. "A theoretical analysis of neuronal variability". In: *Biophys. J.* 5 (1965), pp. 173–194.

[21] R.E. Ewing. *The Mathematics of Reservoir Simulation*. SIAM, Philadelphia, 1983.

[22] T.C. Assiff and D.H. Yen. "On the solutions of clamped reissner-mindlinplates under transverse loads". In: *Quart. Appl. Math.* 45 (1987), pp. 679–690.

[23] V. Barcilon. "Singular perturbation analysis of the fokker-planck equation: Kramer's underdamped problem". In: *SIAM J. Appl. Math.* 56 (1996), pp. 446–479.

[24] M. Van-Dyke. *Perturbation Methods in Fluid Dynamics*. Academic Press, New York, 1964.

[25] Z. Gajic and M.T. Lim. *Optimal Control of Singularly Perturbed Linear Systems and Applications*. Marcel-Dekker, New York, 2001.

[26] D.S. Naidu and A.K. Rao. *Singular Perturbation Analysis of Discrete Control Systems*. Springer-Verlag, Berlin, 1985.

[27] A. Kaushik and M.D. Sharma. "Numerical analysis of a mathematical model for propagation of an electrical pulse in a neuron". In: *Numer. Methods Partial Differ. Equ.* 27 (2008), pp. 1–18.

[28] E.M. De-Jager and J. Furu. *The Theory of Singular Perturbations*. Elsevier, Amsterdam, 1996.

[29] A. Lindstedt. "Über die integration einer für die störungstheorie wichtigen differentialgleichung". In: *Astronomische Nachrichten, volume 103, Issue 14, p. 211* 103 (1882), p. 211.

[30] A. Lindstedt. *Beitrag zur Integration der Differentialgleichnungen der Störungstheorie*. Eggers, 1883.

[31] H. Poincaré. *Les Méthodes Nouvelles de la Mécanique Céleste*. Vol. 2. Gauthier-Villars et fils, imprimeurs-libraires, 1893.

[32] E.L. Reiss. "On multivariable asymptotic expansions". In: *SIAM Review* 13.2 (1971), pp. 189–196.

[33] J.L. Lagrange. *Mécanique Analytique*. Blanchard, Paris, 1788.

[34] B. Van Der Pol. "A theory of the amplitude of free and forced triode vibrations". In: *Radio Review* 1 (1920), pp. 701–710.

[35] N. Bogoliubov and I. Mitropolski. *Les Méthodes Asymptotiques en Théorie des Oscillations Non Linéaires*. Gauthier-Villars, Paris, 1962.

[36] J.J.H. Miller, E. O'Riordan, and G.I. Shishkin. *Fitted Numerical Methods for Singular Perturbation Problems*. World Scientific, Singapore, 2012.

[37] H.G. Roos, M. Stynes, and L. Tobiska. *Numerical Methods for Singularly Perturbed Differential Equations: Convection-Diffusion and Flow Problems*. Springer-Verlag, New york, 1996.

[38] P.A. Farrell, A.F. Hegarty, J.J.H. Miller, E. O'Riordan, and G.I. Shishkin. *Robust Computational Techniques for Boundary Layers*. Chapman and Hall/CRC, Boca Raton, 2000.

[39] G.I. Shishkin and L.P. Shishkina. *Difference Methods for Singular Perturbation Problems*. Chapman and Hall/CRC, Boca Raton, 2009.

[40] K.W. Morton. *Numerical Solution of Convection Diffusion Problems*. Chapman & Hall, London, 2010.

[41] A.N. Tikhonov. "The dependence of the solutions of differential equations on a small parameter". In: *Math. Sb.* 22 (1948), pp. 193–204.

[42] A.N. Tikhonov. "On systems of differential equations containing parameters". In: *Math. Sb.* 27 (1950), pp. 147–156.

[43] A.N. Tikhonov. "Systems of differential equations containing small parameters multiplying some of derivatives". In: *Math. Sb.* 31 (1952), pp. 575–586.

[44] K.O. Friedrichs and W. Wasow. "Singular perturbations of nonlinear oscillations". In: *Duke Math.* 13 (1946), pp. 367–381.

[45] R.W. Wolfgang. "On boundary layer problems in the theory of ordinary differential equations". PhD thesis. New York University, New York, U.S.A, 1941.

[46] S. Kaplun. "The role of coordinate systems in boundary-layer theory". In: *Zeitschrift für angewandte Mathematik und Physik ZAMP* 5 (1954), pp. 111–135.

[47] M.I. Vishik and L.A. Lyusternik. "Regular degeneration and boundary layer for linear differential equations with a small parameter multiplying the highest derivatives". In: *Usp. Mat. Nauk* 12 (1957), pp. 3–122.

[48] P.A. Lagerstrom and R.G. Casten. "Basic concepts underlying singular perturbation techniques". In: *SIAM Review* 14 (1972), pp. 63–120.

[49] P.V. Kokotovic. "Applications of singular perturbation techniques to control problems". In: *SIAM Review* 26 (1984), pp. 501–550.

[50] M.K. Kadalbajoo and K.C. Patidar. "Singularly perturbed problems in partial differential equations: A survey". In: *Appl. Math. Comp.* 134 (2003), pp. 371–429.

[51] M.K. Kadalbajoo and V. Gupta. "A brief survey on numerical methods for solving singularly perturbed problems". In: *Appl. Math. Comp.* 217 (2010), pp. 3641–3716.

[52] H.G. Roos. "Robust numerical methods for singularly perturbed differential equations: A survey covering 2008-2012". In: *ISRN Appl. Math.* 2012 (2012), pp. 1–30.

[53] N. Levinson. "The First Boundary Value Problem for ε-$\Delta U + A(X,Y)UX + B(X,Y)UY + C(X,Y)U = D(X,Y)$ for small ε". In: *Annals of Mathematics* 51 (1950), pp. 428–445.

[54] O.A. Oleĭnik. "On boundary problems from equations with a small parameter in the highest derivatives". In: *Dokl. Akad. Nauk, SSR* 85 (1952), pp. 493–495.

[55] P.A. Lagerstrom and J.D. Cole. "Examples illustrating expansion procedures for the Navier-Stokes equations". In: *J. Ration. Mech. Anal.* 4 (1955), pp. 817–882.

[56] S. Kaplun and P.A. Lagerstrom. “Asymptotic expansions of Navier-Stokes solutions for small Reynolds numbers”. In: *J. Math. Mech.* (1957), pp. 585–593.

[57] M.I. Visik and L.A. Lyusternik. “On elliptic equations containing small parameters in the terms with higher derivatives”. In: *Dokl. Akad. Nauk, SSR* 113 (1957), pp. 734–737.

[58] J. Kevorkian and J.D. Cole. *Perturbation Methods in Applied Mathematics*. Springer, Berlin, 2013.

[59] R.E. O’Malley. *Historical Developments in Singular Perturbations*. Springer, 2014.

[60] C.M. Bender and S.A. Orszag. *Advanced Mathematical Methods for Scientists and Engineers*. McGraw-Hill, New York, 1978.

[61] J. Kevorkian. *The two variable expansion procedure for the approximate solution of certain non-linear differential equations*. Tech. rep. Santa Monica, California, 1962.

[62] D. Dessi, F. Mastroddi, and L. Morino. “A fifth-order multiple-scale solution for Hopf bifurcations”. In: *Comput. Struct.* 82 (2004), pp. 2723–2731.

[63] A. Shooshtari and A.A Pasha Zanoosi. “A multiple times scale solution for non-linear vibration of mass grounded system”. In: *Appl. Math. Model.* 34 (2010), pp. 1918–1929.

[64] O. Coulaud. “Multiple time scales and perturbation methods for high frequency electromagnetic-hydrodynamic coupling in the treatment of liquid metals”. In: *Nonlinear Anal.* 30 (1997), pp. 3637–3643.

[65] W.T. Van Horssen. “On integrating vectors and multiple scales for singularly perturbed ordinary differential equations”. In: *Nonlinear Anal.* 46 (2001), pp. 19–43.

[66] M. Belhaq and F. Lakrad. “Elliptic multiple scales method for a class of autonomous strongly non-linear oscillators”. In: *J. Sound Vib.* 234 (2000), pp. 547–553.

[67] G.E. Kuzmak. “Asymptotic solutions of nonlinear second order differential equations with variable coefficients”. In: *J. Appl. Math. Mech.* 23 (1959), pp. 730–744.

[68] F. Lakrad and M. Belhaq. “Periodic solutions of strongly non-linear oscillators by the multiple scales method”. In: *J. Sound Vib.* 258 (2002), pp. 677–700.

[69] J. Heading. *An Introduction to Phase-Integral Methods*. Methuen, London, 1962.

[70] A. Schlissel. “The initial development of the WKB solutions of linear second order ordinary differential equations and their use in the connection problem”. In: *Hist. Math.* 4 (1977), pp. 183–204.

[71] S. Borowitz. *Fundamentals of Quantum Mechanics, Particles, Waves, and Wave Mechanics*. Benjamin, 1967.

[72] C.R. Steele. “Application of the WKB method in solid mechanics”. In: *Mech. Today* 3 (1976), pp. 243–295.

[73] N.B. Abdallah and O. Pinaud. “Multiscale simulation of transport in an open quantum system: Resonances and WKB interpolation”. In: *J. Comp. Phys.* 213 (2006), pp. 288–310.

[74] L. Gosse and L.N. Mauser. “Multiphase semiclassical approximation of an electron in a one-dimensional crystalline lattice–III. From ab initio models to WKB for Schrödinger-Poisson”. In: *J. Comp. Phys.* 211 (2006), pp. 326–346.

[75] R. Krivec and V.B. Mandelzweig. “Quasilinearization method and WKB”. In: *Comput. Phys. Commun.* 174 (2006), pp. 119–126.

[76] N.N. Nefedov and L. Recke. “A common approach to singular perturbation and homogenization II: Semilinear elliptic systems”. In: *Journal of Mathematical Analysis and Applications* 545.1 (2025), p. 129099.

[77] E. Marušić-Paloka and I. Pažanin. “Homogenization and singular perturbation in porous media”. In: *Communications on Pure and Applied Analysis* 20.2 (2021), pp. 533–545.

[78] O. Khrustalev and S. Vernov. “Construction of doubly periodic solutions via the Poincare-Lindstedt method in the case of massless $\phi 4$ theory”. In: *Math. Comput. Simul.* 57 (2001), pp. 239–252.

[79] T. Öziş and A. Yıldırım. “Determination of periodic solution for a $u^{\frac{1}{3}}$ force by He’s modified Lindstedt–Poincaré method”. In: *J. Sound Vib.* 301 (2007), pp. 415–419.

[80] S. Benbachir. “Lindstedt–Poincaré method and periodic families of the Barbanis-Contopoulos Hamiltonian system”. In: *Math. Comput. Simul.* 51 (2000), pp. 579–596.

[81] A. Marasco. “Lindstedt-Poincarè method and Mathematica applied to the motion of a solid with a fixed point”. In: *Comput. Math. Appl.* 40 (2000), pp. 333–343.

[82] S.H. Chen, J.L. Huang, and K.Y. Sze. “Multidimensional Lindstedt-Poincaré method for nonlinear vibration of axially moving beams”. In: *J. Sound Vib.* 306 (2007), pp. 1–11.

[83] J.F. Navarro. “On the implementation of the Poincaré-Lindstedt technique”. In: *Appl. Math. Comput.* 195 (2008), pp. 183–189.

[84] R. Bauerschmidt, D. C. Brydges, and G. Slade. *Introduction to a Renormalisation Group Method*. Springer Singapore, 2019.

[85] A. Bush. *Perturbation Methods for Engineers and Scientists*. Routledge, New York, 1992.

[86] C.K.R.T. Jones. “Geometric singular perturbation theory”. In: *Dynamical Systems: Lectures Given at the 2nd Session of the Centro Internazionale Matematico Estivo (C.I.M.E.) held in Montecatini Terme, Italy, June 13–22, 1994*. Ed. by Russell Johnson. Berlin, Heidelberg: Springer Berlin Heidelberg, 1995, pp. 44–118.

[87] N. Fenichel. “Geometric singular perturbation theory for ordinary differential equations”. In: *Journal of Differential Equations* 31.1 (1979), pp. 53–98.

[88] M. Wechselberger. *Geometric Singular Perturbation Theory Beyond the Standard Form*. Springer, Cham, 2020.

[89] A.H. Nayfeh. *Perturbation Methods*. Wiley, New York, 1979.

[90] B.K. Shivamoggi. “The method of strained coordinates/parameters”. In: *Perturbation Methods for Differential Equations*. 2003, pp. 41–111.

[91] S. Stahara, A. Crisalli, and J. Spreiter. “Evaluation of a strained-coordinate perturbation procedure-Nonlinear subsonic and transonic flows”. In: *18th Aerospace Sciences Meeting*. 1980, p. 339.

[92] F. Verhulst. *Methods and Applications of Singular Perturbations: Boundary Layers and Multiple Timescale Dynamics*. Springer Science & Business Media, 2005.

[93] L.A. Skinner. *Singular Perturbation Theory*. Springer Science & Business Media, 2011.

[94] R.J. LeVeque. *Finite Difference Methods for Ordinary and Partial Differential Equations*. SIAM, 2007.

[95] H.P. Langtangen and S. Linge. *Finite Difference Computing with PDEs*. Springer Cham, Switzerland, 2017.

[96] J.C. Strikwerda. *Finite Difference Schemes and Partial Differential Equations*. SIAM, 2004.

[97] Z. Chem. *Finite Element Methods and their Applications*. Springer, Berlin, 2005.

[98] D. Boffi, F. Brezzi, and M. Fortin. *Mixed Finite Element Methods and Applications*. Springer, 2013.

[99] F. Brezzi and M. Fortin. *Mixed and Hybrid Finite Element Methods*. Springer Science & Business Media, 2012.

[100] O.C. Zienkiewicz, R. Taylor, and J.Z. Zhu. *The Finite Element Method: Its Basis and Fundamentals*. Elsevier, MA, 2005.

[101] T.J.R. Hughes. *The Finite Element Method: Linear Static and Dynamic Finite Element Analysis*. Dover, New York, 2000.

[102] R. Verfürth. *A Posteriori Error Estimation Techniques for Finite Element Methods*. Oxford University Press, Oxford, 2013.

[103] S. Brenner and L. Scott. *The Mathematical Theory of Finite Element Methods*. Springer-Verlag, New York, 2008.

[104] R.J. LeVeque. *Finite Volume Methods for Hyperbolic Problems*. Cambridge University Press, 2002.

[105] F. Moukalled, L. Mangani, and M. Darwish. *The Finite Volume Method in Computational Fluid Dynamics*. Springer, Switzerland, 2016.

[106] J.N. Reddy, N.K. Anand, and P. Roy. *Finite Element and Finite Volume Methods for Heat Transfer and Fluid Dynamics*. Cambridge University Press, Cambridge, 2022.

[107] N.S. Bakhvalov. "On the optimization of methods for solving boundary value problems with boundary layers". In: *Zh. Vychisl. Mat. Mat. Fis.* 9 (841-859), p. 1969.

[108] A. Gupta and A. Kaushik. "A higher-order accurate difference approximation of singularly perturbed reaction-diffusion problem using grid equidistribution". In: *Ain Shams Engineering Journal* 12.4 (2021), pp. 4211–4221.

[109] A. Gupta and A. Kaushik. "A robust spline difference method for robin-type reaction-diffusion problem using grid equidistribution". In: *Applied Mathematics and Computation* 390 (2021), p. 125597. ISSN: 0096-3003.

[110] S. Saini, P. Das, and S. Kumar. "Computational cost reduction for coupled system of multiple scale reaction diffusion problems with mixed type boundary conditions having boundary layers". In: *Revista de la Real Academia de Ciencias Exactas, Físicas y Naturales. Serie A. Matemáticas* 117.2 (Feb. 2023), p. 66.

[111] E.C. Gartland. "Graded mesh difference schemes for singularly perturbed two point boundary value problems". In: *Math. Comput.* 51 (1988), pp. 631–657.

[112] R. Vulanović and L. Teofanov. "A modification of the Shishkin discretization mesh for one dimensional reaction diffusion problems". In: *Appl. Math. Comput.* 220 (2013), pp. 104–116.

[113] K. Kumar, P.C. Podila, P. Das, and H. Ramos. “A graded mesh refinement approach for boundary layer originated singularly perturbed time-delayed parabolic convection diffusion problems”. In: *Math. Methods Appl. Sci.* 44.16 (2021), pp. 12332–12350.

[114] D. Shakti, J. Mohapatra, P. Das, and J. Vigo-Aguiar. “A moving mesh refinement based optimal accurate uniformly convergent computational method for a parabolic system of boundary layer originated reaction–diffusion problems with arbitrary small diffusion terms”. In: *Journal of Computational and Applied Mathematics* 404 (2022), p. 113167.

[115] S. Priyadarshana, J. Mohapatra, and H. Ramos. “Robust numerical schemes for time delayed singularly perturbed parabolic problems with discontinuous convection and source terms”. In: *Calcolo* 61.1 (Nov. 2023), p. 1.

[116] A. Kaushik, A.K. Vashishtha, V. Kumar, and M. Sharma. “A modified graded mesh and higher order finite element approximation for singular perturbation problems”. In: *J. Comp. Phys.* 395 (2019), pp. 275–285.

[117] A. Kaushik, V. Kumar, M. Sharma, and N. Sharma. “A modified graded mesh and higher order finite element method for singularly perturbed reaction–diffusion problems”. In: *Mathematics and Computers in Simulation* 185 (2021), pp. 486–496.

[118] Aakansha, S. Kumar, and H. Ramos. “A rapidly converging domain decomposition algorithm for a time delayed parabolic problem with mixed type boundary conditions exhibiting boundary layers”. In: *J. Appl. Math. Comput.* 70.2 (2024), pp. 1043–1067.

[119] S. Saini, P. Das, and S. Kumar. “Parameter uniform higher order numerical treatment for singularly perturbed Robin type parabolic reaction diffusion multiple scale problems with large delay in time”. In: *Applied Numerical Mathematics* 196 (2024), pp. 1–21.

[120] P. Das. “Comparison of a priori and a posteriori meshes for singularly perturbed nonlinear parameterized problems”. In: *J. Comput. Appl. Math.* 290 (2015), pp. 16–25.

[121] C.E. Pearson. “On a differential equation of boundary layer type”. In: *J. Math. and Phy.* 47 (1968), pp. 134–154.

[122] C.E. Pearson. “On a nonlinear differential equation of boundary layer type”. In: *J. Math. and Phy.* 47 (1968), pp. 351–358.

[123] E.P. Doolan, J.J.H. Miller, and W.H.A. Schilders. *Uniform Numerical Methods for Problems with Initial and Boundary Layers*. Boole Press, 1980.

[124] A.M. Il’in. “Differencing scheme for a differential equation with a small parameter affecting the highest derivative”. In: *Mathematical Notes of the Academy of Sciences of the USSR* 6 (1969), pp. 596–602.

[125] A. Goeke, S. Walcher, and E. Zerz. “Determining “small parameters” for quasi-steady state”. In: *Journal of Differential Equations* 259.3 (2015), pp. 1149–1180.

[126] F.W. Dorr. “The numerical solution of singular perturbations of boundary value problems”. In: *SIAM J. Numer. Anal.* 7 (1970), pp. 281–313.

[127] F.W. Dorr, S.V. Parter, and L.F. Shampine. “Applications of the maximum principle to singular perturbation problems”. In: *SIAM Review* 15 (1973), pp. 43–88.

[128] M.H. Protter and H.F. Weinberger. *Maximum Principles in Differential Equations*. Springer-Verlag, New York, 1984.

[129] L.R. Abrahamsson, H.B. Keller, and H.O. Kreiss. “Difference approximations for singular perturbations of systems of ordinary differential equations”. In: *Numer. Math.* 22 (1974), pp. 367–391.

[130] K.E. Barrett. “The numerical solution of singular-perturbation boundary-value problems”. In: *Quart. J. Mech. Appl. Math.* 27 (1974), pp. 57–68.

[131] R.B. Kellogg and A. Tsan. “Analysis of some difference approximations for a singular perturbation problem without turning points”. In: *Math. Comp.* 32 (1978), pp. 1025–1039.

[132] V.A. Gushchin and V.V. Shchennikov. “A monotonic difference scheme of second-order accuracy”. In: *USSR Comput. Math. Math. Phys.* 14 (1974), pp. 252–256.

[133] T.M. El-Mistikawy and M.J. Werle. “Numerical method for boundary layers with blowing-The exponential box scheme”. In: *AIAA Journal* 16 (1978), pp. 749–751.

[134] H.B. Keller. *Numerical Methods for Two-Point Boundary-Value Problems*. Blaisdell Publication Co., Waltham, Massachusetts, 1968.

[135] A.E. Berger, J.M. Solomon, and M. Ciment. “An analysis of a uniformly accurate difference method for a singular perturbation problem”. In: *Math. Comp.* 37 (1981), pp. 79–94.

[136] O. Axelsson and I. Gustafsson. “A modified upwind scheme for convective transport equations and the use of a conjugate gradient method for the solution non-symmetric systems of equations”. In: *IMA J. Appl. Math.* 23 (1979), pp. 321–337.

[137] G.I. Shishkin. “A difference scheme on a non-uniform mesh for a differential equation with a small parameter in the highest derivative”. In: *USSR Comput. Math. Math. Phys.* 23 (1983), pp. 59–66.

[138] A.A. Samarskii. *Theory of Difference Schemes*. Nauka, Moscow, 1977.

[139] R. Vulanović. “On a numerical solution of a type of singularly perturbed boundary value problem by using a special discretisation mesh”. In: *Rev. Res. Math. Ser. Univ. Novi Sad* 13 (1983), pp. 187–201.

[140] E.C. Gartland. “Uniform high-order difference schemes for a singularly perturbed two-point boundary value problem”. In: *Math. Comput.* 48 (1987), pp. 551–564.

[141] R.E. Lynch and J.R. Rice. “A high-order difference method for differential equations”. In: *Math. Comput.* 34 (1980), pp. 333–372.

[142] E.J. Doedel. “The construction of finite difference approximations to ordinary differential equations”. In: *SIAM J. Numer. Anal.* 15 (1978), pp. 450–465.

[143] K. Niederdrenk and H. Yserentant. “Die gleichmäßige Stabilität singulär gestörter diskreter und kontinuierlicher Randwertprobleme”. In: *Numer. Math.* 41 (1983), pp. 223–253.

[144] P.A. Farrell. “Sufficient conditions for uniform convergence of a class of difference schemes for a singularly perturbed problem”. In: *IMA J. Numer. Anal.* 7 (1987), pp. 459–472.

[145] P.A. Farrell. “Sufficient conditions for the uniform convergence of a difference scheme for a singularly perturbed turning point problem”. In: *SIAM J. Numer. Anal.* 25 (1988), pp. 619–643.

[146] G.I. Shishkin. “A difference scheme for a singularly perturbed equation of parabolic type with discontinuous boundary conditions”. In: *USSR Computational Mathematics and Mathematical Physics* 28.6 (1988), pp. 32–41.

[147] V. Ervin and W. Layton. “An analysis of a defect-correction method for a model convection-diffusion equation”. In: *SIAM J. Numer. Anal.* 26 (1989), pp. 169–179.

[148] K. Surla and V. Jerković. *An exponentially fitted quadratic spline difference scheme on a non-uniform mesh*. Univ. u Novom Sadu Zb. Rad. Prirod. Mat. Fak. Ser. Mat., 1990.

[149] S. Yu-cheng and C. Quan. “The numerical solution of a singularly perturbed problem for semilinear parabolic differential equation”. In: *Appl. Math. Mech.* 12 (1991), pp. 1047–1056.

[150] G.Q. Liu and Y.C. Su. “A uniformly convergent difference scheme for the singular perturbation problem of a high order elliptic differential equation”. In: *Appl. Math. Mech.* 17 (1996), pp. 413–421.

[151] K. Surla and Z. Uzelac. “A spline difference scheme on a piecewise equidistant grid”. In: *ZAMM-Journal of Applied Mathematics and Mechanics/Zeitschrift für Angewandte Mathematik und Mechanik* 77.12 (1997), pp. 901–909.

[152] D. Herceg, K. Surla, and S. Rapajic. “Cubic spline difference scheme on a mesh of Bakhvalov type”. In: *Novi Sad J. Math* 28.3 (1998), pp. 41–49.

[153] M. Stojanović. “An application of the exponential cubic splines to numerical solution of a self-adjoint perturbation problem”. In: *Approximation Theory and its Applications* 14.2 (1998), pp. 38–43.

[154] M. K. Kadalbajoo and K. C. Patidar. “Spline techniques for solving singularly-perturbed nonlinear problems on nonuniform grids”. In: *Journal of Optimization theory and applications* 114.3 (2002), pp. 573–591.

[155] M. K. Kadalbajoo and K. C. Patidar. “Exponentially fitted spline in compression for the numerical solution of singular perturbation problems”. In: *Computers & Mathematics with Applications* 46.5-6 (2003), pp. 751–767.

[156] S. Natesan and N. Ramanujam. “Booster method for singularly-perturbed one-dimensional convection-diffusion Neumann problems”. In: *J. Optim. Theory Appl.* 99 (1998), pp. 53–72.

[157] S. Natesan and N. Ramanujam. “A computational method for solving singularly perturbed turning point problems exhibiting twin boundary layers”. In: *Appl.Math. Comput.* 93 (1998), pp. 259–275.

[158] J.A. Mackenzie. “Uniform convergence analysis of an upwind finite-difference approximation of a convection-diffusion boundary value problem on an adaptive grid”. In: *IMA J. Numer. Anal.* 19 (1999), pp. 233–249.

[159] M.G. Beckett and J.A. Mackenzie. “Convergence analysis of finite difference approximations on equidistributed grids to a singularly perturbed boundary value problem”. In: *Applied Numerical Mathematics* 35.2 (2000), pp. 87–109.

[160] N. Kopteva and M. Stynes. “A robust adaptive method for a quasi-linear one-dimensional convection-diffusion problem”. In: *SIAM J. Numer. Anal.* 39 (2001), pp. 1446–1467.

[161] T. Linß. “Uniform pointwise convergence of finite difference schemes using grid equidistribution”. In: *Computing* 66 (2001), pp. 27–39.

[162] A.C. Radhakrishna Pillai. “Fourth-order exponential finite difference methods for boundary value problems of convective diffusion type”. In: *Int. J. Numer.Methods Fluids* 37 (2001), pp. 87–106.

[163] T. Linß. “Layer-adapted meshes for convection-diffusion problems”. In: *Comput. Methods Appl. Mech. Eng.* 192 (2003), pp. 1061–1105.

[164] A.R. Ansari and A.F. Hegarty. “Numerical solution of a convection diffusion problem with Robin boundary conditions”. In: *J. Comput. Appl. Math.* 156 (2003), pp. 221–238.

[165] C. Clavero, J.C. Jorge, and F. Lisbona. “A uniformly convergent scheme on a nonuniform mesh for convection–diffusion parabolic problems”. In: *J. Comput. Appl.Math.* 154 (2003), pp. 415–429.

[166] T. Schamberg and W. Heinrichs. “An adaptive refinement method for convection-diffusion problems”. In: vol. 4. 2004, pp. 718–719.

[167] T. Linß. “Error expansion for a first-order upwind difference scheme applied to a model convection-diffusion problem”. In: *IMA J. Numer. Anal.* 24 (2004), pp. 239–253.

[168] K.C. Patidar. “High order fitted operator numerical method for self-adjoint singular perturbation problems”. In: *Appl. Math. Comput.* 171 (2005), pp. 547–566.

[169] J.M.C. Lubuma and K.C. Patidar. “Uniformly convergent non-standard finite difference methods for self-adjoint singular perturbation problems”. In: *J. Comput. Appl. Math.* 191 (2006), pp. 228–238.

[170] M.M. Shahraki and S.M. Hosseini. “Comparison of a higher order method and the simple upwind and non-monotone methods for singularly perturbed boundary value problems”. In: *Appl. Math. Comput.* 182 (2006), pp. 460–473.

[171] J. Rashidinia, M. Ghasemi, and Z. Mahmoodi. “Spline approach to the solution of a singularly perturbed boundary value problems”. In: *Appl. Math. Comput.* 189 (2007), pp. 72–78.

[172] S. Natesan and R.K. Bawa. “Second-order numerical scheme for singularly perturbed reaction-diffusion Robin problems”. In: *J. Numer. Anal. Ind. Appl. Math.* 2 (2007), pp. 177–192.

[173] J.B. Munyakazi and K.C. Patidar. “On Richardson extrapolation for fitted operator finite difference methods”. In: *Appl. Math. Comput.* 201 (2008), pp. 465–480.

[174] T. Linß. “Robust convergence of a compact fourth order finite difference scheme for reaction diffusion problems”. In: *Numer. Math.* 111 (2008), pp. 239–249.

[175] S.C.S. Rao and M. Kumar. “Parameter-uniformly convergent exponential spline difference scheme for singularly perturbed semilinear reaction–diffusion problems”. In: *Nonlinear Analysis: Theory, Methods & Applications* 71.12 (2009), e1579–e1588.

[176] S.C.S. Rao and M. Kumar. “A uniformly convergent exponential spline difference scheme for singularly perturbed reaction-diffusion problems”. In: *Neural Parallel Sci. Comput.* 18 (2010), pp. 121–136.

[177] M.K. Kadalbajoo and A. Awasthi. “The midpoint upwind finite difference scheme for time-dependent singularly perturbed convection-diffusion equations on non-uniform mesh”. In: *Int. J. Comput. Methods Eng. Sci. Mech.* 12 (2011), pp. 150–159.

[178] C. Grossmann, R.K. Mohanty, and H.G. Roos. “A direct higher order discretization in singular perturbations via domain split-A computational approach”. In: *Appl. Math. Comput.* 217 (2011), pp. 9302–9312.

[179] P. Das and S. Natesan. “Higher order parameter uniform convergent schemes for Robin type reaction diffusion problems using adaptively generated grid”. In: *Int. J. Comput. Methods* 9 (2012), pp. 125–152.

[180] J.B. Munyakazi and K.C.Patidar. “A fitted numerical method for singularly perturbed parabolic reaction-diffusion problems”. In: *Comput. Appl. Math.* 32 (2013), pp. 509–519.

[181] S. Gowrisankar and S. Natesan. “Robust numerical scheme for singularly perturbed convection diffusion parabolic initial boundary value problems on equidistributed grids”. In: *Comput. Phys. Commun.* 185 (2014), pp. 2008–2019.

[182] J.B. Munyakazi. “A uniformly convergent nonstandard finite difference scheme for a system of convection-diffusion equations”. In: *Comp. Appl. Math.* 34 (2015), pp. 1153–1165.

[183] K. Gayaz and D. Denys. “On supraconvergence phenomenon for second order centered finite differences on non-uniform grids”. In: *J. Comput. Appl. Math.* 326 (2017), pp. 1–14.

[184] A. Majumdar and S. Natesan. “Alternating direction numerical scheme for singularly perturbed 2D degenerate parabolic convection-diffusion problems”. In: *Appl. Math. Comput.* 313 (2017), pp. 453–473.

[185] L. Ning, S. Haiyan, G. Dongwei, and F. Xinlong. “Multiquadric RBF-FD method for the convection-dominated diffusion problems based on Shishkin nodes”. In: *Int. J. Heat Mass Transfer* 118 (2018), pp. 734–745.

[186] N. Geetha and A. Tamilselvan. “Parameter uniform numerical method for fourth order singularly perturbed turning point problems exhibiting boundary layers”. In: *Ain Shams Eng. J.* 9.4 (2018), pp. 845–853.

[187] A. Das and S. Natesan. “Higher-order convergence with fractional-step method for singularly perturbed 2D parabolic convection-diffusion problems on Shishkin mesh”. In: *Comput. Math. Appl.* 75.7 (2018), pp. 2387–2403.

[188] M.K. Singh and S. Natesan. “Richardson extrapolation technique for singularly perturbed system of parabolic partial differential equations with exponential boundary layers”. In: *Appl. Math. Comput.* 333 (2018), pp. 254–275.

[189] N. A. Mbroh and J. B. Munyakazi. “A fitted operator finite difference method of lines for singularly perturbed parabolic convection–diffusion problems”. In: *Math. Comput. Simulation* 165 (2019), pp. 156–171.

[190] J. L. Gracia and E. O’Riordan. “Parameter-uniform numerical methods for singularly perturbed parabolic problems with incompatible boundary-initial data”. In: *Appl. Numer. Math.* 146 (2019), pp. 436–451.

[191] S. Gowrisankar and S. Natesan. “An efficient robust numerical method for singularly perturbed Burgers’ equation”. In: *Appl. Math. Comput.* 346 (2019), pp. 385–394.

[192] P. Das and J. Vigo-Aguiar. “Parameter uniform optimal order numerical approximation of a class of singularly perturbed system of reaction diffusion problems involving a small perturbation parameter”. In: *J. Comput. Appl. Math.* 354 (2019), pp. 533–544.

[193] C. Clavero and J. C. Jorge. “An efficient numerical method for singularly perturbed time dependent parabolic 2D convection-diffusion systems”. In: *J. Comput. Appl. Math.* 354 (2019), pp. 431–444.

[194] R. Vulanović and T. Nhan. “Robust hybrid schemes of higher order for singularly perturbed convection-diffusion problems”. In: *Appl. Math. Comput.* 386 (2020), p. 125495.

[195] N.A. Mbroh, S.C.O. Noutchie, and R.Y.M. Massoukou. “A uniformly convergent finite difference scheme for Robin type singularly perturbed parabolic convection diffusion problem”. In: *Math. Comput. Simulation* 174 (2020), pp. 218–232.

[196] N. A. Mbroh, S. C. O. Noutchie, and R. Y. M. Massoukou. “A second order finite difference scheme for singularly perturbed Volterra integro-differential equation”. In: *Alex. Eng. J.* 59.4 (2020), pp. 2441–2447.

[197] S. Kumar and H. Ramos. “Parameter-uniform approximation on equidistributed meshes for singularly perturbed parabolic reaction-diffusion problems with Robin boundary conditions”. In: *Appl. Math. Comput.* 392 (2021), p. 125677.

[198] M. J. Kabeto and G. F. Duressa. “Second-order robust finite difference method for singularly perturbed Burgers’ equation”. In: *Heliyon* 8.6 (2022), e09579.

[199] G. Babu, M. Prithvi, K.K. Sharma, and V.P. Ramesh. “A uniformly convergent numerical algorithm on harmonic (H(l)) mesh for parabolic singularly perturbed convection-diffusion problems with boundary layer”. In: *Differ. Equ. Dyn. Syst.* (2022), pp. 1–14.

[200] S. Kumar and J. Vigo-Aguiar. “A high order convergent numerical method for singularly perturbed time dependent problems using mesh equidistribution”. In: *Math. Comput. Simulation* 199 (2022), pp. 287–306.

[201] S. Nagarajan. “A parameter robust fitted mesh finite difference method for a system of two reaction-convection-diffusion equations”. In: *Appl. Numer. Math.* 179 (2022), pp. 87–104.

[202] S. Singh and D. Kumar. “Parameter uniform numerical method for a system of singularly perturbed parabolic convection-diffusion equations”. In: *Math. Comput. Simulation* 212 (2023), pp. 360–381.

[203] S. Singh, D. Kumar, and J. Vigo-Aguiar. “A robust numerical technique for weakly coupled system of parabolic singularly perturbed reaction–diffusion equations”. In: *J. Math. Chem.* 61.6 (2023), pp. 1313–1350.

[204] T.A. Nhan, V.Q. Mai, J. Mohapatra, and Z. Hammouch. “A new upwind difference analysis of an exponentially graded Bakhvalov-type mesh for singularly perturbed elliptic convection-diffusion problems”. In: *J. Comput. Appl. Math.* 418 (2023), p. 114622.

[205] S. Yadav and P. Rai. “A parameter uniform higher order scheme for 2D singularly perturbed parabolic convection-diffusion problem with turning point”. In: *Math. Comput. Simulation* 205 (2023), pp. 507–531.

[206] C. Clavero and J. C. Jorge. “A splitting uniformly convergent method for one-dimensional parabolic singularly perturbed convection-diffusion systems”. In: *Appl. Numer. Math.* 183 (2023), pp. 317–332.

[207] F. W. Gelu and G. F. Duressa. “A parameter-uniform numerical method for singularly perturbed Robin type parabolic convection-diffusion turning point problems”. In: *Appl. Numer. Math.* 190 (2023), pp. 50–64.

[208] K.C. Patidar. “Nonstandard finite difference methods: recent trends and further developments”. In: *J. Difference Equ. Appl.* 22 (2016), pp. 817–849.

[209] R. Shiromani, V. Shanthi, and H. Ramos. “Numerical treatment of a singularly perturbed 2-D convection-diffusion elliptic problem with Robin-type boundary conditions”. In: *Appl. Numer. Math.* 187 (2023), pp. 176–191.

[210] S. Kumar, Aakansha, J. Singh, and H. Ramos. “Parameter-uniform convergence analysis of a domain decomposition method for singularly perturbed parabolic problems with Robin boundary conditions”. In: *J. Appl. Math. Comput.* 69 (2023), pp. 2239–2261.

[211] S.K. Sahoo and V. Gupta. “A robust uniformly convergent finite difference scheme for the time-fractional singularly perturbed convection-diffusion problem”. In: *Comput. Math. Appl.* 137 (2023), pp. 126–146.

[212] A. Panda and J. Mohapatra. “On the convergence analysis of efficient numerical schemes for singularly perturbed second order Volterra integro-differential equations”. In: *J. Appl. Math. Comput.* (2023), pp. 1–24.

[213] A. Panda and J. Mohapatra. “A Robust Finite Difference Method for the Solutions of Singularly Perturbed Fredholm Integro-Differential Equations”. In: *Mediterr. J. Math.* 20.4 (2023), p. 198.

[214] J.E. Flaherty and W. Mathon. “Collocation with polynomial and tension splines for singularly-perturbed boundary value problems”. In: *SIAM Journal on Scientific and Statistical Computing* 1.2 (1980), pp. 260–289.

[215] M. K. Jain and T. Aziz. “Numerical solution of stiff and convection-diffusion equations using adaptive spline function approximation”. In: *Applied Mathematical Modelling* 7.1 (1983), pp. 57–62.

[216] K. Surla and V. Jerkovic. “Some possibilities of applying spline collocations to singular perturbation problems”. In: *Numerical Methods and Approximation Theory* 2 (1985), pp. 19–25.

[217] K. Surla and M. Stojanović. “Solving singularly perturbed boundary-value problems by spline in tension”. In: *Journal of Computational and Applied Mathematics* 24.3 (1988), pp. 355–363.

[218] M. Sakai and R. A. Usmani. “A class of simple exponential B-splines and their application to numerical solution to singular perturbation problems”. In: *Numerische Mathematik* 55.5 (1989), pp. 493–500.

[219] V.V. Strygin, I.A. Blatov, and I.Yu. Pokornaya. “Collocation method for solving singularly perturbed boundary-value problems by using cubic splines”. In: *Ukrainian Mathematical Journal* 46.4 (1994), pp. 433–440.

[220] M. Marušić and M. Rogina. “A collocation method for singularly perturbed two-point boundary value problems with splines in tension”. In: *Advances in Computational Mathematics* 6.1 (1996), pp. 65–76.

[221] Z. Uzelac and K. Surla. “A uniformly accurate collocation method for a singularly perturbed problem”. In: *Novi Sad J. Math* 33.1 (2003), pp. 133–143.

[222] M. K. Kadalbajoo and V. K. Aggarwal. “Fitted mesh B-spline collocation method for solving self-adjoint singularly perturbed boundary value problems”. In: *Applied Mathematics and Computation* 161.3 (2005), pp. 973–987.

[223] M. K. Kadalbajoo and A. S. Yadaw. “B-Spline collocation method for a two-parameter singularly perturbed convection–diffusion boundary value problems”. In: *Applied Mathematics and Computation* 201.1-2 (2008), pp. 504–513.

[224] M. K. Kadalbajoo and V. Gupta. “Numerical solution of singularly perturbed convection–diffusion problem using parameter uniform B-spline collocation method”. In: *Journal of Mathematical Analysis and Applications* 355.1 (2009), pp. 439–452.

[225] M. K. Kadalbajoo and V. Gupta. “A parameter uniform B-spline collocation method for solving singularly perturbed turning point problem having twin boundary layers”. In: *International Journal of Computer Mathematics* 87.14 (2010), pp. 3218–3235.

[226] K. Surla, Z. Uzelac, and L. Teofanov. “On a spline collocation method for a singularly perturbed problem”. In: *PAMM: Proceedings in Applied Mathematics and Mechanics*. Vol. 6. 1. Wiley Online Library. 2006, pp. 769–770.

[227] S.C.S. Rao and M. Kumar. “B-spline collocation method for nonlinear singularly-perturbed two-point boundary-value problems”. In: *Journal of optimization theory and applications* 134.1 (2007), pp. 91–105.

[228] S.C.S. Rao and M. Kumar. “Exponential B-spline collocation method for self-adjoint singularly perturbed boundary value problems”. In: *Applied Numerical Mathematics* 58.10 (2008), pp. 1572–1581.

[229] K. Surla, L. Teofanov, and Z. Uzelac. “A robust layer-resolving spline collocation method for a convection–diffusion problem”. In: *Applied Mathematics and Computation* 208.1 (2009), pp. 76–89.

[230] M. K. Kadalbajoo and P. Arora. “B-splines with artificial viscosity for solving singularly perturbed boundary value problems”. In: *Mathematical and Computer Modelling* 52.5-6 (2010), pp. 654–666.

[231] S.A Khuri and A. Sayfy. “The boundary layer problem: A fourth-order adaptive collocation approach”. In: *Computers & Mathematics with Applications* 64.6 (2012), pp. 2089–2099.

[232] W.K. Zahra and A.M. El Mhlawy. “Numerical solution of two-parameter singularly perturbed boundary value problems via exponential spline”. In: *Journal of King Saud University-Science* 25.3 (2013), pp. 201–208.

[233] Ş. Yüzbaşı. “A collocation method based on the Bessel functions of the first kind for singular perturbated differential equations and residual correction”. In: *Mathematical Methods in the Applied Sciences* 38.14 (2015), pp. 3033–3042.

[234] A. Khan and P. Khandelwal. “Non-polynomial sextic spline solution of singularly perturbed boundary-value problems”. In: *International Journal of Computer Mathematics* 91.5 (2014), pp. 1122–1135.

[235] R.K. Lodhi and H.K. Mishra. “Solution of a class of fourth order singular singularly perturbed boundary value problems by quintic B-spline method”. In: *J. Nig. Math. Soc.* 35 (2016), pp. 257–265.

[236] R.K. Lodhi and H.K. Mishra. “Quintic B-spline method for solving second order linear and nonlinear singularly perturbed two-point boundary value problems”. In: *Journal of Computational and Applied Mathematics* 319 (2017), pp. 170–187.

[237] O.C. Zienkiewicz, R.H. Gallagher, and P. Hood. “Newtonian and non-Newtonian viscous impompressible flow. Temperature induced flows and finite elements solutions. The mathematics of finite elements and applications”. In: *Academic Press, London* (1975), pp. 235–267.

[238] I. Christie, D.F. Griffiths, A.R. Mitchell, and O.C. Zienkiewicz. “Finite element methods for second order differential equations with significant first derivatives”. In: *Int. J. Numer. Meth. Engng.* 10 (1976), pp. 1389–1396.

[239] J.C. Heinrich, P.S. Huyakorn, A.R. Mitchell, and O.C. Zienkiewicz. “An upwind finite element scheme for two-dimensional convective transport equations”. In: *Int. J. Numer. Methods Eng.* 11 (1977), pp. 131–143.

[240] J.C. Heinrich and O.C.Zienkiewicz. “The finite element method and ‘upwinding’ techniques in the numerical solution of convection dominated flow problems”. In: *Finite element methods for convection dominated flows* (1979), pp. 105–136.

[241] M.V. Veldhuizen. “Higher order methods for a singularly perturbed problem”. In: *Numer. Math.* 30 (1978), pp. 267–279.

[242] J.W. Barrett and K.W. Morton. “Optimal finite element solutions to diffusion-convection problems in one dimension”. In: *Int. J. Numer. Methods Eng.* 15 (1980), pp. 1457–1474.

[243] J.W. Barrett and K.W. Morton. “Optimal Petrov-Galerkin methods through approximate symmetrization”. In: *IMA J. Numer. Anal.* 1 (1981), pp. 439–468.

[244] J.W. Barrett and K.W. Morton. “Approximate symmetrization and Petrov-Galerkin methods for diffusion-convection problems”. In: *Comput. Methods Appl. Mech. Eng.* 45 (1984), pp. 97–122.

[245] J. Douglas and T.F. Russell. “Numerical methods for convection-dominated diffusion problems based on combining the method of characteristics with finite element or finite difference procedures”. In: *SIAM J. Numer. Anal.* 19 (1982), pp. 871–885.

[246] E. O’Riordan. “Singularly perturbed finite element methods”. In: *Numer. Math.* 44 (1984), pp. 425–434.

[247] M. Stynes and E. O’Riordan. “An analysis of a singularly perturbed two-point boundary value problem using only finite element techniques”. In: *Math. Comput.* 56 (1991), pp. 663–675.

[248] K. Eriksson and C. Johnson. “Adaptive streamline diffusion finite element methods for stationary convection-diffusion problems”. In: *Math. Comput.* 60 (1993), pp. 167–188.

[249] G. Sun and M. Stynes. “Finite-element methods for singularly perturbed high-order elliptic two-point boundary value problems. I: Reaction-diffusion-type problems”. In: *IMA J. Numer. Anal.* 15 (1995), pp. 117–139.

[250] Z. Zhang. “Finite element superconvergence approximation for one-dimensional singularly perturbed problems”. In: *Numer. Methods Partial Differ. Equ.* 18 (2002), pp. 374–395.

[251] S. Franz and T. Linß. “Superconvergence analysis of the Galerkin FEM for a singularly perturbed convection-diffusion problem with characteristic layers”. In: *Numer. Methods Partial Differ. Equ.* 24 (2008), pp. 144–164.

[252] J. Zhang and X. Liu. “Superconvergence of finite element method for singularly perturbed convection-diffusion equations in 1-D”. In: *Appl. Math. Lett.* 98 (2019), pp. 278–283.

[253] A. Kaushik, V. Kumar, M. Sharma, and A. K. Vashishth. “A higher order finite element method with modified graded mesh for singularly perturbed two-parameter problems”. In: *Math. Meth. Appl. Sc.* (2020), pp. 1–13.

[254] A. Kaushik, A.K. Vashishth, V. Kumar, and M. Sharma. “A modified graded mesh and higher order finite element approximation for singular perturbation problems”. In: *Journal of Computational Physics* 395 (2019), pp. 275–285. ISSN: 0021-9991.

[255] N. Kumar, J. Singh, and R. Jiwari. “Convergence analysis of weak Galerkin finite element method for semilinear parabolic convection dominated diffusion equations on polygonal meshes”. In: *Comput. Math. Appl.* 145 (2023), pp. 141–158.

[256] J. Singh, N. Kumar, and R. Jiwari. “A robust weak Galerkin finite element method for two parameter singularly perturbed parabolic problems on nonuniform meshes”. In: *Journal of Computational Science* 77 (2024), p. 102241.

[257] Ş. Toprakseven and P. Zhu. “Error analysis of a weak Galerkin finite element method for two-parameter singularly perturbed differential equations in the energy and balanced norms”. In: *Appl. Math. Comput.* 441 (2023), p. 127683.

[258] Ş. Toprakseven. “Optimal order uniform convergence in energy and balanced norms of weak Galerkin finite element method on Bakhvalov-type meshes for nonlinear singularly perturbed problems”. In: *Comput. Appl. Math.* 41.8 (2022), p. 377.

[259] Ş. Toprakseven. “Superconvergence of a modified weak Galerkin method for singularly perturbed two-point elliptic boundary-value problems”. In: *Calcolo* 59.1 (2021), p. 1.

[260] Ş. Toprakseven, A. Kaushik, and M. Sharma. “A weak Galerkin finite element method for singularly perturbed problems with two small parameters on Bakhvalov-type meshes”. In: *Numerical Algorithms* 97.2 (2024), pp. 727–751.

[261] Z. Cai and J. Ku. “A Dual Finite Element Method for a Singularly Perturbed Reaction-Diffusion Problem”. In: *SIAM Journal on Numerical Analysis* 58.3 (2020), pp. 1654–1673.

[262] Y. Wang, X. Meng, and Y. Li. “The finite volume element method on the shishkin mesh for a singularly perturbed reaction-diffusion problem”. In: *Comput. Math. Appl.* 84 (2021), pp. 112–127.

[263] K.R. Ranjan and S. Gowrisankar. “Uniformly convergent NIPG method for singularly perturbed convection diffusion problem on Shishkin type meshes”. In: *Appl. Numer. Math.* 179 (2022), pp. 125–148.

[264] A.K. Aziz. *The Mathematical Foundations of the Finite Element Method with Applications to Partial Differential Equations*. Academic Press, 2014.

[265] S.I. Rubinow. *Introduction to Mathematical Biology*. Wiley, 1975.

[266] J.D. Murray. *Mathematical Biology II: Spatial Models and Biomedical Applications*. Vol. 3. Springer New York, 2001.

[267] A. Kaushik. “Singular perturbation analysis of bistable differential equation arising in the nerve pulse propagation”. In: *Nonlinear Anal.* 9 (2008), pp. 2106–2127.

[268] A. Bejan. *Convection Heat Transfer*. John Wiley, New York, 1984.

[269] T. Linss and M. Stynes. “Numerical solution of systems of singularly perturbed differential equations”. In: *Computational Methods in Applied Mathematics* 9.2 (2009), pp. 165–191.

[270] V. Kumar and B. Srinivasan. “A novel adaptive mesh strategy for singularly perturbed parabolic convection diffusion problems”. In: *Differential Equations and Dynamical Systems* 27 (2019), pp. 203–220.

[271] C. Xenophontos and L. Oberbroeckling. “A numerical study on the finite element solution of singularly perturbed systems of reaction–diffusion problems”. In: *Applied mathematics and computation* 187.2 (2007), pp. 1351–1367.

[272] G. Singh and S. Natesan. “A Uniformly Convergent Numerical Scheme for a Coupled System of Singularly Perturbed Reaction-Diffusion Equations”. In: *Numerical Functional Analysis and Optimization* 41.10 (2020), pp. 1172–1189.

[273] Ş. Toprakseven and P. Zhu. “A parameter-uniform weak Galerkin finite element method for a coupled system of singularly perturbed reaction-diffusion equations”. In: *Filomat* 37.13 (2023), pp. 4351–4374.

[274] R. Lin and M. Stynes. “A balanced finite element method for a system of singularly perturbed reaction-diffusion two-point boundary value problems”. In: *Numerical Algorithms* 70 (2015), pp. 691–707.

[275] LB. Liu, G. Long, and Z. Cen. “A robust adaptive grid method for a nonlinear singularly perturbed differential equation with integral boundary condition”. In: *Numerical Algorithms* 83 (2020), pp. 719–739.

[276] A. Gupta and A. Kaushik. “A higher-order hybrid finite difference method based on grid equidistribution for fourth-order singularly perturbed differential equations”. In: *Journal of Applied Mathematics and Computing* (May 2021), pp. 1–29.

[277] A. Gupta and A. Kaushik. “A robust spline difference method for robin-type reaction-diffusion problem using grid equidistribution”. In: *Applied Mathematics and Computation* 390 (2021), p. 125597.

[278] A. Gupta, A. Kaushik, and M. Sharma. “A higher-order hybrid spline difference method on adaptive mesh for solving singularly perturbed parabolic reaction–diffusion problems with robin-boundary conditions”. In: *Numerical Methods for Partial Differential Equations* 39.2 (2023), pp. 1220–1250.

[279] Sumit, S. Kumar, and S. Kumar. “A high order convergent adaptive numerical method for singularly perturbed nonlinear systems”. In: *Computational and Applied Mathematics* 41.2 (2022), p. 83.

[280] P. Das and S. Natesan. “Optimal error estimate using mesh equidistribution technique for singularly perturbed system of reaction–diffusion boundary-value problems”. In: *Applied mathematics and computation* 249 (2014), pp. 265–277.

[281] S. Chawla, J. Singh, and Urmil. “An analysis of the robust convergent method for a singularly perturbed linear system of reaction–diffusion type having nonsmooth data”. In: *International Journal of Computational Methods* 19.01 (2022), p. 2150056.

[282] N. Madden and M. Stynes. “A uniformly convergent numerical method for a coupled system of two singularly perturbed linear reaction diffusion problems”. In: *IMA J. Numer. Anal.* 23 (2003), pp. 627–644.

[283] P. Mahabub Basha and V. Shanthi. “A Uniformly Convergent Scheme for A System of Two Coupled Singularly Perturbed Reaction-Diffusion Robin Type Boundary Value Problems with Discontinuous Source Term”. In: *American Journal of Numerical Analysis* 3.2 (2015), pp. 39–48.

[284] S. Natesan and B.S. Deb. “A robust computational method for singularly perturbed coupled system of reaction-diffusion boundary value problems”. In: *Appl. Math. Comput.* 188 (2007), pp. 353–364.

[285] Z. Cen. “Parameter-uniform finite difference scheme for a system of coupled singularly perturbed convection–diffusion equations”. In: *International Journal of Computer Mathematics* 82.2 (2005), pp. 177–192.

[286] C.G Lange and R.M Miura. “Singular perturbation analysis of boundary value problems for differential-difference equations. V. Small shifts with layer behavior”. In: *SIAM Journal on Applied Mathematics* 54.1 (1994), pp. 249–272.

[287] A. Gupta and A. Kaushik. “A higher-order hybrid finite difference method based on grid equidistribution for fourth-order singularly perturbed differential equations”. In: *Journal of Applied Mathematics and Computing* 68.2 (Apr. 2022), pp. 1163–1191.

[288] M.G. Beckett and J.A. Mackenzie. “On a uniformly accurate finite difference approximation of a singularly perturbed reaction diffusion problem using grid equidistribution”. In: *J. Comput. Appl. Math.* 131 (2001), pp. 381–405.

[289] S. C. S. Rao and M. Kumar. “An almost fourth order parameter-robust numerical method for a linear system of ($m \geq 2$) coupled singularly perturbed reaction-diffusion problems”. In: *International Journal of Numerical Analysis and Modeling* 10.3 (2013), pp. 603–621.

[290] T. Linß and N. Madden. “Accurate solution of a system of coupled singularly perturbed reaction diffusion equations”. In: *Computing* 73 (2004), pp. 121–133.

[291] C. Clavero, J.L. Gracia, and F.J. Lisbona. “An almost third order finite difference scheme for singularly perturbed reaction diffusion systems”. In: *J. Comput. Appl. Math.* 234 (2010), pp. 2501–2515.

[292] S. Singh, D. Kumar, and H. Ramos. “An efficient parameter uniform spline-based technique for singularly perturbed weakly coupled reaction-diffusion systems”. In: *Journal of Applied Analysis & Computation* 13.4 (2023), pp. 2203–2228.

[293] S.C.S. Rao and S. Kumar. “Second order global uniformly convergent numerical method for a coupled system of singularly perturbed initial value problems”. In: *Appl. Math. Comput.* 219 (2012), pp. 3740–3753.

[294] T. Linß and N. Madden. “Layer adapted meshes for a system of coupled singularly perturbed reaction diffusion problems”. In: *IMA J. Numer. Anal.* 29 (2009), pp. 109–125.

[295] C. Xenophontos and L. Oberbroeckling. “A numerical study on the finite element solution of singularly perturbed systems of reaction diffusion problems”. In: *Appl. Math. Comput.* 187 (2007), pp. 1351–1367.

[296] T. Linß and M. Stynes. “Numerical solution of systems of singularly perturbed differential equations”. In: *Computational Methods in Applied Mathematics* 9.2 (2009), pp. 165–191.

[297] C. Clavero, J.L. Gracia, and F.J. Lisbona. “High order schemes for reaction diffusion singularly perturbed systems”. In: *Proc. BAIL* (2009), pp. 107–115.

[298] V. Subburayan and N. Ramanujam. “An initial value method for singularly perturbed system of reaction-diffusion type delay differential equations”. In: *Journal of the Korean Society for Industrial and Applied Mathematics* 17.4 (2013), pp. 221–237.

[299] E. Sekar and A. Tamilselvan. “Parameter uniform method for a singularly perturbed system of delay differential equations of reaction–diffusion type with integral boundary conditions”. In: *International Journal of Applied and Computational Mathematics* 5 (2019), pp. 1–12.

[300] K.C. Patidar and K.K. Sharma. “ε-uniformly convergent non-standard finite difference methods for singularly perturbed differential difference equations with small delay”. In: *Applied Mathematics and Computation* 175.1 (2006), pp. 864–890.

[301] R. Rao and P. Chakravarthy. “A finite difference method for singularly perturbed differential-difference equations with layer and oscillatory behavior”. In: *Applied Mathematical Modelling* 37.8 (2013), pp. 5743–5755.

[302] V. Raja and A. Tamilselvan. “Numerical method for a system of singularly perturbed convection diffusion equations with integral boundary conditions”. In: *Communications of the Korean Mathematical Society* 34.3 (2019), pp. 1015–1027.

[303] M.B. Pathan and S. Vembu. “A parameter-uniform second order numerical method for a weakly coupled system of singularly perturbed convection-diffusion equations with discontinuous convection coefficients and source terms”. In: *Calcolo* 54 (2017), pp. 1027–1053.

[304] H.G Roos and M. Schopf. “Layer structure and the Galerkin finite element method for a system of weakly coupled singularly perturbed convection-diffusion equations with multiple scales”. In: *ESAIM: Mathematical Modelling and Numerical Analysis* 49.5 (2015), pp. 1525–1547.

[305] T. Linß. “Analysis of an upwind finite difference scheme for a system of coupled singularly perturbed convection diffusion equations”. In: *Comput.* 79 (2007), pp. 23–32.

[306] E.R. El-Zahar, G.F. Al-Boqami, and H.S. Al-Juaydi. “Approximate analytical solutions for strongly coupled systems of singularly perturbed convection diffusion problems”. In: *Mathematics* 12.2 (2024), p. 277.

[307] P.P. Chakravarthy and T. Gupta. “Numerical solution of a weakly coupled system of singularly perturbed delay differential equations via cubic spline in tension”. In: *National Academy Science Letters* 43 (2020), pp. 259–262.

[308] LB. Liu and Y. Chen. “A-posteriori error estimation in maximum norm for a strongly coupled system of two singularly perturbed convection-diffusion problems”. In: *Journal of Computational and Applied Mathematics* 313 (2017), pp. 152–167.

[309] LB. Liu and Y. Chen. “A robust adaptive grid method for a system of two singularly perturbed convection-diffusion equations with weak coupling”. In: *Journal of Scientific Computing* 61.1 (2014), pp. 1–16.

[310] LB. Liu, Y. Liang, X. Bao, and H. Fang. “An efficient adaptive grid method for a system of singularly perturbed convection-diffusion problems with Robin boundary conditions”. In: *Advances in Difference Equations* 2021.1 (2021), pp. 1–13.

[311] C. Clavero, J.L. Gracia, and F.J. Lisbona. “An almost third order finite difference scheme for singularly perturbed reaction–diffusion systems”. In: *Journal of Computational and Applied Mathematics* 234.8 (2010), pp. 2501–2515.

[312] T. Linß and N. Madden. “Layer-adapted meshes for a linear system of coupled singularly perturbed reaction–diffusion problems”. In: *IMA journal of numerical analysis* 29.1 (2009), pp. 109–125.

[313] S. Bellew and E. O’Riordan. “A parameter robust numerical method for a system of two singularly perturbed convection–diffusion equations”. In: *Applied Numerical Mathematics* 51.2-3 (2004), pp. 171–186.

[314] E. O’Riordan and M. Stynes. “Numerical analysis of a strongly coupled system of two singularly perturbed convection–diffusion problems”. In: *Advances in Computational Mathematics* 30 (2009), pp. 101–121.

[315] J.D. Lambert. *Numerical Methods for Ordinary Differential Systems*. John Wiley & Sons, New York, 1991.

[316] A. Kaushik, V. Kumar, and A.K. Vashishth. “An efficient mixed asymptotic numerical scheme for singularly perturbed convection diffusion problems”. In: *Appl. Math.Comp.* 218 (2012), pp. 8645–8658.

[317] P.A. Selvi and N. Ramanujam. “An iterative numerical method for a weakly coupled system of singularly perturbed convection–diffusion equations with negative shifts”. In: *International Journal of Applied and Computational Mathematics* 3 (2017), pp. 147–160.

[318] P.C. Podila, T. Gupta, and J. Vigo-Aguiar. “A numerical scheme for a weakly coupled system of singularly perturbed delay differential equations on an adaptive mesh”. In: *Comp and Math Methods* 3.3 (2021), e1104.

[319] C. Xenophontos, S. Franz, and L. Ludwig. “Finite element approximation of convection diffusion problems using an exponentially graded mesh”. In: *Comput. Math. Appl.* 72 (2016), pp. 1532–1540.

[320] R. Vulanović. “A priori meshes for singularly perturbed quasilinear two point boundary value problems”. In: *IMA J. Numer. Anal.* 21 (2001), pp. 349–366.

[321] P. Deepika and A. Das. “A Robust Numerical Scheme via Grid Equidistribution for Singularly Perturbed Delay Partial Differential Equations Arising in Control Theory”. In: *International Journal of Applied and Computational Mathematics* 10.2 (2024), p. 72.

[322] P. Das and S. Natesan. “A uniformly convergent hybrid scheme for singularly perturbed system of reaction diffusion Robin type boundary value problems”. In: *J. Appl. Math. Comput.* 41 (2013), pp. 447–471.

[323] P. Das and S. Natesan. “Optimal error estimate using mesh equidistribution technique for singularly perturbed system of reaction diffusion boundary value problems”. In: *Appl. Math. Comput.* 249 (2014), pp. 265–277.

[324] A. Kaushik, A. Gupta, S. Jain, Ş. Toprakseven, and M. Sharma. “An adaptive mesh generation and higher-order difference approximation for the system of singularly perturbed reaction–diffusion problems”. In: *Partial Differential Equations in Applied Mathematics* 11 (2024), p. 100750.

[325] W.T. Gobena and G.F. Duressa. “Parameter-Uniform Numerical Scheme for Singularly Perturbed Delay Parabolic Reaction Diffusion Equations with Integral Boundary Condition”. In: *International Journal of Differential Equations* 2021.1 (2021), p. 9993644.

[326] W.T. Gobena and G.F. Duressa. “An optimal fitted numerical scheme for solving singularly perturbed parabolic problems with large negative shift and integral boundary condition”. In: *Results in Control and Optimization* 9 (2022), p. 100172.

[327] W. T. Gobena and G. F. Duressa. “Exponentially fitted robust scheme for the solution of singularly perturbed delay parabolic differential equations with integral boundary condition”. In: *International Journal of Applied and Computational Mathematics* 10.1 (2024), p. 30.

[328] W. S. Hailu and G. F. Duressa. “Uniformly Convergent Numerical Scheme for Solving Singularly Perturbed Parabolic Convection-Diffusion Equations with Integral Boundary Condition”. In: *Differential Equations and Dynamical Systems* (2023), pp. 1–27.

[329] V. Raja and A. Tamilselvan. “Numerical method for a system of singularly perturbed reaction diffusion equations with integral boundary conditions”. In: *International Journal of Applied and Computational Mathematics* 5 (2019), pp. 1–12.

[330] J.J.H. Miller, E. O’Riordan, G.I. Shishkin, and L.P. Shishkina. “Fitted mesh methods for problems with parabolic boundary layers”. In: *Math. Proc. Royal Irish Acad.* 98 (1998), pp. 173–190.

[331] T. Linß and N. Madden. “Parameter uniform approximations for time dependent reaction diffusion problems”. In: *Numer. Methods Partial Differ. Equ.* 23 (2007), pp. 1290–1300.

[332] K. Bansal and K. K Sharma. “Parameter-robust numerical scheme for time-dependent singularly perturbed reaction–diffusion problem with large delay”. In: *Numerical Functional Analysis and Optimization* 39.2 (2018), pp. 127–154.

[333] S. Gowrisankar and S. Natesan. “The parameter uniform numerical method for singularly perturbed parabolic reaction–diffusion problems on equidistributed grids”. In: *Applied Mathematics Letters* 26.11 (2013), pp. 1053–1060.

List of Publications

1. Aditya Kaushik, Shivani Jain and Manju Sharma, A uniformly accurate hybrid difference approximation of a system of singularly perturbed reaction-diffusion equations with delay using grid equidistribution, Mathematical Modelling and Analysis, Accepted (2025) **IF 1.3**. **SCIE**

2. Shivani Jain and Aditya Kaushik, A semi-analytical approximation for a coupled system of singularly perturbed convection-diffusion equations with shifts, International Journal of Computational Methods, 2450076 (2024) **IF 1.4**. **SCIE**

3. Aditya Kaushik and Shivani Jain, A Posteriori Error Analysis of Defect Correction Method for Singular Perturbation Problems With Discontinuous Coefficient and Point Source, Journal of Computational and Nonlinear Dynamics, 19, 091005-1 (2024) **IF 2.0**. **SCIE**

4. Aditya Kaushik, Nitika Sharma, Manju Sharma, Monika Arora, and Shivani Jain, A uniformly convergent method for two-parameter singularly perturbed parabolic partial differential equations with a large shift, Journal of Difference Equations and Applications, 69, 1-38 (2024) **IF 1.1**. **SCIE**

5. Aditya Kaushik, Aastha Gupta, Shivani Jain, Şuayip Toprakseven and Manju Sharma, An adaptive mesh generation and higher-order difference approximation for the system of singularly perturbed reaction-diffusion problems, Partial Differential Equations in Applied Mathematics, 11, 100750 (2024) **IF 5.23**. **Scopus**

List of papers presented in International Conferences

1. Presented the paper entitled: “Higher order hybrid difference method for the system of singularly perturbed delay reaction diffusion equations", International Conference on Advances in Pure & Applied Mathematics (ICAPAM) held during 08-10 February 2024 at Shyam Lal College, University of Delhi, Delhi, India.

2. Presented the paper entitled:“Solving system of advance-delay singularly perturbed convection diffusion equations using asymptotic numerical method", International Conference on Mathematical Sciences (ICMA 23) held during 24-25 March 2023 at Sacred Heart College (Autonomous), Tirupattur district, Tamil Nadu, India.

3. Presented the paper entitled:“Asymptotic numerical method for the system of singularly perturbed equations arising in the modelling of enzyme kinetics", International Conference on Computational Mathematics (ICCM-2023) held during 03 February 2023 at Department of Mathematics, Sadguru Gadage Maharaj College, Karad, Kolhapur, India.